Queen Mary
University of London

Antenna and radio channel characterisation for lowpower personal and body area networks

Khan, Mohammad Monirujjaman

For additional information about this publication click this link.
http://qmro.qmul.ac.uk/jspui/handle/123456789/2521

Information about this research object was correct at the time of download; we occasionally make corrections to records, please therefore check the published record when citing. For more information contact scholarlycommunications@qmul.ac.uk

Antenna and Radio Channel Characterisation for Low-Power Personal and Body Area Networks

Mohammad Monirujjaman Khan

A thesis submitted to the faculty of the University of London in partial fulfilment of the requirements for the degree of

Doctor of Philosophy

School of Electronic Engineering and Computer Science
Queen Mary, University of London
London E14NS
United Kingdom

February 2012

2012 © Queen Mary, University of London. All rights reserved.

To my family

Abstract

The continuous miniaturisation of sensors, as well as the progression in wearable electronics, embedded software, digital signal processing and biomedical technologies, have led to new user-centric networks, where devices can be carried in the user's pockets, attached to the user's body. Body-centric wireless communications (BCWCs) is a central point in the development of fourth generation mobile communications. Body-centric wireless networks take their place within the personal area networks, body area networks and sensor networks which are all emerging technologies that have a wide range of applications (such as, healthcare, entertainment, surveillance, emergency, sports and military). The major difference between BCWC and conventional wireless systems is the radio channels over which the communication takes place. The human body is a hostile environment from a radio propagation perspective and it is therefore important to understand and characterise the effects of the human body on the antenna elements, the radio channel parameters and, hence, system performance. This thesis focuses on the study of body-worn antennas and on-body radio propagation channels.

The performance parameters of five different narrowband (2.45 GHz) and four UWB (3.1-10.6 GHz) body-worn antennas in the presence of human body are investigated and compared. This was performed through a combination of numerical simulations and measurement campaigns. Parametric studies and statistical analysis, addressing the human body effects on the performance parameters of different types of narrowband and UWB antennas have been presented. The aim of this study is to understand the human body effects on the antenna parameters and specify the suitable antenna in BCWCs at both 2.45 GHz and UWB frequencies. Extensive experimental investigations are carried out to study the effects of various antenna types on the on-body radio propagation channels as well. Results and analysis emphasize the best body-worn antenna for reliable and power-efficient on-body communications. Based on the results and analysis, a novel dual-band and dual-mode antenna is proposed for power-efficient and reliable on-body and off-body communications. The on-body performance of the DBDM antenna at 2.45 GHz is compared with other five narrowband antennas. Based on the results and analysis of six narrowband and four UWB antennas, antenna specifications and design guidelines are provided that will help in selecting the best body-worn antenna for both narrowband and UWB systems to be applied in body-centric wireless networks (BCWNs). A comparison between

the narrowband and UWB antenna parameters are also provided. At the end of the thesis, the subject-specificity of the on-body radio propagation channel at 2.45 GHz and 3-10 GHz was experimentally investigated by considering eight real human test subjects of different shapes, heights and sizes. The subject-specificity of the on-body radio propagation channels was compared between the narrowband and UWB systems as well.

Acknowledgement

First and foremost, I would like to express my most sincere and deepest gratitude to my supervisors, Prof. Yang Hao, Dr Akram Alomainy and Prof. Clive Parini, for their valuable advice, guidance, beneficial discussions and encouragement throughout my research. Apart from their valuable academic advice and guidelines, they have been extremely kind, friendly, and helpful. I would like to thank Mr. John Dupuy for his help with the antenna fabrication.

Special thanks go to Dr Robert Foster for his valuable and fruitful comments. Many appreciations go to Dr Atiqur Rahman, Dr Masood Ur Rehman, Dr Raffaele Di Bari and George Palikaras for their valuable discussions. Thanks to Sanjoy Mazumdar, Md. Mahbubur Rahman Khan and others for assisting me during measurements. I would like also to thank my colleagues Qammer Hussain Abbasi, Khaleda Ali, Iftekharul, Tuba, Tamer, Xiaodong Yang, Xiaoming Liu, Jiefu Zhang, Oluyemi Peter Falade, Wenxuan Tang and W. Dave Waddoup for having created such a pleasant atmosphere within the research group. I am also grateful to the School of Electronic Engineering and Computer Science, Queen Mary University of London for providing me a good research environment and fund during my PhD.

Above all, I am grateful to my parents (Mohammad Shahabuddin Khan and Siria Begum), my grandparents (Hasmat Ali Fakir and late Ameena Begum), my wife Salma Rahman (Tabassum), my daughter Tasnuva Jaman Khan, my uncles Dr. Atiqur Rahman and Abdus Sobhan, family members (Md Siddiqur Rahman, Shahana Rahman, Md Shahidul Islam Khan, Salina Khanom, Salma Khanom, Liton Khan and Sipon Khan) and friends for their continuous encouragement and support throughout my studies and also for their love.

Mohammad Monirujjaman Khan

London, February 2012

List of Publications

Journal Publications

1. **Mohammad Monirujjaman Khan**, Qammer H. Abbasi, Akram Alomainy, Clive Parini and Yang Hao, ‘‘Experimental Characterisation of Ultra-Wideband Off-Body Radio Channels Considering Antenna Effects,’’ *IET Journal, IET Microwaves Antennas & Propagation*, Special Issue on Body-Centric Wireless Communications. (Accepted for publication).
2. **Mohammad Monirujjaman Khan,** Qammer H. Abbasi, Robert Foster, Akram Alomainy, Clive Parini and Yang Hao, ‘‘Narrowband Antenna Characterisation and Specifications for Body-Centric Wireless Communications,’’ to be submitted in *IEEE Transactions in Antenna and Propagation.*
3. **Mohammad Monirujjaman Khan,** Qammer H. Abbasi, Robert Foster**,** Akram Alomainy, Clive Parini and Yang Hao, ‘‘Ultra Wideband Antenna Characterisation and Specifications for Body-Centric Wireless Communications,’’ to be submitted in *IEEE Transactions in Antenna and Propagation*.
4. **Mohammad Monirujjaman Khan**, Akram Alomainy, and Yang Hao, ‘‘Investigation of Subject-Specific Radio Propagation Channels Characterisation for Body-Centric Wireless Communications,’’ to be submitted in the Special Issue on Wearable Antennas and Systems, *International Journal of Antennas and Propagation,* Hindawi Publishing Corporation.
5. **Mohammad Monirujjaman Khan,** Q. H Abbasi, A. Alomainy, Clive Parini and Yang Hao, ‘‘Comparison of Two Measurement Techniques for Ultra Wideband Off-Body Radio Channel Characterisation,’’ to be submitted in *IEEE Microwave and Optical Technology Letters*.
6. **Mohammad Monirujjaman Khan,** Q. H Abbasi, A. Alomainy, Clive Parini and Yang Hao, ‘‘Wearable Antenna for Power-Efficient On-Body and Off-Body Communications,’’ to be submitted in *Electronics Letters*.
7. **Mohammad Monirujjaman Khan,** Q. H Abbasi, A. Alomainy, Clive Parini and Yang Hao, ‘‘Performance of Ultra Wideband Wireless Tags for On-Body Radio Channel

Characterisation,'' to be submitted in *EURASIP Journal on Wireless Communication and Networking*.

Conference Presentations

1. **Mohammad Monirujjaman Khan**, Qammer H. Abbasi, Akram Alomainy, Clive Parini and Yang Hao, ''Dual-Band and Dual-Mode Antenna for Power-Efficient Body-Centric Wireless Communications,'' the 2011 *IEEE International Symposium on Antennas and Propagation* (APS 2011), July 3-8, 2011, Spokane, Washington, USA.
2. **Mohammad Monirujjaman Khan**, Qammer H. Abbasi, Akram Alomainy and Yang Hao, ''Investigation of Body Shape Variations Effect on the Ultra Wideband On-Body Radio Propagation Channel,'' *International Conference in Electromagnetics in Advanced Applications* (ICEAA) 2011, September 12-17, 2011, Torino, Italy.
3. **Mohammad Monirujjaman Khan**, Qammer H. Abbasi, Akram Alomainy and Yang Hao, ''Radio Propagation Channel Characterisation Using Ultra Wideband Wireless Tags for Body-Centric Wireless Networks in Indoor Environment, '' 2011 *IEEE International Workshop on Antenna Technology,* 7-9 March, Hong Kong, IWAT 2011. (**Nominated for best paper award**).
4. **Mohammad Monirujjaman Khan**, Qammer H. Abbasi, Akram Alomainy and Yang Hao, ''Ultra Wideband Wireless Tags for Off-Body Radio Channel Characterisation with Varying Subject Postures,'' the 14th *European Microwave Week* 2011, 9th-14th October 2011, Manchester Central, Manchester, UK.
5. **Mohammad Monirujjaman Khan**, Qammer H. Abbasi, Akram Alomainy and Yang Hao, ''Study-of-Line-of-Sight (LoS) and Non-Line-of-Sight (NLoS) Ultra Wideband Off-Body Radio Propagation for Body-Centric Wireless Communications in Indoor,'' the 5th *European Conference on Antennas and Propagation*, EuCAP, Rome, Italy, on 11-15 April 2011.
6. **Mohammad Monirujjaman Khan,** Akram Alomainy, Yang Hao, ''Characterisation of Dynamic Radio Propagation Channels in Body-Centric Wireless Networks Using Ultra-Wideband Wireless Tags,'' *Loughborough Antennas & Propagation Conference* 2010 (LAPC2010), 8-9 November 2010, Loughborough, UK.

7. Qammer H. Abbasi, **Mohammad Monirujjaman Khan,** Akram Alomainy and Yang Hao, ‘‘Characterization and Modelling of Ultra Wideband Radio Links For Optimum Performance Of Body Area Network in Health Care Applications’’ 2011 *IEEE International Workshop on Antenna Technology* 7-9 March, Hong Kong, IWAT 2011. (**Nominated for best paper award**).
8. Qammer H. Abbasi, **Mohammad Monirujjaman Khan**, Akram Alomainy and Yang Hao,” Diversity Antenna Techniques for Enhanced Ultra Wideband Body-Centric Communications, the 2011 *IEEE International Symposium on Antennas and Propagation* (APS 2011), July 3-8, 2011, Spokane, Washington, USA.
9. **Mohammad Monirujjaman Khan**, Qammer H. Abbasi, Akram Alomainy and Yang Hao, ‘‘Effect of Various Subject Postures on Ultra Wideband Body Sensor Network Performance,’’ *IET Seminar on Antennas and Propagation for Body-Centric Wireless Communications*, 27 June 2011, the Institute of Physics, London, UK.
10. Qammer H. Abbasi, **Mohammad Monirujjaman Khan**, Akram Alomainy and Yang Hao, ‘‘Sectorial Radio Channel Characterisation for Ultra Wideband Body-Centric Wireless Communications,’’ the 5th *European Conference on Antennas and Propagation*, EuCAP, Rome, Italy, on 11-15 April 2011.
11. **Mohammad Monirujjaman Khan**, Akram Alomainy and Yang Hao, ‘‘Off-Body Radio Channel Characterisation Using Ultra Wideband Wireless Tags,’’ 2010 *International Conference on Body Sensor Networks* (BSN 2010), June 7 - 9, 2010, Biopolis, Singapore.
12. Qammer H. Abbasi, **Mohammad Monirujjaman Khan**, Akram Alomainy and Yang Hao, ‘‘Radio Channel Characterisation and OFDM-based Ultra Wideband System Modelling for Body-Centric Wireless Networks,’’ 2011 *International Conference on Body Sensor Networks* (BSN 2011), May 22, Dallas, USA.
13. Qammer H. Abbasi, **Mohammad Monirujjaman Khan**, Akram Alomainy and Yang Hao, ‘‘Characterisation of Ultra Wideband Body-Centric Radio Channel Dependency on Angular and Spatial Variations,’’ the 14th *European Microwave Week* 2011, 9 th-14th October 2011, Manchester Central, Manchester, UK.
14. Qammer H. Abbasi, **Mohammad Monirujjaman Khan**, Akram Alomainy and Yang Hao, ‘‘Ultra Wideband Low Power System Modelling for Body-Centric Wireless

Networks,'' *IET Seminar on Antennas and Propagation for Body-Centric Wireless Communications,* 27 June 2011, The Institute of Physics, London, UK.

15. **Mohammad Monirujjaman Khan**, Akram Alomainy and Yang Hao, ''Ultra Wideband Off-Body Radio Channel Characterisation and Modelling for Healthcare Applications,'' under review in IEEE 2012 Wireless Telecommunication Symposium, 18-20 April, London, UK.
16. Qammer H. Abbasi, **Mohammad Monirujjaman Khan**, A. Alomainy and Y. Hao, '' Second Order Statistics for UWB On-Body Radio Channels,'' under review in IEEE 2012 Wireless Telecommunication Symposium, 18-20 April, London, UK.

Contents

Abbreviations

BAN	Body Area Network
BCWNs	Body-Centric Wireless Networks
BCWCs	Body-Centric Wireless Communications
CDF	Cumulative Distribution Function
CPW	Co-Planar Waveguide
DBDM	Dual-Band and Dual-Mode
dBm	Decibels relative to 1 mW
EIRP	Equally Isotropic Radiate Power
FCC	Federal Communications Commission
FDTD	Finite Difference Time Domain
FR4	Flame Resistance 4
IEEE	Institute of Electrical & Electronics Engineers
ISM	Industrial, Scientific and Medical
LoS	Line-of-Sight
NLoS	Non-Line-of- Sight
PCS	Personal Communication Services
PICA	Planar Inverted Cone Antenna
SFF	Small Form Factor
RSSI	Received Signal Strength Indicator
Rx	Receiver
SAR	Specific Absorption Rate
TSA	Tapered Slot Antenna
Tx	Transmitter
UWB	Ultra Wide-Band
VNA	Vector Network Analyser
WBAN	Wireless Body Area Network
WPAN	Wireless Personal Area Network
WSN	Wireless Sensor Networks

List of Figures

Lists of Tables

Chapter 1 Introduction

Wireless technology has changed our lives during the past two decades and it has become very popular in recent years. Wireless technology is growing very fast throughout the whole world and larger numbers of people are relying on it, directly or indirectly. Rapid development in wireless technology, in addition with continuous miniaturization of sensors, is leading to a new generation of wearable devices. With the increasing presence of wireless communication in our daily lives, body-centric wireless communications (BCWCs) systems will be a focal point in the development of the fourth generation (4G) mobile communications system [1-3].

Body-centric wireless networks consist of a number of wireless sensors placed on the human body or in close proximity to it. These sensors are required to communicate with other on-body units, with external base stations, or with wireless implants [see Fig. 1.1].

The applications of BCWC vary from low-power low-data-rate communications in healthcare services, to high-data-rate networks used for personal entertainment. The concept of BCWC includes wireless body area networks (WBANs), wireless personal area networks (WPANs) and body sensor networks (BSNs). A WPAN usually refers as the communication between the wearable device and off-body base units, while WBAN consists of several wireless sensor nodes scattered on the human body, communicating with an on-body base unit. The BSN is extended from the wireless sensor network (WSN), and mainly concerned with human physiological data acquisition and communication through a combination of bio-medical and wireless sensors. A very important subject related to BCWC is convergence, in which several functions, capabilities and technologies are merged into a single terminal that will embrace both local and global connectivity.

With the increasing average age of populations in the whole world and the associated rise of healthcare costs, the development of systems for freeing hospital resources is of particular interest in academic and industrial environments. A continuous and remote diagnosis of a patient has been proposed [4-5] by using a “smart” network, where data sets collected from various sensors are analysed in order to allow controlled administration of medicine, as well as the generation of emergency calls. The same concepts discovered an important application in athlete

monitoring. By 2012, it is predicted that on-body wireless sensors could save $25 billion worldwide in annual healthcare costs by providing the capability for remotely monitoring vital signs, such as heart rate, heart electrical activity (ECG), blood glucose monitoring, and blood oxygen, for recovering patients and the elderly [6].

The major drawback of current body-worn systems is the use of wired communication, which is often undesirable because of the inconvenience to the user. Other connection methods have been proposed for alleviating this problem, including the use of smart textiles. Smart clothes imply the need for a special garment to be worn, which may conflict with the user's personal preferences [8]. Body-centric wireless network (BCWN) presents an apparent option and is aiming to provide low power systems with constant availability, re-configurability and unobtrusiveness. However, such networks face many challenges that need to be accounted for before they can be fully deployed for real life applications. Body-worn antennas, on-body wireless communication channels and systems are essential components in the body-centric wireless networks which are the main motivations of the investigations and analyses presented in the thesis.

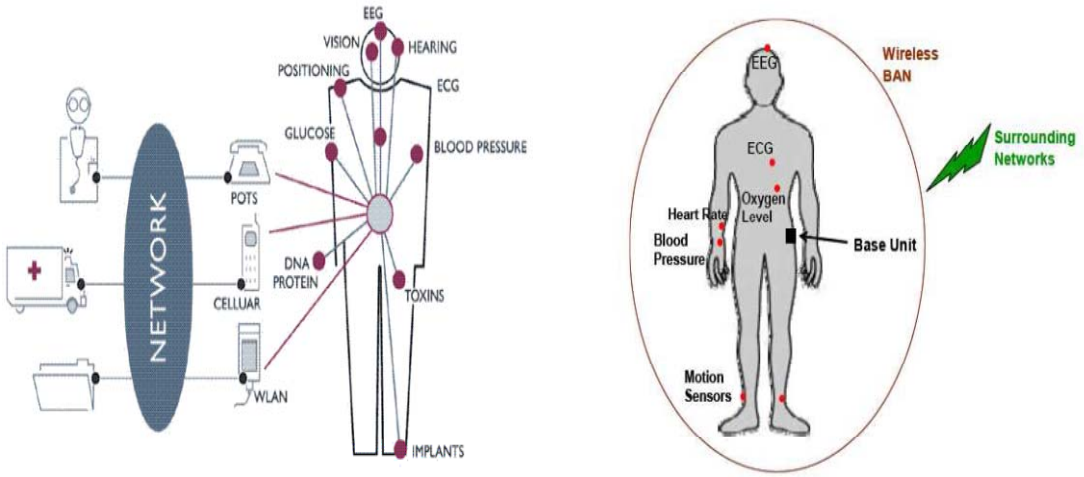

(a) (b)

Fig. 1.1. (a) An example of BCWNs for health monitoring. (Many sensors on the body to collect information and send them to a base station, which is able to communicate with off-body devices to inform about the condition of the user); (b) Wireless BAN in Healthcare Applications [1, 7].

Body-centric wireless networks should provide cost-effective solutions and guarantee the mobility and freedom desired by the users. Therefore the various components of the radio system

should provide light weight and low power consumption to avoid short battery life and unwanted obtrusiveness to the user. One of the major issues in designing such a wireless system is to understand the effect of the human body on the antenna parameters and on the radio propagation channels. The design of body-worn and hand-held devices has many other aspects to take into account, including the safety for the user, the dimensions, and the cost [1].

1.1 Research Motivations

Antennas are the essential component for wearable devices in body-centric wireless networks and they play a vital role in optimizing the radio system performance. When the antenna is placed in or close to a human body (lossy medium), the performances change to that of free space operation. For body-centric antennas, the presence of the human body in the proximity of the radiating structure reduces the radiation efficiency and gain. This is due to electromagnetic absorption in body tissues, which results in frequency detuning, radiation pattern distortion and variation of antenna impedance. The significance and nature of these effects are system-specific, and depend on the propagation environment, the physical constraints on the antenna itself and the antenna type. They are also frequency-dependant; e.g., a radio wave may penetrate more into the human body at low frequencies, whilst dissipate more at high frequencies.

The major difference between BCWC and conventional wireless systems is the radio channel over which the communication takes place. The human body tissue is a lossy medium; hence, the wave propagating within the WBAN faces large attenuation before reaching the specified receiver. Since the human body is hostile in regards to attenuating and distorting the transmitted signal, the design of a reliable and power-efficient wireless system requires accurate analysis and understanding of the radio propagation. Furthermore, the characteristics of body-centric radio channels are subject-specific and depend on many factors, such as the frequency of operation and the antenna radiation. All these issues, if not accurately examined, can lead to increased transmission errors or, in extreme cases, loss of a marginal communication link. Therefore, it is very important to understand the human body effects on the antenna performance parameters and on the radio propagation channels in order to design an ideal wireless system for BCWNs.

Recently, there has been increasing interest in research and development for designing wearable narrowband (2.45 GHz) and UWB (3.1-10.6 GHz) antennas; however, at this point there have been no significant breakthroughs in the design of wearable antennas. Previously

people have studied the human body effects on the antenna performance parameters and on-body radio propagation channels at both narrowband and UWB frequencies. However, the previous studies are limited, because of considering limited number of antennas for both narrowband and UWB cases. In addition, all the performance parameters in close proximity to the body for the narrowband and UWB antennas have not been investigated and analysed thoroughly.

A complete parametrical studies and statistical analysis addressing the human body effects on the performance parameters for various types of narrowband and UWB antennas will help in selecting the best antenna for body-centric wireless communications and enable the development of guidelines useful for the system designers. In addition, there is need of a complete list of antenna specifications and design guidelines for both narrowband UWB body-centric wireless communication systems. As human body tissues behave different for UWB and narrowband antenna performance parameters; hence, a comparison is required for better understanding of the antenna parameters for narrowband and UWB systems. To the best knowledge of the author, the above mentioned work has not been done before.

For power-efficient and reliable body-centric wireless communications there is a need of designing the suitable body-worn antenna. In BCWCs, communications among on-body devices are required, as well as communications with external base stations. Body-centric wireless devices need to be low power consuming in order to extend the battery life of the body-worn devices, and also need to provide power-efficient (minimise link loss) and reliable on-body and off-body communications. Optimisation of antenna radiation pattern at different frequency bands is needed. In this regards, there is a need for an antenna that works at different frequency bands, having diverse radiation modes. However, to the author's knowledge, nothing has been performed so far in designing the antenna for power-efficient cooperative on-body and off-body communications with different radiation modes at different frequencies.

Researchers have been thoroughly investigating narrow band and ultra wideband on-body radio propagation channels. However, the sizes and shapes of the different human bodies will affect the propagation path and lead to different system performances. From the subject-specific on-body radio propagation prospective very limited work is presented in literature that is mostly based on the finite difference time domain technique (FDTD). There was not a sufficiently thorough analysis and the number of digital human phantom test subjects was limited in this study. However, a thorough investigation and analysis of subject-specific on-body radio

propagation channels for a wider number of people with different shapes, sizes and heights both in narrowband and UWB systems are required. A comparison of the on-body radio channels' subject specificity for narrowband and UWB is required in order to be able to specify which technology is more subject-specific.

1.2 Research Objectives

The aim of the research work presented in this thesis is to investigate, characterise, analyse and specify the antenna and the radio propagation channels for body-centric wireless networks. This was done through a combination of numerical simulations and measurement campaigns. The main objectives of the study include:

1. Characterisation and specifications of narrowband antennas for body-centric wireless communications.
2. Design a novel dual-band and dual-mode (diverse radiation pattern) antenna for power-efficient and reliable cooperative on-body and off-body communications.
3. Characterisation and specifications of ultra wideband (3.1-10.6 GHz) antennas for Body Area Networks (BANs).
4. Provide antenna design guidelines for narrowband and ultra wideband body-centric wireless communications.
5. Investigation of subject-specific narrowband (2.45 GHz) and ultra wideband (3.1-10.6 GHz) on-body radio propagation channels for body-centric wireless communications.

1.3 Organisation of the Thesis

Following this introductory chapter, the rest of the thesis is organised as follows:

Chapter 2 introduces the allocation of the frequency spectrum for body-centric wireless communication. An overview of the main technologies available for body-centric wireless communications, such as Bluetooth and UWB is also given. In addition, the features and application of WBANs are described in this section.

Chapter 3 gives an introduction to antenna and radio propagation for body-centric wireless communications. Fundamental antenna parameters are also discussed in this section. Moreover, this chapter illustrates and describes the electrical properties of human body tissues. It also discusses the parameters ruling the radio propagation in multipath channels. Towards the end of

this chapter, an extensive literature review on the state-of-the-art in the development of body-worn antennas and radio propagation channels is provided.

Chapter 4 investigates and compares the on-body performance parameters (frequency detuning, impedance, bandwidth, gain, radiation efficiency, radiation pattern and polarisation) of five different narrowband (2.45 GHz) antennas, including the Wire Monopole, Patch, Printed Monopole, Inverted L and Loop. It also investigates the impact of the five different antenna types on the on-body radio channel characteristics at 2.45 GHz. In addition, this chapter presents a novel dual-band and diverse radiation mode antenna for power-efficient body-centric wireless communications. The free-space and on-body simulated and measured performance parameters of the proposed DBDM antenna are shown and analyzed. In this chapter, the performance parameters at 2.45 GHz of the DBDM antenna are compared with the other five narrowband antennas. Statistical analysis is performed in order to evaluate the on-body antenna parameters. Some parameters that control the on-body performances of the narrowband antennas are also discussed here. Furthermore, at the end of this chapter, narrowband antenna specifications and design guidelines for BCWCs are provided.

Chapter 5 investigates and compares the on-body performance parameters (frequency shifting, impedance matching, bandwidth, gain, radiation efficiency, radiation pattern, pulse fidelity and polarisation) of 4 different ultra wideband (3.1-10.6 GHz) antennas, including the Tapered Slot Antenna (TSA), Planar Inverted Cone (PICA), SWAN-Shaped and Quasi-Self-Complementary Compact antenna. It also investigates the impact of the four different antenna types on the on-body radio channel characteristics at 3-10 GHz. Statistical analysis is performed in order to evaluate the on-body antenna parameters. Some parameters that control the on-body performances of the UWB antennas are also discussed here. UWB antenna specifications and design guidelines for BCWCs are provided. Furthermore, it compares the narrowband and UWB antenna parameters on the body and finally draws some conclusions.

Chapter 6 presents investigation of the subject-specific narrowband and UWB on-body radio propagation channels for body-centric wireless communications. At the end, a comparison of on-body radio channel subject-specificity between narrowband and UWB systems is provided.

Chapter 7 provides a summary of the main contributions and findings of the study and concludes the accomplished work packages. It also introduces suggestions for future research activities.

References

[1] **P. S. Hall and Y. Hao**, *Antennas and Propagation for Body-Centric Wireless Communications*. Artech House, 2006.

[2] The European IST-507102, "My personal adaptive global net (magnet)."

[3] **S. Drude**, "Requirements and Application Scenarios for Body Area Networks," in *Mobile and Wireless Communications Summit, 16th IST*, 2007.

[4] **C. Otto, A. Milenkovic, C. Sanders, and E. Jovanov**, "System architecture of a wireless body area sensor network for ubiquitous health monitoring," *Journal of Mobile Multimedia*, vol. 1, no. 4, pp. 307–326, 2006.

[5] **J. Penders, B. Gyselinckx, R. Vullers, M. De Nil, S. Nimmala, J. Van de Molengraft, F. Yazicioglu, T. Torfs, V. Leonov, P. Merken,** *et al.*, "Human++: from technology to emerging health monitoring concepts," in *Int.Workshop onWearable and Implantable Body Sensor Networks (BSN 2008)*, 2008, p. 948.

[6] WSN for Healthcare: A Market Dynamics Report Published August 2008.

[7] **Y. Hao,** "Numerical and System Modelling Issues in Body-Centric Wireless Communications,'' *The Institution of Engineering and Technology Seminar on Antennas and Propagation for Body-Centric Wireless Communications*, Tuesday, 24 April 2007: The Institute of Physics, London, UK.

[8] "Internet resources, smart textiles offer wearable solutions using nanotechnology," *URL:* http://www.fibre2fashion.com/news/.

Chapter 2 Wireless Communication Standards for Body-Centric Wireless Networks

The IEEE 802.15 task group is responsible for the development of a standard for WPAN and WBAN. This chapter discusses the frequency allocation for body-centric wireless communications, and introduces the main technologies considered by the standard, namely Bluetooth and UWB. Towards the end of this chapter, on-body, off-body and in-body communications are defined in brief.

2.1 Frequency Allocation for Body and Personal Area Networks

Wireless communications systems can operate in unlicensed portions of the spectrum. However the allocation of unlicensed frequencies is not the same in every country. Table 2.1 lists the frequency bands allocated for Wireless Body Area Networks (WBANs) and Wireless Personal Area Networks (WPANs).

- **Medical Implanted Communication Service (MICS):** In 1998, the International Telecommunication Union's Radio sector (ITU-R) allocated the bandwidth 402-405 MHz for medical Implants [1]. MICS devices can use up to 300 kHz of bandwidth at a time to accommodate future higher data rate communications.
- **Industrial Scientific and Medical (ISM):** These frequency bands were originally pre-served internationally for non-commercial use of the radio frequency spectrum. However, many are now used by commercial standards because government approval is not required. These frequency bands are allocated by the ITU-R [2] and every country uses them differently, due to different regional regulations.
- **Wireless Medical Telemetry Services (WMTS):** The Federal Communication Commission (FCC) has allocated these frequency bands in the USA [3] for the purpose of

remote monitoring for patient's health; however, such frequency bands are not available in Europe.

- **Ultra Wide-Band (UWB):** It is a communication system whose spectral occupation is greater than 20%, or higher than 500 MHz. In UWB communications, extremely short pulses are transmitted and higher data rates can be achieved. The FCC authorised the unlicensed use of UWB in the range of 3.1 to 10.6 GHz. Initially, it was available only in the US and Singapore but, on August 13, 2007, Ofcom finally approved the use of ultra wideband technology without a license for use in the UK.

Table 2.1. Unlicensed frequencies available for WBANs and WPANs.

Name	Band [MHz]	Max Tx Power [dBm EIRP]	Comments
MICS	402.0-405.0	-16	Worldwide
ISM	433.1-434.8	+7.85	Europe
ISM	868.0-868.6	+11.85	Europe
ISM	902.8-928.0	+36 w/spreading	Not in Europe
ISM	2400.0-2483.5	+36 w/spreading	Worldwide
ISM	5725.0-0.5875.0	+36 w/spreading	Worldwide
WMTS	608.0-614.0	+10.8	US only
WMTS	1395.0-1400.0	+22.2	US only
WMTS	1427.0-1432.0	+22.2	US only
UWB	100.0-960.0	See Fig. 2.1	US only
UWB	3100.0-10600.0	See Fig. 2.1	US, UK and Singapore

2.2 Wireless Personal Araea Networks (PANs)

A wireless personal area network (WPAN) is a network for interconnecting devices centred around an individual person's workspace in which the connections are wireless. In general, a personal area network uses some technologies that permit communication within about 10 meters (in other words, a very short range). These systems shall be cheap to produce and they are optimized to operate with low power consumption. Such technologies include Bluetooth (which was used as the basis for a new standard), IEEE 802.15 and Ultra Wideband (UWB), which has been recently introduced and is receiving increasing attention for consumer wireless technologies [4].

A wireless personal area network (WPAN) typically interconnects ordinary computing and communicating devices available in the user's surroundings, or it could have a more specialized

purpose, such as authorized and secured communications for military services. WPANs are deployed to facilitate seamless operation among home or business devices and systems. In another usage, a WPAN is a technology that could enable wearable computing devices to communicate with other nearby computers and exchange digital information, using the electrical conductivity of the human body as a data network.

For short, medium and long-range communications, Bluetooth, Zigbee, UWB, Wireless LAN (Wi-Fi), WiMAX, GSM, PCS, GPRS, UMTS and satellite communication are available, allowing a wide coverage area and offering the possibility of ubiquitous worldwide wireless mobility [5].

Short-range devices and networks operate mainly in standalone configurations in home and office environments or large enclosed public areas, while their integration into the wireless wide-area infrastructure is still nearly non-existent. When designing future-short range wireless systems, the increasing pervasive nature of communications and computing must be accounted for. Developers and researchers alike assume that the new wireless systems will be the result of a comprehensive integration of existing and future wireless systems. The Bluetooth and UWB standards are introduced here, due to their popularity within the wireless technology community, with UWB regarded as the most promising technology for high data-rate and low-power systems.

2.2.1 Bluetooth Overview

Bluetooth is an always-on, low power, short range radio system for point to point and point–to-multipoint voice and data transfer. The concept behind Bluetooth is to provide a universal short-range wireless capability, using the 2.4 GHz band, available globally for unlicensed low power uses. Two Bluetooth devices within 10 m of each other can share up to 720 kbps of capacity. Bluetooth is intended to support an open-ended list of applications, including data, audio, graphics, and even video [6]. Bluetooth devices are divided into three classes, which specify the radiated output power [5]:

- Class 1 devices broadcast using up to 100 mW of power, with a maximum range of approximately 100 m;
- Class 2 devices broadcast using up to 2.5 mW of power, with a maximum range of approximately 10 m;

- Class 3 devices broadcast using up to 1 mW of power, and a maximum range of approximately 1 m.

Bluetooth is an open specification for wireless communication of data and voice and is based on a low-cost short-range radio link facilitating protected ad-hoc connections for stationary and mobile communication environments. Bluetooth technology allows for the replacement of many proprietary cables, connecting one device to another, with one universal short-range radio link. It also provides a universal bridge to existing data networks, a peripheral interface and a mechanism to form small private ad hoc grouping of connected devices away from fixed network infrastructures [7].

The Bluetooth system consists of a radio unit, a link control unit, and a support unit for link management and host terminal interface functions. The Host Controller Interface (HCI) provides the means for a host device to access Bluetooth hardware capabilities. Bluetooth provides support for three general application areas using short-range wireless connectivity [7].

- Data and voice access points: Bluetooth facilitates real-time voice and data transmissions by providing effortless wireless connection of portable and stationary communication devices.
- Cable replacement: the technology eliminates the need for numerous, often proprietary cable attachments, for the connection of practically any kind of communication device. Connections are instant and are maintained even when devices are not within line of sight.
- Ad hoc networking: A device equipped with a Bluetooth radio can establish instant connection to another Bluetooth radio as soon as it comes into range.

Another interesting technology for PANs is Zigbee.

2.2.2 Ultra Wideband Technology

Ultra wide band (UWB) technology is an innovative wireless technology which can transmit digital data over a wide frequency spectrum with very low power and a very high data rate. This technology can carry signals through many obstacles that usually reflect signals at more limited bandwidths and higher power [8]. Ultra wideband (UWB) is to become a fundamental

technology for the home entertainment, security, tracking and high data rate transmission markets via wireless personal area networks (WPAN).

The Federal Communication Commission (FCC) issued, in April 2002, UWB regulations, under Part 15 of the Commission's rules, permitting Ultra-wideband international emissions subject to certain frequencies and power limitations that will mitigate interference risk to those sharing the same spectrum [9]. Fig. 2.1 shows the allowed emission spectrum under Part 15 of the FCC's rules. UWB signals may be transmitted between 3.1 GHz and 10.6 GHz at power levels up to -41 dBm/MHz, with higher degree of attenuation required for the out of band region for outdoor communication. It can be thought of an extreme case of spread spectrum technology which offers flexibility, robustness, high-precision, location determination, performance and ranging ability with accuracy in the sub-centimetre range. Lately, most UWB related research and development have been dedicated to short-range wireless systems for personal and body area networks.

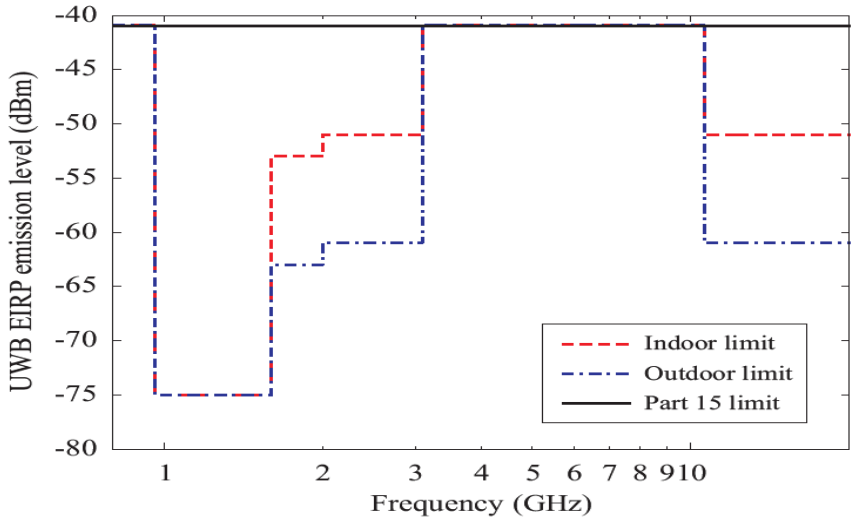

Fig. 2.1. FCC Spectrum Mask for Transmissions by UWB Communication Devices (Reproduced from [9]).

The bandwidth of the UWB systems, as defined by the FCC in [9], is more than 20% of a centre frequency or more than 0.5 GHz. Clearly, this bandwidth is much greater than the bandwidth used by any current communication technology. Ultra-wideband communication systems modulate short duration (nanosecond) pulses to transmit and receive information. The

pulses used in such systems have bandwidths in GHz range and a fractional bandwidth larger than 20% [10]. Fractional bandwidth is defined as

$$B_f = \frac{2(f_h - f_l)}{f_h + f_l}.100\% \tag{2.1}$$

where f_h and f_l are the highest and lowest cut-off frequencies (-10 dB point) of a UWB pulse spectrum, respectively.

The large bandwidth of UWB signals provides robustness to jamming and have low probability of detection properties. UWB devices work below the noise floor so jamming becomes extremely difficult. It is difficult to distinguish the original signal from the noise for the UWB technology. UWB devices usually require low transmit powers, due to the control over the duty cycle, thus supporting a longer battery life for hand-held devices.

Typical UWB pulse waveforms usually used in the literature include rectangular, Gaussian and Gaussian monocycle [11-12]. The rectangular pulse is a simple pulse; however, it has a large DC component, which makes it less appealing for modelling and analysis aspects. One of the most used pulse shapes is a Gaussian pulse, which can be expressed by

$$p(t) = \frac{1}{\sqrt{2\pi\tau}} e^{-\frac{1}{2}(\frac{t-t_0}{\tau})^2} \tag{2.2}$$

where τ determines the width of the pulse and t_0 sets the centre of the pulse. Commonly, derivatives of the Gaussian pulse in eq. 2.2 are applied to describe transmitted and received UWB pulses for characterization and modelling purposes. The first derivative of the Gaussian pulse (known as the Gaussian Monocycle) is given by

$$p_m(t) = A(\frac{t-t_0}{\tau^2}) e^{-\frac{1}{2}(\frac{t-t_0}{\tau})^2} \tag{2.3}$$

where τ determines the monocycle pulse width and A is the pulse amplitude. A useful representation of the pulse is the equivalent frequency spectrum, which is defined as,

$$p_m(f) = A\sqrt{2\pi(2\pi f\tau)} e^{-\frac{1}{2}(2\pi f\tau)^2} . e^{-j(2\pi f t_0 + 0.5\pi)} \tag{2.4}$$

The second derivative of the Gaussian pulse (derivative of Monocycle) is also a popular pulse waveform used in the literature and is given by

$$p_{\delta m}(t) = A[1-(\frac{t-t_0}{\tau^2})^2]e^{-\frac{1}{2}(\frac{t-t_0}{\tau})^2} \qquad (2.5)$$

Fig. 2.2 presents the pulses described above for $\tau = 0.5$ *ns* and $t_0 = 0$ *ns* and the amplitude normalised to 1. The Gaussian monocycle and its derivative do not have a DC component, which makes the radiation more efficient in comparison to rectangular pulses.

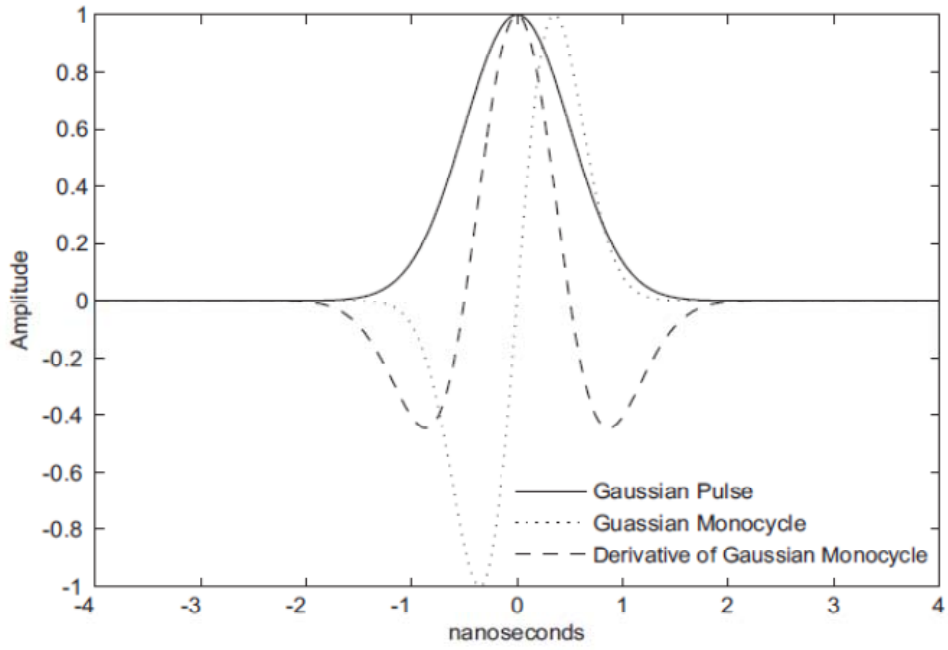

Fig. 2.2. Normalised waveforms of a Gaussian pulse, Monocycle and Monocycle derivative for $\tau = 0.5$ *ns*.

The UWB emission limit is set to the lowest level ever applied to any system, which means that the total power emission of UWB system is in the milliwatt range spread over several gigahertz of bandwidth. However, it is not merely the high data-rate and short range features that make UWB a suitable candidate for body-centric wireless networks: the regulatory limits on power emissions are actually complementary to the requirements for low-power consumption for most body-centric wireless network applications.

2.3 Wireless Body-Area Network Features

WBANs consist of a number of units placed in proximity of the human body (such as in everyday clothing), and are a natural progression of the WPAN concept [13]. Also known as IEEE 802.15.6, WBANs are a low-frequency technology intended to endow a future generation of short-range electronics for exchanging information. The advances in communication and electronic technologies have enabled the development of compact and intelligent devices that have facilitated the introduction of such a network. WBANs may communicate externally with other networks (which may themselves be WBANs), using one of a range of available wireless technologies.

BAN stands for wireless communication between various devices attached to the body such as data spectacles, earphones, microphones and sensors, by its wireless connections between the individual components. A good real-world example of this technology in practice is a pacemaker that can alert, or be controlled by, a wristwatch by using wireless transmission. The military is also considering the use of WBANs to reduce the probability of interference and eavesdropping in battle-field communications.

Body-centric wireless networks are aiming to provide systems with constant availability, re-configurability and unobtrusiveness. High processing and complex body area networks are needed in the future to provide the powerful computational functionalities required for advanced applications. These requirements have led to increasing research and development activities in the area of WBAN applications for many purposes [14-15], with the main interests being healthcare, patient monitoring, sports performances monitoring, and wearable computers.

The idea of WBAN was initiated for medical purposes so that continuous records of patients' health could be kept at all times. Sensors are placed around the human body to measure specified parameters and signals in the body (e.g., blood pressure, ECG, sugar level, temperature, etc.). As an extension to these sensors, base units can be deployed on or close to the human body to collect information or relay command signals to the various sensors in order to perform a desired operation. Body area networks can be applied to many fields; some of its applications include

- Wearable audio-the central device is the headset, applying stereo audio and microphone, with connected devices including (but not limited to): cellular phone, MP3 player, PDA, CD audio player [16];

- Assistance to emergency services, such as police, paramedics and fire fighters;
- Military applications, including soldier location tracking, image and video transmission and instant decentralised communications;
- Augmented reality to support production and maintenance;
- Access/identification systems by identification of individual peripheral devices;
- Navigation support in the car, or while walking, with reliable and efficient communication with existing technologies, such as GPS;
- Bio-Sensors for athletes' performance monitoring and enhancement to improve outcomes in major events.

Body-centric wireless networks would naturally inherit and adhere to attributes defined for wireless personal and body area networks (WPAN/WBAN) by the IEEE 802.15 standardisation group depending on the applications it is intended for (e.g., on-body, off-body or in-body communications). Fig. 2.3 shows example of on-body and off-body communications.

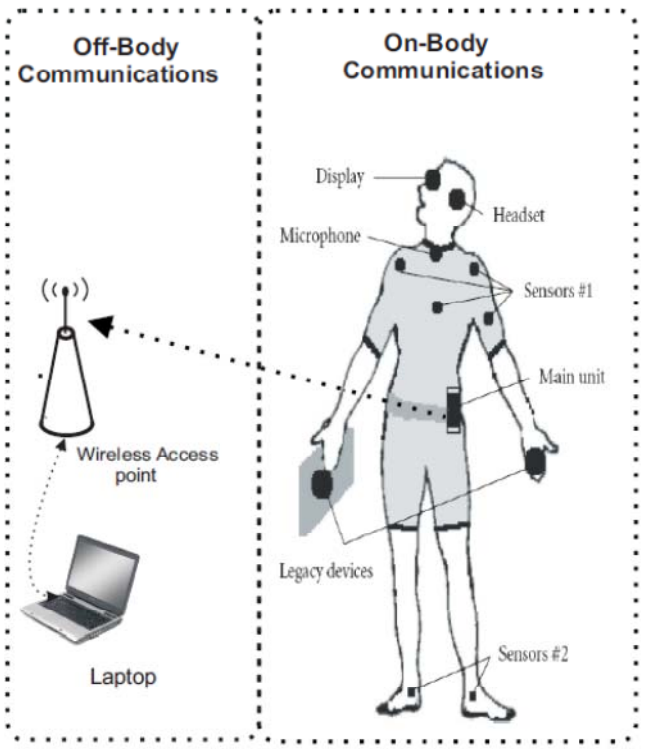

Fig. 2.3. Envisioned BCWN and its possible components showing on-body and off-body communications [reproduced from 17].

- **On-body communications**: describe the link between body mounted devices communicating wirelessly.
- **Off-body communications:** defines the radio links between body-worn devices and base units or mobile devices located in the surrounding environments.
- **In-body communications:** is concerned with relaying and exchanging information between wireless implants and on-body nodes.

2.4 Summary

The frequency allocations for body-centric wireless communications were talked about in this chapter. An overview of the communication standards developed by the IEEE 802.15 task groups for WPAN and WBAN were presented. In addition, features of WPAN and WBAN were introduced. The main features of Bluetooth and ultra wide-band were briefly introduced, and it was highlighted that the UWB technology promises to be a suitable candidate for body-centric wireless communications. At the end of this chapter, basic definitions about the on-body, off-body and in-body communications were provided very briefly.

References

[1] "Federal communications commission (FCC), code of federal regulations (CFR), title 47 part 95, MICS band plan,'' *URL:*www.*fcc.gov,* March'03.

[2] "International telecommunications union-radio communications (ITU-R), radio regulations, section 5.138 and 5.150,'' URL: *www.itu.int/home.*

[3] "Federal communications commission (FCC), code of federal regulations (CFR), title 47 part 95, WMTS band plan,'' *URL:www.fcc.gov,* January'03.

[4] IEEE 802.15, "an international standards working group, IEEE 802.15," *URL:http://grouper.ieee.org/groups/802/15/.*

[5] **R. Foster and Y. Hao,** "Wireless body sensor networks for health-monitoring applications," *Physiological Measurement*, vol. 29, no. 11, pp. 27–56, 2008.

[6] "Bluetooth specifications, vol.2, 2003,'' URL: *http: //www.bluetooth.org,2003*

[7] B. T. Overview, Nokia Forum, vol., Version 1.0, 2003.

[8] **D. Porcino and W. Hirt**, "Ultra-wideband radio technology: potential challenges ahead,'' *IEEE Communications Magazine*, vol. 41, no.7, pp. 66-74, July 2003.

[9] FCC First Report and Order, Revision of the Part 15 Commission's Rules Regarding Ultra-Wideband Transmission Systems, pp. 98-153, April 22, 2003.

[10] **F. Dowla and F. Nekoogar**, "Multiple access in ultra-wideband communications using multiple pulses and the use of least squares filters," *Radio and Wireless Conference, RAWCON*, pp. 211–214, 2003.

[11] **L. Zhao and A. M. Haimovich**, "Performance of ultra-wideband communications in the presence of interference," *IEEE Journal on Selected Areas in Communications*, vol. 20, no. 9, pp. 1684–1691, 2002.

[12] **R. A. Scholtz**, "Multiple access with time-hopping impulse modulation," *Proceedings of IEEE MILCOM* 1993, pp . 447–450, 1993.

[13] "IEEE 802.15, an international standards working group, IEEE 802.15," *URL: http:// grouper.ieee.org/groups/802/15/*.

[14] **E. Jovanov, A. ODonnell-Lords, D. Raskovic, P. Cox, R. Adhami, and F. Andrasik**, "Stress monitoring using a distributed wireless intelligent sensor system," *IEEE Engineering in Medicine and Biology Magazine*, vol. 22, no. 3, pp. 49–55, 2003.

[15] **C. Kunze, U. Grossmann, W. Stork, and K. Muller-Glaser**, "Application of ubiquitous computing in personal health monitoring systems," *Biomedizinische Technik: 36th Annual meeting of the German Society for Biomedical Engineering*, pp. 360–362, 2002.

[16] **S. Drude**, "Tutorial on body area networks -document: IEEE 802.15-06-0331," *IEEE P802.15 Working Group for Wireless Personal Area Networks (WPANs)*, 18 July 2006.

[17] **M. G. Benedetto, T. Kaiser, A. Molisch, I. Oppermann, and D. Porcino,** *UWB communication systems: a comprehensive overview*. Hindawi Publishing Corporation, 2006.

Chapter 3 Basics of Antennas and Propagation for Body-Centric Wireless Networks

This chapter provides an introduction to the fundamentals of antennas and radio propagation for Body-Centric Wireless Communications. Basic antenna performance parameters are discussed. In addition, this chapter illustrates and describes the electric properties of human body tissues. An extensive literature review on the state-of-the-art in the development of body-worn antennas and a review of recent developments in channel characterisation and modelling are provided. The parameters ruling the radio propagation in multipath channels are also discussed.

3.1 Fundamentals of Wearable Antennas

The antennas are an essential part of any wireless system. An antenna is defined as a means for radiating or receiving radio waves. Conventional antenna parameters include impedance bandwidth, return loss, gain, impedance, directivity, radiation pattern, polarisation and efficiency which are usually applied to fully characterise an antenna and determined whether an antenna is suitable for specific applications. These parameters are usually presented considering the classical situation of the antenna placed in free space; however, when the antenna is placed in or close to a lossy medium the performance changes to that of free space operation and the parameters defining the antenna needs to be revisited and redefined. In this thesis, the commonly-used antenna parameters (such as return loss, impedance bandwidth, radiation pattern, radiation efficiency, directivity, gain, input impedance and polarisation) in close proximity to the human body for various narrowband and UWB body-worn antennas are studied. A well-designed antenna can relax system requirements and improve overall system performance. The characteristics and behaviour of the antenna need to adhere to certain specifications set by the wireless standard and system technology requirements. A list of useful guidelines helps to select the proper antenna for specific applications. The common antenna specifications are the size of the antenna, shape, weight, operating frequency, bandwidth, gain, radiation pattern, polarisation, antenna feed impedance, radiation efficiency, type of connector, VSWR (return loss), power rating of antenna, antenna placement location and so on. The antenna

specification is set for specific application. Based on specific applications and system technology requirement, the antenna specifications are usually set. However, for body-centric wireless communications antenna specifications are very essential which are provided in the next two chapters. To describe the performance of an antenna, definitions of various parameters are necessary.

❖ Return Loss

Return loss is a measure of the difference between the power input to and the power reflected from a discontinuity in a transmission circuit. It is often expressed as the ratio in decibels of the power incident on the antenna terminal to the power reflected from the terminal at a particular frequency or band of frequencies.

The return loss is defined as

$$RL(dB) = 10\log_{10}(\frac{P_{in}}{P_{ref}}) \qquad (3.1)$$

where RL (dB) is the return loss in dB, P_{in} is the incident power on the antenna and P_{ref} is the reflected power to the source [1, 2].

❖ Impedance

Antenna impedance is the ratio of the voltage to the current at the input to the antenna. If the antenna input impedance isn't well matched to the source impedance, not very much power will be delivered to the antenna. A good impedance match is indicated by a return loss less than -10 dB. The degree of mismatch can be measured using reflection coefficient Γ which is the ratio of the amplitude of the reflected wave V_r to the amplitude of the incident wave V_i [1, 3].

$$\Gamma = \frac{V_r}{V_i} \qquad (3.2)$$

❖ Bandwidth

The bandwidth of an antenna can be considered to be the range of frequencies, on either side of the centre frequency, where the antenna characteristics are within an acceptable value of those at the centre frequency. Usually, in wireless communications, the antenna is required to provide a

return loss less than -10 dB over its frequency bandwidth. The bandwidth specifications are set in each case to meet the needs of particular application.

The bandwidth of an antenna can be expressed as either an absolute bandwidth (*ABW*), or a fractional bandwidth (*FBW*). If F_H and F_L denote the upper edge and the lower edge (at -10 dB impedance) of the antenna bandwidth, respectively, then the *ABW* is defined as the difference between the two edges (equation 3.3) and the *FBW* is designated as the percentage of the frequency difference over the centre frequency, as described in the chapter two [4, 5].

$$ABW = F_H - F_L \tag{3.3}$$

For narrowband antennas, the bandwidth is expressed as a percentage of the frequency difference (upper minus lower) over the centre frequency of the bandwidth, which is given as

$$BW = \frac{F_H - F_L}{F_C} \times 100\% \tag{3.4}$$

❖ Radiation Pattern

The radiation pattern is a graphical representation of the radiation properties of the antenna as a function of space coordinates. In most cases, it is determined in the far-field region and is represented as a function of the directional coordinates.

For a linearly polarised antenna, its performance is often described in terms of its principle *E*-plane and *H*-plane patterns.

- The *E*-plane is defined as the plane containing the electric field vector and the direction of maximum radiation.
- The *H*-plane is defined as the plane containing the magnetic field vector and the direction of maximum radiation [4]

There are three common radiation patterns that are used to describe an antenna's radiation property:

- **Isotropic**- A hypothetical lossless antenna having equal radiation in all directions.
- **Directional**- An antenna having the property of radiating or receiving electromagnetic waves more effectively in some directions than in others.
- **Omni-directional**- An antenna having an essentially non-directional pattern in a given plane and a directional pattern in any orthogonal plane.

Directional or omni-directional radiation properties are needed depending on the practical application. Omni-directional patterns are normally desirable in mobile and hand-held systems.

❖ Directivity, Gain and Efficiency

Directivity D is defined as the ratio of the radiation intensity U in a given direction from the antenna to the radiation intensity over that of an isotropic source [4-6]. For an isotropic source, the radiation intensity U_0 is equal to the total radiated power P_{rad} by the antenna divided by 4π; therefore, the directivity can be calculated by,

$$D = \frac{U}{U_0} = \frac{4\pi U}{P_{rad}} \tag{3.5}$$

The **gain** of an antenna is defined as 4π times the ratio of the radiation intensity $U(\theta,\phi)$ in a given direction to the total power P_{in} (input power) received by the antenna. This can be stated as,

$$G(\theta,\phi) = \frac{4\pi U(\theta,\phi)}{P_{in}} = \frac{Radiation \quad \text{int}ensity \quad in \quad the \quad direction \quad (\theta,\phi)}{Total \quad received \quad power} \tag{3.6}$$

Directivity and gain are closely related; the difference between them is the power value they use. Therefore, the gain of an antenna also can be defined as the product of the directivity and the radiation efficiency, which can be written as [4-5]

$$G = e_{rad} D \tag{3.7}$$

The **radiation efficiency** is the ratio of the total radiated power to the net power accepted by the antenna [4-5]. It can be written in the following form,

$$Radiation \quad efficicncy \quad (e_{rad}) = \frac{P_{rad}}{P_{in}} = \frac{P}{P_{in} + P_L} \tag{3.8}$$

where P_{rad} is the power radiated, P_{in} is the power supplied to the antenna and P_L is the power loss in the antenna.

❖ Polarisation

The polarization of an antenna is the polarization of the wave radiated in a given direction by the antenna when transmitting. When the direction is not stated, the polarization is taken to be the polarization in the direction of maximum gain. The polarization of a radiated wave is the property of an electromagnetic wave describing the time varying direction and relative magnitude of the electric field vector [4].

If the polarization of the receiving antenna is not the same as the polarization of the incoming (incident) wave, there is polarization mismatch and a resulting power loss. The requirement of the antenna polarization depends on the applications [4-5].

Polarization can be categorized as linear, circular and elliptical.

- **Linear polarization**- If the electric field vector moves back and forth along a line it is assumed to be linearly polarised. A linearly polarised wave is considered as **horizontally** polarised if the electric field is parallel to the earth and **vertically** polarized if the electric field is perpendicular to the earth. The antennas studied in this thesis, are linearly polarised.
- **Circular polarization**- If the electric field vector remains constant in length but rotates around in a circular path then it is considered circularly polarized. For circular polarization, the field's components have same magnitude and the phase between two components is 90 degree.

For a linearly-polarized antenna, the radiation pattern is taken both for a co-polarized and cross-polarized response.

- **Co-polarisation** represents the polarisation the antenna is intended to radiate (receive),
- **Cross-polarisation** represents the polarisation orthogonal to a specified polarization (co-polarization) [4].

❖ Pulse Fidelity

Consistency of radiated pulse shape is a critical issue in UWB antenna performance. It is helpful to have a measure of the energy radiated and a measure of fidelity for a given input waveform, when describing UWB antennas. A correlation between the transmitted, or received, waveform

and a template is used to assess how an antenna affects a waveform and to quantify the level of distortion.

A fidelity parameter involving the auto-correlation of the difference of the time domain transmitted field and a template function is described by Lamensdorf *et al.* in [7]. In certain UWB transceivers, correlation detection is applied to recover sent data correctly and introducing a correlation pattern involving the cross-correlation between the transmitted/received signal and the template function would provide an excellent measure for antenna performance. Descriptors of energy patterns are useful for specific applications where the signal level varies depending on system parameters and propagation environments.

In time-domain formulation, the fidelity between waveforms $x(t)$ and $y(t)$ is generally defined as a normalised correlation coefficient [8]:

$$F = \tau_{\max}\left[\frac{\int_{-\infty}^{\infty} x(t).y(t-\tau).dt}{\sqrt{\int_{\infty}^{\infty}\left|x(t)^2.dt\right|\int_{-\infty}^{\infty}\left|y(t)^2.dt\right|}}\right] \tag{3.9}$$

where $x(t)$ and $y(t)$ are normalized by their energy, respectively and the fidelity is the maximum integration by varying time delay τ . Fig. 3.1 illustrates the definition of pulse fidelity characterisation.

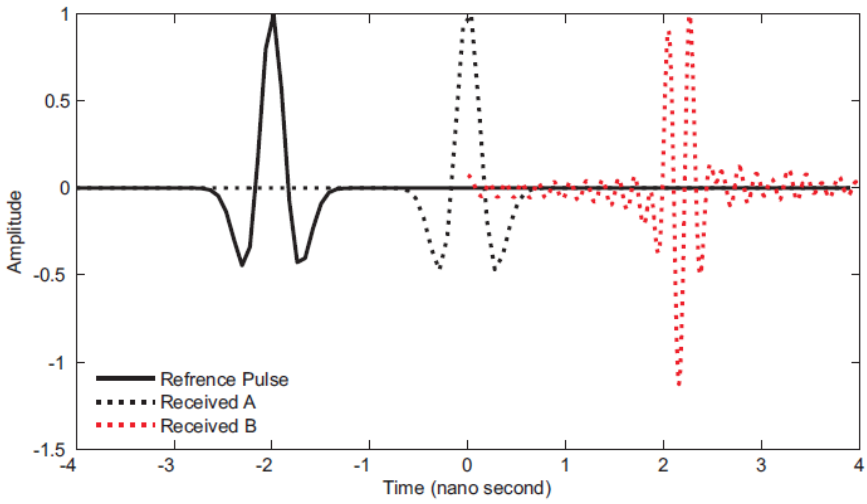

Fig. 3.1. Examples of transmitted UWB pulses to illustrate pulse fidelity concept. Fidelity of reference pulse compared to Received A is 100% and compared to Received B is 85% to demonstrate that fidelity compares pulse shape only regardless of pulse amplitude and phase offsets.

In practice, signal fidelity is calculated for a given direction in space in order to fully characterise the spatial radiation properties of an antenna. The fidelity depends not only on the antenna characteristics, but also on the excitation pulse; thus, it is also a system dependent parameter.

3.2 Electric Properties of Human Body Tissues

Body-centric communications involve the interaction of electromagnetic waves with the body. Body-worn devices will be in different places on the human body. In studying this interaction, it is important to understand the electromagnetic properties of the body tissues. These properties vary significantly with tissue type and frequency [9]. Specific parameters regarding the human tissue are required in order to model the electromagnetic fields in and around the body correctly. This includes the conductivity σ (S/m) and the relative permittivity ε_r of all different tissues used for the calculations, and also the frequency dependency of these parameters which must be considered appropriately.

Studies of the effect of electromagnetic waves on humans, and vice versa, are usually performed using physical phantoms that are limited to homogeneous models or, very expensive and limited inhomogeneous phantoms. Numerical modelling of electromagnetic fields on and around the human body can have a setup that can be chosen almost freely in a broad frequency range. Parameters can be easily and simply changed in the computation domain, such as operating frequency and various human tissue electric properties.

Fig. 3.2 shows measured permittivity data for a number of human tissues at different frequencies. The conductivity values are presented in Fig 3.3. The results are obtained from a compilation presented in [10-11] that covers a wide range of different body tissues and can help in producing modelling equations to determine the appropriate dielectric values at each desired frequency. Table 3.1 presents the electric properties of specified human tissues at 2.45 GHz in the ISM band including dielectric permittivity (ε_r), conductivity and penetration depth in mm. In order to well understand the EM propagation in the body area, an important parameter to take into account is the skin depth (δ) which is given from

$$\delta = \frac{1}{\sqrt{\pi \mu f \sigma}} \tag{3.10}$$

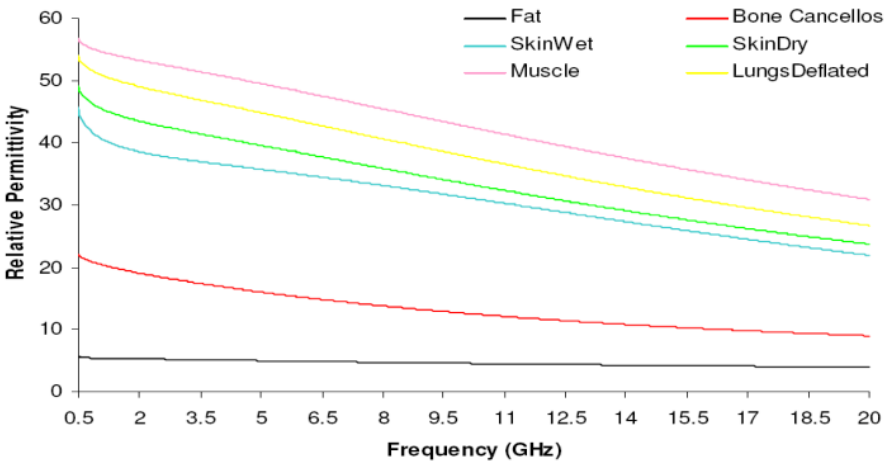

Fig. 3.2. Measured data of human tissue permittivity for various tissue types [10].

The decline in current density versus depth is known as the skin effects and the skin depth is a measure of the distance over which the current falls to 1/e of its original value. At lower frequencies, the permittivity is relatively high and the conductivity is low; the human body behaves as a conductor as the EM wave propagates through it. At higher frequencies the lossy effects are higher, so the skin depth decreases.

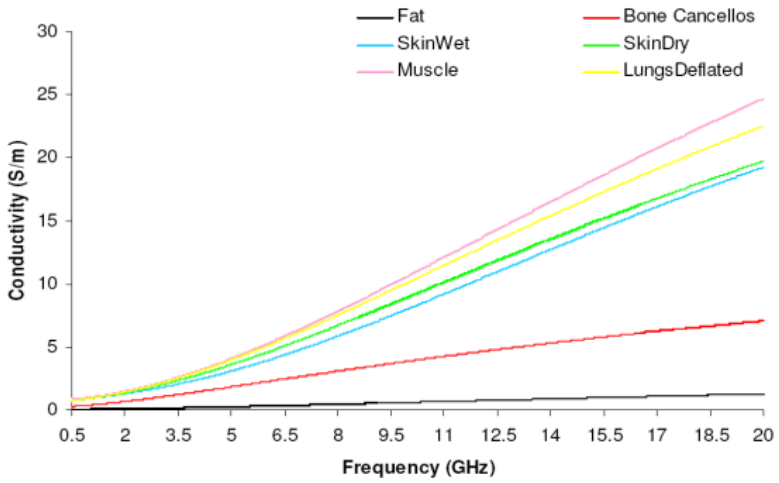

Fig. 3.3. Measured data of human tissue conductivity [10] for various tissue types.

In a medium with complex permittivity and non-zero conductivity, the effective permittivity $\varepsilon_e ff$ and conductivity $\sigma_e ff$ are usually expressed as

$$\varepsilon_e ff = \varepsilon' - \frac{\sigma''}{\omega} \tag{3.11}$$

$$\sigma_e ff = \sigma' - \omega \varepsilon'' \tag{3.12}$$

Where ε' is the real part of the permittivity and ε'' is the imaginary part of the permittivity related to the loss of energy within the medium. σ' is the real part of the conductivity and σ'' is the imaginary part of the conductivity related to the magnetic losses.

Table 3.1. Electric properties of specific human tissues used within the visible man model at 2.45 GHz [10] (σ is the tissue conductivity, ε_r r is the dielectric constant and δ is the penetration depth in mm).

	2.45 GHz		
Tissue	**σ (dB)**	**ε_r**	**δ (mm)**
Aorta	1.44	42.53	24.30
Bladder	0.69	18.00	33.18
Blood	2.54	58.26	16.12
Body Fluid	2.48	68.21	17.85
Bone	0.81	18.55	28.75
Grey Matter	1.81	48.91	20.72
White Matter	1.22	36.17	26.47
Breast Fat	0.14	5.15	88.30
Fat	0.10	5.28	117.02
Gall Bladder	2.06	57.63	19.74
Gland	1.97	57.20	20.56
Heart	2.26	54.81	17.61
Kidney	2.43	52.74	16.09
Liver	1.69	43.04	20.86
Lung Deflated	1.68	48.38	22.12
Lung Inflated	0.80	20.48	30.18
Muscle	1.74	52.73	22.33
Pancreas	1.97	57.20	20.56
Prostrate	2.17	57.55	18.75
Skin Dry	1.46	38.01	22.57
Skin Wet	1.59	45.85	22.03
Spleen	2.24	52.45	17.38
Stomach	2.21	62.16	19.09
Tendon	1.68	43.12	20.90
Testis	2.17	57.55	18.75

where the permittivity and conductivity are defined in their real and imaginary parts,

$$\varepsilon = \varepsilon' - j\varepsilon'' \tag{3.13}$$

$$\sigma = \sigma' - j\sigma'' \tag{3.14}$$

The permittivity of a medium or substrate is usually scaled to that of the vacuum for simplicity,

$$\varepsilon_r = \frac{\varepsilon_{eff}}{\varepsilon_0} \tag{3.15}$$

where $\varepsilon_0 = 8.854 \times 10^{-12}$ F/m.

The equations above indicate the differences between free space and lossy material; hence, the imaginary part of the permittivity includes the conductivity of the material which defines the loss that is usually expressed as dissipation or loss tangent.

$$\tan\delta = \frac{\sigma_{eff}}{\omega\varepsilon_{eff}} \tag{3.16}$$

This implies that, when an antenna is placed on a lossy medium, such as the human body, the conventional parameters need to be re-examined. The biological system of a human is an irregularly-shaped dielectric medium with frequency-dependent permittivity and conductivity; the distribution of the internal electromagnetic fields and the scattered energy depends on the body's physiological parameters and geometry, as well as the frequency and polarisation of the incident wave.

One major difference that can be identified directly when placing antenna on a lossy medium (in this case the human body) is the deviation of the wavelength value from the free space one. The effective wavelength λ_{eff} at the specified frequency will become shorter, since the wave travels more slowly in lossy medium,

$$\lambda_{eff} = \frac{\lambda_0}{\mathrm{Re}\left[\sqrt{\varepsilon_{eff} - j\frac{\sigma_{eff}}{\omega\varepsilon_0}}\right]} \tag{3.17}$$

However, in this case, the effective permittivity as seen by the antenna, depends on the distance between the antenna and the body and also on the location, since the human electrical properties are different for various tissue types as shown in Table 3.1. The general rule of thumb

is that the further the antenna is from the human body, the closer its performance is to free space. This also depends on the antenna type used and the structure of the antenna itself and its matching circuit. Wire antennas operating in standalone modes and planar antennas directly printed on substrate will experience changes in wavelength and, hence a deviation in resonance frequency, depending on the distance from the body. On the other hand, antennas with ground planes or reflectors incorporated in their design will experience less effect when placed on the body, independent of their distance from the body.

The effective permittivity, as explained and applied in this thesis, represents all factors affecting the antenna input impedance and current distribution. This includes the scattered wave from nearby objects, (in this case, the human body which is considered a conducting highly reflective medium at this frequency of 2.45 GHz). Scattered waves from the body will induce additional currents on the antenna, distorting the resonance distribution of the structure, and hence, causing frequency detuning and pattern degradation. The maximum reflection index of a wave incident from free space on the human skin layer is around 0.77, which is obtained from a simple 1-D multi-layer analytical wave propagation analysis. This indicates the significance of the backscattered wave components on antennas placed on the body.

An important factor in characterising antennas is the radiation pattern and, hence, the gain and efficiency of the antenna. The antenna patterns and efficiency definitions are not obvious and cannot be directly derived from conventional pattern descriptors, when the antenna is placed on the lossy medium. This is due to the fact that losses in the medium cause waves in the far-field to attenuate quicker initially to zero. The antenna efficiency is proportional to the gain.

Calculating the antenna efficiency when placed on the body is different to the efficiency in free space, due to changes in far field patterns and also in the electric field distribution at varying distance from the body, which leads to the different efficiency definition.

In direct relation to antenna patterns and with great interest for wearable antennas is the front-to-back ratio that defines the difference in power radiated in opposite directions wherever the antenna is placed. The ratio varies depending on antenna location on the body and also on the antenna type applied. For example, the presence of the ground plane in the microstrip patch antenna causes the current and electric field travelling backwards to be reflected; hence, the front –to-back ratio when antenna is placed in free space and on the body is not significantly different, which is not the case for conventional dipole and monopole antennas.

3.3 Fundamentals of Radio Propagation Channels

3.3.1 The Radio Link

The radio channel is defined as a path over which electrical signals can pass. The radio link can be represented as three distinct blocks, namely, the transmitting antenna (with transfer function $H_{Tx}(\omega)$), the radio channel (with transfer function $H_{ch}(\omega)$), and the receiving antenna (with transfer function $H_{Rx}(\omega)$. Therefore, the receiving signal $S_{Rx}(\omega)$ can be defined as

$$S_{Rx}(\omega) = S_{Tx}(\omega)\ H_{Tx}(\omega)\ H_{Ch}(\omega)\ H_{Rx}(\omega) \tag{3.18}$$

where $S_{Tx}(\omega)$ is the input signal. The path gain, which is given by the ratio between received and transmitted power, can be calculated adopting the Friis transmission formula

$$PG = \frac{P_r(\omega)}{P_t(\omega)}(1-|\Gamma_t(\omega)|^2)(1-|\Gamma_r(\omega)|^2)G_r(\omega)G_t(\omega)\left|\hat{\rho}_t(\omega).\hat{\rho}_r(\omega)\right|^2(\frac{\lambda}{4\pi d})^2 \tag{3.19}$$

where:

- G_t is the peak gain of the transmitting antenna;
- G_r is the peak gain of the receiving antenna;
- P_t is the average input power of the transmitting antenna;
- P_r is the average output power of the receiving antenna;
- Γ_t is the return loss at the input of the transmitting antenna;
- Γ_r is the return loss at the output of the receiving antenna;
- $\left|\hat{\rho}_t.\hat{\rho}_r\right|^2$ is the polarization matching factor between Tx and the output at Rx;
- λ is the wavelength at the operating frequency;
- d is the distance between transmitting and receiving antennas.

Often, the inverse of the path gain (path loss) is adopted.

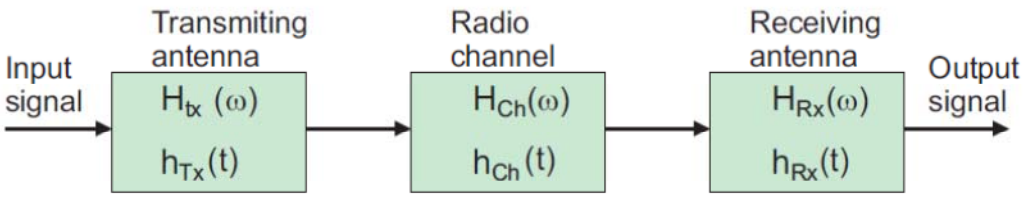

Fig. 3.4. Block diagram representing the radio link.

In conventional mobile communications systems, between a mobile terminal and a base station, the variation in the channel is due to interference between multiple rays scattered from the local environment. In WBANs, in addition to the local scattering, significant changes in the channel are also due to the changes in posture and movement of the body. Thus, characterisation of the radio channel needs to consider both the change in position of the mobile terminals, and for the change in geometry of the body [9].

Furthermore, the presence of the body, and its changes in posture, affect the radiation pattern, and the impedance of the antenna. The aforementioned Friis transmission formula 3.19 is valid in the case of free space propagation, and when the receiver is located in the far-field region. In a scattered environment, the wave reaches the receiver through multiple paths and more complex path loss models need to be considered. For on-body communications, the scenario is even more complex, and the propagation is a combination of free space waves, reflections from body parts and surrounding scatterers, and creeping waves along the body surface. Moreover, the impedance matching and the antenna gain depend on many factors, such as its position on the body, and the separation distance between the antenna and the body. For all these reasons, the three blocks of Fig 3.4 are not independent anymore, and the antenna characteristics need to be included in the on-body radio channel.

3.3.2 Radio Channel Characterisations

A radio channel model is a complex mathematical attempt to describe the propagation phenomenon through free space, physical and biological objects. The interaction among electromagnetic waves and the real world is extremely difficult to predict reliably and is clearly strongly dependent on the precise details of the propagation scenario chosen to represent the

typical case under analysis. There are many approaches attempting to define a radio channel with a high degree of confidence. Two major branches can be identified as

- Statistical models;
- Deterministic propagation models.

Statistical models are generally derived from measurements conducted in different environments and then characterized statistically, while a deterministic model tries to predict the exact characteristics of electromagnetic wave through use of geometry, Maxwell's equations and models of the boundary conditions of the media. Examples of deterministic modelling are ray-tracing, and the Finite Difference Time Domain full wave electromagnetic numerical technique (FDTD) [12-13].

Many studies have been made on the development of wearable devices using human body as a transmission channel [14, 15]. The human body is a complex and hostile environment for the propagation of a wireless signal. On-body propagation links can be roughly categorized according to the parts of the body at which the transmitting and receiving antennas are attached: for example, trunk-to-trunk, trunk-to-head and trunk-to-limb. Characteristics of the propagation channels, corresponding to different types of such links, can be expected to differ considerably, due to link geometry variability. For example a trunk-to-limb-link is expected to be subject to significant variation, due to the movement of the link, while a trunk-to-trunk link will be more stable [15]. From an electromagnetic point of view, the human body can be seen an irregular, stratified, lossy, and frequency-dependant dielectric object located in close proximity to an antenna. Wireless body-centric networks have special properties and requirements in comparison with other available wireless networks, and that is due to the rapid changes in communication channel behaviour on the body during the network operation. This raises important issues regarding the propagation channel characteristics, radio systems compatibility with such environments, and the effect that it has on the human. The diffraction and scattering from body parts, in addition to the tissue losses, lead to a strong attenuation, distortion and time-spreading of the signal; therefore, in order to design a power-efficient on body communication system, an accurate study of the radio channel is necessary [9, 16].

3.3.3 Radio Propagation Measurement Techniques

Different propagation measurement setups have been presented in the literature to characterize the radio channel. The measurement techniques can be generally characterized as time-domain measurements and frequency-domain measurements [17-21]. These two techniques are the bases for many other radio propagation sounders commonly used in characterizing wideband radio channels for indoor, outdoor and body-area network scenarios [22-24]. In time-domain measurements (see Fig 3.5.a), a digital oscilloscope is used to receive the signal, and it is relatively easy to detect multipath components if their delay with respect to the direct component is greater than the UWB pulse duration.

Channel measurements can also be performed using a vector network analyzer (VNA) in the frequency domain; see Fig. 3.5.b. Measurement antennas are connected to the ports of the analyzer and a sweep of discrete frequency tones, which include the S-parameters of the wireless channel, is taken by the analyzer. The S_{21} response measures the transmission from one antenna to the other and it also represents the channel frequency response $(H(\omega))$. Analyzing both magnitude and phase of S_{21} enables a transition to the time domain, simply by applying an Inverse Discrete Fourier Transform (IDFT); Fig. 3.5. (a). However, one of the disadvantages of the frequency-domain method is the restriction applied on measurement area freedom, since both transmit and receive antennas are connected to the same VNA; however, this problem can be avoided by the use of ultra low-loss long cables and applying advanced calibration techniques. This problem can also be overcome by application of VNA measurement set-ups using RF-on-fibre-optic connections, in scenarios where electrically small antennas are used [22].

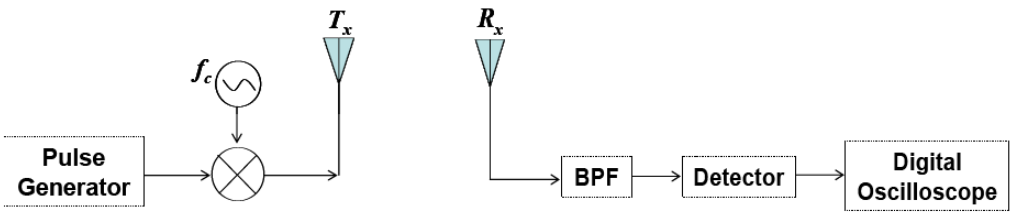

(a) Time domain method

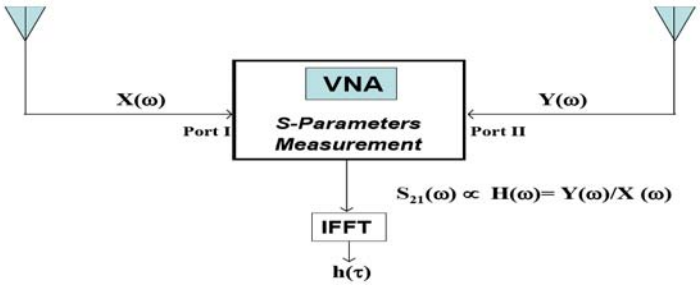

(b) Frequency domain method

Fig. 3.5. Radio propagation measurement techniques for indoor communication [17].

3.3.4 Path Loss and Large Scale (Slow) Fading

One of the most important aspects of statistical characterization is the derivation of a model describing the fluctuations of the received signal with respect to the distance. Models of this kind are called large-scale propagation models and the output of these models is usually the estimation of the path loss at a certain distance. The path loss represents the attenuation of the signal and it is defined as

$$PL = \frac{P_r}{P_t} \tag{3.20}$$

where P_r and P_t received and transmitted power, respectively. The prediction of the average received signal strength at a certain distance from the transmitter has been usually applied to model the radio channel. Path loss is usually examined using the Friis transmission formula, which provides a means for predicting this received power. The formula, in general, predicts that signal power will decrease at a rate of frequency squared (which has little effects on narrow-band systems) and by the square of the separation distance between transmitter and receiver. The free space power received by an antenna at a distance d from a transmitter is given by [17]

$$P_r(d) = \frac{P_t G_t G_r \lambda^2}{(4\pi d)^2 L} \tag{3.21}$$

where P_t and P_r are the transmitted and received power, respectively. G_t and G_r are the transmitter and receiver antenna gain, respectively. The distance between the transmitter and receiver is defined by d and L is the system loss (not related to propagation and is equal to 1 for lossless environment, e.g. free space).

Many theoretical and measurement-based studies presented in the literature have shown that the average received signal decrease logarithmically with distance (for both indoor and outdoor environments) [17-18, 9, 25, 26-28]. Therefore, the average path loss for a distance d between transmitter and receiver is expressed as

$$PL(d) \propto \left(\frac{d}{d_0}\right)^{\gamma} \text{ for } d \geq d_0 \tag{3.22}$$

where γ is the path loss exponent that indicates the rate at which path loss increases with distance, and d_0 is a reference distance set in measurement, d_0 normally set to 1 m for indoor channels; for on-body channel characterisation, it is usually set to 0.1 m. The average path loss can be presented in dB as

$$PL_{dB}(d) = PL_{dB}(d_0) + 10\,\gamma\,\log\left(\frac{d}{d_0}\right) \tag{3.23}$$

which leads to the average received power, represented as

$$P_r(d) = P_r(d_0)\left(\frac{d}{d_0}\right)^{\gamma} \tag{3.24}$$

The path loss observed at any given point will deviate from this average value due to variations in the environment, as reported in [17], and this variation has been shown to follow a log-normal distribution in many measurements. Therefore, the average path loss can be represented as:

$$PL_{dB}(d) = PL_{dB}(d_0) + 10\,\gamma\,\log\left(\frac{d}{d_0}\right) + X_{\sigma} \tag{3.25}$$

where X_{σ} is a zero-mean Gaussian-distributed random variable with standard deviation σ (both values in dB).

In UWB systems, the path loss is obtained by averaging the received power across the band for the specified number of sweeps, taken with reference value of 1 m, and is calculated by

$$PL(d) = \frac{1}{NK}\sum_{i=1}^{N}\sum_{j=1}^{K}\left|H(f_i, x_j; d)\right|^2 \tag{3.26}$$

Where $H(f_i, x_j; d)$ is the frequency response of the channel, which represents the received power relative to the transmitted power per frequency component. N represents the number of

frequency components *f* measured in the channel, K is the number of sweeps defined by *x* and *d* is the separation distance between transmit and receive antennas.

3.3.5 Small-Scale (Fast) Fading

In addition to modelling the channels large-scale behaviour, it is necessary to consider small-scale effects on the received signal. Small-scale statistics describe the variation of the channel over an area or period of time where the channel can be considered wide-sense stationary. Due to the constructive or destructive interference of the received paths, the received power has a fast and significant variation around the average path loss; we refer to this as small-scale channel fading. Multipath fading degrades the performance of the wireless communication systems because, in the propagation environment, the signal arriving at a receiver experiences the effects of various propagation-dependent mechanisms: multiple reflections, detractions, absorption, etc. Unfortunately, it is hard to eliminate multipath disturbances. However, if the channel is well-characterised, it is possible to reduce the effect of these disturbances by designing the proper transmitter and receiver. Therefore, accurate channel characterisation would be particularly useful for system designers to provide a reliable simulation model.

The amplitude of the fading can follow different distributions, such as Rician, Rayleigh, Nakagami, Log-normal, Gamma, Normal and Weibull. Rician occurs when a strong path exists in addition to the low level scattered paths. The Rician distribution is usually applied to model line of sight (LOS) channels. In this case, random multipath components are superimposed to a dominant signal, so that the received signal is the combination of a fixed deterministic component and some scattered components with stochastic amplitude and phase. If it is not a LOS channel, it is not possible to identify a dominant component, and the amplitude of the signal is often modelled by the Rayleigh distribution. Both Rayleigh and Rice distributions are applied to channels with a large number of unresolved multipath components, such as in the narrow-band case. However, in UWB channels, more flexible empirical distributions are used to describe the path amplitude within a delay interval. In the multipath fading environment, if the received scattered signal has random amplitude and phase, then a Nakagami distribution is suitable for slow-and fast-fading scenarios. The Nakagami and Weibull distributions have been applied to model the small-scale fluctuations of UWB indoor channels [29]. The lognormal distribution has been usually applied to model the large-scale fluctuations of the signal amplitudes in a multipath

fading environment; however, in [30], it was shown that the lognormal provides a good fit for the small-scale fading in UWB on-body radio channels and narrowband off-body communication channels where Rayleigh is a poor fit.

3.4 Literature Review for Narrowband Antennas and Radio Propagation for Body-Centric Wireless Communications

Antennas play a vital role in optimizing the radio system performance, since they are used to transmit/receive the signal through free space as electromagnetic waves from/to the specified destination. Wearable antennas are mainly designed to operate in GSM/PCS band, the unlicensed ISM band (2.45 GHz) and UWB (3.1 GHz -10.6 GHz). First of all, for wireless BAN to be accepted by the majority consumers, the radio system components need to be somehow hidden, conformal to the body, small in size and light weight. This requires a possible integration of these systems within everyone's daily clothes. Therefore, the antennas for body area networks need to be compact, light weight, smart, conformal, low-cost and easily integrated with body-worn devices and low-power consuming, to maximise battery life and promote green radio systems. For on-body applications, the antenna needs to be immune to the effect of the human body; a low mutual influence between antennas and body is required in order to get better performances. In BCWCs, communications among on-body devices are required, as well as communications with external base stations, which therefore require antennas with different radiation characteristics and possibly multi-band functionality.

The miniaturisation of the antenna presents a significant problem, as its performance is directly related to its physical size, involving a trade off between design parameters, such as efficiency, bandwidth, and radiation characteristics. To design body-mounted antennas, an understanding of how the presence of human body affects the behaviour of the antenna (in terms of frequency detuning, radiation pattern modification, changes of input impedance, variation of bandwidth and gain and efficiency reduction) must be utilised. It is widely accepted that antenna performance is significantly affected by close proximity to the human body; for example, radiation pattern distortion (varying propagation conditions), antennas suffered from reduced efficiency due to bulk power absorption, resonance frequency shift (antenna detuning) and variations in impedance at the feed due to antenna-body capacitive coupling as reported in [31-

33]. Furthermore, these effects will vary between different antennas, ground plane size, separation distances, and near field proximity coupling [34-35]. For on-body applications, the antenna must be more immune to the human body**,** with low mutual influence between antennas and body for high radiation efficiency, low specific absorption rate (SAR) and radiation omnidirectional to the body surface for minimized link loss in on-body communications.

Many studies have been made on the operation of antennas located in close proximity of the body [33-38], as well as on the SAR [39-40]. Studies show that the antennas with full ground plane have minimum sensitivity to the body presence, due to the effects of the ground plane, which acts as a shield between the antenna and the body. In [34], a parametric study to evaluate how the antenna-body spacing affects the antenna performance has been presented. The further the antenna is from the body, the lower is the absorption from the human body. The use of a lossy material to keep this spacing is beneficial, as it leads to SAR reduction, since part of the power is dissipated in the lossy material rather than in the body tissues. For many applications, printed antennas also offer favourable characteristics, such as lower profile construction, physical robustness, low cost, ease of construction, and, in some cases, conformability.

There are two primary requirements for antennas for on-body links. First, the antenna needs to be insensitive to the proximity to the body; and second, the antenna needs to have a radiation pattern shape that minimizes the link loss [9]. To date, there has been no significant breakthrough in the design of low profile narrowband antennas for body-centric wireless communication but studies of body-worn or wearable antennas have recently received much attention with some reported in the open literature so far [34-35,16, 38-45].

Peter Hall *et al.* have done extensive studies on narrowband antennas (2.45 GHz) [15, 41] for on-body applications and found that, for communication over the body surface, wire monopole antennas shows good performances with respect to path loss, due to their omnidirectional radiation pattern in the azimuth plane. In [43, 45] a dual-band (2.4 GHz, 5.2 GHz) button antenna for WLAN applications was presented by John Batchelor. The antenna has the size of a standard metal button used in denim jeans, and can be easily integrated in clothes. The antenna has monopole-like radiation performances in both frequency bands of operation.

In [42], Scanlon *et al*. presented a set of higher-mode microstrip patch antennas operating at 2.45 GHz. The antennas are excited at the higher TM21 resonant mode, which has the advantage of having a vertical monopole-like radiation pattern. In this way, despite a total antenna height of

only $\lambda/20$, the on-body coupling performance is comparable to that achievable with a quarter wavelength monopole and significantly higher than that measured with a fundamental microstrip patch antenna. In [46], a cavity-slot antenna was proposed for communication at 2.45 GHz. The polarization of the antenna is normal to the body, thus leading to minimized path loss in the on-body link and relatively high efficiency (50%) when it is body-mounted. William G. shows stacked-patch antenna with switchable propagation mode for UHF BCWCs [44].

Alomainy *et al.* presented a study of a compact antenna used in sensors aimed at healthcare applications in the 2.4 GHz ISM band [35]. A thorough numerical investigation of the antenna performance, including full sensor details and the presence of the human body, was performed. The results demonstrated that the power radiated from the compact embedded antenna is comparable to the one of an external monopole.

To enable the integration of wireless devices in garments, antennas made out of textile materials have been proposed [47-53]. In [52], a patch antenna integrated into protective clothing for fire-fighters was introduced. The antenna was printed on a flexible pad of foam, which is commonly used in protective clothing. In [49, 50, and 54], narrowband antennas were printed above Electromagnetic Band Gap (EBG) structures to reduce the radiation towards the human body, and minimize the detuning effect. In [50], Langley *et al*. proposed a flexible dual-band patch antenna (2.45 and 5.5 GHz) printed on an EBG textile substrate made of felt. Results demonstrated that by introducing the EBG, the radiation into the body is reduced by over 10 dB, and the antenna gain is improved by 3 dB. However, the antenna is big in size (120 x 120 mm). Salonen *et al.* has presented a flexible planar inverted F antenna (PIFA) that can be applied to smart clothing intended for use with wearable computers as part of WBANs [53].

On-body radio propagation has been studied and investigated for narrowband (2.45 GHz) communication [9, 15, 38, 41]. In [9, 15, 41], on-body channel characterization was presented at the unlicensed frequency band of 2.45 GHz, with the human body standing, various body positions and postures and body movements, using different kinds of antennas (such as Wire Monopole on large ground plane, Loop, Dipole, Patch and Patch array). Results show that the Monopole-Monopole combination gives the lowest link loss (lowest path loss) for all on-body channels of positions and postures scenarios. The Wire Monopole antenna has a quite omnidirectional radiation pattern in the horizontal plane with the maximum gain, which provides good coverage over the body surface when it is placed on the human body.

Based on the literature, although there were some studies of the human body effects on the antenna parameters, they were not thorough and the antennas were limited. However, a complete parametric study addressing the effects of the human body on the performance parameters for a wider number of antennas are required in order to understand what are the requirements to design suitable antennas for body-centric wireless communications.

3.5 Literature Review of UWB Antennas and Propagation for Body-Centric Wireless Communications

The antenna designed for a UWB radio system plays a more important role that it does for a conventional system. In such a system, the antenna behaves like a filter in both spatial and frequency domains and tends to introduce unpleasant signal distortion and degradation [55]. A variety of UWB antennas have been proposed already for different applications. Complete details of almost all kinds of UWB antennas can be found easily from [55-66]. Body-centric UWB antennas and systems have attracted a lot of researchers recently. Antennas for UWB/WBAN/WPAN applications are easily found in the literature [56-57, 9, 61-66].

In UWB communications, the antennas are significant pulse-shaping filters. Any distortion of the signal in the frequency domain causes distortion of the transmitted pulse shape, thereby increasing the complexity of the detection mechanism at the receiver. Fundamental antenna parameters such as impedance bandwidth, radiation patterns, half-power beam-width, antenna gain, polarisation and efficiency [67], should be considered in designing antennas for ultra wideband radio; however, there are additional challenges for UWB antenna design. When designing UWB antennas, group delay must be taken into account, given by the derivative of the unwrapped phase of an antenna. If the phase is linear throughout the frequency range, the group delay will be constant and, hence, delivered pulses will be transmitted with no distortion in all directions. Any strong resonance at any frequency causes large group delay variation, thus causing much distortion of the pulse shape. So, it is not reasonable to design ultra-wideband antennas with multiple deep resonances, as far as pulse fidelity is concerned.

UWB antennas require a constant return loss across the whole bandwidth of operation. A very wide operational fractional bandwidth of UWB systems makes the design and evaluation of

antennas more difficult than in narrowband systems [68-69]. For more specific applications, such as wireless BAN, the antenna design becomes more complicated than for simple free-space operation scenarios, due to the complex human body medium presence and additional factors and constraints. All these factors need to be taken into account for designing an efficient antenna to provide reliable radio links for on-body communications. For UWB antennas, an additional criterion has to be taken into account, in addition to conventional antenna characteristics, which is the frequency variation of the antenna radiation pattern. This criterion is considered essential in designing suitable UWB antennas, due to the large relative bandwidth of UWB antennas; the variation of the antenna pattern over the considered frequency range is more distinct. In addition, the emission rules for UWB radiation specify that the power spectral density must be limited in each possible direction. The regulations enforce a limit on the emitted power in the frequency-angle domain [70].

In [64], Chen *et al.* proposed three different microstrip-fed wearable UWB antennas. Such antennas were designed to operate in the lower UWB frequency band (3-5 GHz), and they present different radiation characteristics. Chen *et al.* proposed a novel diversity antenna with two different radiating elements, providing different and symmetric coverage regions.

In [62], Klemm *et al.* presented time-domain characteristics of an aperture-stacked patch antenna for UWB body-worn devices through numerical modelling. Both frequency-and time-domain characteristics of the proposed antenna are analysed and discussed with regards to applicability in wearable computing. Three different modes were investigated: transmit, receive and 'two antennas' mode (where one antenna is transmitting and the other is receiving in free space), with a Gaussian pulse excitation. The spatial and impulse performance of the antenna was studied by obtaining fidelity of pulses radiated in different directions in comparison to a reference pulse. High fidelity values suggested that the antenna is a good candidate for UWB wireless body area networks.

Promwong *et al.* used a three-antenna method to characterise the UWB transfer function of two antennas with one placed on the human body. The measurement results are then used to evaluate the extended Friis transmission formula used for calculating transmission gain [66]. The biconical antenna is used for transmitting and the Skycross antennas for receiving. Both transmitted waveform and matched filter system are used to characterise the antenna with the extended Friis formula.

In [25, 73], the miniaturised CPW-fed Tapered Slot Antenna (TSA) and the Planar Inverted Cone antenna (PICA) were proposed for body-centric wireless communications. There is little work presented in the literature regarding human body presence effects on UWB antenna performance parameters. Most literatures considered the antennas as a part of the propagation system and apply commonly and widely available antenna types to characterise the channels. However, a complete parametric study addressing the human body effects on the performance parameters of different types of UWB antenna is very important and should be investigated.

Accurate prediction of radio propagation behaviour is crucial to system design. In order to design power-efficient systems for personal communication environments, it is important to provide reliable models of the radio propagation channels. The case is even more complex when it comes to on-body channel characterisation, due to its stochastic and dynamic nature. It is important to characterise the radio propagation channel to ensure satisfactory performance of a wireless communication system. UWB body area network channel characterisation was presented in [72] for pre-defined sets of nodes, with multi-hopping networking in mind, to determine energy and power requirements. However, a more realistic representation of the human body behaviour, such as different body positions and postures for various antenna systems, was introduced in [74, 75]. Results and analysis show that, due to different body postures and positions, the variation in path loss occurs.

In [25, 73], modelling of path loss for UWB on-body radio channels was performed with two different antennas (the TSA and PICA), both in the chamber and in an indoor environment, to study the effects of the antenna type on the channel parameters. Results and analysis show that different antenna shows different path loss exponent values, due to different radiation characteristics. Lower path loss exponent values were found for both antenna cases when measurements are performed in the indoor environment, due to the reflecting environment. UWB on body radio channels for a pseudo-dynamic human body have been characterised in [25, 75-76]. Results show that, due to human body movements, a variation in the on-body path loss occurs.

Two different UWB antennas with different radiation characteristics were presented in [72]. The first antenna is a printed horn-shaped self complementary antenna (HSCA), and the second is a vertical planar inverted cone antenna (PICA) as shown in Figs. 3.6 (a) and (b). The HSCA is tangentially polarised (with respect to the body), while the vertical PICA is vertically polarised.

As shown in [72], antennas with different radiation characteristics lead to different channel parameters. In particular, the use of a vertically polarized UWB monopole, rather than a planar antenna, reduces the attenuation but increases the time spread of the signal. Therefore, it was concluded that the hybrid use of different antennas can improve the channel performance. However, such antennas are relatively big and not conformal to the body, and the aim of the authors was to demonstrate the effect of different antenna types on the UWB on-body radio channel parameters.

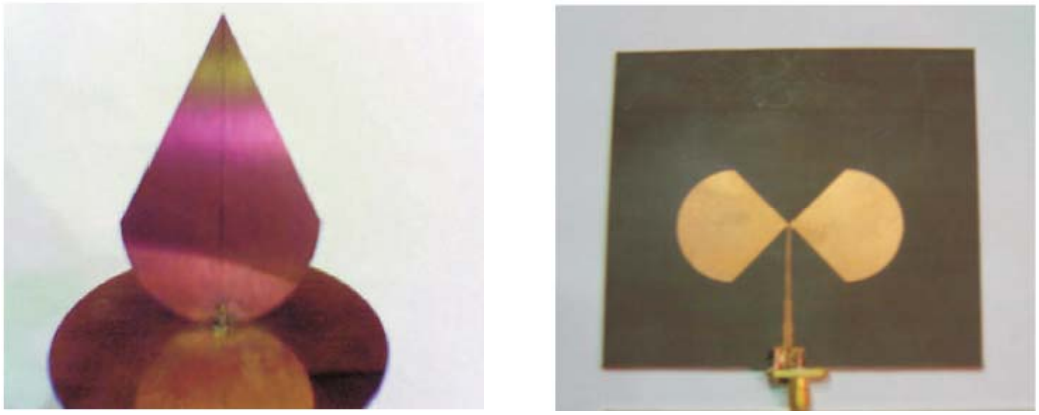

(a) Vertical Planar Inverted Cone Antenna (b) Printed Horn-Shaped Self Complementary Antenna

Fig. 3.6. The two UWB antennas proposed in [72].

UWB on-body propagation and system modelling for body-centric networks was investigated in [72-77]. In addition to experimental characterisation of UWB on-body radio channels, they were analysed using numerical modelling technique to highlight various propagation mechanisms and also to provide a more deterministic means to model the radio channel. In [78], the on-body radio channel was investigated with several body postures using a dispersive finite difference time domain (FDTD) technique that is in turn to ray-tracing methods and theories of diffraction. Researchers have investigated the impact of the different antenna types on the on-body radio channel characteristics at 3-10 GHz using very limited number of antennas and the sizes of the antennas used were also bigger. However, the UWB on-body radio channel performance needs to be investigated using wider number of compact antennas.

Recently, researchers have investigated ultra wide-band on-body radio channels thoroughly, while little has been performed for UWB off-body radio channels, which need further

investigation. UWB off-body communication channels measurement results in an anechoic chamber were investigated and analyzed in [79]. In this case, measurements were performed placing one transmitter antenna on the access point off the body and another antenna mounted on the belt position of the human body under test, where the height between transmitter and receiver antenna was the same. UWB off-body measurement results in the hospital environment using fibre optics set-up measurements are presented in [80-81].

3.6 Summary

This chapter discussed the fundamentals of antennas and radio propagation for body-centric wireless communications. The electric properties of human body tissues are also illustrated and discussed. A literature review of wearable antennas highlighted the need for developing compact and conformal antennas and understanding the behaviour when placed in close proximity of the human body is also provided.

This chapter also gave a literature review on the state-of-the-art in radio channel characterisation in body-centric wireless communications. The parameters governing the radio propagation channel in multipath environments (large scale path loss and small scale fading analysis) were described with respect to different modelling and characterisation techniques.

References

[1] Return loss, URL: *en.wikipedia.org/wiki/Return_loss*

[2] Sky cross, URL: *www.skycross.com/technology/terminology.asp*

[3] **S. R. Saunders and A. A-Zavala**, Antenna and propagation for wireless Communication Systems, John Wiley and Sons, Ltd, Second edition, 2007.

[4] **C. A. Balanis**, Antenna Theory Analysis and design, John Wiley and sons, New York, third edition, 2005.

[5] **W. L. Stutzman, G A. Thiele**, Antenna theory and design, John Wiley and Sons, Inc. New York, second edition, ISBN 0-471-02590-9, pp.56-57, 1998.

[6] **J. D. Kraus, R. J. Marhefka**, Antennas for all applications, third edition, Mc Graw Hill, 2002.

[7] **D. Lamensdorf and L. Susman,** "Baseband-pulse-antenna techniques," *IEEE Antennas and Propagation Magazine*, vol. 36, no. 1, February 1994.

[8] **J. S. McLean, H. Foltz, and R. Sutton**, "Pattern descriptors for UWB antennas," *IEEE Transactions on Antennas and Propagation*, vol. 53, no. 1, January 2005.

[9] **P. S. Hall, Y. Hao**, Antennas and Propagation for Body-Centric Wireless Communications, Artech House, 2006.

[10] ''Calculation of the dielectric properties of body tissues," *Institute for Applied Physics*, *Italian National Research Council, URL: http://niremf.ifac.cnr.it/tissprop/*.

[11] **C. Gabriel and S. Gabriel**, "Compilation of the dielectric properties of body tissues at RF and microwave frequencies,'' *URL: http://www.brooks.af.mil/AFRL/HED/hedr/reports/dielectric/Title/Title.html,1999.*

[12] **B. Allen, M. Dohler, W. Q. Malik, D. J. Edwards, A.K Brown**, Ultra-wideband Antennas and Propagation For Communications, Radar and Imaging. John Wiley and sons Ltd, The Atrium, Southern Gate, Chichester, West Sussex England, 2007.

[13] **D. Porcino**, "Simulation of an indoor radio channel at mm-wave frequencies,'' Final Year Project, Dott. Ing. Thesis, Politecnico Di Torino, Italy 1997.

[14] **A. Alomainy, Y. Hao and F. Pasveer**, "Numerical and Experimental Evaluation of a Compact Sensor Antenna for HealthCare Devices,'' *IEEE Transaction on medical circuits and systems,* vol.1, no.4, December 2007.

[15] **P.S. Hall, Y. Hao, Y.I. Nechayev, A. Alomainy, C.C. Constantinou, , C.G Parini , M.R Kamruddin, T. Z. Salim, D. T. M. Hee, R. Dubrovka, A. Wadally, W. Song, A. Serra, P. Nepa, M. Gallo, and M. Bozzetti**, "Antennas and propagation for on body communication systems," *IEEE Antenna Technology and Propagation Magazine,* vol. 49, no 3, June 2007.

[16] **A. Sani, A. Alomainy, and Y Hao,** " Characterisation of Ultra Wideband wearable Antennas and Body-Centric Wireless Networks in Indoor Environment,'' *Proceeding of the 1st European Wireless technology conference*, October 2008, Amsterdam, the Netherland.

[17] **T.S. Rappaport***, Wireless Communications Principles and Practice.* Prentice Hall, Inc., New Jersey, 1996.

[18] **H. Hashemi,** " The indoor radio propagation channel,'' *Proceedings of IEEE*, vol.81, no.7, pp. 943-968,1993.

[19] **A.A. Saleh and R. A. Valenzuela**, "A statistical model for indoor multipath propagation,'' *IEEE Journal on Selected Areas in Communications,* vol. 5, no. 2, pp. 128-137, February 1987.

[20] **H. Suzuki**, "A statistical model for indoor multipath propagation,'' *IEEE Transactions on communications*, vol. 25. no 7, pp.673-680, July 1977.

[21] **M. Z. Win and R. A. Scholtz**, "Impulse radio: how it works, '' *IEEE Communications Letter,* pp. 36-38, February 1998.

[22] **I. S. Kovacs, G. Pedersen, P. Eggeres, and K. Olsen**, "Ultra wideband radio propagation in body area network scenario,'' *in ISSSTA Proceedings*, pp.120-106, 2004.

[23] **S. L. Cotton and W. Scanlon**, "A statistical analysis of indoor multipath fading for a narrowband wireless body area network,'' *IEEE 17th International Symposium on Personal, Indoor and Mobile Radio Communications*, pp. 1-5, September, 2006.

[24] **D. Neirynck**, "Channel *Characterization and Physical Layer Analysis for Body and Personal Area Network Development*,'' PhD Thesis, University of Bristol, November 2006.

[25] **A. Sani, Y. Hao**, "Modeling of Path Loss for Ultrawide Band Body-Centric Wireless Communications,'' Electromagnetics in Advanced Applications, 2009. *ICEAA '09. International Conference* on 14-18 Sept. 2009.

[26] **S.R. Saunders**, *Antennas and Propagation for Wireless Communications*. John Wiley & Sons, Ltd., 2004.

[27] --, *Antennas and Propagation for Wireless Communications*, 2nd Edition. John Wiley & Sons, Ltd., 2007.

[28] **S.S Gassemzadeh, R. Jana, C. W. Rice, W. Turin, and V.** , "A statistical path loss model for in-home UWB channels,'' *IEEE Conf. Ultrawide Band Systems and Technologies Baltimore,* P. 5964, 2002.

[29] **C. Chong and S. Yong,** " A Generic statistical-based UWB channel model for high-rise apartments," *IEEE Transactions on Antennas and Propagation*, vol. 53, no. 8, pp. 2389–2399, 2005.

[30] **A. Fort, C. Desset, P. D. Doncker, and L. V. Biesen**, "Ultra wideband body area propagation: from statistics to implementation," *IEEE Transactions on Microwave Theory and Technique*, vol. 54, no. 4, pp. 1820–1826, June 2006.

[31] **W. G. Scanlon and N.E .Evans**, "Numerical analysis of body worn UHF antenna systems,'' *IEEE Electron. Commun. Eng.* J., vol. 13, no.2, pp.53-64, 2001.

[32] **M. Okoniewski and M.A Stuchly**, "A study of the handset antenna and human body interaction,'' *IEEE Trans. Microw. Theory Tech,.* vol. 44 no. 10, pp 1855-1864, Oct. 1996.

[33] **K.L Wong and C. I. Lin**, "Characteristics of a 2.45 GHz compact shorted patch antenna in close proximity to a lossy medium,'' *Microw. Opt. Technol. Lett.*, vol 45, no 6, pp 480-483, 2005.

[34] **A. Alomainy, Y. Hao and D. M Davenport**, "Parametric Study of Wearable Antennas Varying Distances from the Body and Different On-Body Positions,'' *Antennas and Propagation for Body-Centric Wireless Communications, 2007 IET Seminar on* 24-24 April 2007 Page(s):84 – 89.

[35] **A. Alomainy, Y. Hao and F. Pasveer**, "Numerical and Experimental Evaluation of a Compact Sensor Antenna for HealthCare Devices,'' *IEEE Transaction on medical circuits and systems,* vol.1, no.4, December 2007.

[36] **H. R. Chuang and W. T. Chen**, " Computer simulation of the human-body effects on a circular-loop-wire antenna for radio-pager communications at 152, 280, and 400 MHz," *IEEE Transactions on Vehicular Technology*, vol. 46, no. 3, pp. 544–559, 1997.

[37] **P. Salonen, Y. Rahmat-Samii, and M. Kivikoski**, "Wearable antennas in the vicinity of human body," *IEEE Antenna and Propagation Society Symposium*, vol. 1, pp. 467–470, June 2004.

[38] **A. Alomainy, Y. Hao, A. Owadally, C. G. Parini, P. S. Hall, and C. C. Constantinou**, " Statistical analysis and performance evaluation for on-body radio propagation with microstrip patch antennas," *IEEE Transactions on Antenna and Propagation*, vol. 55, no. 1, pp. 245–248, January 2007.

[39] **B. Sinha,** " Numerical modelling of absorption and scattering of EM energy radiated by cellular phones by human arms," *IEEE Region 10 International Conference on Global Connectivity in Energy, Computer, Communication and Control, New Delhi, India*, vol. 2, pp. 261–264, December 1998.

[40] **J.Wang, O. Fujiwara, S.Watanabe, and Y. Yamanaka**, "Computation with a parallel FDTD system of human-body effect on electromagnetic absorption for portable telephone," *IEEE Transactions on Microwave Theory and Techniques*, vol. 52, no. 1, pp. 53–58, January 2004.

[41] **M. R. Kamruddin, Y. Nechayev, and P.S. Hall,** "Performances of Antennas in the On-Body Environment," *IEEE Antennas and Propagation Society International Symposium*, 2005, Page(s): 475-478 vol. 3A.

[42] **G. A. Conway and W.G. Scanlon**, "Antennas for over Body- Surface Communication at 2.45 GHz,'' *IEEE Transactions on Antennas and Propagation.* Vol. 57. No. 4, April 2009.

[43] **B. Sanz-Izquierdo, F. Huang, and J.C. Batchelor**, "Covert dual-band wearable button antenna,'' *IEEE Electron. Lett.* vol. 42, no.12, pp.3-4, 2006.

[44] **W.G. Scanlon and A. Chandran**, " Stacked-Patch Antenna with Switchable Propagation Mode for UHF Body-Centric Communications,'' *2011 IEEE International Workshop on Antenna Technology*, March 2-7, Santa Monica California, IWAT 2009.

[45] **B. A. Sanz-Izquierdo**, "Compact Multiband Antennas for Wireless systems,'' PhD Thesis, University of Kent at Canterbury, December 2006.

[46] **N. Haga, K. Saito, M. Takahashi, and K. Ito**, "Characteristics of cavity slot antennas for body-area networks," *IEEE Transactions on Antennas and Propagation*, vol. 57, no. 4, pp. 837–843, 2009.

[47] **P. Salonen, Y. Rahmat-Samii, and M. Kivikoski**, "Wearable antennas in the vicinity of human body," *IEEE Antenna and Propagation Society Symposium*, vol. 1, pp. 467–470, June 2004.

[48] **P. Salonen and Y. Rahmat-Samii**, "Textile antennas: effects of antenna bending on input matching and impedance bandwidth," *IEEE Aerospace and Electronic Systems Magazine*, vol. 22, no. 3, pp. 10–14, 2007.

[49] **S. Zhu and R. Langley**, "Dual-band wearable antennas over EBG substrate," *Electronics Letters*, vol. 43, no. 3, pp. 141–142, 2007.

[50] ——, "Dual-band wearable textile antenna on an EBG substrate," *IEEE Transactions on Antennas and Propagation*, vol. 57, no. 4, pp. 926–935, 2009.

[51] C**. Hertleer, A. Tronquo, H. Rogier, L. Vallozzi, and L. Van Langenhove**, "Aperturecoupled patch antenna for integration into wearable textile systems," *IEEE antennas and wireless propagation letters*, vol. 6, 2007.

[52] **C. Hertleer, H. Rogier, L. Vallozzi, and L. van Langenhove**, "A textile antenna for off-body communication integrated into protective clothing for fire-fighters," *IEEE Transactions on Antennas and Propagation*, vol. 57, no. 4, pp. 919–925, 2009.

[53] **P. Salonen and J. Rantanen**, "A dual-band and wide-band antenna on flexible substrate for smart clothing," *27th Annual Conference of the IEEE Industrial Electronics Society*, 2001.

[54] **J. Kim and Y. Rahmat-Samii**, "Exterior antennas for wireless medical links: EBG backed dipole and loop antennas," *Antennas and Propagation Society International Symposium, IEEE*, 2005.

[55] **T. G. Ma and C. H. T Seng**, "An Ultra Wideband Coplanar Waveguide –Fed Tapered Ring slot antenna,'' *IEEE Transactions on Antenna and Propagation*, vol. 54, no.4, April 2006.

[56] **A. Rahman, A. Alomainy, and Y. Hao**, "Compact Body-Worn Coplanar Waveguide Fed Antenna for UWB Body- Centric Wireless Communications,'' A*ntennas and Propagation, 2007. EuCAP 2007.* The Second European Conference on 11-16 Nov. 2007 Page(s):1 – 4.

[57] A**. Alomainy, A. Sani, J. Santas, A. A Rahman, and Y. Hao**, "Transient characteristics of wearable antennas and radio propagation channels for Ultra wideband body-centric wireless communications,*'' IEEE Transactions in Antenna and Propagation,* vol. 57, no.4, pp.875-884, April 2009.

[58] **A. Alomainy Y.Hao Frank Pasveer**, Antennas for portable device. Chapter 6 page 197-229 Ed Zhi Ning Chen, ISBN 978-0-470-03073-8. Copyright 2006, John Wiley and Sons Ltd. West Sussex, UK.

[59] **T.G. Ma and C. H. T Seng**, "An Ultra Wideband Coplanar Waveguide –Fed Tapered Ring slot antenna,'' *IEEE Transactions on Antenna and Propagation*, vol. 54, no.4, April 2006.

[60] **J. Liang, L. Guo, C.C. Chiau, X, Chen and C.G Parini**, "Study of CPW Fed circular disk monopole antenna for Ultra wideband application,'' *IEEE Proc.-microw. Antenna Propag* vol, 152, no 6, November 2006.

[61] **T.S.P. See, A. Alomainy, Y. Hao, and Z. N. Chen**, "On-body Craterisation of a compact planar UWB antenna,'' Proc, *EuCAP 2006,* Nice France 6-10 November 2006.

[62] **M. Klemm, I. Kovacs, G. Pedersen, and G. Toster**, "Novel small-size directional antenna for UWB WBAN/ WPAN applications,'' *IEEE Transactions and Propagation*, vol. 53, no. 12, pp. 3884-3896, Dec. 2005.

[63] **A. Alomainy, Y. Hao, X. Hu, C.G Parini, and P.S Hall**, " UWB on-body radio propagation and system modelling for wireless body-centric networks,'' *IEE proceedings communications*-Special Issue on Ultra Wideband Systems, technologies and Applications, vol. 153, no.1, pp 107-114, Feb. 2006.

[64] **T. P. See and Z. N. Chen**, "Experimental characterization of UWB antennas for on-body communications," *IEEE Transactions on Antennas and Propagation*, vol. 57, no. 4, pp. 866– 874, April Apr. 2009.

[65] **Klemm and G. Troster**, "Characterisation of an aperture-stacked patch antenna for ultra-wideband wearable radio systems," *15th International Conference on Microwaves, Radar and Wireless Communications, 2004*, vol. 2, pp. 395–398, May 2004.

[66] **S. Promwong, W. Hachitani, G. S. Ching, and J. Takada,** " Characterization of ultrawide band antenna with human body," *International Symposium on Communications and Information Technology (ISCIT 2004), Sapporo, Japan*, pp. 1213–1217, October 2004.

[67] **W. L. Stutzman and G. A**. Thiele, Antenna theory and design. John Wiley & Sons, Ltd., 1998.

[68] **K. Y. Yazdandoost and R. Kohno**, "Ultra wideband antenna," I*EEE Communications Magazine,* vol. 42, no. 6, pp. S29–S32, June 2004.

[69] **P. R. Foster**, "UWB antenna issues," *IEE Seminar on UWB Communication*s, London, UK, July 2004.

[70] **H. G. Schantz**, "Introduction to ultra-wideband antennas," *IEEE Conference on Ultra Wideband Systems and Technologies,* pp. 1–9, November 2003.

[71] F.C.C (FCC), "FCC first report and order, revision of the part 15 Commission's rules regarding Ultra-Wideband transmission systems,'' *ET Docket,* pp.98-153, April 22, 2002.

[72] **A. Alomainy,, Y. Hao, C. G. Parini, and PS Hall**, "Comparison between two different antennas for UWB on body propagation measurements,*'' IEEE Antennas and Wireless Propagation Letters.*

[73] **A. Sani, A. Alomainy, G. Palikaras, Y. Nechayev, C. Parini and P. S. Hall**, "Experimental Characterization of UWB on-Body Radio Channel in Indoor Environment Considering Different Antennas,*'' IEEE Transactions on Antennas and Propagation,* Vol. 8, page 238-241, Jan. 2010.

[74] **Q. Wang, J. Wang**, "Performance of on-body chest to waist UWB communication links,'' *IEEE microwave and wireless components let*, vol.19. 2. Feb. 2009.

[75] **Q.H. Abbasi, A. Sani, A. Alomainy and Y.Hao**, "Arm movements effect on Ultra wideband on-body propagation channels and radio systems, *Antenna and prop. Conference, 2009,* Loughborough, UK.

[76] **A. Alomainy, Q. H. Abbasi, A. Sani, and Y.Hao**, "System level modelling of optimal ultra wideband body centric wireless network,'' *APMC 2009, Singapore*.

[77] **A. Alomainy, Y. Hao, X. Hu, C.G Parini, and P.S Hall**, "UWB on-body radio propagation and system modelling for wireless body-centric networks,'' *IEE proceedings communications*-Special Issue on Ultra Wideband Systems, technologies and Applications, vol. 153, no.1, pp 107-114, Feb. 2006.

[78] **Y. H. Y. Zhao, and Clive Parini**, "FDTD characterization of UWB indoor radio channel including frequency dependent antenna directivities, *IEEE antenna and wireless propagation letters* vol. 6. Pp-191-194, 2007.

[79] **A. A. Goulianos, T. W. Brown and S. Stavrou**, "Ultra-Wideband measurement and results for sparse off-body communication channels,'' 2008 *Loughborough Antennas and Propagation Conference,* 17-18 March, 2008, Loughborough, UK.

[80] **P. A. Caterwood and W. G. Scanlon**, "Link characteristics for an off-body UWB transmitter in a hospital environment, *Loughborough antennas and propagation conf.*, Nov. 2009.

[81] **P.A. Catherwood & W.G. Scanlon**, " Off-body UWB channel characterisation within a hospital ward environment,' *Intl. J. Ultra Wideband Communications & Systems*, Special issue on Applications of Ultra Wideband Systems in Biomedicine, Vol. 1, 4, pp. 263-272, 2010.

Chapter 4 Narrowband Antenna Characterisation and Specifications for Body-Centric Wireless Communications

With the rapid development of biosensors and wireless communication devices bring new opportunities for body-centric wireless networks (BCWNs) which have recently received increasing attentions due to their promising applications in medical sensor systems and personal entertainment technologies [1-5]. Antennas play a vital role in optimizing the radio system performance. The design of a power-efficient and reliable on-body communication system, requires suitable antennas which therefore require accurate understanding of the human body effects on the antenna performance parameters and radio propagation channels. This chapter investigates and compares the on-body performance parameters of five different narrowband antennas at 2.45 GHz, specially the Wire Monopole, Patch, Printed Monopole, Inverted L and Loop antennas. It provides an understanding of the human body effect on antenna parameters such as frequency detuning, impedance bandwidth, gain, impedance, radiation pattern, polarisation and radiation efficiency. The effects of body-worn antenna types on the on-body radio channels are also investigated. Based on the study, a novel dual-band and dual-mode (DBDM) antenna is proposed for power-efficient cooperative on-body and off-body communications. The on-body performance parameters of the DBDM antenna at 2.45 GHz are compared with the other five narrowband antennas. The main aim of this study is to specify the suitable narrowband antenna for body-centric wireless communications. Based on the study in this chapter, narrowband antenna specifications and design guidelines for body-centric wireless communications are provided at the end of this chapter. These conclusions may be broadly applicable in narrowband systems at other frequencies.

4.1 Narrowband Wearable Antennas

4.1.1 Microstrip-Fed Patch Antenna

Rectangular patches represent the simplest and most widely-used configuration of microstrip printed antennas. The Patch is a low-cost printed antenna that can be easily fabricated and

integrated with other radio system components and potentially made conformal to the human body. Microstrip patches only radiate close to their resonance frequency; which leads to the fact that their main dimension is usually a half wavelength at the operating frequency. The microstrip patch was designed to operate at 2.45 GHz with radiator length of $\lambda_{eff}/2$ Fig. 4.1 shows the schematic design of the rectangular patch with detailed dimensions [6]. The radiator dimensions are 34 mm×39.5 mm; the total board size is 60×80 mm^2, printed on RT/Duroid board with $\varepsilon_r = 3$ and a thickness of 1.524 mm. The antenna is fed by 50 Ω coaxial cable, which requires good matching with the antenna impedance to obtain sufficient matching. The matching configuration used is the quarter-wavelength transformer between the 50 Ω (Z_0) input and antenna impedance (Re [Z]) = 120 Ω, [6] where the $\lambda/4$ impedance is defined as

$$Z_{\lambda/4} = \sqrt{Z_L Z_0} \qquad (4.1)$$

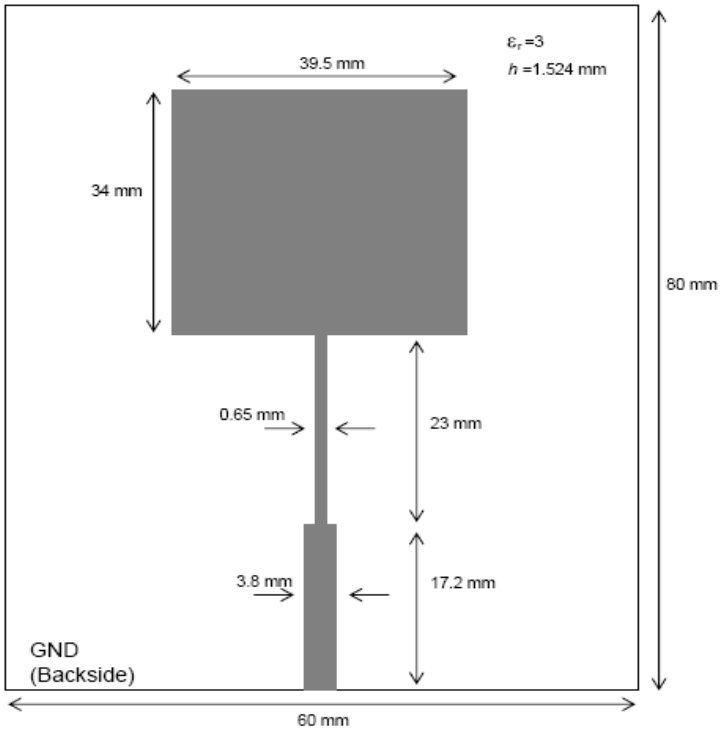

Fig. 4.1. Schematic diagram of the rectangular patch antenna for on-body communications at 2.45 GHz [6].

The ground plane in the patch antenna covers the back of the board, providing good shielding of the radiating element from the lossy human tissues when the antenna used for body-worn applications. The patch shows directive radiation characteristics. Major operational disadvantages of microstrip antennas include their lower efficiency, lower power, poor polarisation purity, high Q factor, spurious feed radiation and very narrow bandwidth [7]. The impedance bandwidth of a patch antenna is strongly influenced by the spacing between the patch and the ground plane. As the patch is moved closer to the ground plane, less energy is radiated and more energy is stored in the patch capacitance and inductance: that is, the quality factor Q of the antenna increases.

4.1.2 Wire Monopole Antenna

Monopole antennas have found extensive applications in many wireless communication systems, such as airborne and ground-based communication systems, over a wide range of frequencies. This is because of their desirable features; pure vertical polarisation and an omnidirectional radiation pattern in the horizontal plane. The schematic diagram of Wire Monopole is shown in the Fig. 4.2. The antenna is fed through a ground plane by a coaxial probe. The antenna is quarter-wavelength vertical Monopole which has been used in many measurments of on-body communication at the University of Birmingham [8-9]. The length of the vertical wire is 29 mm with the diameter of 3 mm and the overall ground plane size is 90×90 mm^2.

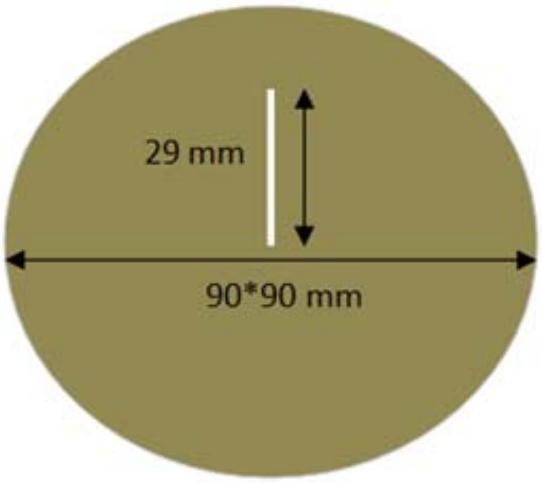

Fig. 4.2. Schematic diagram of the Wire Monopole antenna on the ground plane for on-body communications at 2.45 GHz [8-9].

4.1.3 Printed Monopole Antenna

An antenna operating near a perfect ground plane produces two rays at each observation angle, a direct ray from the antenna and a reflected ray from the ground plane [10]. This is the basis of the image theory applied in antenna designs to provide modified antennas with reduced size and improved gain and efficiency. The monopole is a dipole with the lower half of the antenna replaced by the ground plane, against which the radiator is fed. The radiating element of the planar monopole antenna is designed on the FR4 board with $\varepsilon_r = 4.6$ and thickness of 1.6 mm. Fig. 4.3 shows the schematic diagram of the printed monopole antenna for on-body communication at 2.45 GHz [11]. The total board size is 80×70 mm^2, with the ground plane printed on the back of the board with size optimised to obtain good matching at the frequency band of interest to produce the corresponding image of the electric field induced on the monopole [12]. A 50 Ω impedance line is applied to feed the radiator, which is of the same width. The antenna shows an omnidirectional radiation pattern. There is a partial ground plane at the back of the printed monopole antenna; see Fig. 4.3.

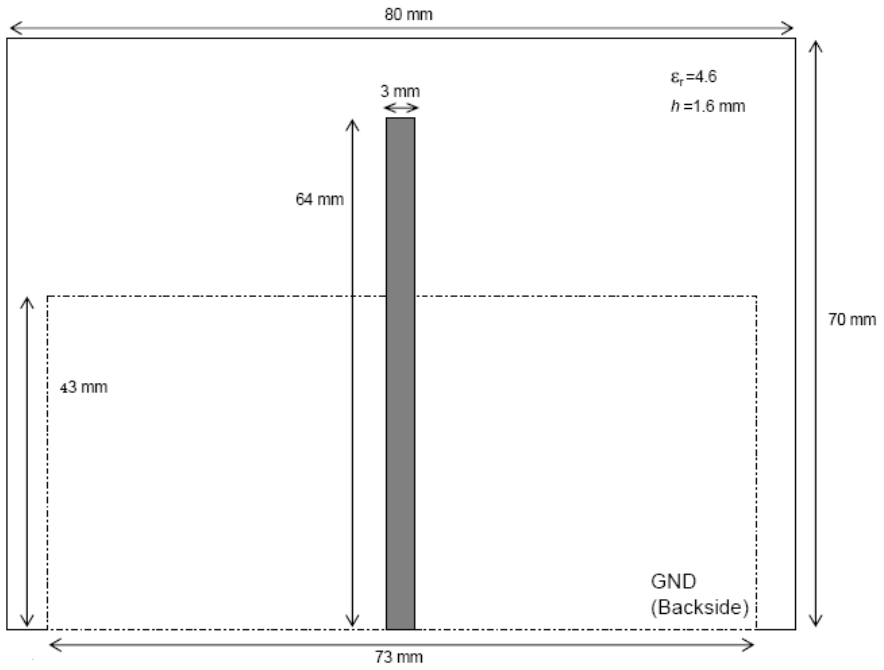

Fig. 4.3. Schematic diagram of the Printed Monopole antenna for on-body communications at 2.45 GHz [11-12].

4.1.4 Inverted L Antenna

The Inverted L is a modified monopole (bent monopole), aiming for antenna size reduction and improved omnidirectional radiation. The antenna is printed on FR4 substrate, with a total board size of 50×70 mm^2, 1.6 mm thickness, with $\varepsilon_r = 4.6$ and conductivity 0.001 S/m. Fig. 4.4 shows the schematic diagram of the Inverted L. There is a partial ground plane at the back of the antenna, with a size of 50 mm×45 mm^2. The antenna radiation pattern shows directive patterns, with a slight deformation compared with conventional monopole patterns, due to the addition of the horizontal radiating section of the antenna [13-14].

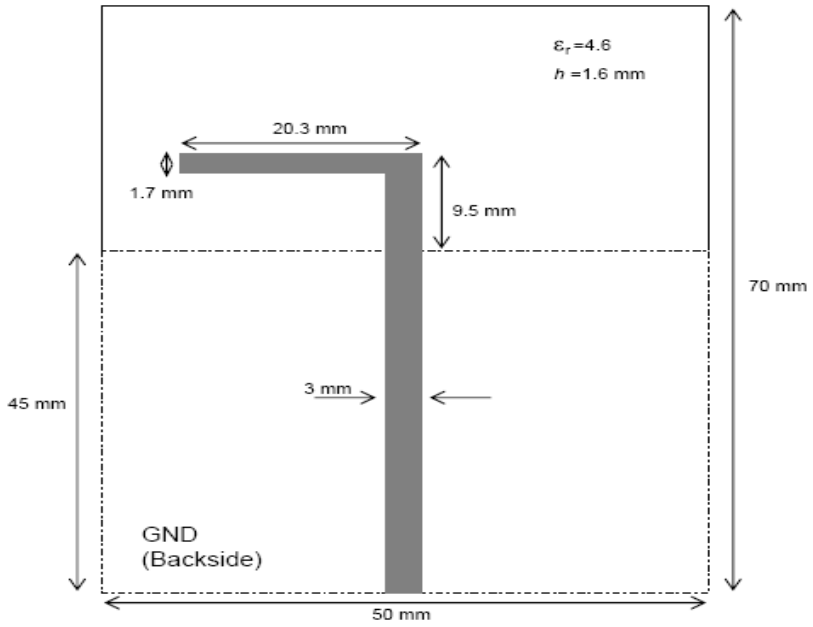

Fig. 4.4. Schematic diagram of the Inverted L antenna for on-body communications at 2.45 GHz [13-14].

4.1.5 Printed Circular Loop Antenna

The circular loop is printed on FR4 board with ε_r=4.6 and thickness of 1.6 mm. The total size of the board is 60 x 60 mm^2 [15]. There is also a partial ground plane at the back of the proposed circular loop antenna. The size of the ground plane of the loop is the lowest of all the narrowband antennas used in this study. Fig. 4.5 shows the schematic diagram of printed circular loop. The antenna radiation performance shows slightly directive patterns [7, 15].

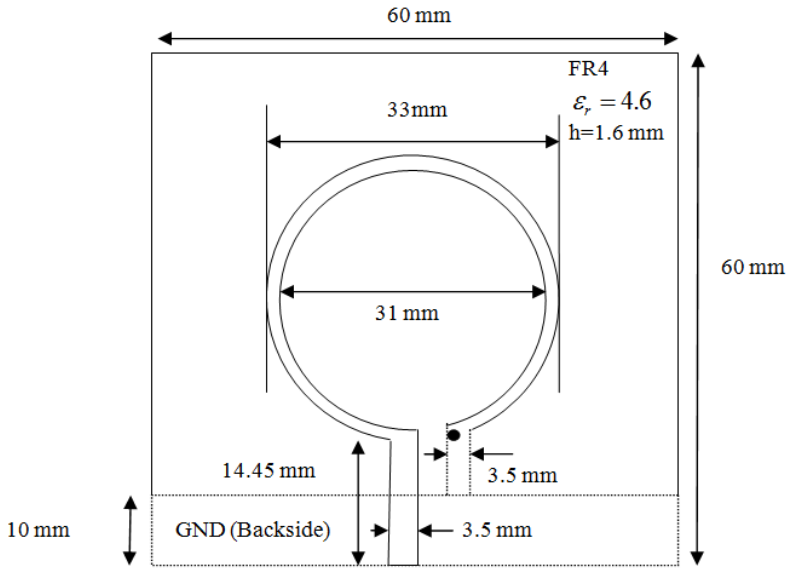

Fig. 4.5. Schematic diagram of the Printed Circular Loop antenna for on-body communications at 2.45 GHz [7, 13].

4.1.6 Volume and Size Comparison of the Narrowband Antennas

The size and volume of the narrowband antennas used in this study are shown in Table 4.1. All antennas are printed on FR4 substrate, excpet for the Patch (RT/Duroid) and Wire Monopole. Out of the six antennas, two (Patch, Wire Monopole) have a full ground plane at the back and the other three (Printed Monopole, Loop, Inverted L) have partial ground plane. The proposed antennas used for this study work in the frequency band of 2.45 GHz. Out of the five antennas, the Loop has the smallest ground plane size; in comparison, the Wire Monopole has the highest volume.

Table 4.1. Comparison of volume and size of the narrowband antennas used in this study.

Antenna	**Substrate L×W (mm^2)**	ε_r	**Ground Plane L×W (mm^2)**	**Height (mm)**	**Volume L×W×H (mm^3)**	**Antenna Element L×W(mm^2)**
Patch	80×60	3	80×60	1.524	80×60×1.524	74.2×39.5
Wire Monopole	-	-	90×90	29.3	90×90×29.3	23.3×0.35
Printed Monopole	70×80	4.6	43×73	1.6	70×80×1.6	64×3
Inverted L	70×50	4.6	45×50	1.6	70×50×1.6	54.5×20.3
Circular Loop	60×60	4.6	10×60	1.6	60×60×1.6	47.5×33

4.2 Narrowband Antenna Performance Parameters Comparison

4.2.1 Frequency Detuning

For this study, S11 measurement campaigns were performed in an anechoic chamber at Queen Mary, University of London. An average-sized male, with a height of 1.74 m and a weight of 80 kg was used. The presented five different narrowband antenans were placed on various locations of the human body, varying the distance between the antenna and the body; see Fig. 4.6. During the measurement, the antennas were placed directly on the body, and then placed at 1, 4, 8 and 16 mm away from the body. Due to the back feed, the Wire Monopole antenna was placed at 16 mm away form the body only. The spacing was realised by putting foam blocks (ε_r=1.08) between the antennas and the body.

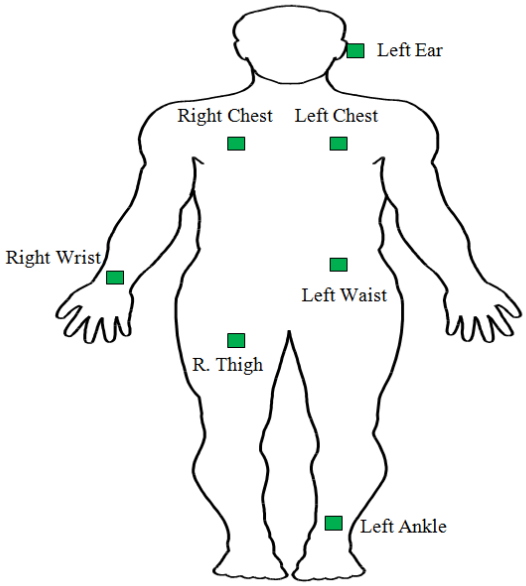

Fig. 4.6. Antenna positions on the human body for S11 measurements.

Fig. 4.7 presents the percentage of frequency detuning from free space resonance for the different antennas when placed at various distances away from the body (left side of the waist). The resonance frequency detunes from the free space value, up to maximum of 33 % (Inverted L

antenna), when the antenna placed on the body. The frequency detuning is due to the changes in the antennas effective length, caused by the presence of the human lossy tissue. The antennas with partial ground plane (Printed Monopole, Loop, and Inverted L) experience the highest frequency detuning, while the antennas with full ground plane (Patch and Wire Monopole) do not experience any frequency detuning. The ground plane acts as a shield between the antenna and the body, resulting in no frequency detuning for patch and wire monopole antennas. Results show that, as the distance between the antenna and the body increases, the frequency detuning reduces.

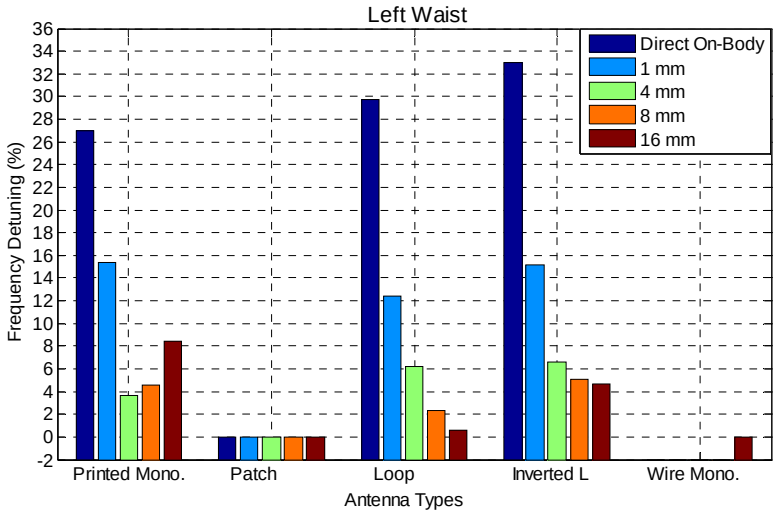

Fig. 4.7. Comparison of frequency detuning in percentage for presented five narrowband antennas when placed at different distances from the left side of the waist (due to back feed the wire monopole antenna was placed 16 mm away from the body only).

The distance to place the antenna from the human body has higher effect in frequency detuning for the Printed Circular Loop, Inverted L and Printed Monopole antennas (antenna with partial ground plane) while it has no effect for the Patch antenna (antenna with full ground plane). For different distances to place the antenna from the body, maximum of 29.14 % variation of frequency detuning occurs which is noticed for the Loop antenna when it is placed direct on the body and 16 mm away from the body. The frequency detuning for each antenna is averaged over the antenna placement distances from the body (direct on the body, 1, 4, 8, and 16 mm). Table 4.2 summarises the mean frequency detuning and standard deviation of different antenna placement distances for different narrowband antennas. On the body, the Inverted L antenna shows the highest average frequency detuning. The highest standard deviation values are

noticed for the Inverted L and Loop antennas which show that these two antennas have higher variation of frequency detuning due to different antenna placement distances from the body.

Table 4.2. Average frequency detuning and standard deviation of different antenna placement distances for five narrowband antennas. (Frequency detuning for each antenna was averaged over various distances to place the antenna on the body).

Antenna	Mean (%)	Standard Deviation (%)
Printed Monopole	11.84	9.65
Patch	0	0
Loop	10.24	11.80
Inverted L	12.89	12.02
Wire Monopole	0	0

Fig. 4.8 shows a comparison of frequency detuning in percentage for the different narrowband antennas when placed at various locations, direct on the body. When antenna placed on different locations of the body due to changes in human tissue physiological and electrical properties the frequency detuning varies, up to maximum 23.8 %. This happens for the Loop antenna when it is placed directly on the left ankle and right side of the chest. Fig. 4.9 and 4.10 show the return loss curves of the Loop and Patch antennas when placed on seven different locations of the body directly.

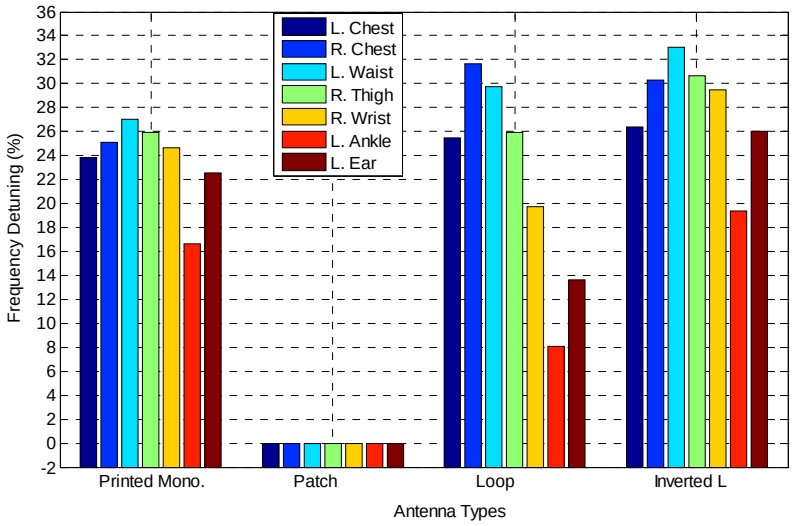

Fig. 4.8. Comparison of frequency detuning in percentage for four narrowband antennas when placed at different locations on the body directly (Since wire monopole was placed only at 16 mm away from the body, it was not included in the graph).

For different locations on the body, the variation of frequency detuning is significant for the antennas with partial ground plane and insignificant for antenna with full ground plane. Due to having the smallest ground plane (Table 4.1), the Loop antenna experiences the highest effects from the human lossy body, resulting the highest variation of frequency detuning when placed at different locations on the body. The maximum frequency detuning variation for the other antennas (Printed Monopole, Inverted L and Patch) is 13.11 %, 13.6 %, 0 %, respectively. For all antennas, the frequency detuning is the greatest when the antenna is placed on the left waist and right side of the chest, while the lowest is on the left ankle.

For each antenna, the frequency detuning (as shown in Fig. 4.8) of different on the body locations was averaged. Table 4.3 lists the average frequency detuning and standard deviation of different on body locations for four different antennas. The Inverted L antenna shows the highest average frequency detuning of 27.88 %. Results show that the Loop antenna shows the highest standard deviation value which indicates that, for different on-body locations, it has higher effect in the frequency detuning.

Table 4.3. Average frequency detuning and standard deviation of seven different locations of the body for four narrowband antennas. (Frequency detuning for each antenna was averaged over different locations of the body).

Antenna	Mean (%)	Standard deviation (%)
Printed Monopole	23.68	3.41
Patch	0	0
Loop	22.03	8.66
Inverted L	27.88	4.46

For the on-body case, due to capacitive coupling between the antenna and the body, the antenna impedance changes, which causes variation of the return loss; see Figs. 4.9 and 4.10. As compare to the Loop, the antenna impedance changes less for the Patch antenna and, hence lower variation of the return loss is observed for the later case.

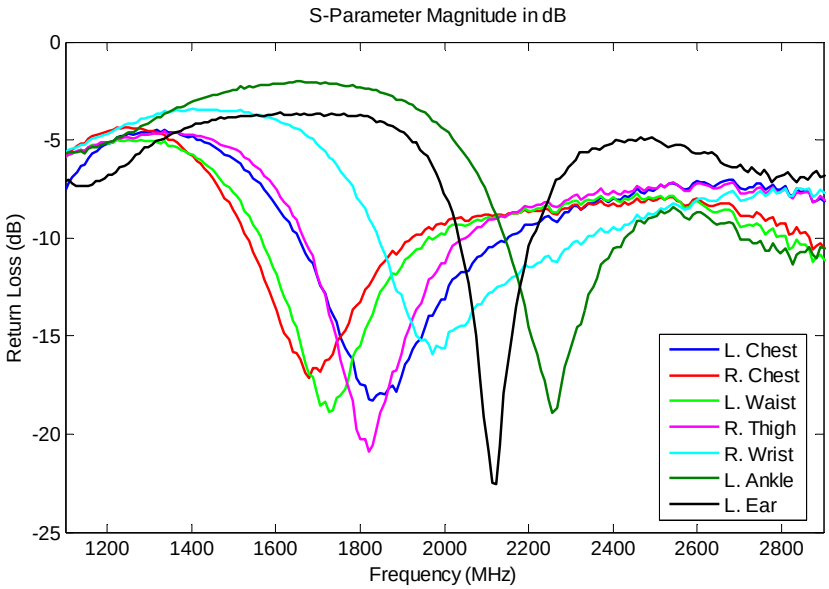

Fig. 4.9. Return loss curves of the loop antenna when placed on seven different locations of the body directly.

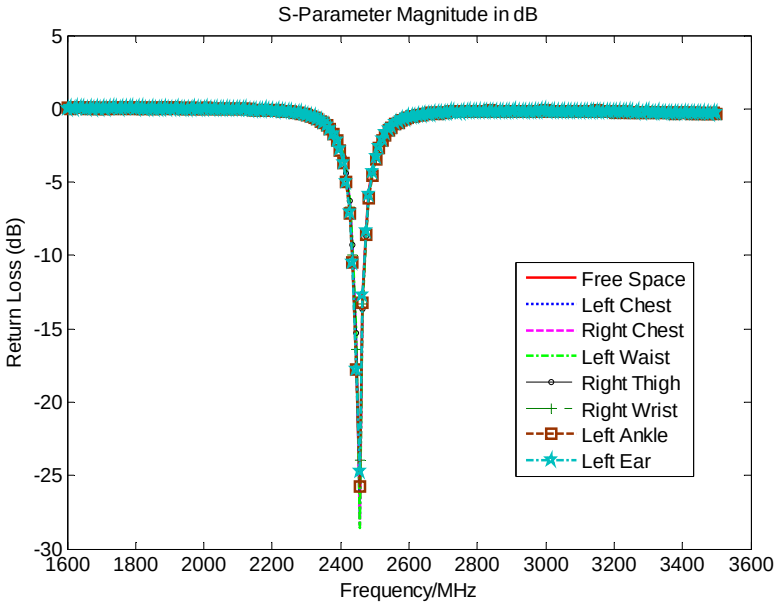

Fig. 4.10. Return loss curves of the patch antenna when placed on seven different locations of the body directly.

4.2.2 On-Body Bandwidth

The impedance bandwidth of the five different narrowband antennas was extracted from the measured S11 results; see Fig. 4.6. For this study, impedance bandwidth was calculated for a

return loss of -10 dB. Fig. 4.11 shows a comparison of impedance bandwidth as a percentage for the five different narrowband antennas, with respect to distance from the body (right side of the chest). In this study, when antennas were placed on the body, the impedance bandwidth mostly increased from the free space value, up to a maximum of 84.52% (Printed Monopole antenna). On the body, the impedance bandwidth of the antenna increases due to the loss from the human body. The impedance bandwidth increase is significant for the antennas with partial ground plane. The use of Printed Monopole, Inverted L and Loop antennas on the body, the frequency detunes from free space significantly; however, the impedance bandwidth increases greatly. Varying the distance between the antenna and the body doesn't affect the impedance bandwidth much for the Patch antenna, whereas the impedance bandwidth varies to a large extent with separation for the Printed Monopole, Inverted L and Loop. Out of these five antennas, the Path antenna shows the lowest on body impedance bandwidth (maximum up to 1.38 %).

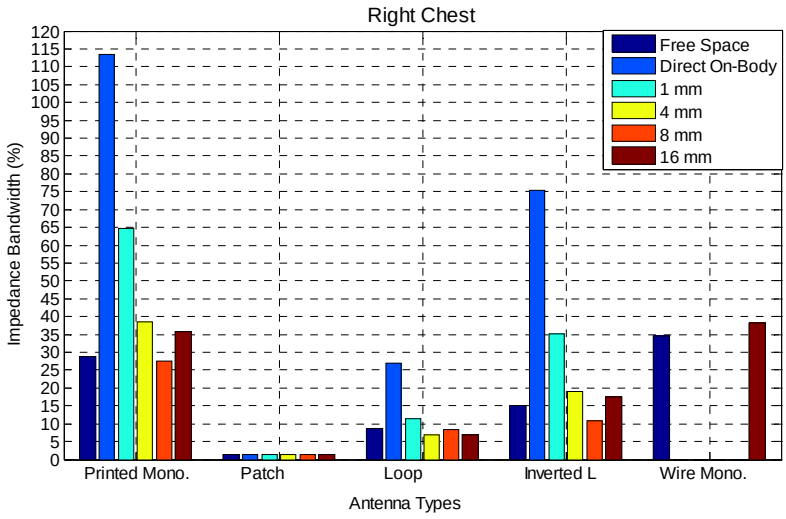

Fig. 4.11. Comparison of impedance bandwidth in percentage for five different narrowband antennas when placed at different distances from the right side of the chest. (-10 dB return loss impedance bandwidth is considered).

The on-body impedance bandwidth for different distances from the body of each antenna case was averaged as a function of distance. Table 4.4 summarises the average on-body impedance bandwidth and standard deviation of different distances from the body for four narrowband antennas. On the body, the highest average impedance bandwidth is noticed for the Printed

Monopole antenna, whereas the highest standard deviation value is noticed for the Inverted L and Printed Monopole antennas.

Table 4.4. Comparison of average on-body impedance bandwidth and standard deviation of various antenna placement distances for four narrowband antennas (the on-body bandwidth of different distances from the body was averaged as a function of distance).

Antenna	Mean (%)	Standard Deviation (%)
Printed Mono.	55.94	35.00
Patch	1.38	0
Loop	12.11	8.58
Inverted L	31.58	26.03
Wire Mono.	-	-

Fig. 4.12 shows the comparison of on-body impedance bandwidth as a percentage for the different narrowband antennas when placed at various locations, direct on the body. When antennas placed on various locations direct on the body, the impedance bandwidth varies up to a maximum of 85.35 %. This occurred for the Printed Monopole when it is placed on the right side of the chest and on the left ear. Due to different on body locations, the impedance bandwidth variation is significant for the Printed Monopole (maximum 85.34 %), Inverted L (maximum 43.46 %) and Loop (maximum 19.09 %) and insignificant for the Patch antenna (maximum 0.08 %). In most of the cases, the highest on-body impedance bandwidth is noticed when antenna placed on the right side of the chest.

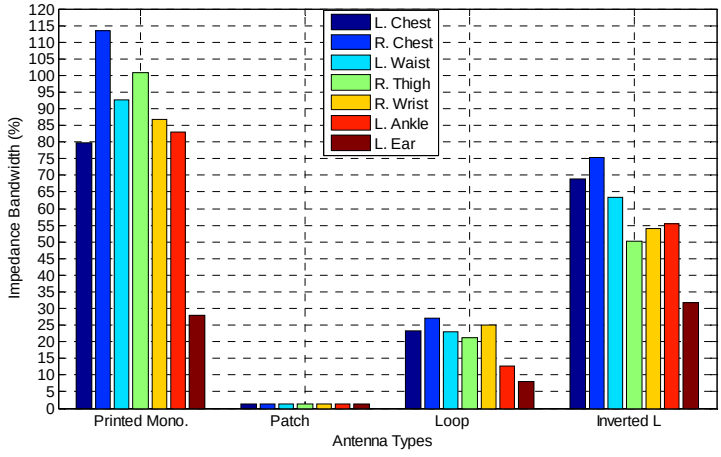

Fig. 4.12. Comparison of on-body impedance bandwidth in percentage for different narrowband antennas when placed at different locations directly on the body.

Similarly to what has been done for the frequency detuning, the on-body impedance bandwidth for each antenna is averaged over different locations of the body. Table 4.5 lists the average impedance bandwidth and standard deviation of different on body locations for four different narrowband antennas. Out of these four antennas, the average on-body impedance bandwidth and standard deviation are found to be the highest for the Printed Monopole antenna.

Table 4.5. Average on-body impedance bandwidth and standard deviation of different locations of the body for four narrowband antennas.

Antenna	Mean (%)	Standard Deviation (%)
Printed Mono.	83.50	27.01
Patch	1.41	0.03
Loop	20.04	7.01
Inverted L	57.00	14.21

4.2.3 Radiation Efficiency

The antenna radiation efficiency parameter was extracted from the simulation results. The on-body simulation set-up is shown in Fig. 4.13. In this case, the antenna was simulated placing in free space and then at 1, 4, 8 and 16 mm away from the human phantom (right side of the chest) using CST microwave studio ^{TM}. The human body employed is the commonly available detailed multi-layer model (Fig. 4.13) namely the 'visible male model' developed by the US air force [17]. The resolution of the model applied is 4 mm with the electrical properties of human tissues defined at 2.45 GHz for all organs and tissues used including heart, lungs, muscle, fat, skin, etc [18-19].

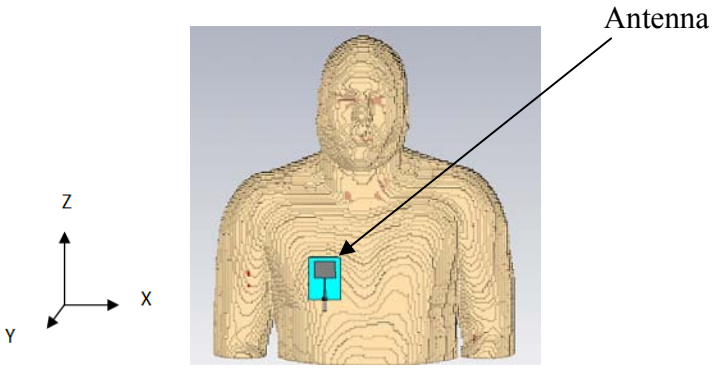

Fig. 4.13. Human phantom used for simulation showing antenna location and orientation on the body during simulation.

Due to power absorption by the human lossy tissues, the radiation efficiency for all five presented antennas reduces from free space when placed on the body. Fig. 4.14 shows the reduction of radiation efficiency from that of free space (in percentage) for the narrowband antennas when placed at various distances from the body (right side of the chest). Placing the antennas at 1 mm away from the body, the highest radiation efficiency reduction of 96 % is noticed for the Inverted L, while the lowest is noticed for the Patch (20%). The Loop, Inverted L and Printed Monopole show nearly the same trends of the radiation efficiency reduction. Due to having full ground plane at the back, the radiation efficiency reduces less for the Patch and Wire Monopole. For all narrowband antenna cases, as the distance between the body and the antenna increases the radiation efficiency reduces the less. Results show that regardless of the antenna type, reasonable on-body radiation efficiency is noticed when placed at 8 mm away from the body. However, for the antenna with full ground planes, reasonable radiation efficiency is still achieved at very lower distance (1 mm).

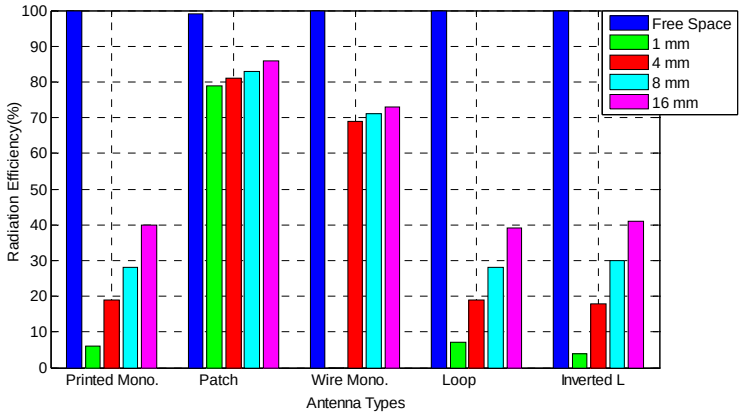

Fig. 4.14. Comparison of radiation efficiency in percentage for five different narrowband antennas when placed on various distance from the body on right side of the chest. (In simulation, the Wire Monopole antenna was placed on 4, 8 and 16 mm from the body).

The on-body radiation efficiency of different distances from the body for each antenna was averaged as a function of distance. Table 4.6 summarises the average on-body efficiency and standard deviation of different distances from the body for five narrowband antennas. On the body, the Patch antenna shows the highest average on-body radiation efficiency (82%) while the other three antennas (Printed Monopole, Loop and Inverted L) show the lowest (23%). The lower standard deviation values (3, 2) are noticed for the Patch and Wire Monopole which indicate that

for different separation distances, these two antennas have the lowest effect on the on-body radiation efficiency.

Table 4.6. Average radiation efficiency and standard deviation of various separation distances between the antenna and the body for five narrowband antennas (the radiation efficiency was averaged over various distances).

Antenna	Mean (%)	Standard Deviation (%)
Printed Mono.	23.25	14.36
Patch	82.25	3
Wire Mono.	71	2
Loop	23.27	13.57
Inverted L	23.20	15.90

4.2.4 Gain

The gain parameter in free space and 1, 4, 8 and 16 mm away from the body of five narrowband antennas was extracted from the simulated results as was done for the radiation efficiency.

Peak Gain

Fig. 4.15 shows the comparison of free space and on-body gain for the presented five different narrowband antennas, when placed at different distances on the body (right side of the chest). Placing the antenna on the body, the gain drops by a maximum of 12.39 dB (Inverted L); however, gain increases by a maximum of 1.6 dB for the Wire Monopole. On the human body, the gain drops for the antennas with partial ground planes (Printed Monopole, Inverted L and Loop) and increases mostly for the antennas with full ground plane (Patch and Wire Monopole). For the antennas having partial ground plane, higher power absorption occurs from the human lossy tissues resulting in a dramatic decrease of antenna gain. When the antenna placed on the human body, the curvature of the human body contributes to improve the directivity of the antenna which results higher gain for some on-body antennas.

In this study, when the antenna was placed at 1 mm away from the body, the lowest gain is noticed for the Inverted L (-8.68 dBi), while the highest is noticed for the Patch (6.58 dBi). Even though, the free space gain of the Inverted L is the same as Printed Monopole, it shows the lowest gain on the body, which can be due to the smaller size of the Inverted L. For on-body applications, if we don't want the full ground plane at the back of the wearable antennas, they need to be placed at 8 or 16 mm away from the body, because at these distances the antennas

show acceptable gain (Fig. 4.15). The optimum distance to place the narrowband antenna from the body is therefore recommended to be 8 mm or 16 mm.

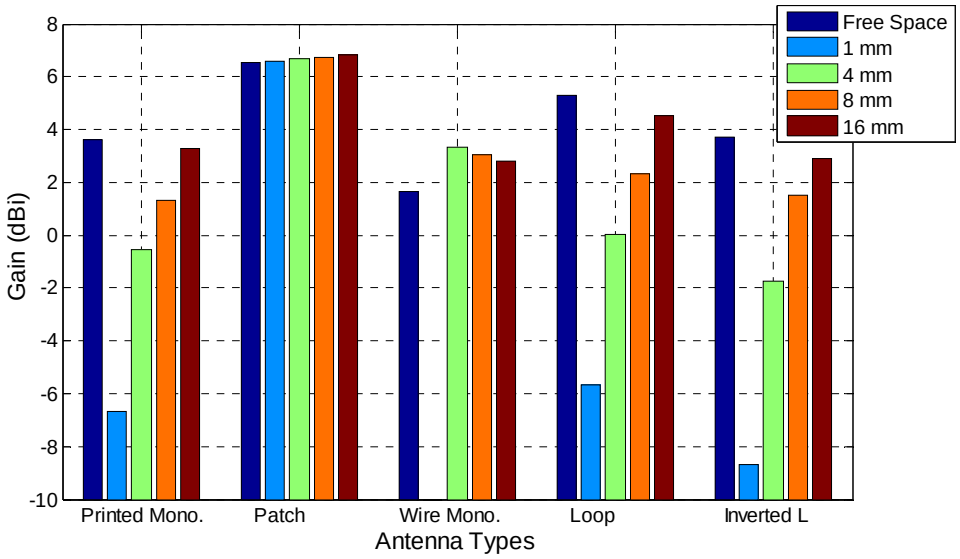

Fig. 4.15. Comparison of gain for five different narrowband antennas when placed at various distances from the body on right side of the chest. (The gain has been considered for the maximum radiation). Due to back feed, in simulation, the Wire Monopole was placed at 4, 8 and 16 mm from the body.

The on-body peak gain of different separation distances from the body for each antenna case was averaged. Table 4.7 lists the average on-body peak gain and standard deviation of different distances from the body for five narrowband antennas. Results show that when the antenna placed at various distances from the body, the variation of on body gain is smaller for the Patch and the Wire monopole antennas while it is found to be higher for the Inverted L antenna. The antenna placement distance has very high effect on the on-body gain for the Inverted L, Loop and Printed Monopole antennas. However, varying the distance between the antenna and the body does not have much effect on the on-body gain for the Patch and Wire Monopole antennas. For these two antennas, even at very close to the body, very good on-body gain is noticed. For different narrowband antennas used in this study, the average on-body peak gain varies maximum up to 8.20 dB which is significant (Table 4.7). The use of Loop, Printed Monopole, Inverted L increases the impedance bandwidth; however, high absorption from the human body reduces drastically the radiation efficiency and gain.

Table 4.7. Average peak gain and standard deviation of different separation distances for five narrowband antennas (the on-body peak gain for each antenna was averaged over four separation distances of antenna placement).

Antenna	Mean (dBi)	Standard Deviation (dBi)
Printed Mono.	-0.65	4.32
Path	6.70	0.10
Wire Mono.	3.07	0.27
Loop	0.30	4.37
Inverted L	-1.48	5.17

The on body gain for the presented five different narrowband antennas has been analysed plane wise such as XZ and YZ planes.

XZ Plane Gain

Fig. 4.16 shows the comparison of XZ (azimuth) plane gain for five different narrowband antennas when placed at various distances from the body (right side of the chest). The Wire Monopole antenna has the highest on-body gain in the XZ plane; thus will contribute to power efficient on-body communication. In this plane, the lowest gain (-11 dBi) is noticed for the Inverted L antenna (at 1 mm away from the body). The gain drops significantly compared to free space for the Loop (maximum 15.6 dB).

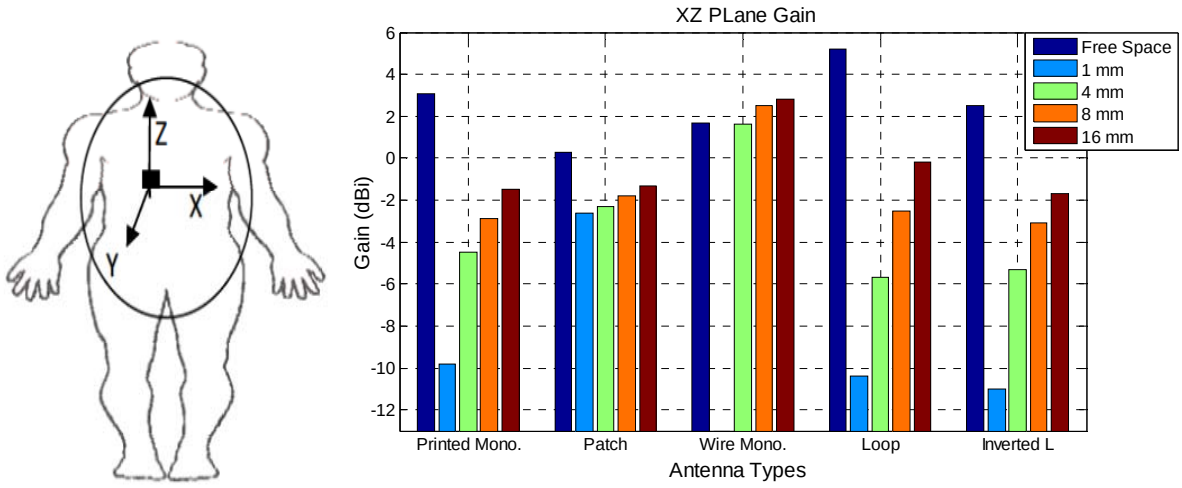

Fig. 4.16. Comparison of XZ plane gain for five different narrowband antennas when placed at various distances from the body (right side of the chest).

The XZ plane average on-body gain and standard deviation of different separation distances for five narrowband antennas are tabulated in Table 4.8. In the XZ plane, the Patch has an average of 4.3 dB less gain compared to the Wire Monopole. Though the patch antenna has good on-body performances in terms of frequency detuning, efficiency and peak gain, it shows very low gain in the XZ plane. The XZ plane gain values for the Loop, Printed Monopole and Inverted L are very low compared to the Wire Monopole antenna. For different antennas, a maximum variation of averaged gain is noticed to be 7.58 dBi.

Table 4.8. Average XZ plane gain and standard deviation of different separation distances from the body for five narrowband antennas.

Antenna	Mean (dBi)	Standard deviation (dBi)
Printed Mono.	-4.67	3.62
Patch	-2	0.57
Wire Mono.	2.30	0.63
Loop	-4.70	4.42
Inverted L	-5.28	4.10

YZ Plane Gain

The YZ plane gain of the five narrowband antennas in terms of distances is shown in Fig. 4.17. Though the patch shows less on body gain in the XZ plane, it has the highest gain in the YZ plane (off-body direction). The Inverted L antenna also shows the lowest gain in this plane. The antenna with higher gain in the YZ plane will contribute to provide power-efficient communication for off-body radio channels (i. e,. communication from on-body devices to off-body devices). Table 4.9 lists the YZ plane average on-body gain and standard deviation of different separation distances for five narrowband antennas. The Wire Monopole also shows good on-body gain in the YZ plane and the gain is nearly stable at various separation distances from the human body.

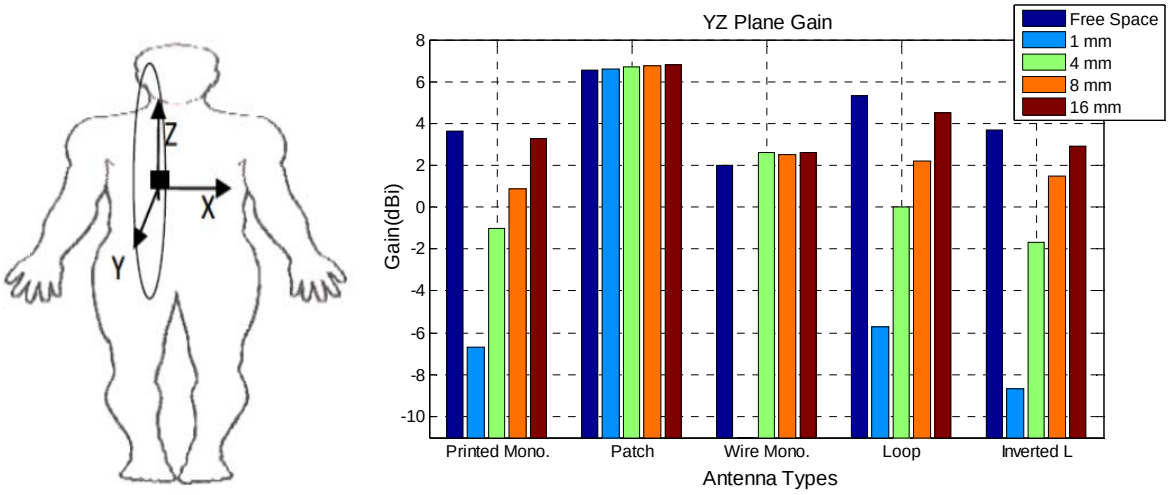

Fig. 4.17. Comparison of YZ plane gain for five different narrowband antennas when placed at various distances from the body (right side of the chest).

Table 4.9. Average YZ plane gain and standard deviation of different separation distances for five narrowband antennas.

Antenna	Mean (dBi)	Standard Deviation (dBi)
Printed Mono.	-0.87	4.25
Patch	6.71	0.10
Wire Mono.	2.56	0.06
Loop	0.25	0.44
Inverted L	-1.5	5.17

4.2.5 Radiation Pattern

The free space radiation pattern of the Wire Monopole antenna is quite omnidirectional over the body surface (in the XZ plane) and there is a presence of null in the Y direction [8-9] while the free space radiation of the Patch antenna is directive towards the Y direction (off-body direction) [6-7]. The Printed Monopole and Inverted L antennas show nearly the same free space radiation performances as omnidirectional in the XY plane. There is a presence of null to the Z direction in the radiation pattern of the Printed Monopole and Inverted L antennas [12, 13]. The free space radiation pattern of the Loop antenna is directive towards the Z direction; however, it also radiates omnidirectional in the XY direction with slight loss in the radiation pattern in both

direction of X [15]. Placing the narrowband antennas on the body, the radiation patterns do not deform for the Patch and Wire Monopole antennas while for the Printed monopole, Inverted L and Loop antennas, the radiation patterns deform notably (the radiation patterns become directive towards off-body direction).

The radiation patterns of the five different narrowband antennas at 2.45 GHz was measured in the anechoic chamber by placing them on the same subject used for S11 measurement. The on-body radiation patterns of five antennas were analysed for two different principle planes such as XZ (over body surface) and YZ (off-body direction). Figs. 4.18 (a) and (b) show the simulated XZ (azimuth) plane co-and cross-polar on-body radiation patterns of the five narrowband antennas when placed 1 mm away from the body, while Figs 4.18 (c) and (d) show the measured patterns. During simulation, the Wire Monopole was placed 4 mm away from the body and 16 mm during measurement. The simulated co-and cross-polar radiation patterns broadly agree with the measurements, except for a slight variation in some cases, which can be due to the effects of the cables.

The Wire Monopole shows quite omnidirectional co-polar radiation patterns in the XZ plane, both for simulation and measurement. For on-body communications, antennas with omnidirectional radiation in this plane (XZ) is desired, because it provides power-efficient communications (minimise on body link loss). The on-body radiation performances of the Loop, Printed Monopole, and Inverted-L are the worst, in comparison to other antennas used. In this plane (XZ), both Patch and Wire Monopole show the best co-and cross-polar on-body radiation performances (Fig. 4.18 (b) and (d)). The on-body co-and cross-polar radiation patterns do not vary much for the Loop, Inverted L and Printed Monopole antennas. Placing the narrowband antennas on the human body, the de-polarisation was noticed. Usually in free space, the co-polar radiation patterns of the used five narrowband antennas show higher performance (in terms of patterns and power level) as compared to cross-polar radiation patterns. However, when the narrowband antennas are placed on the body, the cross-polar radiation patterns show higher performance compared to the ones in free space. For the Inverted L, Loop and Printed Monopole antennas, the on-body cross-polar and co-polar performances are nearly the same and even in some cases, the cross-polar radiation is higher than co-polar, and hence the antenna becomes un-polarised.

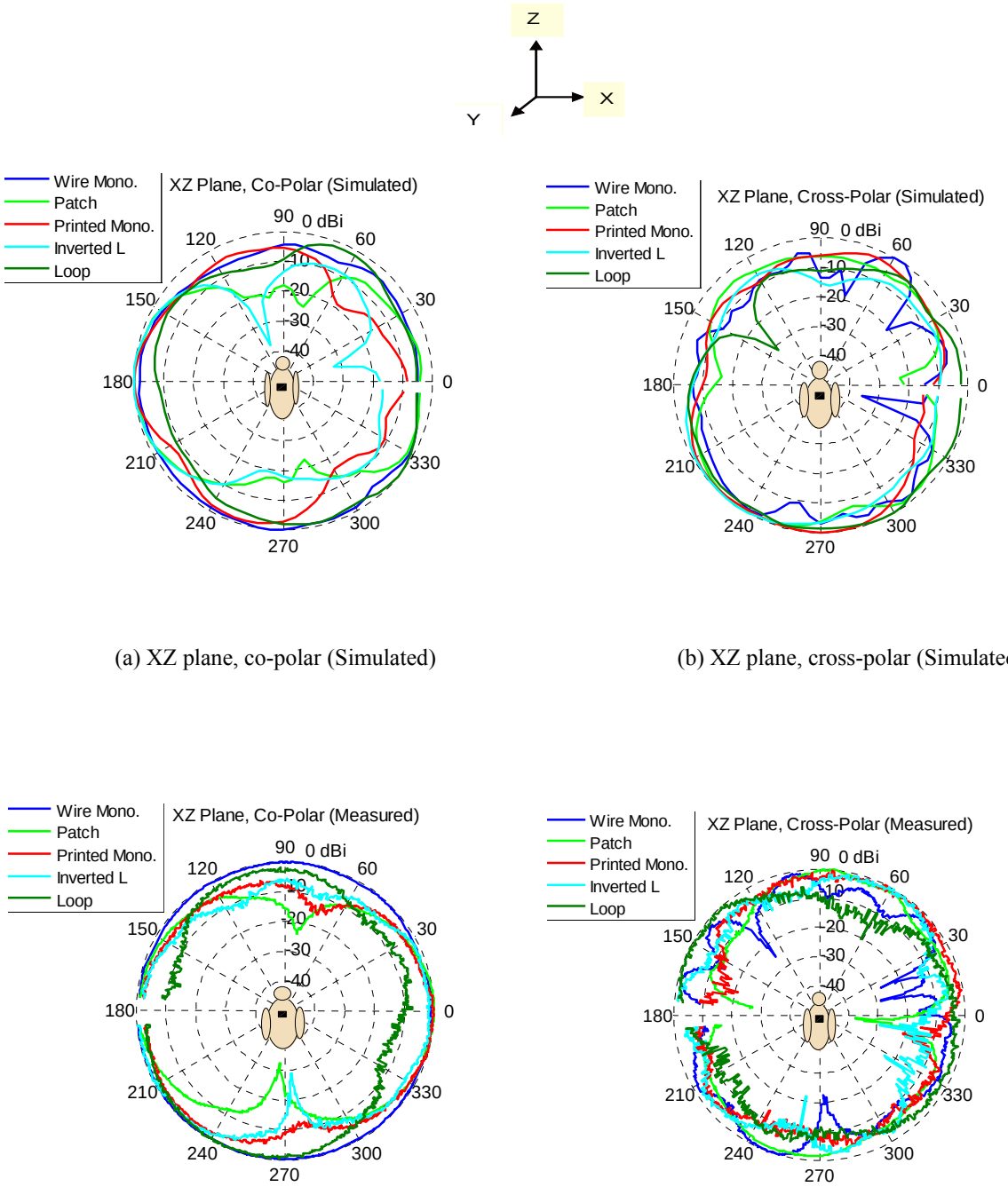

(a) XZ plane, co-polar (Simulated)

(b) XZ plane, cross-polar (Simulated)

(c) XZ plane, co-polar (Measured)

(d) XZ plane, cross-polar (Measured)

Fig. 4.18. XZ plane (co-and cross-polar) on-body radiation patterns of used five narrowband antennas when placed 1 mm away from the body (a-b) simulated and (c-d) measured. The radiation patterns have been normalised (maximum=0 dB). During simulation the Wire Monopole was placed at 4 mm from the body and in measurement 16 mm).

Figs. 4.19 (a) and (b) show the simulated YZ plane co-and cross-polar on-body radiation patterns of the five narrowband antennas when placed 1 mm away from body, and Figs. 4.19 (c) and (d) show the measured. In the YZ plane, all five antennas show directive radiation patterns towards off the body, except there is a presence of null in the front beam for the Wire Monopole. The Patch antenna shows the best co-and cross-polar radiation patterns in the YZ plane (off-body direction). Due to human body effects, there is power loss at the back lobe which is significant for the Loop, Inverted L and Printed Monopole. On the body, the YZ planes radiation patterns distort very much for Loop, Inverted L and Printed Monopole antennas. When the antennas are worn on the body, all five (antennas) show very good cross-polar radiation performance in the YZ plane. The co-and cross-polar radiation patterns in the YZ plane of the five narrowband antenna look the same except slight variation in the power level. However, on the body, the antennas become un-polarised in the YZ plane as well. From the study, it is noted that the on-body radiation patterns is nearly stable as free space for the antennas with full ground plane (Patch and Wire Monopole) while distorts remarkably compared with free space for the antennas with partial ground plane (Inverted L, Loop and Printed Monopole).

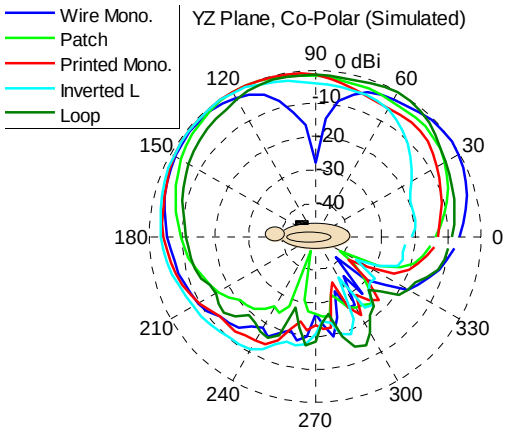

(a) YZ plane, co-polar (Simulated)

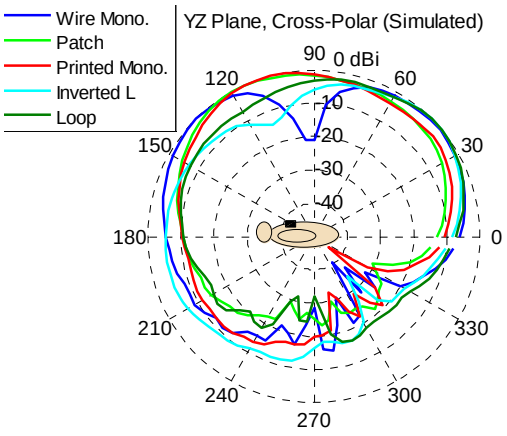

(b) YZ plane, cross-polar (Simulated)

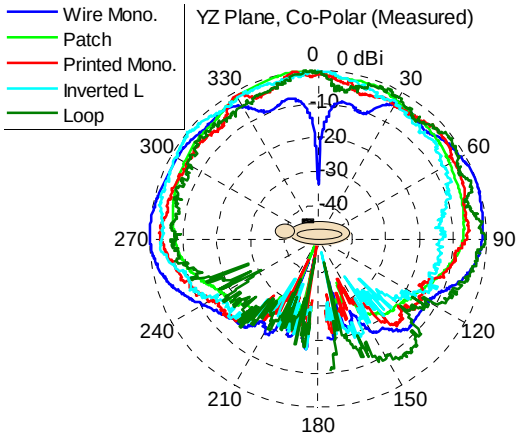

(c) YZ plane, co-polar (Measured)

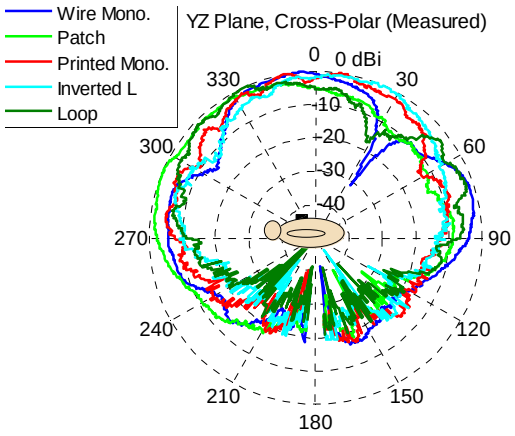

(d) YZ plane, cross-polar (Measured)

Fig. 4.19. YZ plane (co-and cross-polar) on-body radiation patterns of five narrowband antennas when placed 1 mm away from the body (a-b) simulated and (c-d) measured. The radiation patterns have been normalised (maximum=0 dB).

The radiation pattern was also investigated as a function of distance between the antenna and the human body. In this case, the Patch and Printed Monopole have been chosen as suitable examples. Figs. 4.20 (a) and (b) show the simulated XZ plane co-and cross-polar radiation patterns of the Printed monopole and Figs. 4.20 (c) and (d) show the simulated XZ plane co-and cross-polar radiation patterns of the Patch. Results show that varying the distance between the antenna and the body does not distort the radiation pattern but changes the power level.

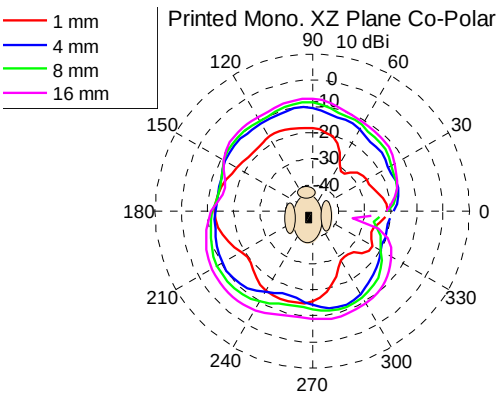

(a) Printed Monopole, XZ plane co-polar

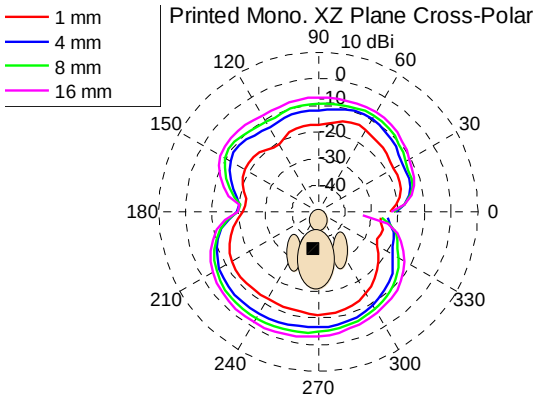

(b) Printed Monopole, XZ plane cross-polar

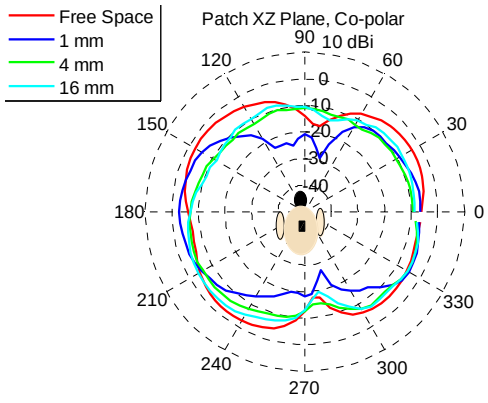

(c) Patch, XZ plane co-polar

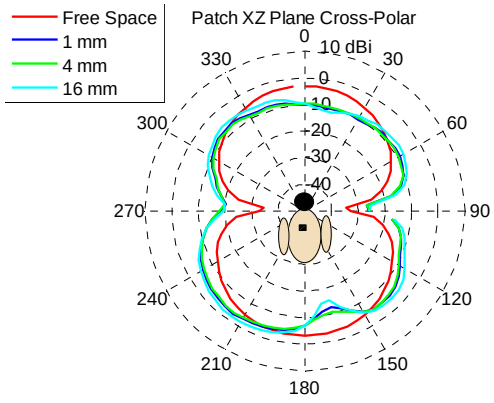

(d) Patch, XZ plane cross-polar

Fig. 4.20. (a) XZ plane co-polar radiation patterns of the Printed Monopole, (b) XZ plane, cross-polar radiation patterns of the Printed Monopole (c) XZ plane, co-polar radiation patterns of the Patch (d) XZ plane, cross-polar radiation patterns of the Patch.

The performances of the Printed Monopole, Inverted L and Loop antennas degrade significantly in close proximity to the human body except the increase of the bandwidth. These types of antenna need to be placed far away from the human body in order to get good on-body performance. The overall on-body performances of the Inverted L, Printed Monopole and Loop are comparable, while slight improve performance is noticed for the Printed Monopole antenna. The performance of the Wire Monopole and Patch antenna is less sensitive to the presence of the human body due to having full ground plane at the back. These two antennas show very good (nearly stable) performance even very close to the body. The wire monopole antenna has the advantage of performance compared with the Patch (in terms of impedance bandwidth, XZ plane gain and radiation pattern). It has omnidirectional radiation pattern with higher on-body gain over the body surface plane while the patch has the radiation towards the off-body direction with higher gain. The wire monopole shows 36.60 % higher on-body impedance bandwidth and 4.5 dB higher on-body gain in the XZ plane compared with the patch. The major drawback of the wire monopole is the shape which is not conformal to the body. In addition, the volume of the wire monopole is the highest compared with other four antennas. However, for on-body applications, the behaviour of the antenna as a part of the on-body radio channels needs to be investigated in order to study the effects of overall on-body performance of each antenna on the on-body radio propagation channels.

4.2.6 Radio Propagation for Narrowband (2.45 GHz) Body-Centric Wireless Networks

The five narrowband antennas were used to characterise the path loss for communication along the front part of the human body.

Measurement Settings

A frequency-domain measurement set-up was applied. The measurements were performed on the same test subject as used for the S11 measurements. A HP8720ES vector network analyzer (VNA) was used to measure the transmission response (S21) between two antennas of the same kind placed on the body. During the measurement, the transmitter antenna was placed on the left waist, while the receiver antenna was successively placed on 34 different locations on the front part of the human body (Fig. 4.21). The subject was wearing a T-shirt and Trousers and the antennas were placed directly on them. The two similar antennas placed on the body are connected to the VNA by two 3 metre long cables (cable effects on channel responses were calibrated out). Table 4.10 shows the network analyser settings for the narrowband on-body measurements. During the measurement, the subject was standing still; for each receiver location, 10 sweeps were considered. The path loss for different receiver location was calculated directly from the measurement data of S21 (10 sweeps) averaging at 2.45 GHz. The measurement was first performed in the anechoic chamber to eliminate multipath reflections from the surrounding environment, and then repeated in the Body-Centric Wireless Sensor Laboratory at Queen Mary, University of London, to consider the effect of the indoor environment in the on-body radio propagation channels; see Fig. 4.22.

Table 4.10. Network analyser settings.

Frequency Band	2.35 to 2.55 GHz
Frequency Points	201
Sweep Time	100 ms
Number of Sweep	10
VNA Transmit Power	0 dBm

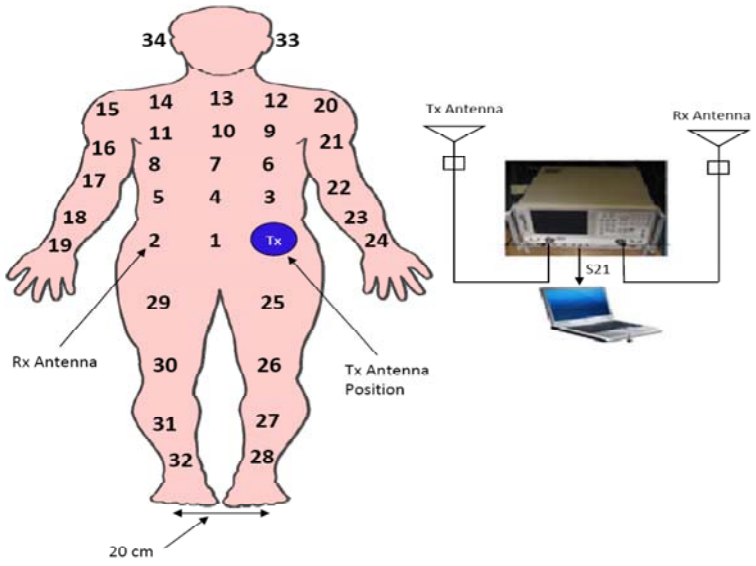

Fig. 4.21. On-body radio propagation measurement settings showing the transmitter antenna is on the left waist while the receiver antenna is on 34 different locations of the body.

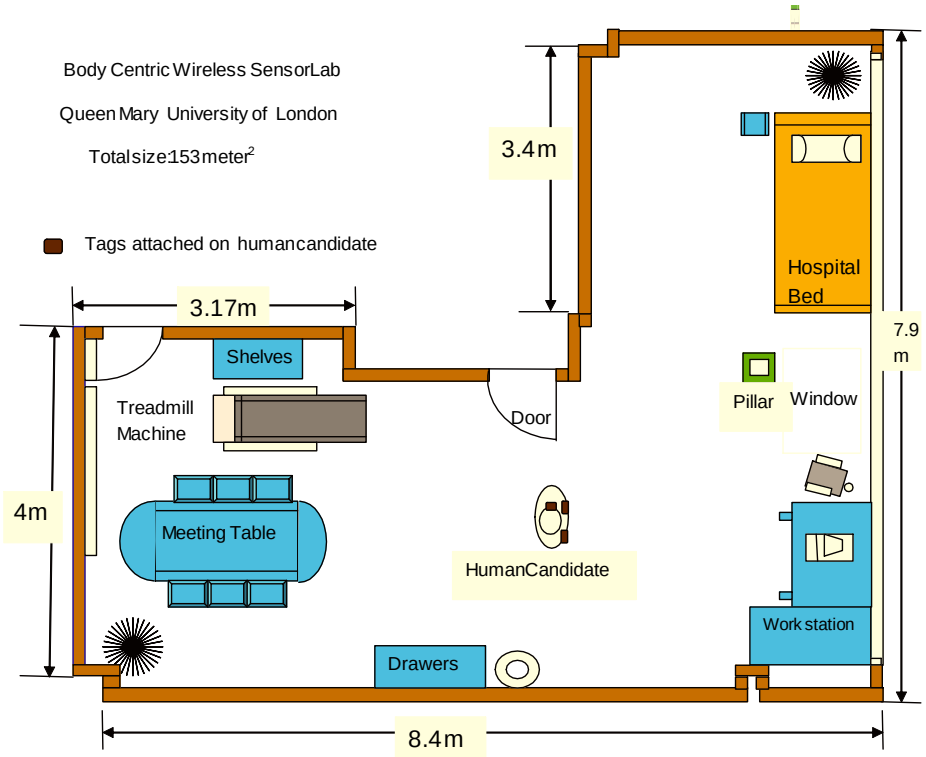

Fig. 4.22. Dimensions and geometry of the Body-Centric Wireless Sensor Laboratory (housed within the Department of Electronic engineering, Queen Mary University of London, London, U.K) where the indoor on-body radio propagation measurements for the presented work is performed.

It is well known that the average received signal decreases logarithmically with distance. The path loss can be modelled as a linear function of the logarithmic distance between transmitter and receiver as explained in [16],

$$PL_{dB}(d) = PL_{dB}(d_0) + 10\gamma \log(\frac{d}{d_0}) + X_\sigma \qquad (4.2)$$

where d is the distance between transmitter and receiver, d_0 is a reference distance set in measurement (set to 10 cm in this study), $PL_{dB}(d_0)$ is the path loss value at the reference distance. The parameter γ is the path loss exponent that indicates the rate at which the path loss increases with distance. X_σ is a zero-mean Gaussian-distributed random variable with standard deviation σ.

A least-square (LS) fit technique is applied on the measured path loss results for the 34 different receiver locations on the body, to extract the path loss exponent and the mean path loss at the reference distance d_0 for the five antenna cases (Table 4.11). Figs. 4.23(a) and 4.23(b) show measured and modelled path loss for on-body channel versus logarithmic Tx-Rx separation distance, for all five antennas, measured in the chamber and indoor environment, respectively. The slope of each line represents the path loss exponent γ, for the five body-worn antennas.

Due to the quite omnidirectional on-body radiation pattern, higher gain on the XZ (azimuth) plane and good on-body performances (in terms of efficiency, frequency detuning, gain, radiation distortion and so on), the Wire Monopole shows the lowest path loss exponent (2.76, 2.56) and path loss (23.1, 25.2 dB) at the reference distance both in the chamber and indoor. Out of these five antennas, the highest path loss exponent (4.08, 3.65) is noticed for the Printed Monopole, while the highest path loss (43.7, 45.1 dB) at the reference distance is noticed for the Loop antenna.

For the Loop, Inverted-L and Printed Monopole antennas, the radiation pattern is not quite omni-directional in the XZ plane, the gain is the lowest in the XZ plane and they show poor on-body performances (in terms of frequency detuning, efficiency, gain, radiation patterns distortion and so on), which all result in higher path loss exponent and path loss at the reference distance.
The Printed Monopole shows the lower path loss value compared with the Loop and inverted L. Due to improved on-body performance, the Patch antenna shows considerable lower path loss compared to the Loop, Inverted-L and Printed Monopole. Although the patch shows good on-

body performance but it shows higher path loss value compared with the wire monopole which is due the facts that the patch has lower gain in the XZ plane and the radiation pattern in the XZ plane is not quite omnidirectional to the body surface plane. Compared to the Patch, the Wire Monopole has 20.21 % lower path loss exponent and 9 dB lower path loss value, suggesting that the Wire Monopole is more power-efficient for on-body communications. However, due to its structure (non conformal shape) and the highest volume (32 times higher than the Patch), the Wire Monopole will not be suitable for on-body communication in Wireless Body Area Networks (WBANs). Therefore, a conformal antenna with full ground plane at the back having omnidirectional radiation pattern over the body surface with good gain may provide good on-body radio channel performances (less link loss) and it can be considered a suitable candidate for narrowband on-body applications in WBANs.

The path loss exponent for all antennas are found to be lower in the indoor due to indoor multipath components (MPCs), which increase the received signal strength, resulting in a lower path loss exponent.

X_σ is a zero-mean, normal distributed statistical variable, and is introduced to consider the deviation of the measurements from the calculated average path loss. Figs. 4.24(a) and 4.24(b) show the deviation of measurements from the average path loss fitted to a normal distribution for five antenna cases in the anechoic chamber and indoor, respectively. The highest standard deviation is noticed for the Loop and Inverted L and the lowest is for the Wire Monopole. The standard deviation is higher (path loss data more spreads around to the linear fit line) for the antennas with directive radiation compared to the antennas with omnidirectional radiation patterns.

Table 4.11. Comparison of path loss parameters for five different narrowband antennas used in this study.

	Chamber			Indoor		
Antenna	γ	$PL_{dB}(d_0)$	σ	γ	$PL_{dB}(d_0)$	σ
Loop	3.60	43.7	8.53	3.10	45.1	7.24
Inverted L	3.85	40.1	8.57	3.46	41.7	8.20
Printed Mono.	4.08	38.0	7.08	3.65	40.0	6.24
Patch	3.33	32.0	7.01	2.88	33.5	6.27
Wire Mono.	2.76	23.1	5.61	2.56	25.2	5.32

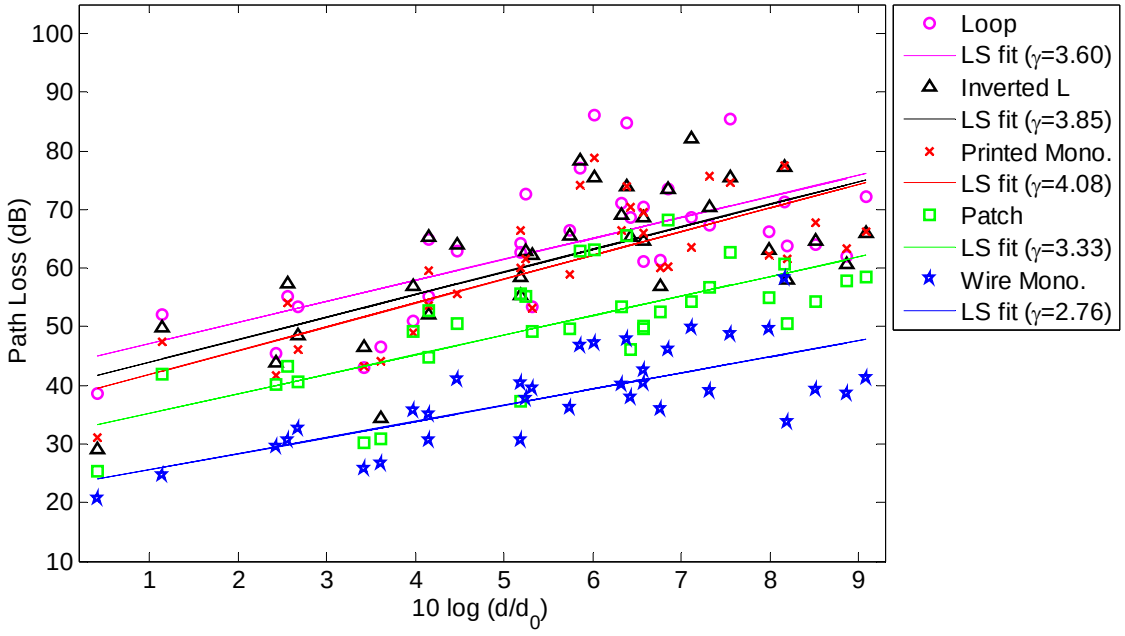

(a) Chamber

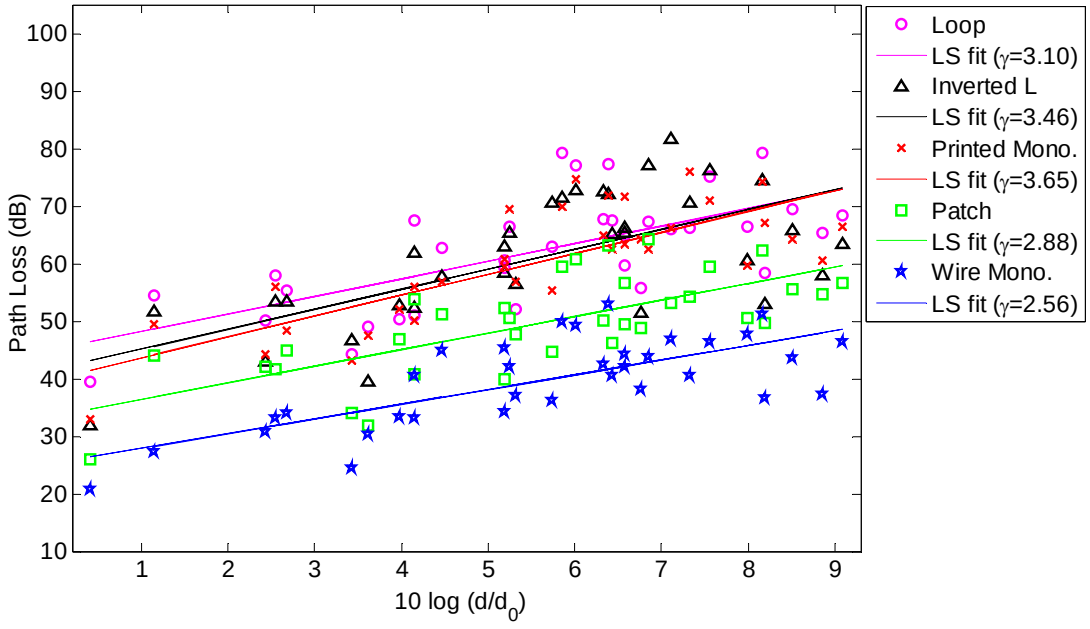

(b) Indoor

Fig. 4.23. Measured and modelled (best fit model) path loss for the on-body channel versus logarithmic Tx-Rx separation distance for five different narrowband antennas used; (a) Chamber and (b) Indoor.

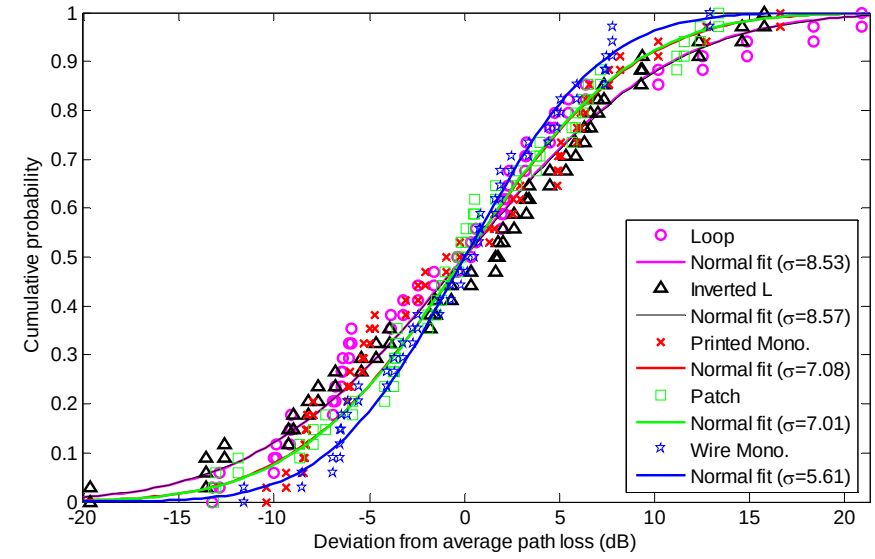

(a) Chamber

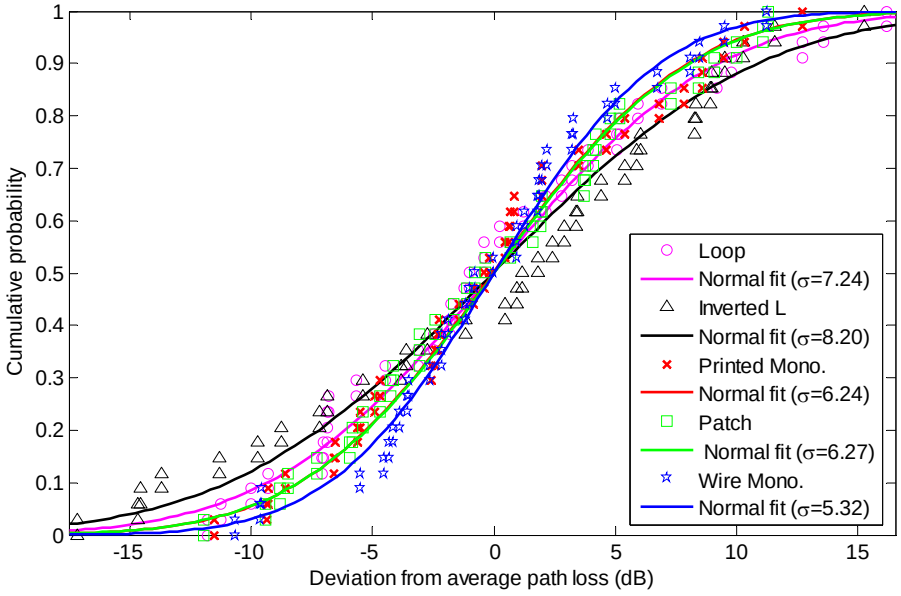

(b) Indoor

Fig. 4.24. Deviation of measurements from the average path loss fitted to a normal distribution for five different narrowband antennas used; (a) Chamber and (b) Indoor.

From the investigation in this chapter, it is noted that the full ground plane is very effective at minimising the human body effects on the performance of the narrowband antennas. In addition, antenna radiation pattern and gain have a significant influence on the on-body propagation channels. It is noted that the antenna having radiation pattern omnidirectional over the body

surface with maximum gain provides the best on-body link performances by improving the path gain. Antenna (like patch) having directive radiation towards off the body direction with higher gain will provide good off-body radio channels performance by improving the path gain.

In common healthcare monitoring scenarios, it is very important for the antenna to radiate over the body surface omni-directionally and also be directive towards off-the-body units, in order to get the best on-body and off-body radio channel performances i.e. minimise the link loss to ensure power-efficient and reliable on-body and off-body communications and maximise the battery life of the body-worn devices. Body-centric wireless devices need to be low power consumable in order to extend the battery life of the body-worn devices. By considering the above mentioned facts, a novel dual-band antenna having diverse radiation mode is proposed for power-efficient and reliable cooperative on-body and off-body communications. The antenna is dual-band with omnidirectional radiation pattern over the body surface at 2.45 GHz (ISM band) to communicate power-efficiently with other co-located body-worn devices scattered on the body or body-worn base station. At 1.9 GHz (PCS band), it has with directive radiation pattern towards off-the body to communicate power-efficiently from on-body device to off-body units/access point or other wider e-health networks.

The on-body performance parameters of the DBDM antenna at 2.45 GHz is compared with the other five narrowband antennas studied in the previous section with the aim of verifying the suitability of the antenna for on-body applications for narrowband system.

4.3 Dual-Band and Dual-Mode Antenna for Power-Efficient Body-Centric Wireless Communications

Figs. 4.25 (a) and (b) show the schematic diagram and fabricated version of the proposed dual-band and dual-mode antenna. The antenna is modelled on FR4 substrate with a thickness of 1.57 mm and a relative permittivity of 4.6. There is a full ground plane at the back of the substrate with the size of 60×60 mm. The antenna has two radiating elements a disk-loaded Monopole and a circular Patch. The DBDM antenna is excited by single microstrip line feed connected to the circular patch printed on the substrate. The upper and lower disks are connected placing a small cylinder with a diameter of 5 mm and a height of 2.23 mm on the lower disk; see Fig. 4.25. Table 4.12 shows the dimensions of the antenna along with its electrical size.

The inner cylinder works on the same principle as Wire Monopole and placing the disk on the top the size has been reduced which otherwise would radiate at much higher frequency. For the DBDM, the upper resonance frequency depends on the size of the inner cylinder and also on the size of top disk but for the lower frequency it depends on the diameter of the lower Patch and the size of the top disk. Both disks were aligned asymmetrically because of the optimum impedance matching and radiation performances.

In this structure, the top-loaded disk monopole structure has been chosen to achieve the resonance at 2.45 GHz (ISM band), with an omnidirectional radiation pattern over the body surface to communicate with other body-worn devices, especially the body worn base station whereas the printed disk-like patch on the FR4 board have been designed for 1.9 GHz (PCS band) with an off-the-body directive radiation pattern mode to communicate power-efficiently from the on-body device to off-body units/access points or other wider e-health networks. The disk-loaded Monopole works on same principle as a Wire Monopole on the large ground plane, where the current distribution is significant on the radiating wire near to the feed and null at the edge of the radiating wire, achieving the omnidirectional radiation pattern on the azimuth plane. The size of the antenna reduces dramatically with the same radiation principle by loading a capacitive disk on the edge of the radiating wire of the monopole. For the top-loaded disk monopole, the current flows near the feed to the radiating element and spreads till to the bottom part of the disk. The current distribution is null on the top part of the disk. The lower circular disk works on the same principle as Patch. The fundamental microstrip Patch radiates from the edge of the rectangular Patch which produces directive radiation characteristics [1].

Table 4.12. Dimensions and electrical size of the proposed DBDM antenna components.

Components	**Unit (mm)**	**Electrical size (guided λ_g)**	**Electrical size (free space λ)**
Top disk diameter	39	λ_g / 1.46	λ / 3.13
Lower disk diameter	34	λ_g / 2.16	λ / 4.64
Cylinder height	2.23	λ_g / 25 .65	λ / 55
Ground plane size	60×60	λ_g / 1.22	λ / 2.63
Total antenna height	4.5	λ_g / 12 .61	λ_g / 12 .27
Total Volume	60×60×4.5		

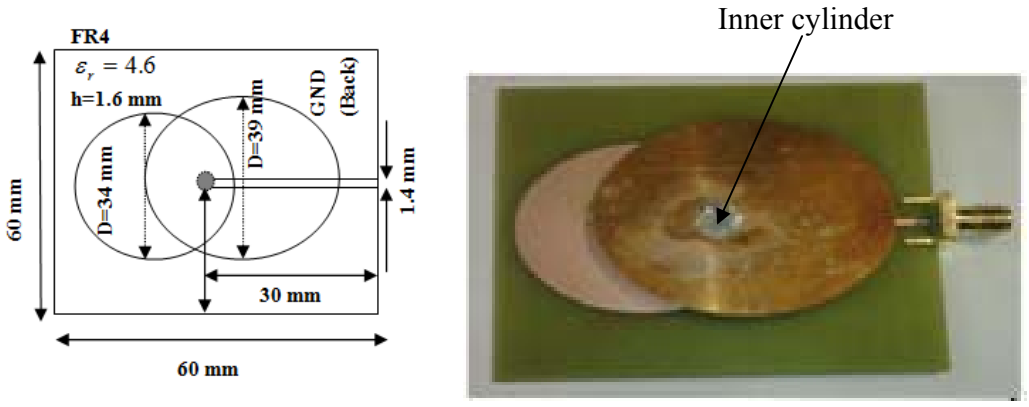

(a) (b)

Fig. 4.25. (a) Schematic diagram, (b) Fabricated version of the proposed dual-band and dual-mode (DBDM) antenna.

Current Distribution of the DBDM Antenna

The free space simulated surface current of the DBDM is shown in Fig. 4.26 (a) and (b) for the higher frequency band (2.45 GHz) and Fig. 4.27 (a) and (b) for the lower frequency band (1.9 GHz). At the upper frequency band, the current flows via the inner cylinder to the lower part of the top disk and the current flow is significant on the inner cylinder, under the top disk and on the lower disk near the cylinder. There is a current null at the centre of the top part of the upper disk. For the lower band, at 1.9 GHz current flow is significant on around the lower disk, the inner cylinder and also to the edge of the top disk.

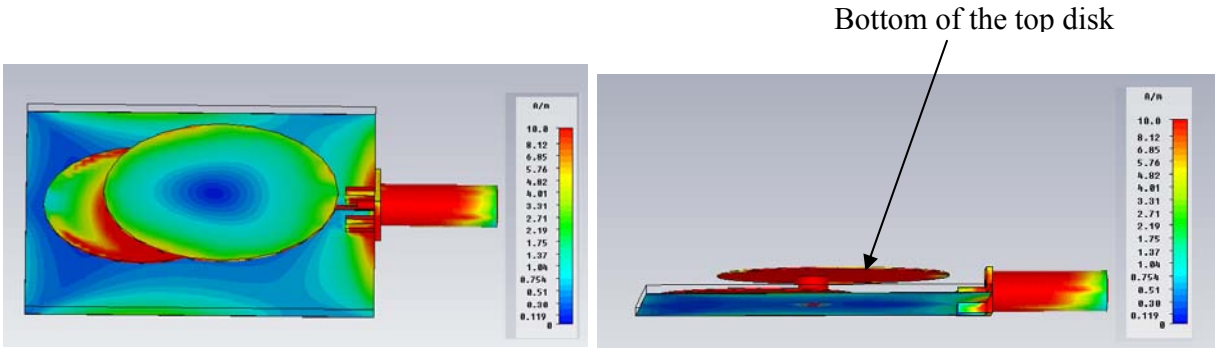

(a) (b)

Fig. 4.26 Surface current of the DBDM antenna at 2.45 GHz.

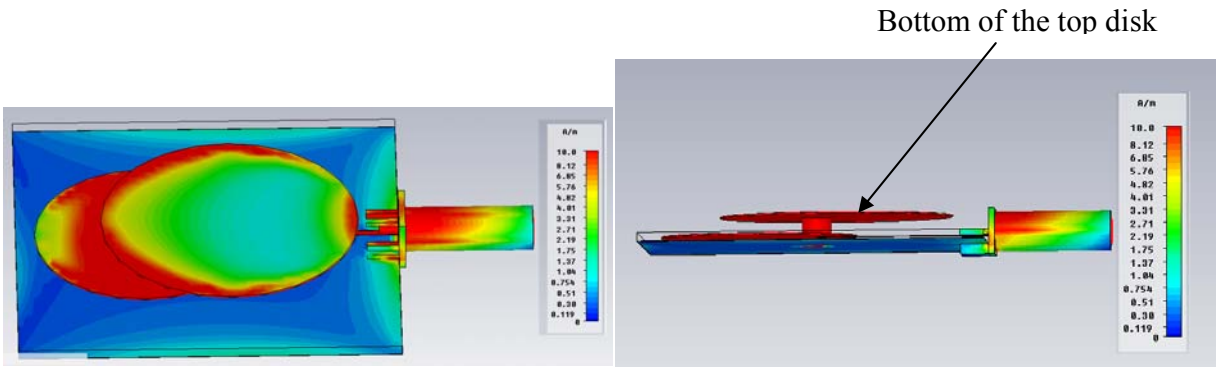

(a) (b)

Fig. 4.27. Surface current of the DBDM antenna at 1.9 GHz.

4.3.1 Investigation of On-Body Performance Parameters of the DBDM Antenna

In order to study the performance parameters in close proximity to the human body, the DBDM antenna is simulated on the same human phantom as shown Fig. 4.13. The resolution of the model applied is 4 mm with the electrical properties of human tissues defined at 2.45 GHz and 1.9 GHz, respectively, for all organs and tissues used including heart, lungs, muscle, fat, skin, etc [17-18]. For 1.9 GHz and 2.45 GHz, the DBDM antenna was simulated separately. The on-body performance of the DBDM antenna was measured on the same real human body as was used for other five narrowband antennas case. The simulation and measurement settings were the same as were made for the other five narrowband antenna cases.

Frequency Detuning of the DBDM

Fig. 4.28 shows the simulated and measured free space and on body return loss curves of the proposed dual-band dual-mode antenna when placed at 1 mm away from the body. Slight variation of the free space simulated and measured resonances are noticed which can be due to fabrication perfectness. When DBDM antenna measured on the body (1 mm away from the body), a very slight frequency detuning from free space resonance (0.32%) is observed for the upper frequency band whereas for the lower frequency band no frequency detuning is noticed. Simulation results show little higher frequency detuning in compare to measurement.

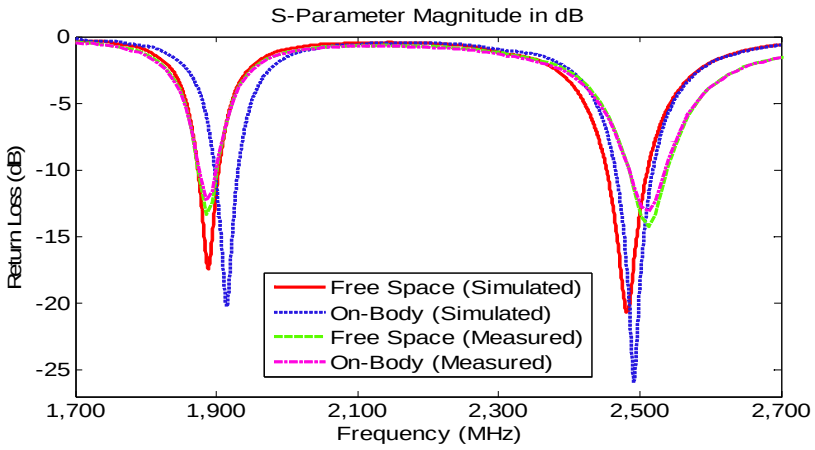

Fig. 4.28. Simulated and measured free space and on-body return loss curves of the proposed dual-band and dual-mode antenna (The antenna was placed at 1 mm away from body).

Like other five narrowband antennas, the frequency detuning of the DBDM antenna at 2.45 GHz also measured placing at various distances from the body and various locations on the body. The results were compared with the other five narrowband antennas used in previous case. Fig. 4.29 shows the frequency detuning of the DBDM antenna in comparison with the other five narrowband antennas when it is placed at various distances from the human body (left side of the waist). Results show that for various gaps between the antenna and the body, there is not much effect in the frequency detuning for the DBDM antenna. Due to different distances from the body, the frequency detuning of the DBDM varies very slight (maximum 0.36 %). The average frequency detuning and the standard deviation of various separation distances for the DBDM antenna are 0.22 % and 0.15 respectively.

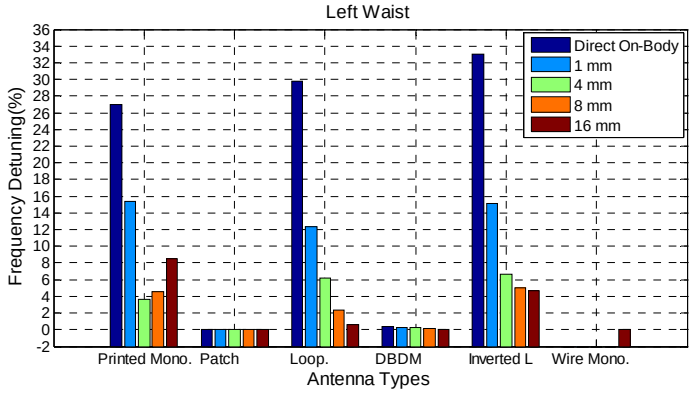

Fig. 4.29. Frequency detuning of the DBDM antenna in comparison with the other five narrowband antennas when placed at various distances away from the body.

From the graph 4.29, it is noted that the frequency detuning of the DBDM is extremely smaller compared to the Printed Monopole, Loop and Inverted L. As compared to the Patch, the DBDM shows slightly more frequency detuning which can happen for the bigger ground plane size of the patch. The DBDM shows 0.36 % frequency detuning when placed directly on the body, but no frequency detuning is observed when it is placed at 16 mm away from the body. In the study, it was found that, although there was a full ground plane in the back of the antenna structure, the frequency detuning was still observed which is attributed to the smaller size of the ground plane. It is also found that antennas with partial ground planes have shown significant frequency detuning, even when placed 16 mm away from the body. For wearable antennas, there has to be a full ground plane at the back of the antenna and it needs to be placed more than 8 mm from the body if the frequency detuning is to be avoided. If the antenna used only has a partial ground plane, it needs to be placed as far from the body as possible (more than 16 mm) or the antenna needs to be designed with a frequency-tuning mechanism, or new material must be introduced to the antenna structure.

The DBDM also shows nearly stable performance in terms of frequency detuning when placed at various locations on the body directly; see Fig. 4.30. Due to different locations on the body, the maximum variation of frequency detuning of the DBDM antenna is 0.36 % which is incredibly little compared to the Inverted L, Loop and Printed Monopole. The DBDM antenna experiences no frequency detuning when placed on the right wrist and left ankle. For the DBDM, the average frequency detuning and standard deviation of different locations on the body are 0.25% and 0.17 respectively.

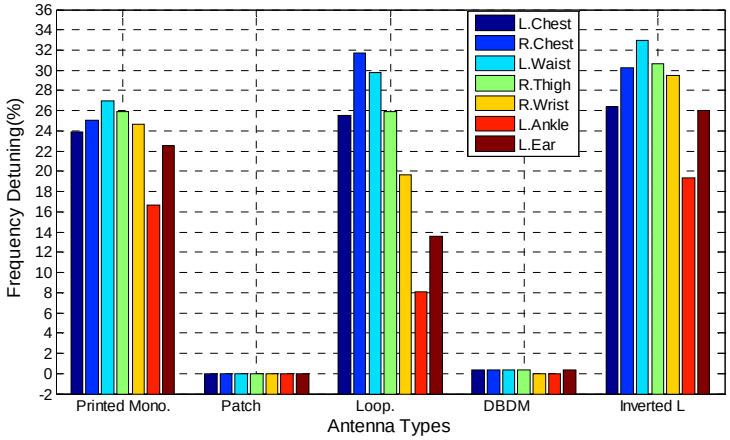

Fig. 4.30. Frequency detuning of the DBDM antenna in comparison with the other five narrowband antennas when placed at various locations direct on the body.

On-Body Bandwidth of the DBDM

The impedance bandwidth (-10 dB impedance) of the DBDM is extracted from the S11 results measured on the body varying the gap between the antenna and the body. At lower frequency band, in free space, the DBDM antenna shows reasonable impedance bandwidth (1.8 %) which is nearly stable when placed on the body (1 mm away). At higher frequency band, the on-body impedance bandwidth of the DBDM is also nearly the same as free space. It shows good on-body impedance bandwidth (2.45 %) at upper frequency band that is close to the required bandwidth (3.2 %) of ISM band; however, the impedance bandwidth of upper frequency band can be increased by increasing the thickness of the inner ring.

Fig. 4.31 shows the on-body impedance bandwidth of the DBDM antenna at 2.45 GHz in comparison with the other five narrowband antennas when placed at various distances from the human body. Placing the DBDM antenna different distances from the body, a slight variation of the impedance bandwidth is noticed while for the other antennas, the variation of on-body impedance bandwidth is noticed to be very higher except for the Patch. For the DBDM, the average impedance bandwidth and standard deviation of different distances from the body are 2.38% and 0.03 respectively. In comparison with the Wire Monopole, the DBDM antenna shows lower on-body impedance bandwidth. However, the DBDM has the advantage of 1.07% higher on body impedance bandwidth as compared to the Patch.

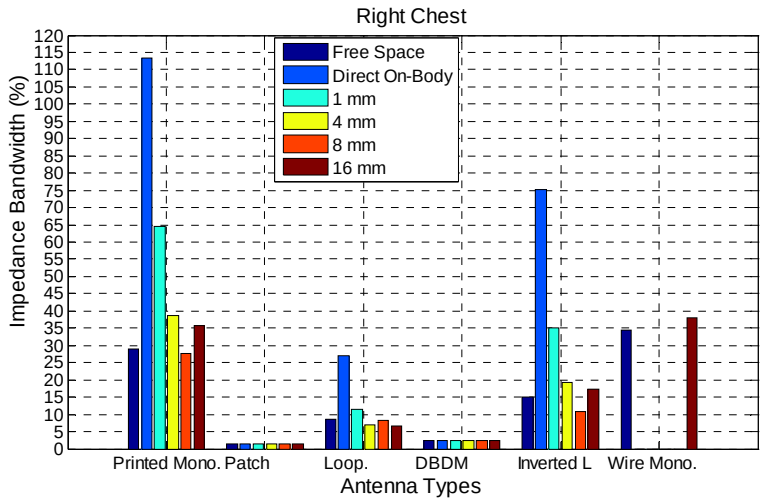

Fig. 4.31. Free space and on-body impedance bandwidth at 2.45 GHz in percentage for the DBDM antenna in comparison with other five narrowband antennas when placed at different distances from the right side of the chest. (-10 dB return loss impedance bandwidth was considered).

Fig. 4.32 shows the comparison of on-body impedance bandwidth of the DBDM antenna at 2.45 GHz in comparison with other four narrowband antennas when placed various locations on the body directly. For different locations on the body, the DBDM antenna shows insignificant variation of impedance bandwidth as 0.08 %; this was found for the patch antenna as well. For the DBDM, the average impedance bandwidth and standard deviation of different locations direct on the body are 2.30 % and 0.10 respectively. For the different locations on the body, the DBDM antenna follows nearly the same trends (variation of impedance bandwidth) as patch.

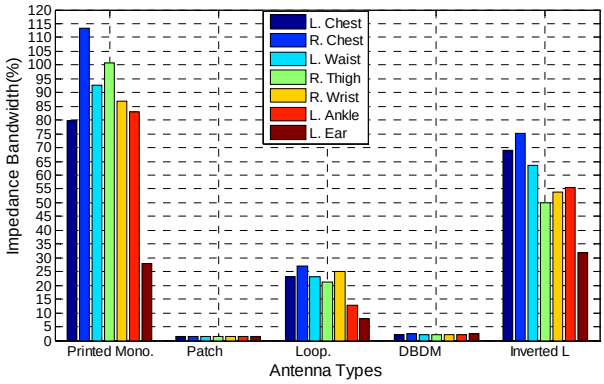

Fig. 4.32. The on-body impedance bandwidth in percentage for the DBDM antenna at 2.45 GHz in comparison with other four narrowband antennas when placed at different locations directly on the body.

Radiation Efficiency of the DBDM

The radiation efficiency of the DBDM antenna is extracted for the simulation results. In this case, the antenna was simulated placing at 1 mm away from the body (right side of the chest) for 1.9 GHz and 1, 4, 8 and 16 mm away from the body for the higher frequency band. At lower frequency band, the free space radiation efficiency of the DBDM is 99 % which reduces by 38 % when placed on the body.

At higher frequency band, the DBDM antenna shows very good on-body radiation efficiency at various distances away from the body. Fig. 4.33 shows the on-body radiation efficiency of the DBDM antenna (at 2.45 GHz) in comparison with the other five narrowband antennas when placed at various distances away from the body. The variation of gap between the antenna and the body has very less effects on the on-body radiation efficiency of the DBDM compared to the printed Monopole, Inverted L, and Loop antennas.

The average radiation efficiency and the standard deviation of various separation distances for the DBDM antenna are 61 % and 6 respectively. The patch and wire monopole antennas show

slightly higher on-body radiation efficiency compared with the DBDM antenna. On the other hand, the Printed Monopole, Inverted L and Loop antennas show much reduced on-body radiation efficiency. For the patch and wire monopole antenna, the ground plane sizes are bigger compared with the DBDM resulting in less radiation efficiency reduction for these two antennas. However, the on-body radiation efficiency of the DBDM antenna is very good.

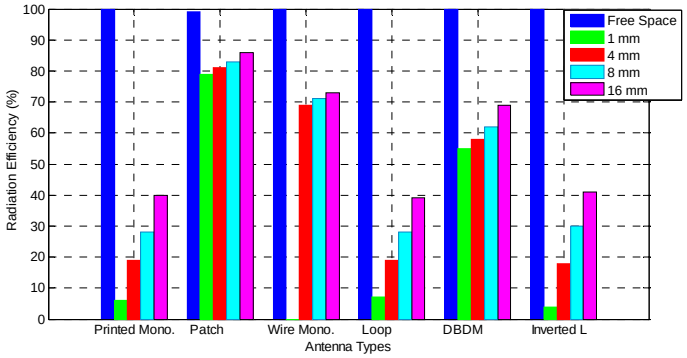

Fig. 4.33. Radiation efficiency of the DBDM antenna (at 2.45 GHz) in comparison with other five narrowband antennas when placed at various distances away from the human body.

Gain of the DBDM

The gain of the DBDM antenna is also extracted for the simulation results. For 1.9 GHz, the gain was extracted for free space and 1 mm away from the body. For 2.45 GHz, the gain was extracted for free space and 1, 4, 8 and 16 mm away from the body (right chest). At lower frequency band, the free space gain of the DBDM antenna is 4.31 dBi which increases by 3.24 % when placed on the body.

At higher frequency band, in free space the DBDM has 4.01 dBi gain which increases when the antenna is body-worn. Fig. 4.34 shows the XZ plane gain of the DBDM antenna at 2.45 GHz in comparison with the other five narrowband antennas in terms of various distances from the body. Out of these six antennas, the DBDM shows the highest on-body gain in the XZ plane. The XZ plane averaged gain and standard deviation of a range of separation distances for the DBDM antenna is 4.28 dBi and 0.30 respectively. Results show that the variation of the gap between the antenna and the body has minor effect on the gain of the DBDM antenna which is improved compared with other five narrowband antennas. In this plane, the DBDM shows averaged 6.5 dB, 2 dB higher on-body gain compared with the patch and wire monopole antennas, respectively.

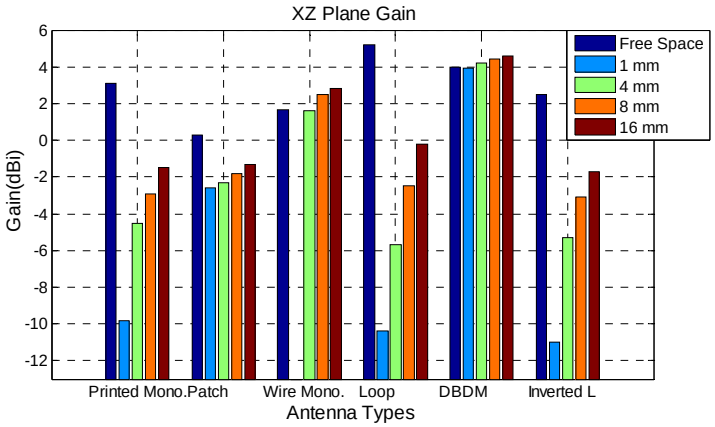

Fig. 4.34. XZ plane gain of the DBDM antenna (at 2.45 GHz) in comparison with the other five narrowband antennas when placed various distances away from the body.

YZ Plane Gain

Fig. 4.35 shows the YZ plane gain of the DBDM antenna at 2.45 GHz in comparison with the other five narrowband antennas when placed on various distances away from the body. In the YZ plane, in free space, the DBDM has 4 dBi gain which also increases when the antenna is body-worn. For the DBDM antenna, the YZ plane averaged gain and standard deviation of different separation distances are 4.21 dBi and 0.30 respectively. Out of these six antennas, the patch shows the highest on-body gain in the YZ plane. However, the DBDM shows higher gain in the both plane (XZ and YZ). Compared to the other four narrowband antenans (Wire Monopole, Loop, Inverted L and Printed Monopole), the DBDM shows the higher on-body gain in the YZ plane.

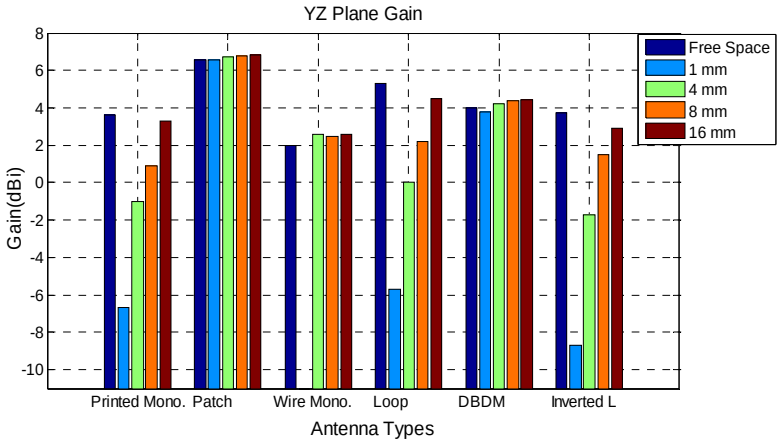

Fig. 4.35. YZ plane gain of the DBDM antenna (at 2.45 GHz) in comparison with the other five narrowband antennas when placed various distances away from the body.

Radiation Pattern of the DBDM Antenna

Radiation Pattern at 1.9 GHz

The antenna is proposed to be used in body-centric wireless communications where communication is necessary both to the devices on-body and to the external off-body network nodes. With the antenna mounted on the body, it is observed that at 1.9 GHz the radiation pattern is directive towards off the body; see Fig. 4.36 (a) and 4.36 (b). It has a very good coverage at the forward of the user body in the Y direction with the maximum gain which is very good to communicate power-efficiently by improving path gain from the body-worn base station to the off-body devices. Due to the presence of human body, at lower frequency band, loss in back lobe of the radiation pattern is noticed both in measurement and simulation.

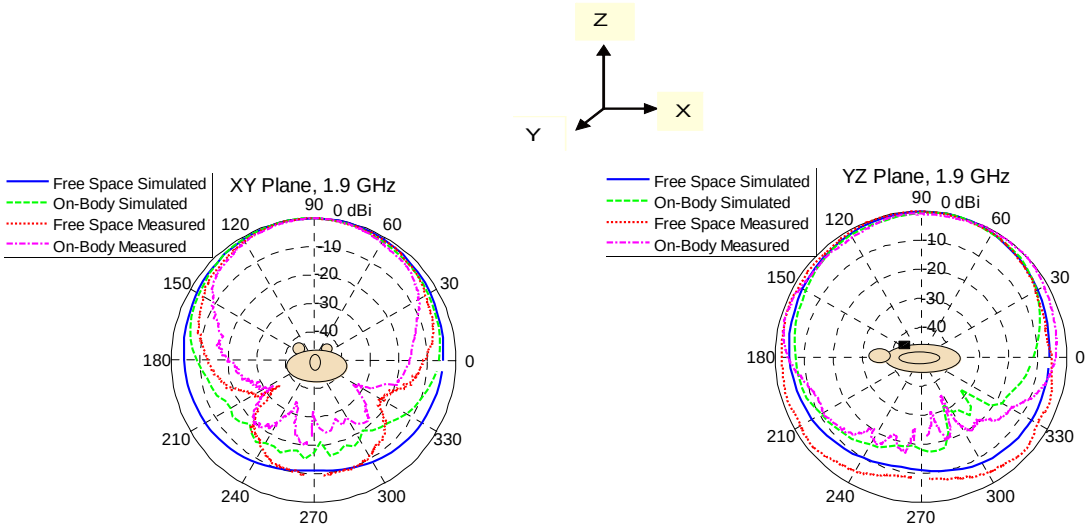

(a) XY plane, 1.9 GHz

(b) YZ plane, 1.9 GHz

Fig. 4.36. Simulated and measured free space and on-body radiation patterns of the DBDM antenna at 1.9 GHz (a) XY plane, (b) YZ plane. Normalised (maximum= 0 dB).

Radiation Pattern at 2.45 GHz

The free space and on-body co-polar radiation patterns (simulated and measured) of the DBDM antenna at 2.45 GHz are illustrated in the Fig. 4.37 (a) for the XZ plane and 4.37 (b) for the YZ plane respectively. The simulation and measured results broadly agree except trivial variation

which can be due to the effects of the cable. At 2.45 GHz, the DBDM antenna radiates omnidirectional to the user surface or the front part of the body in the XZ (azimuth) plane; see Fig. 4.37 (a). Fig. illustrates that for on-body case there is also omnidirectional radiation in the XZ plane with very little loss in the simulation results but for measurement case the radiation pattern looks nearly stable as free space. As user needs to wear various sensors integrated with antenna system on many different places of the body for reading the vital electrical signs of the human body where power-efficient communication is important from each other nodes and also in the human worn base controller. For this scenario, this kind of radiation pattern as omnidirectional on the front part of the body with maximum gain is very useful to establish power-efficient reliable on-body communications or minimise the on-body link loss by improving the on-body path gain. In the YZ plane at 2.45 GHz, the DBDM antenna shows directive radiation pattern with little null in the front beam as shown in Fig. 4.37 (b). At 2.45 GHz, the radiation pattern of the DBDM antenna is similar to the Wire Monopole.

The free space and on-body corss-polar radiation patterns (simulated and measured) of the DBDM antenna at 2.45 GHz are illustrated in Fig. 4.37 (c) for the XZ plane and 4.37 (d) for the YZ plane respectively. In both planes, the DBDM antenna shows very good on-body cross-polar radiation performances. On the body, the co-and cross-polar radiation patterns (YZ plane) of the the DBDM antenna are nearly the same.

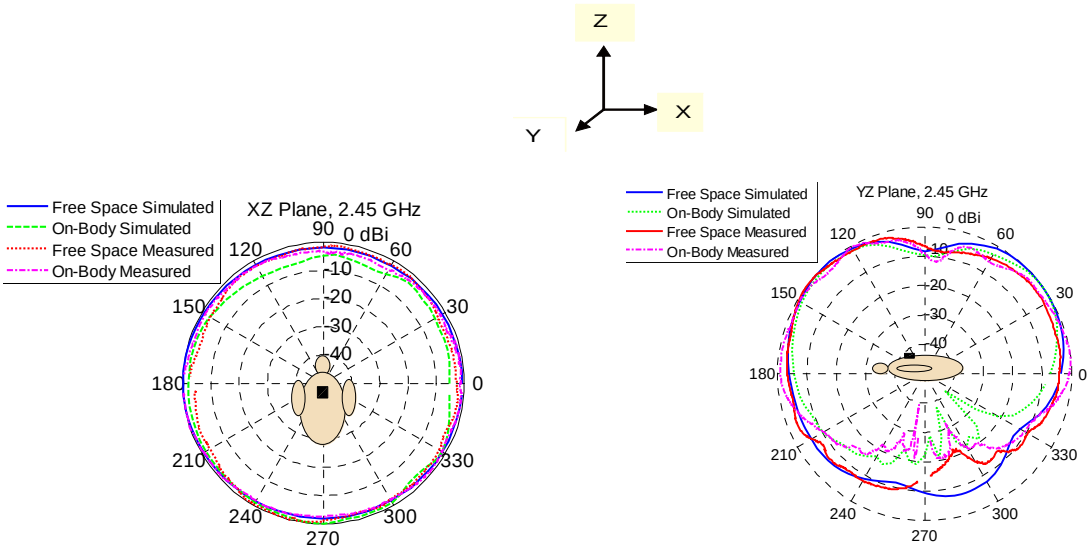

(a) XZ Plane, co-polar (on-body 1 mm)

(b) YZ Plane, co-polar (on-body 1 mm)

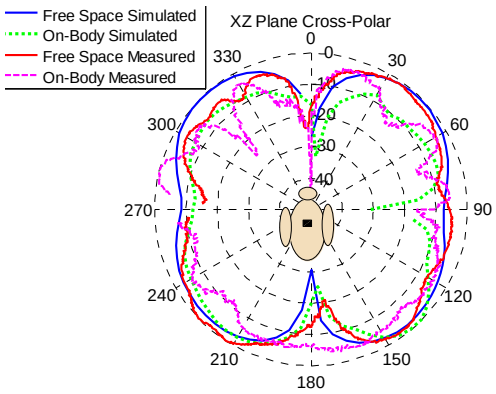

(c) XZ plane cross-polar (on-body 1mm)

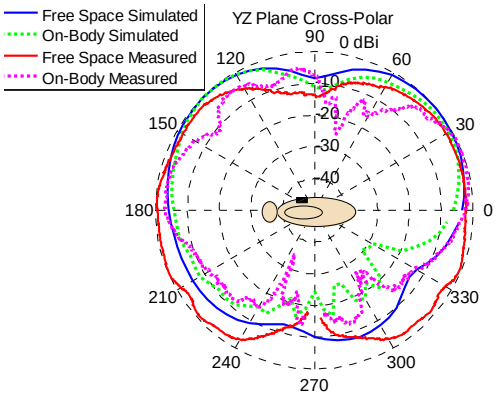

(d) YZ plane cross-polar (on-body 1 mm)

Fig. 4.37. Simulated and measured free space and on-body radiation patterns of the DBDM antenna at 2.45 GHz (a) XZ plane co-polar, (b) YZ plane co-polar, (c) XZ Plane cross-polar and (d) YZ plane cross-polar. Normalised (maximum= 0 dB).

The radiation pattern of the DBDM antenna was also investigated as a function of distance between the antenna and the human body. Figs. 4.38 (a) and (b) show the simulated YZ plane co- and cross-polar radiation patterns of the DBDM antenna at 2.45 GHz, when placed various distances away from the body. Results show that varying the distance between the antenna and the body does not distort the radiation pattern as was found in the previous section.

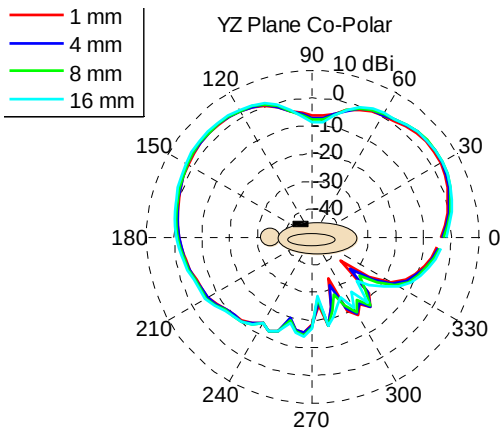

(a) DBDM, YZ plane, co-polar

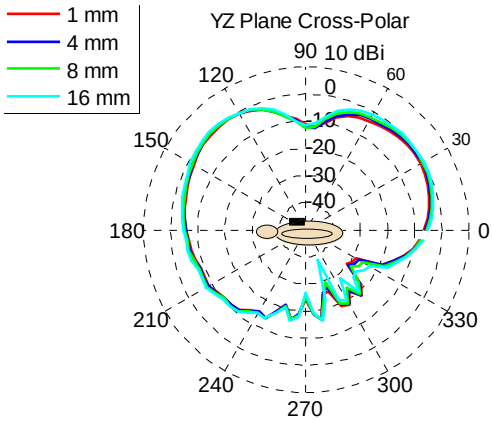

(b) DBDM, YZ plane, cross-polar

Fig. 4.38. YZ plane co-polar radiation patterns of the DBDM at 2.45 GHz (b) YZ plane cross-polar radiation patterns of the DBDM at 2.45 GHz, when placed various distances away from the human body.

The Inverted L, Loop, and Printed Monopole antennas are found to be very sensitive to the close proximity of the human body and these three antennas show very poor on-body performances as compared with the DBDM, except the impedance bandwidth, which is found to be higher for the previous three. The performance of the DBDM is found to very less sensitive to the close proximity of the human body as was noticed for the Patch and Wire monopole. The distance and various locations of the body to place the antenna have very slight effects on the performance of the DBDM, Wire monopole and Patch antenna compared with other three. The DBDM at 2.45 GHz shows the same radiation performances as the wire monopole and the radiation pattern does not deform on the body. As compared to the Wire Monopole, the DBDM has 2 dB higher on-body gain but lower on-body bandwidth; however, the DBDM shows good on-body bandwidth. Although the DBDM experiences trivial frequency detuning, it has 6.5 dB improved on-body gain in the XZ plane, 1.07% higher on-body bandwidth compared with the patch antenna. Other important advantage of the DBDM antenna over patch is the omnidirectional radiation pattern over the body surface. However, the on-body radio channel performance of the DBDM needs to be investigated and compared with the other five narrowband antennas.

4.3.2 On-Body Radio Propagation Using DBDM Antenna at 2.45 GHz

The DBDM antenna was used to characterise the path loss for communication along the front part of the human body. Same real test subject was used for this experiment as was used previously. Exactly same set of measurements were performed for the DBDM antenna as was made for the other five narrowband antenna in previous section. The measurement settings were the same as was done for the other five narrowband antennas; see Fig. 4.21. The radio channel measurement campaigns for the DBDM were also performed in the same anechoic chamber and in the indoor environment (Fig. 4.22).

A least-square fit method is performed on the measured data for the 34 different receiver locations on the body to extract the path loss exponent and the average path loss at the reference distance for the DBDM antenna. Figs. 4.39(a) and 4.39(b) show the measured and modelled path loss for on-body channel versus logarithmic Tx-Rx separation distance for the DBDM antenna in comparison with other five narrowband antennas.

Out of these six antennas, the DBDM antenna shows the lowest path loss exponent values (2.49, 2.29) both in the chamber and in indoor environment. The DBDM shows quite omnidirectional radiation pattern with the higher gain on the XZ plane. In addition, having a full ground plane at the back, the DBDM antenna is less sensitive to the human body resulting in very good on-body performances (in terms of frequency detuning, radiation distortion, efficiency, gain and so on) which all contribute to the lower path loss exponent and path loss values for this antenna.

The DBDM shows considerable lower path loss compared to the Loop, Inverted-L and Printed Monopole. Although the volume of the DBDM is 15 times lower (Table 4.1 and Table 4.12) than the wire monopole, it shows very good on-body radio channel performances (11 % less path loss exponent) compared with the wire monopole. Compared to Patch, the DBDM has 25.23 % lower path loss exponent and 6 dB lower path loss value, suggesting that the DBDM is more power-efficient for on-body communications. Overall the DBDM has the advantages of 1.07% higher on-body impedance bandwidth, omnidirectional radiation, 6 dB lower path loss and 25.23% lower path loss exponent, smaller ground plane size and dual-band and dual-mode functionality compared with the patch. Although the current volume of the DBDM is slightly bigger, it will be a suitable candidate for-body centric wireless communications with the required size-reduction and system integration.

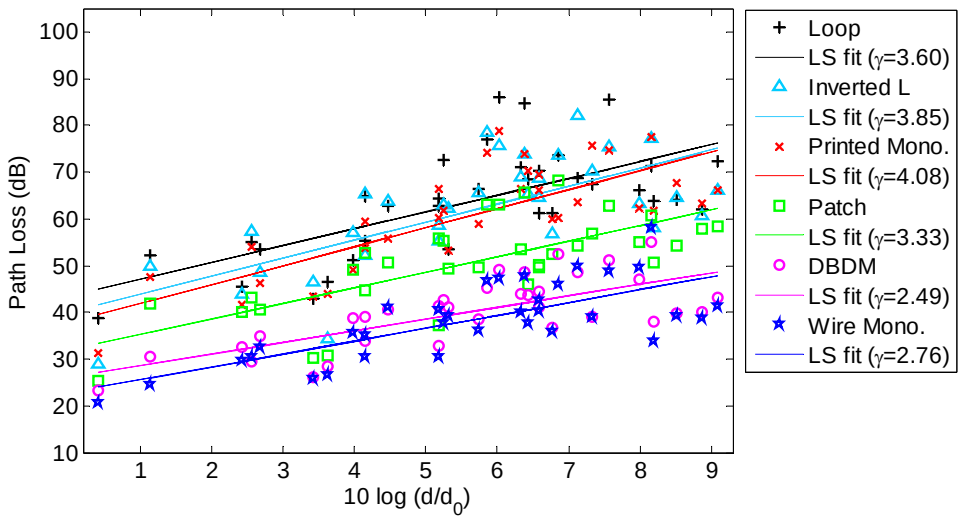

(a) Chamber

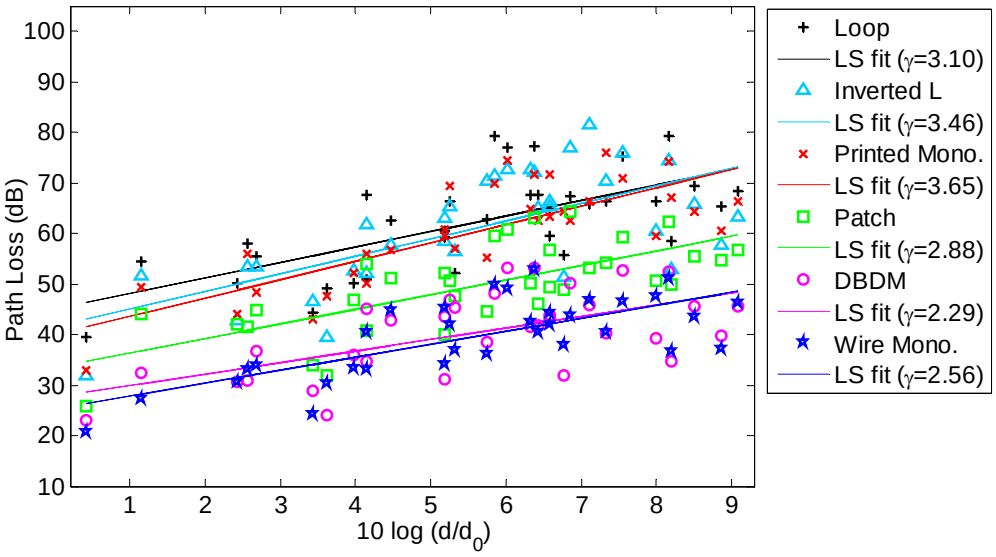

(b) Indoor

Fig. 4.39. Measured and modelled path (best fit model) loss for the on-body channel versus logarithmic Tx-Rx separation distance for six different narrowband antennas used; (a) Chamber and (b) Indoor.

Figs. 4.40 (a) and 4.40 (b) show the deviation of measurements from the average path loss fitted to a normal distribution for the DBDM antenna in comparison with the other five narrowband antennas measured in the chamber and in indoor respectively. The highest standard deviation is noticed for the Loop and Inverted L and the lowest is for the DBDM and Wire Monopole.

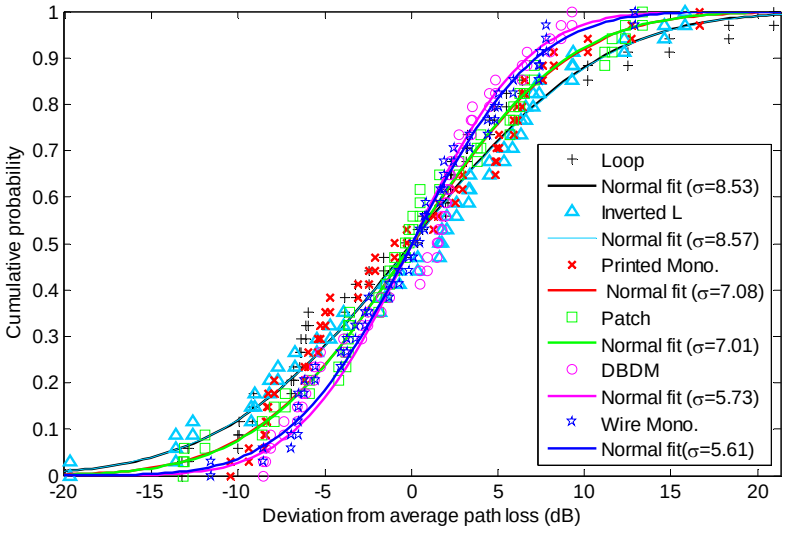

(a) Chamber

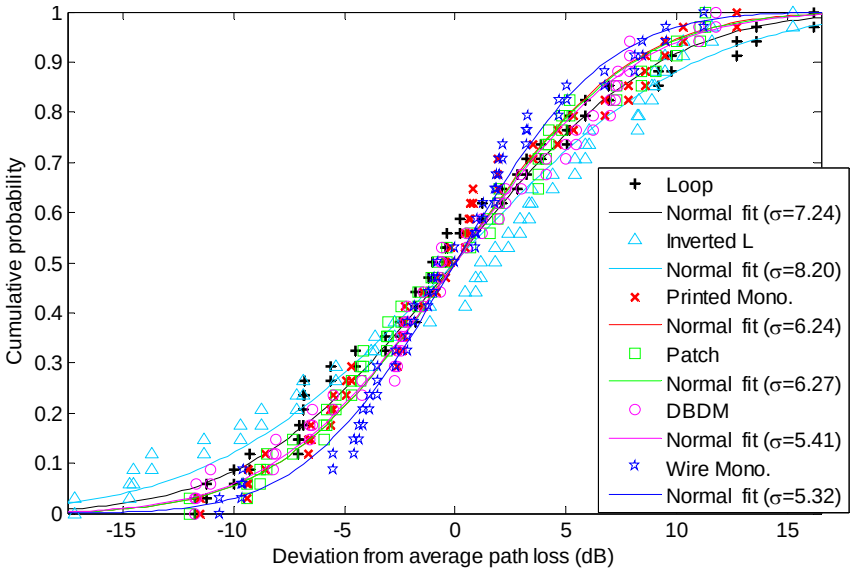

(b) Indoor

Fig. 4.40. Deviation of measurements from the average path loss fitted to a normal distribution for six different narrowband antennas used; (a) Chamber and (b) Indoor.

The DBDM is a model antenna for power-efficient and reliable narrowband wireless body-centric communications; however, based on the results analysed in this chapter, narrowband (2.45 GHz) antenna specifications and guidelines for body-centric wireless communications are summarised. These antenna specifications and guidelines will be helpful for the system design to choose and design the suitable antenna for future efficient and reliable body-centric wireless communications.

4.4 Narrowband Antenna Specifications for Body-Centric Wireless Communications

- **Size and shape**: The size and shape of wearable antennas are very important issues since the wearable devices will be attached on the human clothes or on the body. The narrowband wearable antennas for body-centric wireless communications need to be compact, light-weight, conformal to the body, low-cost and easily integrated with body-worn devices. The antenna is also required to consume low power concerning to battery life and green radio systems. In addition to these, the antenna has to be unobtrusive to the

users, so that they can move freely without any discomfort. The shape and size of the antenna depend primarily on the antenna type and feeding technique.

- **Operating frequency**: The operating frequency for the narrowband wearable antennas is in the unlicensed ISM band of 2.45 GHz. In the previous section, it was reported that, on the body, the operating frequency of the narrowband antennas detunes, with respect to free space, by as much as 33%. When a narrowband antenna is placed directly on the body, antennas with a full ground plane show only slight frequency detuning by a maximum of 0.36 %, while antennas with a partial ground plane show significant frequency detuning by up to 33%. The antennas with partial ground planes show significant frequency detuning even when placed 16 mm away from the body. Furthermore, from the study in the previous sections, it is found that, for wearable narrowband antennas, even though there is a full ground plane at the back, a slight frequency detuning still occurred when antenna is very close to the body; however, at 16 mm, there is no frequency detuning. In order to overcome frequency detuning, there has to be full ground plane at the back of the antenna structure and it needs to be placed more than 8 mm from the body or the antenna needs to be designed with a frequency tuning technique; or new material must be introduced to the antenna structure. The frequency detunes less as the gap between the antenna and the body increases. The frequency detuning of narrowband antennas varies for the different locations of the body, by up to 23.8 %. Smaller antennas experience higher frequency detuning compared to antennas bigger in physical size, which must also be taken under consideration when designing a body-worn narrowband antenna. For on-body applications, a very narrowband antenna will not be a good choice, unless the operating frequency is tuned properly when placed on the body. Due to antenna frequency detuning, the on-body communication links may drop; hence, on the body, the operating frequency of narrowband antennas needs to be tuned properly. The frequency detuning of five narrowband antennas (DBDM, Patch, Printed Monopole, Inverted L and Loop) for each separation distance between the antenna and the body was averaged. Table 4.13 shows the average frequency detuning and standard deviation of five narrowband antennas for various separation distances. The highest antenna-averaged frequency detuning of 18.02 % is noticed, when the antenna

placed directly on the human body. The highest standard deviation value of 16.42 % is noticed when the antenna is placed directly on the body. This shows that for different kinds of antennas, the frequency detuning will show the greatest variation when placed directly on the body. At higher distances from the body, the standard deviation values are found to be less which shows that the frequency detuning for different narrowband antennas varies a smaller amount at higher distances.

Table 4.13. Average frequency detuning and standard deviation of five narrowband antennas for various antenna placement distances. (the frequency detuning for each distance was averaged over 5 antennas).

Distance from the body	Mean (%)	Standard deviation (%)
Direct on the body	18.02	16.42
1 mm	8.65	7.84
4 mm	3.35	3.14
8 mm	2.43	2.38
16 mm (without wire mono)	2.75	3.74
16 mm (with wire mono)	2.29	3.53

- **Bandwidth**: The operational bandwidth for the narrowband wearable antennas is required to be from 2400 MHz-2483.5 MHz or 83.5 MHz (3.40 %) at -10 dB impedance. When a narrowband antenna is placed on the body, the impedance bandwidth for most of the antennas examined increases with respect to free space, by up to 84.52 %. On the body, the return losses for narrowband antennas remain below -10 dB; therefore, the bandwidth for this case can be considered at -10 dB impedance. The bandwidth for patch antennas is found to be very narrow, while the printed monopole antenna can show very wide bandwidth. In order to get higher on-body impedance bandwidth, antennas with partial ground planes are a better choice but these types of antennas show huge on-body performance degradation in concern of frequency detuning, radiation pattern deformation, and gain reduction. Antennas with full ground planes show moderate bandwidth, but are less sensitive to the human body; hence it is a trade off. Due to different on-body locations, the impedance bandwidth of different narrowband antennas varies by up to 85.35 %. Bandwidth is dependent on antenna type. Like frequency detuning, the impedance bandwidth of five narrowband antennas (DBDM, Patch, Printed Monopole, Inverted L and Loop) for various separation distances between the antenna and the body

was averaged. Table 4.14 shows the average impedance bandwidth and standard deviation of five narrowband antennas for various separation distances. The highest antenna-averaged impedance bandwidth (43.91 %) is noticed when the antenna is placed on the body directly. Results show that, the on-body impedance bandwidth varies significantly for different narrowband antennas.

Table 4.14. Average on-body impedance bandwidth and standard deviation of five narrowband antennas for various antenna placement distances. (the impedance bandwidth for each distance was averaged over 5 narrowband antennas).

Distance from the body	Mean (%)	Standard deviation (%)
Direct on the body	43.91	49.08
1 mm	22.95	26.95
4 mm	13.66	15.59
8 mm	10.12	10.51
16 mm (without wire mono)	12.70	14.32
16 mm (with wire mono)	16.94	16.48

- **Impact of different locations of the body:** Antennas with partial ground planes are extremely location dependant on-body. The results presented earlier show that antenna with partial ground planes have a huge variation of impedance bandwidth and frequency detuning for different locations of the body, while antennas with full ground planes show trivial variation. It is reported earlier that on the body, the highest frequency detuning is noticed when antenna is on the left waist, while the lowest is on the left ankle. The highest on-body impedance bandwidth is noticed when the antenna is placed on the right chest and the lowest is noticed when the antenna is on the left ear. The on-body impedance bandwidth and frequency detuning of five narrowband antennas (DBDM, Patch, Printed Monopole, Inverted L and Loop) for each different location on the body was averaged respectively. Fig. 4.41 illustrates the average frequency detuning and standard deviation of five narrowband antennas for various locations on the body, while Fig 4.42 shows the average impedance bandwidth and standard deviation. When the antenna placed directly on the body, for each on-body location, the frequency detuning and on-body impedance bandwidth for narrowband antenna varies significantly. On the body, maximum antenna-averaged frequency detuning is found to be 18 % (on left waist) whereas maximum impedance bandwidth is noticed to be 44 %.

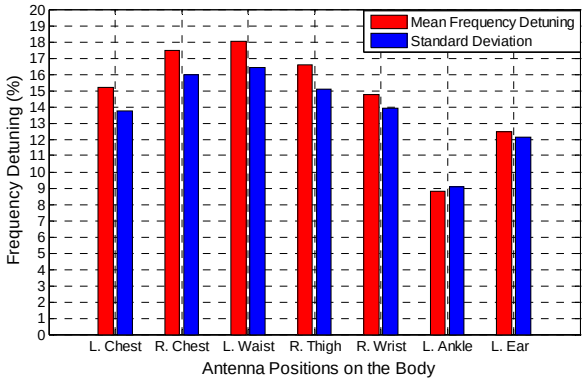

Fig. 4.41. Average frequency detuning and standard deviation of five narrowband antennas for various locations on the body when antenna placed directly on the body (the frequency detuning was averaged over the five antennas for each location).

Fig. 4.42. Average impedance bandwidth and standard deviation of five narrowband antennas for various locations on the body when antenna placed directly on the body (the on-body impedance bandwidth was averaged over the five antennas for each location).

- **Impedance:** Since the line impedance is 50 **Ω,** the wearable antenna input impedance should be 50 Ohm. On the body, the antenna input impedance changes. However, the return loss for most of the antenna studied in this thesis is below -10 dB; hence, the antennas show a good impedance match. For very compact narrowband antennas an extra matching network may be necessary to match the antenna impedance. Impedance changes less for the full ground plane antennas, compared to the partial ground plane antennas.
- **Radiation pattern:** The antenna radiation pattern has a significant influence on the on-body communication channels. For on-body applications, an antenna with omnidirectional radiation pattern over the body surface is recommended as this type of

antenna will provide more power-efficient and reliable communication links (minimise the on-body link loss). Due to their omnidirectional radiation over the body surface, the DBDM and Wire Monopole antennas experience the lowest path loss values for on-body radio channels, as reported in the previous section. However, for off-body communications antenna (patch) with directive radiation towards off the body will provide better communication link. On the body, the antenna radiation needs to be as stable as in free space. On the body, the radiation pattern distorts for the antennas with partial ground plane but remains nearly the same as free space for the antenna with full ground plane, except for slight variations of power level. The radiation pattern is antenna-dependent; therefore, the right antenna needs to be designed for the desired performance. When the narrowband antennas are placed on the body, the de-polarisation is noticed. On the body, the cross-polar radiation patterns show higher performance (in terms of patterns and power level) compared to the ones in free space. In the previous section, it was noted that the on-body cross-polar and co-polar radiation performances for some antennas were nearly the same and even in some cases, the cross-polar radiation was higher than co-polar radiation and hence, the antenna became un-polarised.

- **Radiation efficiency:** For body-centric wireless communications, an efficient antenna is required. Placing the narrowband antennas on the body, the radiation efficiency decreases with respect to free space for all proposed antennas as reported in previous section. Antennas with partial ground planes experience significant radiation efficiency reduction compared with the antennas with full ground planes. When the antenna is 1 mm away from the body, the wearable narrowband antenna experiences up to 96 % reduction of radiation efficiency. In the previous section, it was found that, at 8 mm away from the body, all antennas show acceptable levels of radiation efficiency; therefore, narrowband antennas should be placed at this distance (8 mm) from the body. At this distance, the on-body radiation efficiency for the proposed narrowband antennas is in the range of 28% to 82%. Table 4.17 summarises the on-body performances of the proposed narrowband wearable antennas when placed at 8 mm away from the body. The higher the antenna efficiency, the better the performances; therefore, narrowband antenna should be designed with full ground plane at the back. The radiation efficiency of six narrowband antennas including the wire monopole for different antenna placement distances was

averaged. Table 4.15 shows the average radiation efficiency and standard deviation of six narrowband antennas for various separation distances. On the body, the lowest antenna-averaged radiation efficiency (32.2 %) is noticed when the antenna placed at very close to the body (1 mm away). The standard deviation values are found to be very high for every separation distance which indicates that for different narrowband antennas, the radiation efficiency varies greatly.

Table 4.15. Average radiation efficiency and standard deviation of six narrowband antennas for various separation distances (the radiation efficiency was averaged over six narrowband antennas).

Distance from the body	Mean (%)	Standard deviation (%)
Free space	99.83	0.40
1 mm	32.20	34.67
4 mm	44.00	28.69
8 mm	50.33	24.66
16 mm	58.00	20.51

- **Gain:** When narrowband antennas are placed very close to the body (1 mm away), the maximum gain drops significantly for the antennas with partial ground planes but increases (mostly) for the antennas with full ground planes. When the narrowband antennas are worn on the body, the gain reduces by as much as 12.40 dB and increases up to 1.6 dB, with respect to free space. In the previous section, it was found that very close to the body (1, 4 mm), the gain for the antennas with partial ground planes is a negative value. For short-range indoor on-body communications, the antenna gain with positive value (1 dBi or more) is better. For-body-centric wireless communications, in order to get good on-body gain, there has to be a full ground plane at the back of the antenna. If we don't want the ground plane at the back of the narrowband wearable antenna, it has to be placed at least 8 mm away from the body. At this distance, all narrowband antennas show good on-body gain, which is in the range of 1.34 to 6.75 dBi, as shown in Table 4.17. The wearable antenna gain in the XZ plane (over the body surface) needs to be higher in order to minimise the on-body link loss. Table 4.16 lists the average peak gain and standard deviation of six narrowband antennas for various separation distances from the human body. At very close to the body (1 mm), the antenna-averaged gain is very low (-2 dBi) with the highest standard deviation value (6.86). The standard deviation value reduces as the distance between the antenna and the body increases. At higher distances, the lower

standard deviation values indicate that the on-body gain for different narrowband antennas varies very less when placed far away from the body.

Table 4.16. Average peak gain and standard deviation of six narrowband antennas for various separation distances (the peak gain was averaged over six narrowband antennas).

Distance from the body	Mean (dBi)	Standard deviation (dBi)
Free space	4.14	1.65
1 mm	-2.10	6.86
4 mm	2.00	3.24
8 mm	3.23	2.05
16 mm	4.16	1.52

- **Polarisation**: Polarization of the antenna is one of the important properties which is mainly determined by the propagation channel characteristics. Proper choice of the polarization of the antenna can improve the communication channel. The narrowband antenna polarisation should be normal to the body surface for minimised link loss in on-body communications. For body-centric wireless communications, a dual-polarised (vertical and horizontal polarization) antenna is better. When human body moves, the sensors located on the legs and ankles change the position and the orientation in relative to the body worn base station located on the left waist. During the movements (such as walking, running and so on) of the human body, the sensors located on the legs and wrists of the human body will provide better radio channel performance if the polarisation of the antenna is vertical and horizontal. On the other hand, the horizontal polarised antenna will provide better radio channel performance for the sensors located on the trunk (such as chest, waist and so on) of the human body. Considering these facts, a dual-polarised antenna will provide better radio channel performance for on-body radio channels. The polarisation is antenna-dependent. It is clear that, because of the lossy dielectric properties of the body tissues, vertically-polarised antennas should have better path gain compared with the horizontally polarised ones. For the wireless application, such as mobile system different dual polarised antennas are used. The antennas used in the thesis all are linearly polarised.
- **Ground plane:** Ground-plane size is one of the biggest issues for narrowband wearable antennas with respect to on-body performance reduction. This study has shown that for narrowband wearable antennas, the performance degrades significantly in close proximity

to the human body for the antennas with partial ground planes. Therefore, a full ground plane at the back of the antennas is preferred as it reduces the influence of lossy human tissues on antenna performances. The bigger the antenna ground plane size, the lesser the body effects. One of the drawbacks for the antenna with full ground plane is lower bandwidth; however, bandwidth is dependent on antenna types which can be improved.

- **Antenna placement distance from the body:** The gap between the antenna and the body is a very important issue for wearable antenna in body-centric wireless communications. Results indicate that, as the gap between the antenna and the body increases the antenna behaves like free space. It is very important to know the best distance to place the wearable antenna on the body, in order to get the optimal performance. The optimum distance to place the narrowband antenna from the body is suggested to be 8 mm. At 8 mm from the body, most of the narrowband antennas show acceptable levels of on-body performances, even if the antenna does not have a full ground plane at the back. Varying the distance between the antenna and the body does not have much effect on the antenna radiation pattern, but the gain, operating frequency shifting, impedance bandwidth and radiation efficiency are all significantly affected. The performance of the antennas with full ground plane does not change much as the distance between the body and the antenna varies; on the other hand, antennas with partial ground plane show huge variation in performance as the gap between the antenna and the body changes. The antenna placement distance is very effective for the narrowband antennas with partial ground planes/without ground planes.
- **SAR:** SAR (specific absorption rate) is a measurement of how much electromagnetic radiation is absorbed by body tissue whilst using the antenna on the body. The higher the SAR, the more radiation is absorbed; hence, antennas with low SAR are required, in order to minimise the electromagnetic radiation absorption by body tissue. This topic has been extensively studied by others for the investigation of mobile-human interaction. Further work needs to be done for body-centric wireless communications, however, it is out of the scope of my current study.
- **Multifunction and multiband antenna**: In BCWC, communications among on-body devices are required, as well as communications with external base stations. This

therefore requires antennas with different radiation characteristics and possibly, multi-band function. The antenna shape will be complex.

Table 4.17. Comparison of the on-body performance parameters of the proposed six narrowband antennas when placed at 8 mm away from the body.

Performance parameters	Printed Mono.	Patch	Wire Mono.	Loop	DBDM	Inverted L
Frequency Detuning (%)	4.62	0	-	2.32	0.16	5.06
Impedance Bandwidth (%)	27.51	1.38	-	8.4	2.37	10.96
Radiation Efficiency (%)	28	83	71	28	62	30
Peak gain (dBi)	1.34	6.75	3.06	2.31	4.41	1.53
XZ plane gain (dBi)	-2.9	-1.8	2.51	-2.5	4.40	-3.1
YZ Plane gain (dBi)	0.9	6.75	2.5	2.2	4.4	1.5

The leading parameters that control the narrowband antenna performance when placed on the body are the ground plane size, full or partial ground plane, antenna type and size, antenna placement distance from the body and locations of the body. A general summary of the effects of these parameters on the antenna performances on the body is given below in Table 4.18.

Table 4.18. General summary of the effects of the leading parameters that control the narrowband antenna performances when placed on the body.

Parameters	Frequency detuning	Impedance bandwidth	Radiation efficiency	Gain	Radiation pattern	Impedance matching	Path loss
Ground plane size	Very sensitive. Depends on ground plane size. Decreases as ground plane size increases.	Very sensitive. Decreases as ground plane size increases.	Very sensitive. Efficiency reduction decreases as ground plane size increases	Very sensitive. Increases as ground plane size increases.	Very sensitive. Radiation pattern becomes nearly the same as free space as the ground plane size increases.	Sensitive. Impedance changes very slight as the ground plane size decreases	-
Partial ground plane behind antenna	Significant frequency detuning. Very much dependent on the gap between antenna and the body and locations of the	Significant increase of impedance bandwidth. Very much dependent on the gap between the antenna and the body and locations of	Reduces significantly. Very much dependent on the gap between the antenna and the body. Reasonable efficiency at 8 mm.	Reduces significantly. Very much dependent on the gap between the antenna and the body. Negative gain very close to the body. Reasonable	Distorts significantly. Doesn't depend on the gap between the antenna and the body.	Changes significantly. Dependent on the gap between the antenna and the body.	Depends on antenna radiation pattern and gain. Higher path loss.

	body.	the body.		gain at 1mm			
Full ground plane behind antenna	Slight frequency detuning. Depends very slightly (ignorable) on the gap between the antenna and the body and locations of the body.	Slight increases (ignorable). Nearly independent of the gap between antenna and the body and also locations of the body.	Reduces less. Adequate efficiency even antenna placed very close to the body. Less dependent on the gap between antenna and the body. Reasonable efficiency at 1mm	Increases mostly. Less dependent on the gap between the antenna and the body. Positive gain on the body at all distances. Reasonable gain at 1mm	Less distortion; nearly as stable as free space in the XZ plane. Very slight distortion in the YZ plane.	Nearly independent of distance between the antenna and the body.	Depends on antenna radiation pattern and gain. Lower path loss.
Antenna type	Less dependent.	Very much dependent.	Dependent on antenna type.	Dependent on antenna type.	Completely dependent on antenna type; also, the polarisation is dependent on antenna	Less dependent on antenna type	Dependent on antenna type.
Antenna placement distance from the body	Extremely sensitive. Reduces as gap increases. Very effective for the antennas with partial ground planes.	Dependent very much. Very effective for the antenna with partial ground plane.	Dependent very much. Very effective for the antenna with partial ground plane.	Dependent very much. Very effective for the antenna with partial ground plane.	Does not influence the radiation pattern but the power level.	Dependent on the distance. Sensitive for the antennas with partial ground planes	Dependent but very less.
Antenna size	Dependent. Frequency detunes more for smaller antennas.	Dependent. Depends also on the antenna type and structure.	Dependent. Smaller antenna shows less efficiency.	Dependent. Smaller antenna shows less gain.	No dependence.	Less dependent.	-

The narrowband antenna specifications provided here will serve as a guideline in order to design suitable antenna for future efficient and reliable body-centric wireless communications. The DBDM antenna meets the specifications and guidelines. Based on the specifications, out of these six studied antennas, the DBDM antenna appears the best candidate for narrowband body-centric wireless communications. However, more suitable narrowband antenna for on-body applications can be designed, based on the specifications above.

4.5 Summary

The performance parameters in the presence of the human body of five narrowband antennas (namely, the Wire Monopole, Patch, Inverted L, Loop and Printed Monopole) were investigated and compared. The performance of the antennas with partial ground plane (Printed Monopole, Inverted L and Loop) degrades significantly in close proximity to the body except the increase of bandwidth. On the other hand, antennas with full ground plane (Patch and Wire Monopole) are very less sensitive in close proximity to the human body and show nearly stable performance when they are body-worn; therefore the ground plane is recommended for the wearable antennas. The on-body performance of the Printed Monopole, Loop and Inverted L is greatly dependent on the gap between the antenna and the body and also the locations on the body, while for the Patch and Wire Monopole, the on-body performance is nearly stable for various distances and locations on the body. However, results show that at 8 and 16 mm away from the body all antennas show satisfactory levels of efficiency and gain, so the optimum distance to place the narrowband antenna from the body is recommended to be 8 or 16 mm. The on-body performance of the Printed Monopole, Inverted L and Loop are comparable, while slight improved performance is noticed for the first one. These three antennas show very poor on-body radio channel performances compared with the Patch and Wire Monopole. However, the advantages of these three antennas are the higher on-body bandwidth and smaller volume. The wire monopole shows better on-body performance in terms of impedance bandwidth, radiation and XZ plane gain compared with the patch; it is found to be the most power-efficient for BCWCs. However, due to its shape, the wire monopole will not be suitable for on-body applications. A novel conformal dual-band and dual-mode antenna is proposed for power-efficient and reliable on-body and off-body communications. The performance of the DBDM at 2.45 GHz is compared with other five narrowband antennas, where it shows the advantage of on-body performance compared to other five antennas and it will be suitable candidate for future power-efficient and reliable BCWCs.

Based on the results analysis of six antennas, narrowband antenna specifications and design guidelines for BCWCs are provided. For efficient and reliable BCWCs, the antenna needs to show good on-body performance in terms of efficiency, gain, radiation pattern, frequency detuning, bandwidth, impedance matching, polarisation and so on. The human body effects on the wearable antenna performances need to be minimised as much as possible. Furthermore, the size, shape and radiation pattern of the antenna are very important.

References

[1] **P. S Hall and Y. Hao,** *Antennas and propagation for Body-Centric Wireless Communications.* Artech House, 2006.

[2] **C. Kunze, U. Grossmann, W. Stork, and K. Muller-Glaser,** " Application of ubiquitous computing in personal health monotoring systems, '' in *Biomedizinische Technik*: *36 th Annual Meeting of the German Society for Biomedical Engineering,* 2002, pp. 360-362.

[3] **N. F. Timmons and W. G. Scanlon**, " Analysis of the perfromances of IEEE 802.15.4 for medical sensor body area networking,'' in *1st Annual IEEE Communications Society Conf. Sensor Ad. Hoc Communications and and Networks (SECON)*, Oct. 4-7, 2004, pp 16-24.

[4] WSN for Healthcare: A Market Dynamics Report Published Aug. 2008.[Online] Available: http:// www.onworld.com/healthcare/index.html.

[5] **M. Presser, T. Brown, A. Goulianos, S. Stavrou and R. Tafazolli,** "Body Centric Context Aware Application Scenarios,''Antennas and Propagation for Body-Centric Wireless Communications,''2007 *IET Seminar* on 24-24, April 2007.

[6] **A. Alomainy, Y. Hao, A. Owadally, C. G. Parini, P. S. Hall, and C. C. Constantinou,** " Statistical analysis and performance evaluation for on-body radio propagation with microstrip patch antennas," *IEEE Transactions on Antenna and Propagation*, vol. 55, no. 1, pp. 245–248, January 2007.

[7] **Constantine A. Balanis**, Antenna theory analysis and design, Third edition, John Wiley and Sons, Inc. Hoboken, New Jersey, 2005.

[8] **P. S. Hall, Y. Hao, Y. I. Nechayev, A. Alomainy, C. C. Constantinou, , C. G Parini , M. R Kamruddin, T. Z. Salim, D. T. M. Hee, R. Dubrovka, A. Wadally, W. Song, A. Serra, P. Nepa, M. Gallo, and M. Bozzetti**, "Antennas and propagation for on-body communication systems," *IEEE Antenna Technology and Propagation Magazine,* vol. 49, no 3, June 2007.

[9] **P.S. Hall, Y. Nechayev, Y. Hao, A. Alomainy, M. R. Kamruddin, C.C. Constantinou, R. Dubrovka, and C.G Parini**, "Radio channel characterization and antennas for on body communications," *Proceeding of Loughborough Antennas and Propagation Conference, Loughborough, UK,* pp.330-333, April 2005.

[10] **W. L. Stutzman, and Gary A. Thiele**, Antenna Theory and design. John Wiley and Sons Ltd. 1988.

[11] **A. Alomainy, Y. Hao and D. M Davenport**, "Parametric Study of Wearable Antennas Varying Distances from the Body and Different On-Body Positions,'' *Antennas and Propagation for Body-Centric Wireless Communications, 2007 IET Seminar on* 24-24 April 2007 Page(s):84 – 89.

[12] **M. N Suma, P.C Bybi, and P. Mohanan**, "A wideband printed monopole antenna for 2.45 GHz WLAN applications,'' *Microwave and optical technology letter*, vol, 48, no, 5, pp 871-873, May 2006.

[13] **H. D. Chen, J. S. Chen, Y. T. Chen,** "Modified inverted-L monopole antenna for 2.4/5 GHz dual-band operations'', *Electronics Letters*, Volume 39, Issue 22, October 2003, pp: 1567-1568.

[14] **A. Alomainy**, Antennas and Radio Propagation for Body-Centric Wireless Networks, PhD thesis, Electronic Engineering, Queen Mary University Of London, May 2007.

[15] **Akhoondzadeh-Asl L., Khan I., Nechayev Y I, Hall P. S**, "Investigation of polarization in on-body propagation channels,'' *Antennas and Propagation, EuCAP 2009*. 3rd European Conference on, 2009, Page(s): 466–469.

[16] **S. S. Gassemzadeh, R. Jana, C. W. Rice, W. Turin, and V. Tarohk**, "A statistical path loss model for in-home UWB channels,'' *IEEE Conf. Ultrawide Band Systems and Technologies*, Baltimore, p. 5964, 200.

[17] "Electronic imaging: Board of regents, "National Institute of Health National Library of Medicine USA, Bard of regents, Bethesda, MD, Tech, Rep. NH 90-2197, 1990.

[18] **C. Gabriel and S. Gabriel**, "Compilation of the dielectric properties of body tissues at RF and microwave frequencies," *URL: http://www.brooks.af.mil/AFRL/HED/hedr/reports/dielectric/Title/Title.html,1999.*

[19] ''Calculation of the dielectric properties of body tissues," *Institute for Applied Physics*, *Italian National Research Council, URL: http://niremf.ifac.cnr.it/tissprop/*.

Chapter 5 Ultrawide Band Antenna Characterisation and Specifications for Body Area Networks

The UWB technology has attracted much attention and experienced considerable growth over the past few years due to its distinctive characteristics. In 2002, the Federal Communication Commission (FCC) [1] has allocated the spectrum from 3.1 to 10.6 GHz for unlicensed UWB communication applications. One of the most promising areas of UWB applications is the body-centric wireless communication, where the wireless connectivity between body-centric units is provided through the deployment of light-weight and compact UWB antennas [2-4]. This chapter investigates and compares the on-body performance parameters of 4 different ultra wideband (3.1-10.6 GHz) antennas including the Tapered Slot Antenna (TSA), Planar Inverted Cone Antenna (PICA), SWAN Shaped Antenna and Self-Complementary Compact Antenna. It provides an understanding of the human body effects on the UWB antenna parameters. The behaviour of the antenna types on the ultra wide-band (UWB) on-body radio channels is also experimentally investigated in this chapter. Based on the study, ultra wideband antenna specifications and design guidelines for body-centric wireless communications are provided. In addition, a comparison of narrowband and UWB on-body antenna parameters is also provided at the end of this chapter. The presented results will be useful to design the suitable body-worn ultra wideband antenna for efficient and reliable body-centric wireless communication applications.

5.1 Ultra Wideband Wearable Antennas

5.1.1 Tapered Slot Antenna (TSA)

A far as the design of a UWB antenna is concerned, a broadband impedance matching network is needed and it can be achieved by employing two tapered radiating slots at the end of the

Coplanar Waveguide CPW feeding line [5] by gradually varying the feed-gap [6] and with the help of a pair of tapered radiating slots [7]. A tapered slot antenna (TSA) is proposed using a similar approach to [8-9]. The CPW fed miniaturised TSA is fabricated on RT/Duroid board with permittivity of ε_r=3 and a thickness of 1.524 mm [8-10]. Fig. 5.1 shows the dimensions and geometry of the proposed Tapered Slot Antenna.

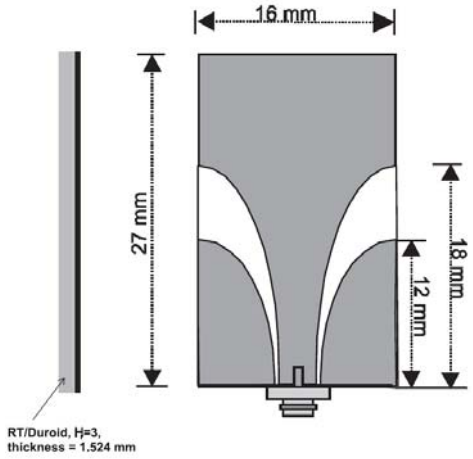

Fig. 5.1. Dimensions and geometry of the designed CPW-fed Tapered Slot Antenna (TSA) [8-10].

The total size of the TSA antenna is 27 mm×16 mm^2 which is around $0.27\lambda_0 \times 0.16\lambda_0$ in electrical length, where λ_0 is the free space wavelength at 3 GHz. Unlike the traditional CPW-fed antenna (such as the PICA discussed below), the tapered slot antenna is designed to allow for the smooth transition of line impedance. The ratio of semi-major to semi-minor axis within the design is the most significant parameter to affect the impedance matching [5].There is no ground plane at the back of the proposed TSA.

5.1.2 Planar Inverted Cone Antenna (PICA)

The Planar Inverted Cone Antenna (PICA) is also fed with coplanar waveguide. The PICA [10-14] consists of two elements; the top element planar cone and rectangular-shaped metal incorporating a CPW feed. The antenna is fabricated on RT/Duroid substrate with thickness of *h*=1.524 mm, relative permittivity of $\varepsilon_r = 3,$ and loss tangent tan (δ) =0.0013. Fig. 5.2 shows

the dimensions and geometry of the proposed PICA. The total size of the antenna is 47.5× 50 mm^2 which is around 0.48 λ_0 × 0.5 λ_0 in electrical length, where, λ_0 is the free space wavelength at 3 GHz. The gap dimension between the metallic part and the cone is 0.3 mm; the gap plays a major role in matching the antenna with Ω 50 input. There is no ground plane at the backside of the PICA.

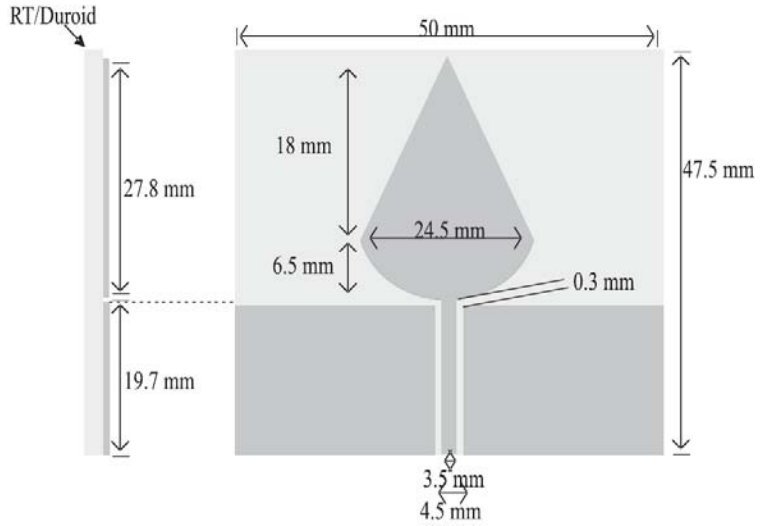

Fig. 5.2. Dimensions and geometry of the designed CPW-fed Planar Inverted Cone Antenna (PICA) [10-13].

5.1.3 SWAN Shaped Antenna

The SWAN Shaped Monopole Antenna is a miniaturised microstrip-line fed antenna. It is fabricated on a PCB board Rogers 4003 with the thickness of 1.5 mm and relative permittivity of $\varepsilon_r = 3.38$ [11-13]. Fig. 5.3 shows the dimensions and geometry of the proposed SWAN Shaped Antenna. The total size of the antenna is 25×25 mm^2 which is around 0.25 λ_0 × 0.25 λ_0 in electrical length, where, λ_0 is the free space wavelength at 3 GHz. In order to reduce the antenna size, and also improve polarisation performance, the monopole has been slotted and an additional horizontal section is added (hence the antenna takes the shape of a swan). Two bevels were cut to improve the impedance matching at higher frequencies. There is a partial ground plane at the back of the SWAN shaped antenna.

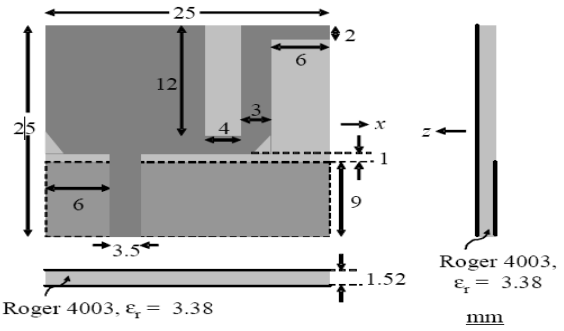

Fig. 5.3. Dimensions and geometry of the designed microstrip line fed SWAN Shaped Monopole antenna [15-17].

5.1.4 Quasi-Self Complementary Compact Antenna

The proposed small printed Quasi-Self Complementary antenna is fed by a microstrip line. The antenna is fabricated on FR4 substrate with thickness of h=1.6 mm and relative permittivity of $\varepsilon_r = 3$. The total size of the antenna is 25×16 mm^2 which is around 0.25 λ_0 ×0.16 λ_0 in electrical length, where, λ_0 is the free space wavelength at 3 GHz [18]. Fig. 5.4 shows the dimensions and geometry of the proposed Quasi-Self Complementary Compact Antenna. A triangular slot is cut on the ground plane in order to improve the impedance matching of the antenna. There is a partial ground plane at the back of the self complementary compact antenna.

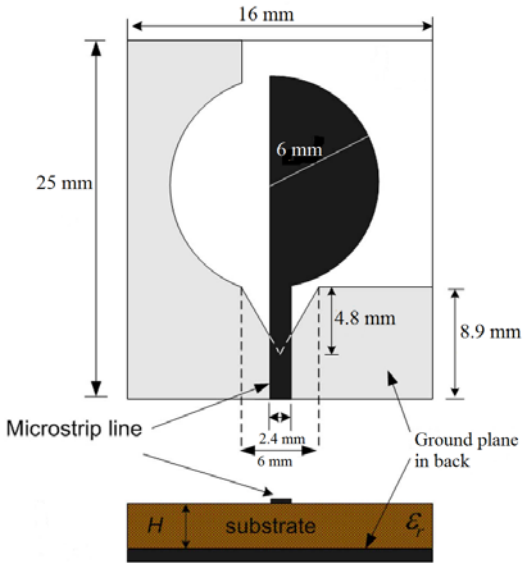

Fig. 5.4. Dimensions and geometry of the designed microstrip line fed Quasi-Self-Complementary antenna [18].

5.1.5 Volume and Size Comparison of the UWB Antennas

The size and volume of the ultra-wideband antennas used for this study are shown in Table 5.1. The TSA and PICA are printed on RT/Duroid board, the SWAN shaped on Rogers 4003 and the Self complementary is on FR4 substrate. Out of these four antennas, two (SWAN shaped and self complementary compact) have partial ground planes at the back of the antenna and the other two (TSA and PICA) dont have ground plane. Of the four antennas, the self complementary compact has the smallest substrate size and the PICA has the highest volume.

Table 5.1 Comparison of volume and size of the ultra wideband antennas used in this study.

Antenna	**Substrate L×W (mm^2)**	ε_r	**Ground Plane L×W (mm^2)**	**Height (mm)**	**Volume L×W×H (mm^3)**	**Antenna Element L×W(mm^2)**
TSA	27×16	3	-	1.524	27×16×1.524	27×16
PICA	47.5×50	3	-	1.524	47.5×50×1.524	47.5×50
SWAN	25×25	3.38	9×25	1.52	25×25×1.52	25×25
Self Complementary	25×16	3.0	25×8.9	1.6	25×16×1.6	25×16

5.2 UWB Antenna Performance Parameters Comparison

5.2.1 Return Loss Comparison

The S11 measurement campaigns of four UWB antennas were performed in an anechoic chamber at Queen Mary, University of London. In this study, the same male test subject was used as in the narrowband case. Like the narrowband experiment, the four different UWB antenans were placed on seven different locations (Right/left chest, left waist, left thigh, right wrist, left ear and left ankle) of the human body, varying the distance between the antenna and the body; see Fig.4.6. During the measurement, the antennas were placed direct on the body and then 1, 4, 8 and 16 mm away from the body. The antenna was oriented with radiating elements parallel to the body and facing outward.

Figs. 5.5 (a-d) show free space and on-body return loss responses of the presented four UWB antennas when placed at various distances from the body (left side of the waist). The figures illustrate that, in free space, all four antennas have excellent impedance matching across the UWB band, with return loss less than -10 dB. The free-space working frequency of the TSA, PICA, SWAN and Self Complementary is in the range of 3.168–10.96, 3.170-12.04, 3.003-12.57, and 3.195-11.19 GHz, at -10 dB impedance, respectively. When the antenna is placed on human body, the lower frequency band at -10 dB impedance shifts from free space for all antenna cases.

Fig. 5.6 shows the comparison of the lower frequency shifting, with respect to free space at -10 dB impedance for the four different UWB antennas when placed at various distances from the human body. Placing the UWB antennas on the body, the lower frequency at -10 dB impedance shifts down to 2 GHz with respect to free space. The lower frequency shifting is the highest for the TSA, while the lowest is noticed for the PICA. Results indicate that antennas bigger in size (PICA, SWAN) show lower frequency shifting in compared to the antennas smaller in size (TSA, Self complementary). It is noted that, although the size of the self complementary is smaller compared to the TSA but shows less frequency detuning, which is due to the partial ground plane at the back of the self complementary antenna. The partial ground plane helps to reduce the frequency shifting for the SWAN and Self complementary antennas as compared to the TSA. On the body, most of the UWB antennas show leftwards lower frequency shifting trends except for the PICA. This suggests potential reduction of the UWB antenna size for BAN applications. The lower frequency shifting is at its maximum when the antenna is very close to the body, and decreases as the gap between the antenna and the body increases.

In this study of UWB antennas, when the antennas are placed on the body due to capacitive coupling between body and antenna, the antenna input impedance changes this causes the variation in return loss for all antennas (Fig. 5.5). The impedance matching for the PICA, SWAN shaped and Self Complementary antennas is sensitive to the human body. In some cases, at various distances from the body, the on-body return loss of these three antennas reach a maximum -5.5 to -6.5 dB, which is acceptable, because some mobile phone antennas work with the return loss of -6 dB. In terms of impedance matching, the TSA shows very good on-body performance as compared to the other aforesaid UWB antennas (Fig. 5.5).

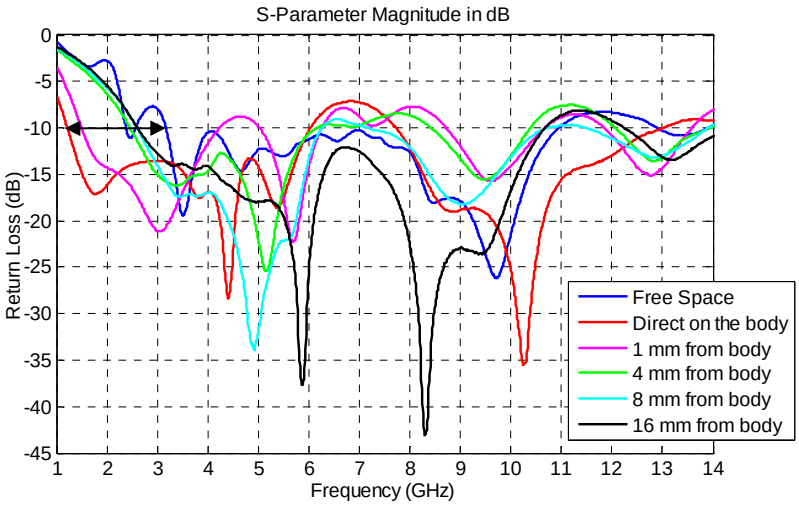

(a) TSA

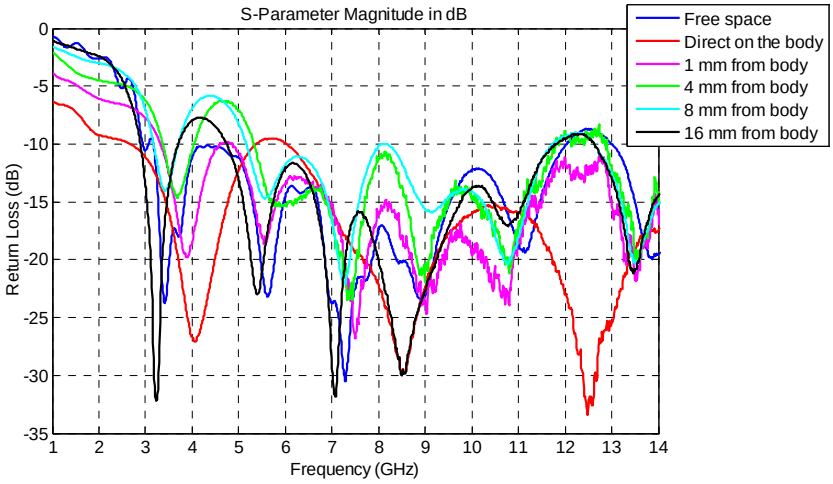

(b) PICA

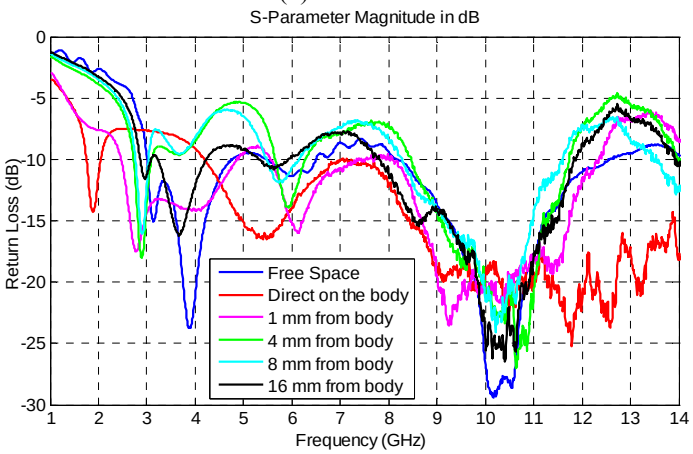

(c) SWAN Shaped

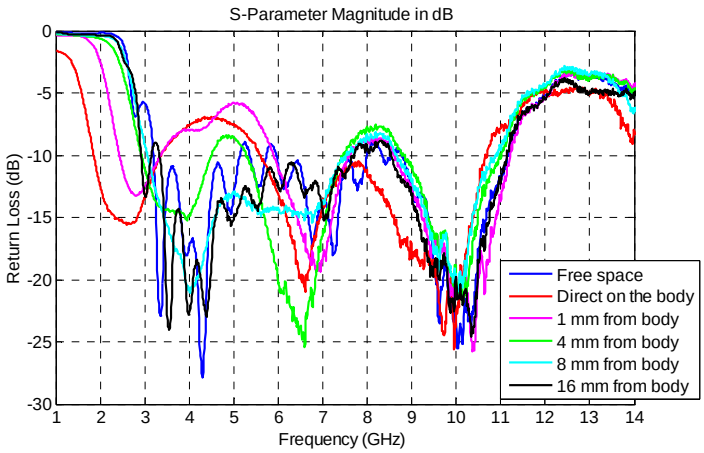

(d) Self Complementary

Fig. 5.5. Return loss responses of the four proposed UWB antennas (a) TSA (b) PICA (c) SWAN (d) Self Complementary, when placed at various distances from the left side of the waist.

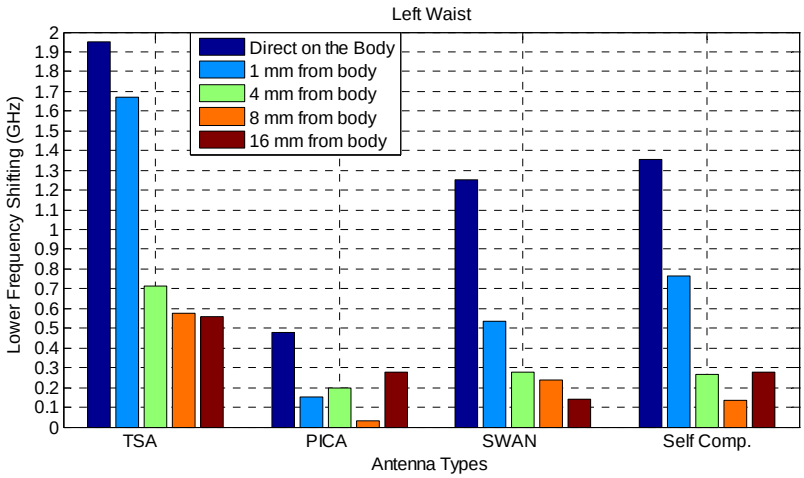

Fig. 5.6. Comparison of lower frequency shifting at -10 dB impedance with respect to free space for four UWB antennas when placed at different distances from the left side of the waist.

The lower frequency shifting at -10 dB impedance for each UWB antenna was averaged over various antenna placement distances (direct on the body, 1, 4, 8, 16 mm) from the human body. Table 5.2 shows the average lower frequency shifting and standard deviation of various antenna placement distances from the human body for four UWB antennas. The distance to place the antenna from the human body, has lower effect in lower frequency shifting for the PICA antenna while it has higher effect for the TSA and Self complementary antennas.

Table 5.2. Average lower frequency shifting and standard deviation of different antenna placement distances from the body for four UWB antennas (lower frequency shifting at -10 dB impedance of each antenna was averaged over the various antenna placement distances).

Antenna	Mean (GHz)	Standard deviation (GHz)
TSA	1.093	0.664
PICA	0.222	0.177
SWAN	0.490	0.451
Self Comp.	0.560	0.505

The four UWB antenna return loss responses on different body parts were also investigated. Fig. 5.7 shows the return loss responses of the TSA and PICA when placed directly on seven different locations of the body. Due to changes in human tissue physiological and electrical properties, the lower frequency shifting with respect to free space at -10 dB impedance varies up to 0.916 GHz; see Fig. 5.8. This happens for the TSA when it is placed directly on the right chest and right wrist. For different locations of the body, the variation of lower frequency shifting is the highest for the antennas without ground planes (TSA and PICA) and the lowest for the antennas with partial ground planes (SWAN Shaped and Self Complementary compact antennas). The SWAN Shaped is less sensitive (least frequency shifting) to the changes in on-body position while the TSA is the most sensitive.

Due to different on-body locations, the maximum lower frequency shifting variation for the PICA, SWAN, and Self Complementary antennas is 0.717 GHz, 0.313 GHz and 0.511 GHz respectively. For all UWB antenna cases, the lower frequency shifting is the most when antennas are placed on the left waist, right thigh and right wrist and the lowest is on the right chest; see Fig. 5.8. For UWB antenna cases, the lower frequency shifting at -10 dB impedance ultimately leads to the increase of antenna impedance bandwidth.

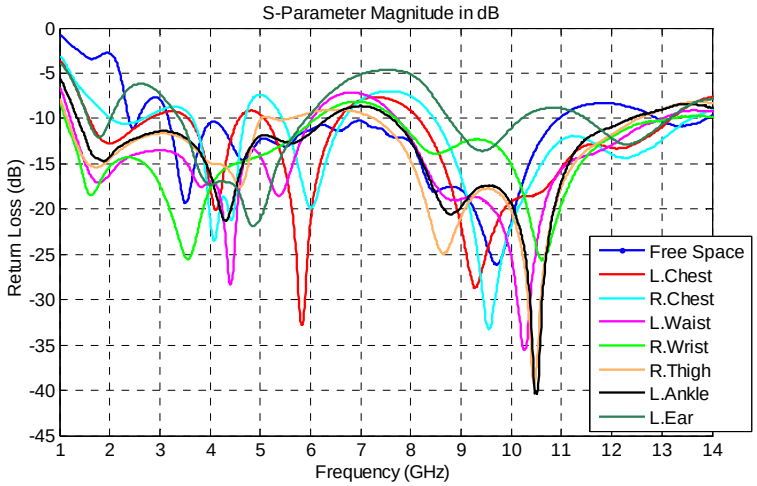

(a) TSA

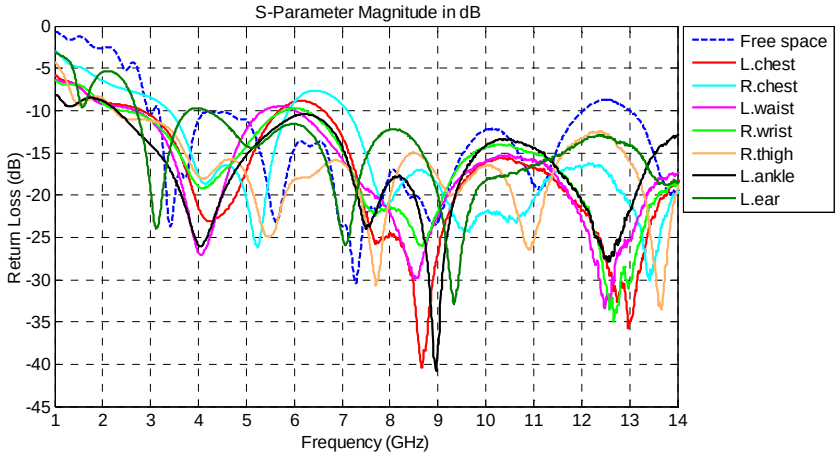

(b) PICA

Fig. 5.7. Return loss responses of the proposed UWB antennas when placed on seven different locations of the body directly (a) TSA (b) PICA.

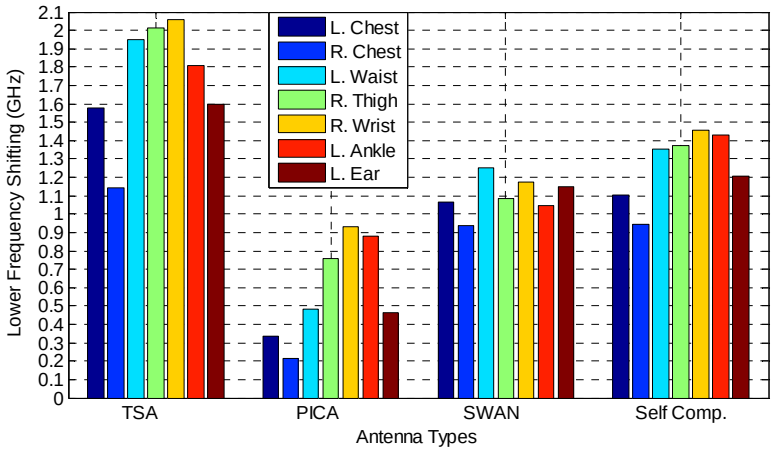

Fig. 5.8. Comparison of lower frequency shifting at -10 dB impedance with respect to free space for four UWB antennas when placed at different locations on the human body.

The lower frequency shifting at different locations direct on the body was averaged for each UWB antennas; see Table 5.3. The SWAN shaped and Self complementary antennas show the lower standard deviation values. Results indicate that the location to place the antenna on the human body, has lower effect in the lower frequency shifting for the SWAN shaped and Self complementary antenna while it has higher effect for the TSA and PICA antennas. However, the standard deviation values for four UWB antennas are very close to each other.

Table 5.3. Average lower frequency shifting and standard deviation of various locations on the body for four UWB antennas (the lower frequency shifting at -10 dB impedance of each antenna was averaged over the various locations on the body).

Antenna	Mean (GHz)	Standard deviation (GHz)
TSA	1.736	0.324
PICA	0.581	0.277
SWAN	1.101	0.101
Self Comp.	1.269	0.192

5.2.2 Radiation Efficiency

The antenna radiation efficiency parameter was extracted from the simulation results. During the simulation, the antenna was placed on the middle of the three-layer human body model which was modelled using CST microwave studio ^{TM}. The three layers considered were: a skin layer of 2-mm thickness; a fat layer of 15-mm thickness; a muscle layer of 100-mm thickness. The overall dimensions of this model were 300 ×700 ×117 mm^3. The dielectric properties of the three layers human body for 3 to 10 GHz were obtained from [19-20]. The human tissues are dispersive and their electrical properties are therefore changing over frequencies. In this case, the antenna was simulated first in free space, and then at 1, 4, 8 and 16 mm away from the body.

The antenna was oriented with radiating elements parallel to the body and facing outward. Figs. 5.9 (a-c) show a comparison of free space and on-body radiation efficiency as a percentage at 3, 6 and 9 GHz, for the four ultra wideband antennas when placed at various distances from the body (middle of the three layers model). In this study, when the UWB antennas are placed on the body, the radiation efficiency for all four presented antennas reduces from the free space across the whole UWB band due to power absorption by the lossy human tissues.

Placing the UWB antenna on the human body a maximum of 90.77, 81.25 and 59.7% radiation efficiency reduction is noticed at 3 GHz, 6 GHz and 9 GHz respectively. In the lower

frequency band, the radiation efficiency reduction is the highest compared with the higher frequency band, which shows that the body impact is greater at lower frequencies, as was expected. A radio wave penetrates more into the human body at low frequencies, whilst dissipate more at high frequencies. At higher frequencies, the penetration depth is lower but the power losses due to the presence of lossy human body tissues increase as compared to lower frequencies.

Fig. 5.10 shows the comparison of on-body radiation efficiency for the four UWB antennas across the band (3 to 10 GHz) when placed 4 mm away from the body. The on-body radiation efficiency, as shown in Fig. 5.10 for each antenna at 4 mm away from the body was averaged over the frequency band of 3 to 10 GHz. The average radiation efficiency for TSA, PICA, SWAN and Self Complementary was found to be 53.30 %, 60.32 %, 58.19 % and 48.16 % respectively. Being the smallest in size, the Self Complementary UWB antenna experiences the lowest on-body radiation efficiency, as compared to the other three.

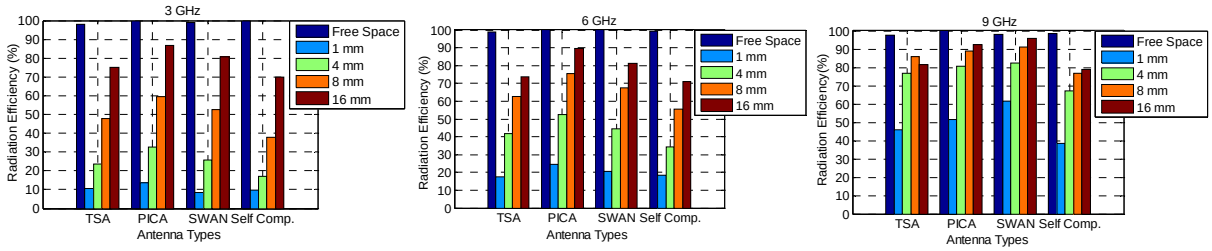

(a) 3 GHz (b) 6 GHz (c) 9 GHz

Fig. 5.9. Comparison of free space and on-body radiation efficiency in percentage for four different UWB antennas at (a) 3 GHz (b) 6 GHz (c) 9 GHz when placed at various distances away from the body.

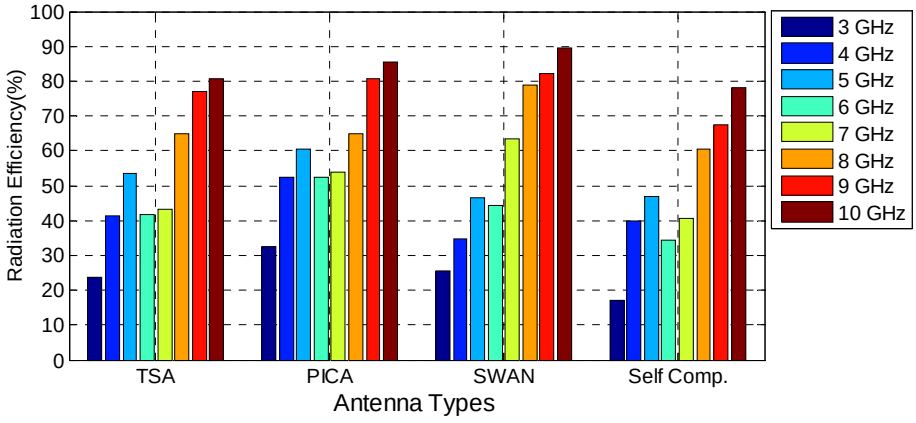

Fig. 5.10. Comparison of on-body radiation efficiency in percentage for four different UWB antennas across the band (3 to 10 GHz) when placed at 4 mm away from the body.

The human body has less effect on the UWB antenna impedance but has a significant effect on the antenna radiation efficiency. For the UWB case, having no ground plane or a partial ground plane has limited effect on the on-body radiation efficiency, but the antenna size seems to be more significant. However, it is possible that having a full ground plane on the rear of the antenna may improve the on-body radiation efficiency for the UWB antenna.

For all antennas, the radiation efficiency reduces less as the distance between the antenna and the body increases. Results show that, when the antenna is placed at 4 mm away from the body, most of the antennas show an acceptable level of radiation efficiency across the whole frequency band.

The radiation efficiency for the other separation distances (1, 8, 16 mm away from the body) was also averaged over the frequency band of 3-10 GHz for the four UWB antennas. The frequency-averaged radiation efficiency of various separation distances (1, 4, 8, 16 mm) was averaged for each antenna. Table 5.4 summarises the frequency-averaged mean radiation efficiency and standard deviation of various separation distances for the four UWB antennas. The PICA and SWAN shaped antennas show the highest distance-averaged on-body radiation efficiency. The standard deviation values for four UWB antennas are very close to each other. Results show that, the antenna placement separation distance has nearly the same effects on the on-body radiation efficiency for the four UWB antennas.

Table 5.4. Frequency-averaged mean radiation efficiency and standard deviation of various separation distances for four UWB antennas (the frequency averaged efficiency was averaged over various antenna placement distances).

Antenna	Mean (%)	Standard Deviation (%)
TSA	57.83	23.55
PICA	66.24	25.04
SWAN	64.81	24.74
Self Comp.	54.73	22.88

5.2.3 Gain

The gain parameters for the UWB antennas were also extracted from the simulation results. The on-body simulation set up was the same as describes in previous section 5.2.2. In this case, the antenna was simulated placing first in the free space and then 1, 4, 8 and 16 mm away from the body.

Peak Gain

Fig. 5.11 illustrates a comparison of free space and on-body peak gain at 3, 6 and 9 GHz of the four UWB antennas when placed at different distances away from the body. When the UWB antenna is placed very close to the body (1 mm away), in the lower frequency bands (3 and 6 GHz), the peak gain reduces with respect to free space but in the higher frequency band (9 GHz), the gain increases. Placing the UWB antenna on the body a maximum of 7.59 dB reduction of gain is noticed at 3 GHz, while an increase of maximum 5.94 dB gain is noticed at 9 GHz. On the body, the directivity of the antenna increases because the wave is reflected from the body, while the efficiency decreases due to tissue absorption. In free space, the peak gain is always in broadside direction (x=0 and y=0), when the antenna is body-worn, the wave reflected from the body may be recombined in phase with the direct one in a different direction, and hence the direction of the peak gain changes with frequency and it is slightly tilted with respect to the free space case.

Placing the full ground plane at the back of the UWB antenna, the on-body gain can be improved. Results show that at 4 mm away from the body, all proposed UWB antennas show acceptable level of gain hence the optimum distance to place the UWB antenna from the body is recommended to be 4 mm. However, when the antenna is placed 8 mm away from the body, the gain with respect to free space enhances for all antennas across the whole frequency band of operation (3.1-10.6 GHz).

Fig. 5.12 gives the comparison of on-body gain as a function of frequency for the four UWB antennas when placed at 4 mm away from the body. The on-body gain at 4 mm away from the body, as shown in Fig. 5.12, is averaged over the frequency band of 3 to 10 GHz for each antenna. The on-body gain for TSA, PICA, SWAN and Self Complementary antennas is found to be 6.02 dBi, 7.09 dBi, 6.55 dBi and 5.15 dBi respectively. The PICA and SWAN shaped antennas show the highest on body gain, while the lowest is noticed for the self complementary. Being bigger in size, the PICA shows the highest on-body average gain, while the Self complementary show the lowest because of its smallest size. Placing the Self complementary antenna on the body, a reduced amount of gain and radiation efficiency is noticed as compare to the other three. However, it is noted that the size of the TSA and SWAN is very small compared

to the PICA, but there is not much difference in gain parameters which shows the suitability of these two antennas for on-body applications.

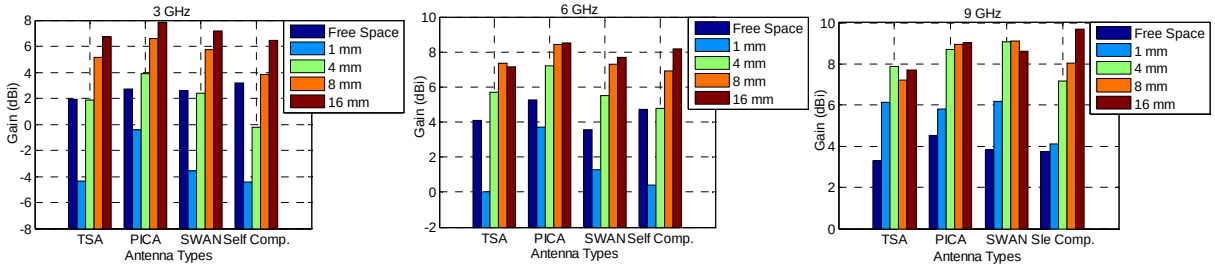

(a) 3 GHz (b) 6 GHz (c) 9 GHz

Fig. 5.11. Comparison of free space and on-body gain of the proposed UWB antenna at (a) 3 GHz, (b) 6 GHz, (c) 9 GHz when placed at various distances from the body.

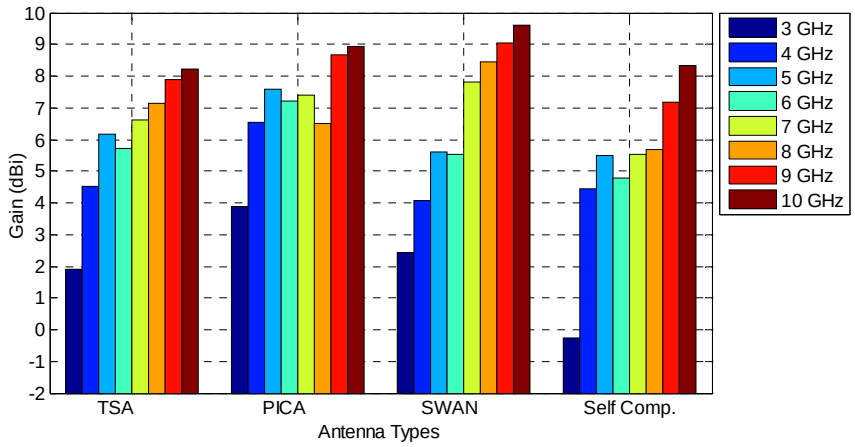

Fig. 5.12. Comparison of on-body peak gain across the band (3 GHz to 10) GHz for four different UWB antennas when placed at 4 mm away from the body.

Like the radiation efficiency, the peak gain for the other separation distances (1, 8, 16 mm) was also averaged over the frequency band of 3-10 GHz for the four UWB antennas. The frequency-averaged peak gain of various separation distances (1, 4, 8, 16 mm) is averaged for each antenna. Table 5.4 summarises the frequency-averaged mean peak gain and standard deviation of various separation distances for the four UWB antennas. Results show that for different separation distances, the peak gain varies less for the PICA compared to other three antennas. The standard deviation values of the other three antennas are found to be very close to each other.

Table 5.5. Frequency-averaged mean peak gain and standard deviation of various separation distances for four UWB antennas (the frequency-averaged peak gain was averaged over various antenna placement distances).

Antenna	Mean (dBi)	Standard deviation (dBi)
TSA	5.39	2.77
PICA	6.96	1.92
SWAN	6.23	2.64
Self Comp.	5.28	2.85

The on-body gain for the four UWB antennas has been investigated plane wise as XY, YZ and XZ.

XY Plane Gain

Fig. 5.13 shows a comparison of free space and on-body XY (azimuth) plane gain at 3, 6 and 9 GHz for the four UWB antennas when placed at various distances from the body. When the antenna placed on the body, in this plane a maximum of 7.8 dB reduction of gain with respect to free space is noticed at 3 GHz, while an increase of 6.9 dB gain is noticed at the higher frequency band of 9 GHz. At 4 mm away from the body, the on-body gain is plotted as function of frequency in Fig. 5.14. The gain at 4 mm away from the body, as shown in Fig. 5.14, is averaged over the frequency band of 3 to 10 GHz for each antenna. The average on-body gain in the XY plane for the TSA, PICA, SWAN and Self Complementary antennas is 4.9 dBi, 6.26 dBi, 6.3 dBi, 3.43 dBi, respectively.

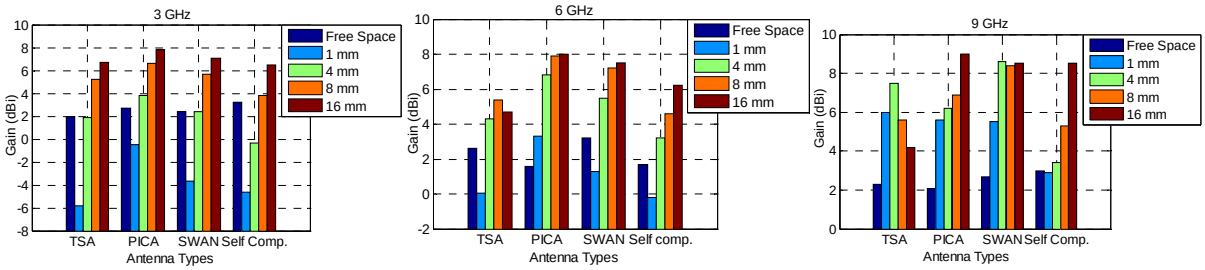

(a) 3 GHz (b) 6 GHz (c) 9 GHz

Fig. 5.13. Comparison of XY plane free space and on-body gain of the proposed UWB antenna at (a) 3 GHz, (b) 6 GHz, (c) 9 GHz when placed at various distances from the body.

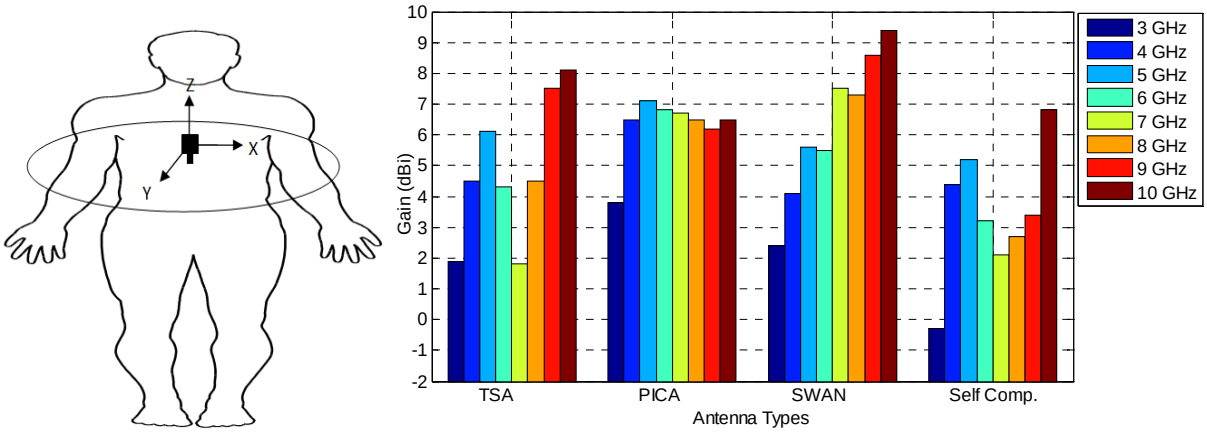

Fig. 5.14. Comparison of XY plane on-body gain across the band (3 GHz to 10) GHz for four different UWB antennas when placed 4 mm away from the body.

For the other separation distances, the XY plane gain was also averaged over the frequency band of 3-10 GHz for the four UWB antennas. The frequency-averaged XY plane gain of various separation distances is averaged as a function of distance for each antenna; see Table 5.6. In this plane, the SWAN Shaped and the PICA show the highest average on-body gains while the Self complementary shows the lowest.

Table 5.6. Frequency-averaged mean XY plane gain and standard deviation of various separation distances for four UWB antennas.

Antenna	Mean (dBi)	Standard deviation (dBi)
TSA	5.0	2.17
PICA	6.40	1.82
SWAN	6.0	2.60
Self Comp.	4.07	2.63

XZ Plane Gain

Fig. 5.15 shows a comparison of free space and on-body XZ plane gain at 3, 6 and 9 GHz, for the UWB antennas as a function of distance from the body. In this plane, on the body, the gain for all proposed antennas drops with respect to free space across the whole band (3-10 GHz), where the drop is most significant in the lower frequency band. When the antenna is body worn, maximum of 17 dB drop in gain is noticed in this plane. In free space, most of the used UWB antennas show omnidirectional radiation behaviours in the XY plane but, on the body, the radiation patterns become directive in the XY and YZ (off-body) directions, which results in lower gain on

this plane (XZ). However, for UWB application antenna with quite omnidirectional radiation patterns in this plane (XZ) may provide better on-body gain, hence improved radio channel performances.

Fig. 5.16 shows the on-body gain as function of frequency when the antenna is placed at 4 mm away from the body. At this distance, the on-body gain (averaged over the frequency band of 3~10 GHz) in the XZ plane for the TSA, PICA, SWAN and Self Complementary antennas is -11.82 dBi, -9.38 dBi, -8.23 dBi and -10 dBi, respectively. In this plane, the SWAN shaped antenna shows the best on-body gain performance.

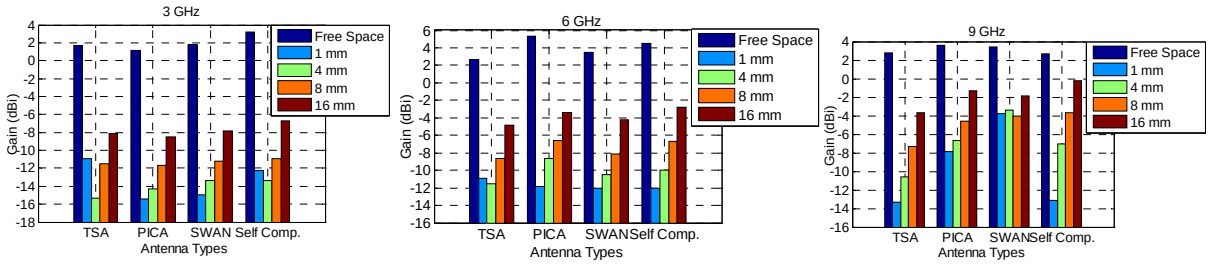

(a) 3 GHz (b) 6 GHz (c) 9 GHz

Fig. 5.15. Comparison of XZ plane free space and on-body gain of the proposed UWB antenna at (a) 3 GHz, (b) 6 GHz, (c) 9 GHz when placed at various distances from the body.

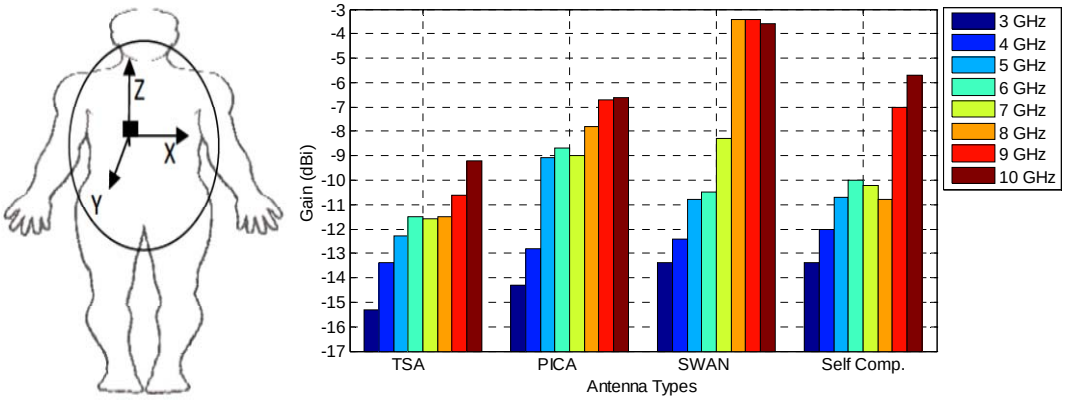

Fig. 5.16. Comparison of XZ plane on-body gain across the band (3 GHz to 10 GHz) for four different UWB antennas when placed at 4 mm away from the body.

The XZ plane frequency averaged on-body gains of 1, 4, 8, and 16 mm separation distances are averaged over the separation distances for four UWB antennas. Table 5.7 shows the frequency-averaged XZ plane mean on-body gain and standard deviation of various separation distances.

Table 5.7. Frequency-averaged mean XZ plane gain and standard deviation of various separation distances for four UWB antennas.

Antenna	Mean (dBi)	Standard deviation (dBi)
TSA	-9.26	2.82
PICA	-7.84	3.62
SWAN	-7.12	2.38
Self Comp.	-8.04	3.81

YZ Plane Gain

Fig. 5.17 illustrates free space and on-body YZ (elevation) plane gain at 3, 6 and 9 GHz for the UWB antennas when placed at various distances from the body. In this plane, when antenna placed on the body, the gain drops by maximum of 6.8 dB in the lower band whereas increases by 6 dB in the upper band with respect to free space. On the body, the radiation patterns of four UWB antennas become directive in both XY and YZ planes; therefore, the on-body gain for the proposed UWB antennas is the highest on these two planes (XY and YZ).

Fig. 5.17 shows the YZ plane on-body gain as function of frequency when antenna is at 4 mm away from the body. At this distance, the on-body gain (averaged over the frequency band of 3~10 GHz) in the YZ plane for the TSA, PICA, SWAN and Self Complementary antennas is 6.02 dBi, 5.6 dBi, 6.25 dBi and 4.71 dBi, respectively. In this plane, the SWAN shaped and TSA show the best on-body gain performances. In all planes, the self complementary antenna shows the lowest gain except in the XZ plane.

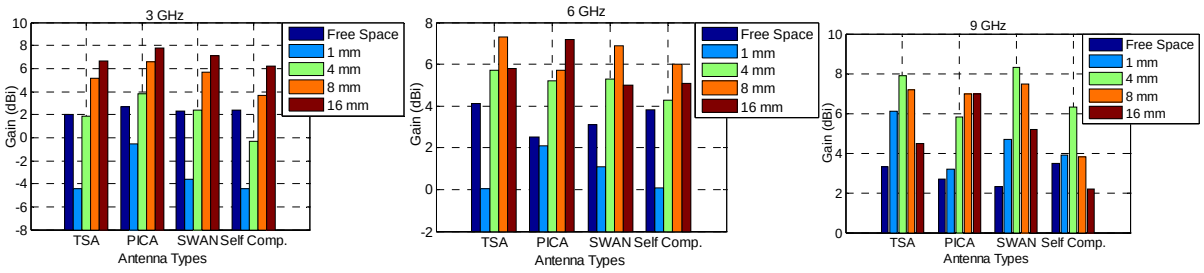

(a) 3 GHz (b) 6 GHz (c) 9 GHz

Fig. 5.17. Comparison of YZ plane free space and on-body gain of the proposed UWB antenna at (a) 3 GHz, (b) 6 GHz, (c) 9 GHz when placed at various distances from the body.

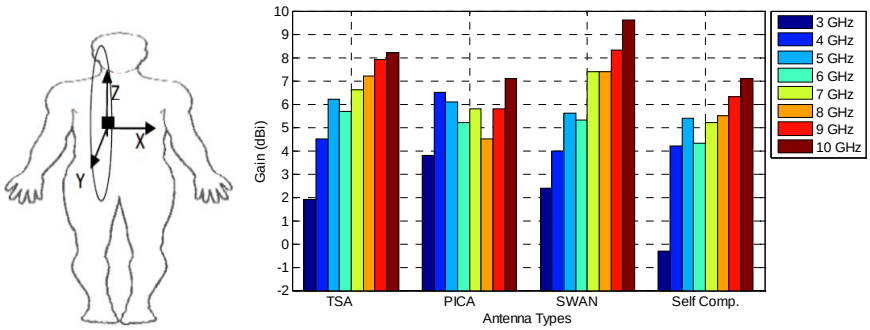

Fig. 5.18. Comparison of YZ plane on-body gain across (3 to 10 GHz) for four different UWB antennas when placed 4 mm away from the body.

Table 5.8 lists the frequency-averaged YZ plane mean on-body gain and standard deviation of various separation distances (1, 4, 8 and 16 mm) for the four UWB antennas. In this study, for the on-body gain, it is noted that the standard deviation values of different separation distances for the four UWB antennas are very close to each other. While for the narrowband case, the standard deviation values of different separation distances for the six narrowband antennas were found to be very high.

Table 5.8. Frequency-averaged YZ plane mean gain and standard deviation of various separation distances for four UWB antennas.

Antenna	Mean (dBi)	Standard deviation (dBi)
TSA	5.27	2.55
PICA	5.54	1.95
SWAN	5.37	2.24
Self Comp.	4.13	1.96

5.2.4 Radiation Pattern

The radiation pattern of the four UWB antennas has been measured at 3, 6 and 9 GHz in the anechoic chamber, placing the antennas on the same test subject used for S11 measurements. During the radiation measurements, the antenna was placed at 1 mm away from the middle of the upper trunk (chest). The antenna was oriented with radiating elements parallel to the body and facing outward. The free space radiation patterns of the four UWB antennas are mostly omnidirectional in the XY (azimuth) plane, except for some distortions in the higher frequency

band [8-10, 12, 15-16, 18]. The radiation presents a null in the Z direction. In free space, at higher frequency bands, the antenna radiation patterns produce peak in different directions other than the main beam. The on-body radiation pattern is investigated plane-wise.

XY Plane On-Body Radiation Pattern

When UWB antenna is placed on the human body, due to presence of the lossy human body tissues (with increased conductivity at higher frequencies), the XY plane omnidirectional radiation distorts and becomes directive towards the off the body direction for all antenna cases. Figs. 5.19 (a), (b) and (c) show the measured XY (azimuth) plane co and cross-polar on body radiation patterns at 3, 6, and 9 GHz for the four UWB antennas when placed at 1 mm away from the body. The XY plane on-body co-polar radiation patterns are directive across the UWB frequency band for all four antennas, except at the higher frequency where there are nulls present in the front beam for the Self complementary antenna. The front-back ratio of the antenna on-body radiation patterns is 20-40 dB.

When comparing the four antennas, the TSA shows constant directive co-polar radiation performance in this plane across the whole band. Placing the UWB antenna on the body has little effect on the impedance matching but higher effects are noticed for the antenna radiation pattern, gain and radiation efficiency. The proposed four UWB antennas are vertically polarised. The on-body cross-polar radiation patterns of the four antennas are also directive across the UWB band, with the presence of deep nulls in the front beam except for SWAN shaped at 3 and 6 GHz. In this plane, on-the-body the SWAN shaped antenna shows good cross-polar radiation performance compared to the other three. The SWAN shaped has a better cross-polar radiation pattern at 3 and 6 GHz compared to its co-polar. Placing the UWB antennas on the body, the on-body cross-polar radiation pattern shows higher performance compared as free space. In some cases for the UWB antennas, the on-body cross-polar radiation patterns show the same performance as co-polar patterns or even higher; hence, the antenna becomes un-polarised. On the body, antennas with high levels of co-and cross-polar radiation characteristics are desired for body-centric wireless communications.

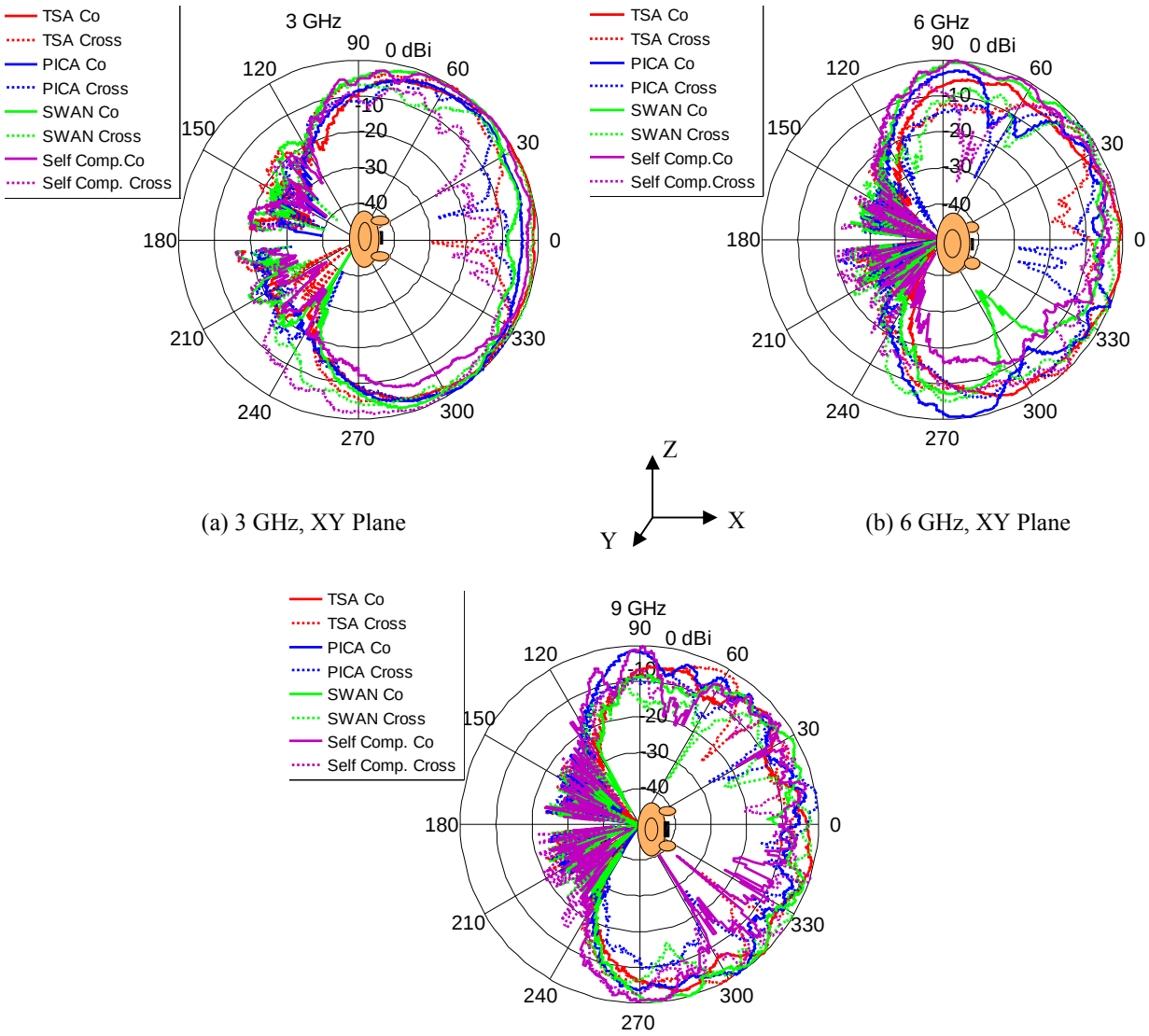

Fig. 5.19. Measured XY plane (co-and cross-polar) on-body radiation patterns of the presented four UWB antennas when placed at 1 mm away from the body (a) 3 GHz (b) 6 GHz (c) 9 GHz. Co-polar: solid lines cross polar: dotted lines. (The radiation patterns have been normalised).

XZ Plane On-Body Radiation Pattern

Figs. 5.20 (a), (b) and (c) show measured XZ plane co and cross-polar on body radiation patterns at 3, 6 and 9 GHz for the four UWB antennas when placed at 1 mm from the body. The co-polar on-body radiation patterns for the four UWB antennas are comparable to each other, apart from slightly more omnidirectional patterns for the PICA and SWAN shaped. The cross-polar

radiation patterns of these four antennas are also very similar except there is presence of more nulls in the patterns for the self complementary antenna. In this plane, an omnidirectional radiation pattern is desired for power-efficient and reliable body-centric wireless communications and, in this regard, the PICA and SWAN shaped antennas show the best radiation performances. However, antennas with full omnidirectional radiation on this plane are required for future power-efficient and reliable UWB body- centric wireless communications.

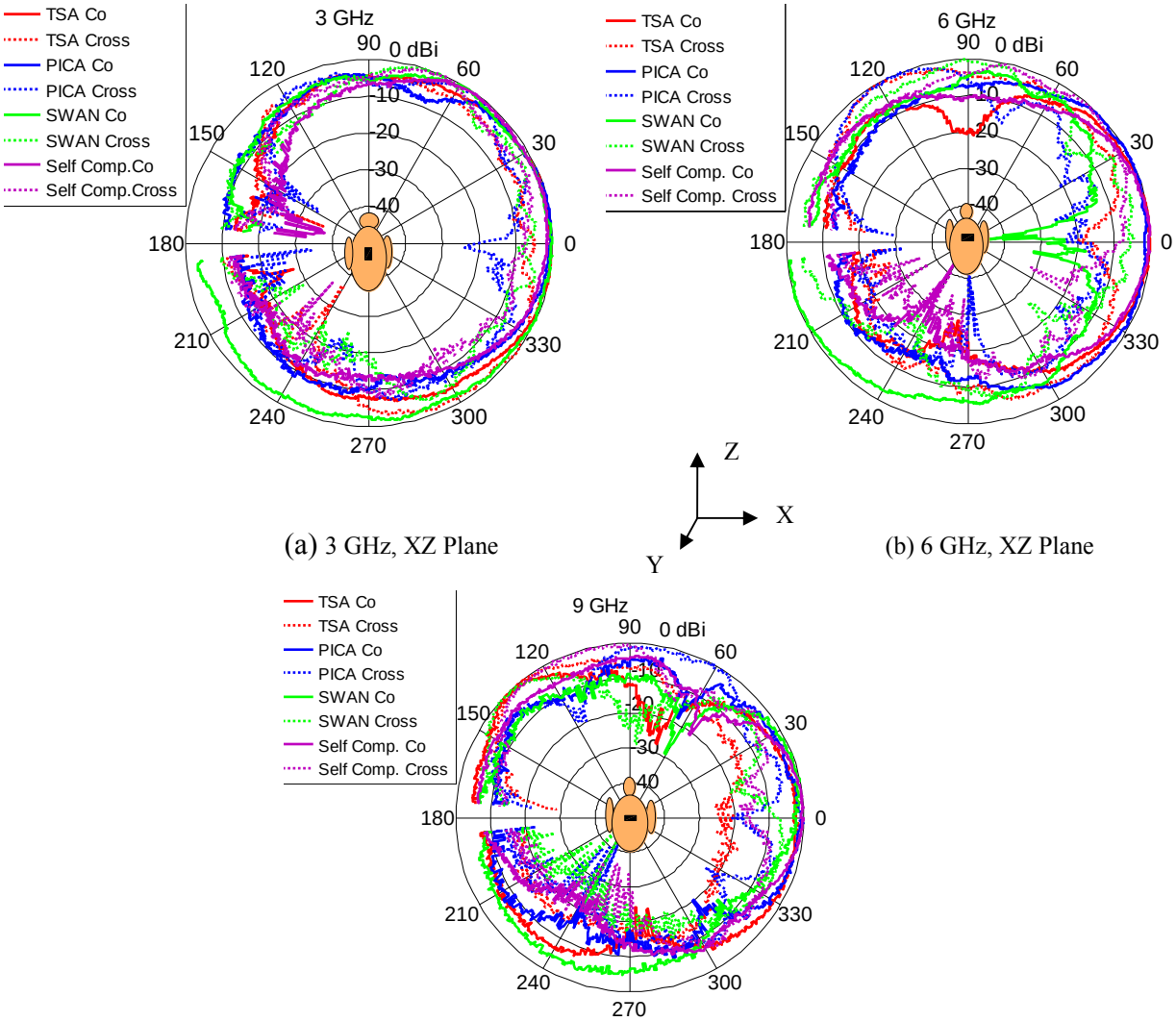

Fig. 5.20. Measured XZ plane (co-and cross-polar) on-body radiation patterns of the presented four UWB antennas when placed at 1 mm away from the body (a) 3 GHz (b) 6 GHz (c) 9 GHz. Co-polar: solid lines cross polar: dotted lines.

YZ Plane Radiation Pattern

The measured YZ plane co- and cross-polar on body radiation patterns at 3, 6, and 9 GHz of the four UWB antennas are shown in Figs. 5.21 (a), (b) and (c), respectively.

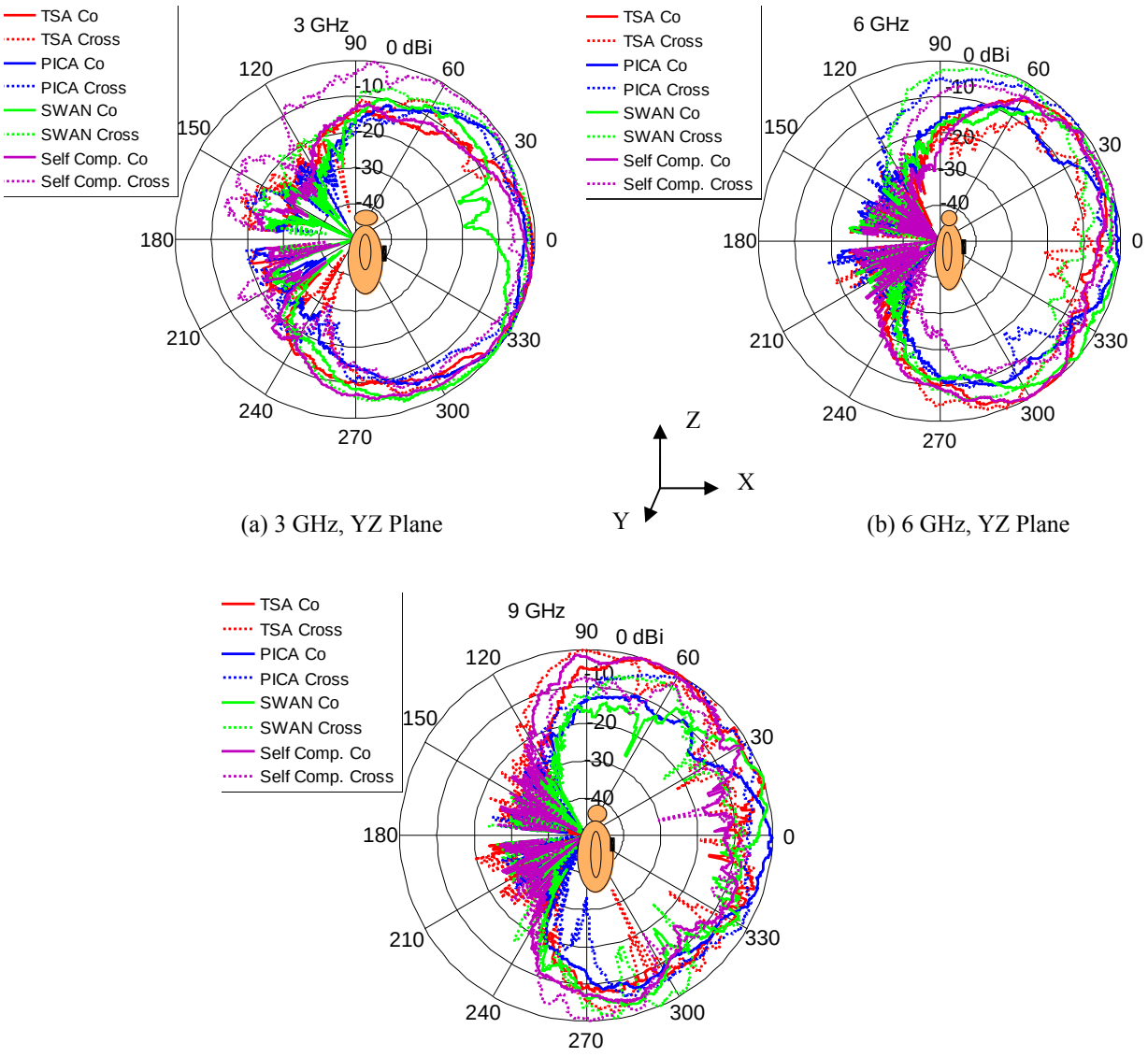

(a) 3 GHz, YZ Plane

(b) 6 GHz, YZ Plane

(c) 9 GHz, YZ Plane

Fig. 5.21. Measured YZ plane co-and cross-polar radiation patterns of the UWB antennas when placed at 1 mm away from the body (a) 3, (b) 6, (c) 9 GHz. Co-polar: solid lines and cross-polar: dotted lines.

In this plane, all antennas show directive co-polar radiation patterns except there is present of null in the front beam at 3 GHz and 9 GHz for the Self Complementary and SWAN shaped antennas. In this plane, the TSA and PICA show the best co-polar radiation performances as compare to other two antennas. The cross-polar radiation patterns in this plane are also comparable for the four antennas. The cross-polar radiation performances of the PICA and SWAN in this plane are better than those of the other two antennas. The SWAN shaped antenna shows reasonably good cross-polar radiation in all the planes across the band. On the body, the radiation distorts on the XY and YZ planes very much while very less is noticed on the XZ plane.

Simulated On-Body Radiation Pattern

Figs. 5.22 (a) and (b) show the simulated XY (azimuth) and YZ (elevation) planes co and cross-polar on body radiation patterns at 6 GHz of the four UWB antennas when placed at 1 mm from the body. The simulated co and cross-polar radiation patterns broadly agree with the measurements, except for a slight variation in some cases, which can be due to the effects of the cables. In the measured radiation patterns, there is presence of ripples, which is due to the effects of the cable. When the small UWB antennas are connected with the cable during pattern measurement, it (cable) may contribute to the radiation. The PICA being bigger in physical size has less effect from the cable, resulting less ripple in the measured patterns.

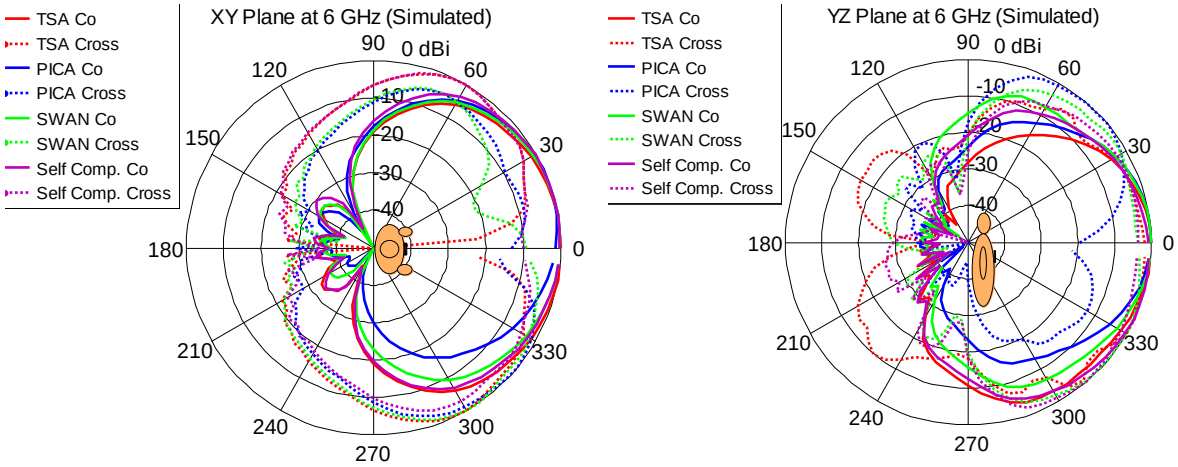

(a) Simulated XY plane at 6 GHz (b) Simulated YZ plane at 6 GHz

Fig. 5.22. Simulated on-body co-and cross-polar radiation patterns at 6 GHz of the four UWB antennas (a) XY plane, (b) YZ plane.

Impact of Distance on the Radiation Pattern

The on-body radiation patterns of four UWB antennas were also investigated as a function of distance. Figs. 5.23 (a), (b), (c) and (d) show the XY (azimuth) plane simulated on-body co-and cross-polar radiation patterns at 6 GHz of the four UWB antennas when placed at 1, 4, 8 and 16 mm away from the body. Results show that varying the distance between the antenna and the body does not distort the radiation pattern, but changes the power level.

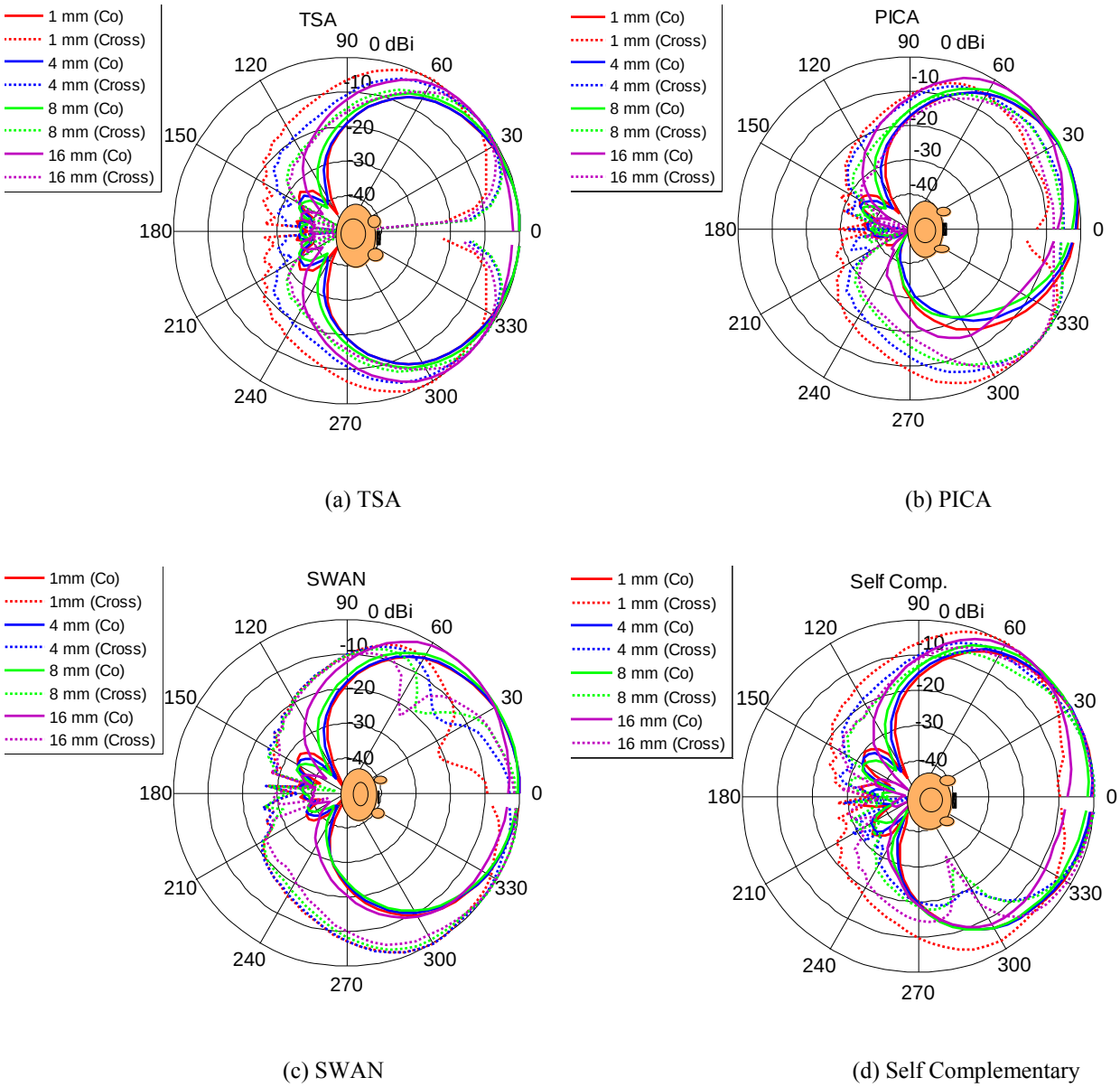

(a) TSA (b) PICA

(c) SWAN (d) Self Complementary

Fig. 5.23. 6 GHz XY (azimuth) plane radiation patterns of the analysed four UWB antennas when placed at various distances away from the body (1 mm, 4 mm, 8 mm and 16 mm). Co-polar: solid lines and cross-polar: dotted lines.

5.2.5 Pulse Fidelity

To investigate both frequency domain and transient antenna characteristics, the channel between two identical antennas set face-to-face, face-to-side and side-by-side (most appropriate setting for WBAN applications of the proposed printed antenna) is measured when the distance between the antennas is 50 cm, as shown in Fig. 5.24.

Measurement Settings

The antennas are connected to a vector network analyser (Hewlett Packard 8720ES-VNA) to measure the transmission response (S21) with port I and port II of the analyser serving as transmit and receive nodes, respectively. Two cables, of length 3 meters, are used to connect the antennas to the analyser ports. Measurements have been made in the anechoic chamber to eliminate multipath reflections from the surrounding scatterers. The analyser is set on the response mode in the range 3 GHz to 10 GHz with intervals of 3.75 MHz, at a sweep rate of 800 ms. The magnitude and phase of each frequency components are recorded.

For this measurement, the same test subject was used as for the S11 measurements. The transmitter antenna was placed on the foam at 125 cm height from the ground, while the receiver antenna was attached on the middle chest of the test subject with the same height as the transmitter antenna was set on the foam. But for the reference pulse, both transmitter and receiver antennas were placed on the foam (free space). In this study, the chosen distance between the antennas is 50 cm, which is 5 times the wavelength at the lower frequency in the band (3 GHz). Thus, the interaction between the antennas is minimal and most of the distortion in the frequency channel responses is due to impedance mismatch and the inherent radiation properties of the antenna. The time domain responses of the radio channel with the antennas are obtained by direct application of the IFFT on the measured real frequency responses S21 [21].

In UWB communications, specifically impulse radio systems, a correlation between the transmitted or received waveform and a template is often used to assess how the system affects a waveform and quantify the level of pulse distortion. A fidelity parameter involving the cross-correlation between the time domain transmitted field and a template function is described by Lamensdorf *et al.* [22], and it was defined in (3.17). For many applications, fidelity analysis is applied to investigate the preservation of pulse shape (not amplitude) with respect to space and

time. Usually, a pattern is defined, which is simply the normalized correlation coefficient of the electric field with the template, as a function of direction [22-25].

The choice of template function is not restricted to a specific reference pulse or stringent requirements [24]. The template function in fidelity analysis can be the transmitted pulse, input pulse or transmitted pulse in a reference direction (usually maximum radiation density direction) and the later is the case chosen in this study [22–24]. The reference impulse response is thus when both antennas are set face-to-face in free space (maximum density direction). In this case, the template pulse is set when both antennas are at 50 cm distance away attached on the foam with the setting of face to face (Fig. 5.24). The correlation with pulses radiated and received at various directions is experimentally evaluated using two identical antennas [25, 27].

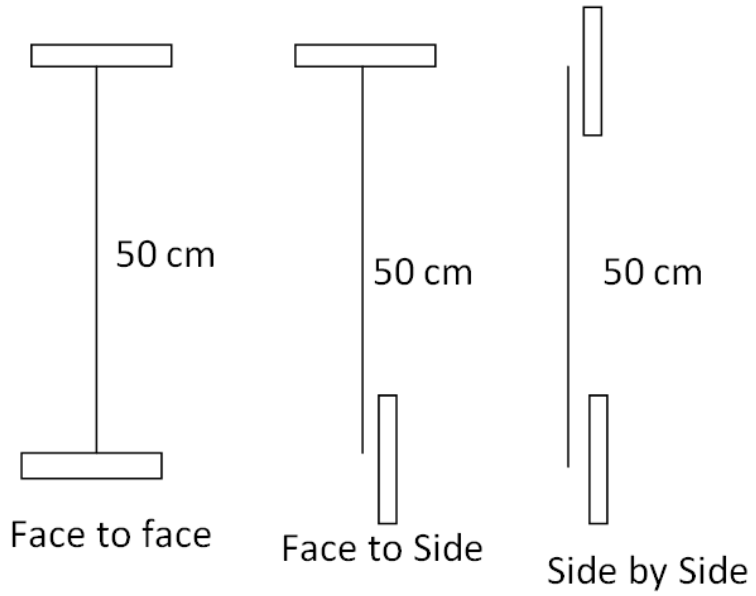

Fig. 5.24. Measurement settings for pulse fidelity showing the orientation of the transmitter antenna and the test subject with the antenna.

The fidelity values for the measured band for the four antennas in the three different alignments are shown in the Fig. 5.25 with the response at free space face to face set as reference. The results show good transient performance of the antennas at different orientations. Mostly, the highest fidelity values are noticed for face to face settings, due to maximum radiation density as expected. When the antennas are set side by side, the SWAN shaped and PICA show higher fidelity values/less distortion of pulse shape, compared with the TSA and Self

complementary antennas because of the more omnidirectional radiation on the XZ plane. Since, for the on-body case, the side by side settings is commonly used, therefore, the antenna with omnidirectional radiation over the body surface will give less distortion of pulse or higher fidelity. When the antenna is setting face to face and face to side the TSA antenna shows the best performance because of good radiation performance on the forward coverage.

The average pulse fidelity over the three different settings for each antenna is 93.50 %, 93.68 %, 94.81 % and 90.29 % for TSA, PICA, SWAN and Self Complementary, respectively. The fidelity values for the TSA, PICA and SWAN are very close; the Self complementary antenna is slightly degraded compared to the SWAN, PICA and TSA. This may be related to the fact that the Self complementary antenna has a size reduction.

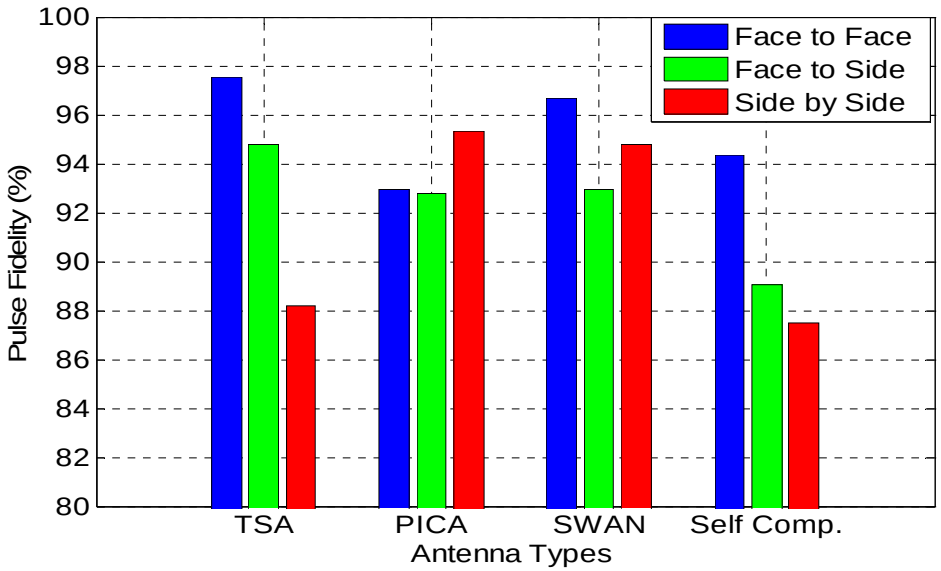

Fig. 5.25. Comparison of pulse fidelity for four different UWB antennas of different settings as face to face, face to side and side by side.

Fidelity studies of commonly-used antennas, such as monopoles and resistively loaded dipoles presented in [22–25, 27], has shown that a spatially averaged fidelity factor as low as 70 % is often deduced. In the wireless BAN specific study presented in [23], a value of 76-99% was derived for fidelity, when numerically comparing the input pulse to a transmitted pulse for various antenna types. This indicates that the acceptable minimum value for fidelity is application and environment specific. In the study presented here, the average values obtained for TSA, PICA, SWAN and Self complementary antennas are considerably sufficient

performance for the proposed applications, considering the short communication distance between the body-centric network devices.

The overall on-body performances of the TSA, PICA and SWAN shaped UWB antennas are comparable, while slight degradation of performance is noticed for the self complementary antenna compared to the other three. Due to significant size reduction (four times smaller in volume as compared to the PICA), with good overall on-body performances, the TSA and SWAN shaped will be ideal candidate for body area networks (BANs). However, for on-body applications, the behaviour of the antenna as a part of the on-body radio channel needs to be investigated.

5.2.6 Radio Propagation for Ultra Wideband (3.1-10.6 GHz) Body-Centric Wireless Networks

The four UWB antennas were also used to characterise the path loss for communication along the front part of the human body.

Measurement Settings

The measurements were performed in the frequency domain, using a Vector Network Analyser (Hewlett Packard 8720ES-VNA) and two cables, connecting two stand-alone, identical antennas, to measure the transmission response (S21) in the frequency range of 3-10 GHz. The measurements were performed on the same test subject as used for the narrowband case. The frequency range was set to 3-10 GHz at a sampling rate of 1601 with sweep time of 800 ms subsequently. Table 5.9 shows the network analyser settings for the ultra wideband on-body radio channel measurements. The transmitter antenna was placed on the left waist, while the receiver antenna was placed at 34 different locations on the front part of the human body as in the narrowband case; see Fig. 4.21. To eliminate the coupling effect between the two antennas, we ensure a minimum distance of 10 cm between transmitting and receiving antenna (corresponding to one free space wavelength at the minimum frequency of 3 GHz). During the measurements, the subject was standing still and, for each receiver location and measurement scenario, 10 sweeps were considered. The antennas were placed directly on the T-shirt and Trousers of the test subject.

Measurements were first performed in the anechoic chamber, to eliminate multipath reflections from the surrounding environment, and then repeated in the Body-Centric Wireless Sensor Laboratory at Queen Mary, University of London, to consider the effect of the indoor environment in the on-body radio propagation channels; see Fig. 5.22, in Chapter 4.

Table 5.9. Network analyser settings for UWB on-body radio link measurements.

Frequency Band	3-10 GHz
Frequency Points	1601
Sweep Time	800 ms
Number of Sweep	10
VNA Transmit Power	0 dBm

Path Loss Characterisation

The path loss for each receiver location is directly calculated from the measurement, averaging over the frequency band of 3~10 GHz. The path loss can be modelled as a function of the distance between transmitter and receiver using the equation 4.2. A least-square fit is performed on the measured data for the 34 different receiver locations on the body to evaluate the path loss exponent and the average path loss at the reference distance for the four UWB antenna cases (Table 5.10).

Figs. 5.26 (a) and 5.26 (b) show the measured and modelled path loss for on-body channels versus logarithmic Tx-Rx separation distance, for the four UWB antennas measured in the chamber and indoor, respectively. The slope of each line represents the path loss exponent γ. The PICA shows the highest path loss exponent (3.56, 2.91) while the TSA shows the lowest (2.34, 2.01), both in the chamber and in the indoor environment. The path loss exponents for all antennas are found to be lower in the indoor environment. When the measurements were performed in the indoor environment, the reflections from the surrounding scatterers increased the received power, causing a reduction of the path loss exponent. The reduction of the path loss exponent is significant for the PICA, due to it having more omnidirectional radiation compared to the other three UWB antennas.

The lowest path loss at the reference distance is noticed for both PICA (44, 46) and SWAN shaped antenna (48, 50), while the highest is for the TSA (50, 51.3) and Self Complementary compact antenna (49, 50.8). The PICA and SWAN shaped antenna show higher gain, slightly

more omnidirectional radiation patterns in the XZ plane and slight improved on-body performance compared to the TSA and Self complementary antenna, which results in less path loss for these two antennas (PICA and SWAN).

Although, the PICA has the lower path loss value at the reference distance, it shows the highest path loss exponent value compared to the other three antennas. In addition to this, the volume of the PICA is nearly four times higher than the other three UWB antennas used for this study. The SWAN, TSA and Self complementary are very compact compared to the PICA, but they show good on-body radio channel performance despite this.

The path loss values of the SWAN, TSA and Self complementary are very close to each other. Although, there is little difference in path loss of the Self complementary antenna compared with the SWAN and TSA, it shows poorer overall on-body performances. The TSA and SWAN shaped will be good candidates for body area networks, due to their overall on-body performance close to the human body and their significant size reduction compared to the PICA. Since, none of the antennas used for this study has quite omnidirectional radiation characteristics in the XZ plane (over the body surface), an antenna with full omnidirectional radiation on this plane may provide improved on-body radio channel performances.

Figs. 5.27(a) and 5.27(b) show the deviation of measurements from the average path loss fitted to a normal distribution for the four antenna cases, in the chamber and in the indoor, respectively. The highest standard deviation (σ) is noticed for the TSA and Self complementary compact antenna while the lowest is for the PICA and SWAN shaped. The more directive the antenna is, the less valid is the linear relation between path loss and logarithmic distance; hence the more spread the data is. This explains the higher value of standard deviation (σ) for the TSA and self complementary cases.

Table 5.10. Comparison of path loss parameters for different ultra wideband antennas used in this study.

	Chamber			Indoor		
Antenna	γ	$PL_{dB}(d_0)$	σ	γ	$PL_{dB}(d_0)$	σ
TSA	2.34	50.0	9.14	2.01	51.3	8.85
PICA	3.56	44.1	8.46	2.91	46.1	7.61
SWAN	3.00	48.0	8.97	2.44	50.0	8.71
Self Comp.	2.57	49.0	10.28	2.15	50.8	10.11

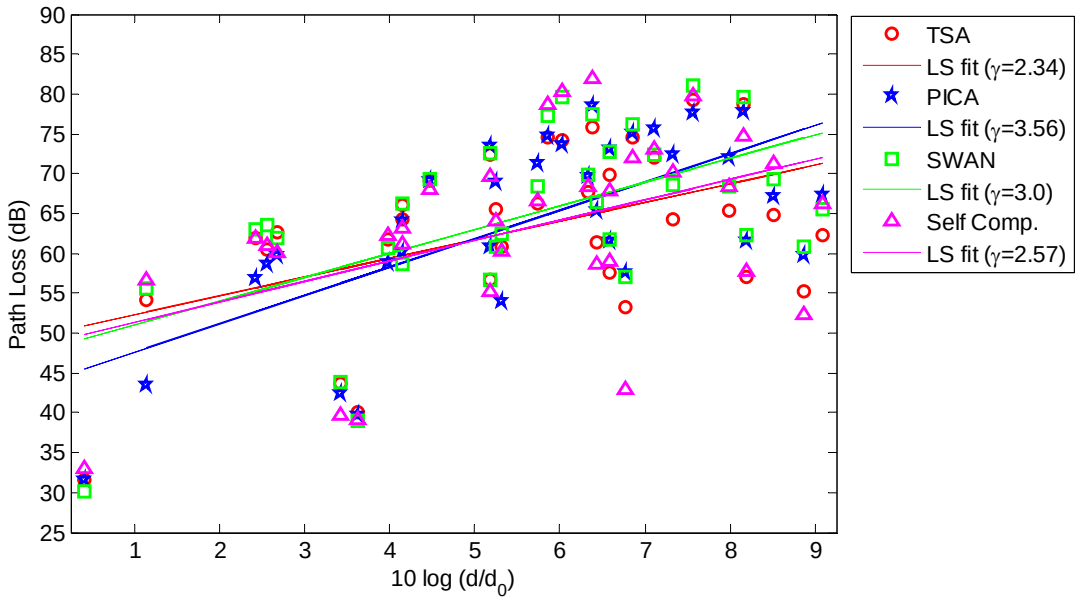

(a) Chamber

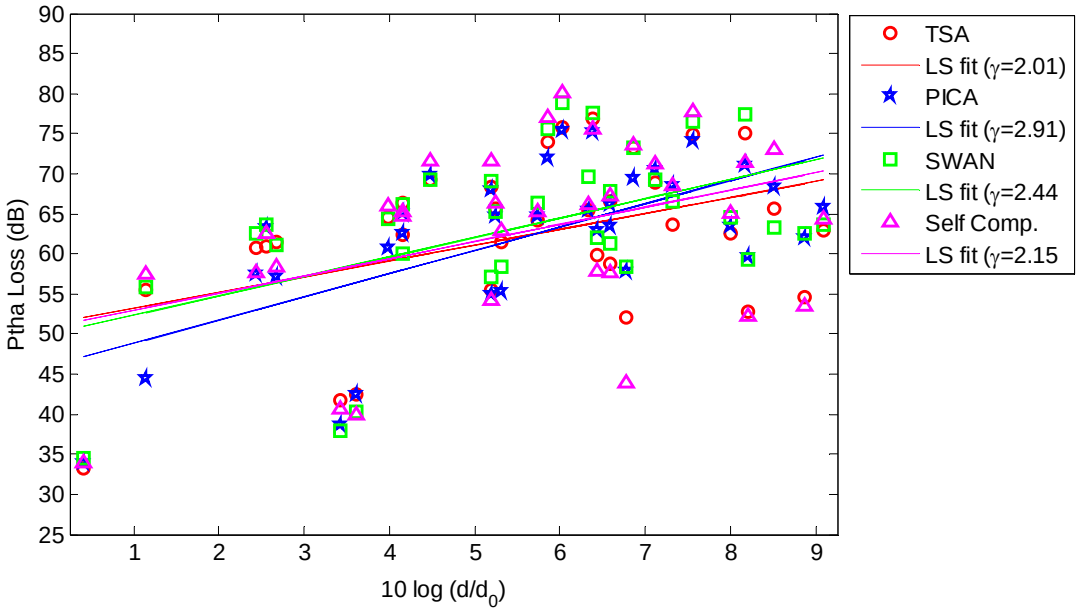

(b) Indoor

Fig. 5.26. Measured and modelled (best fit model) path loss for the on-body channel versus logarithmic Tx-Rx separation distance for four different ultrawide band antennas used; (a) Chamber and (b) Indoor.

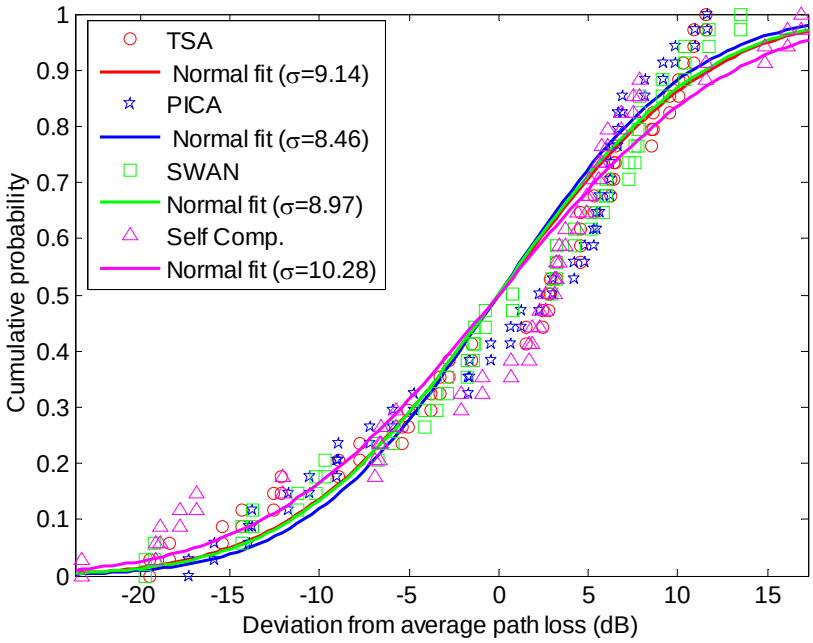

(a) Chamber

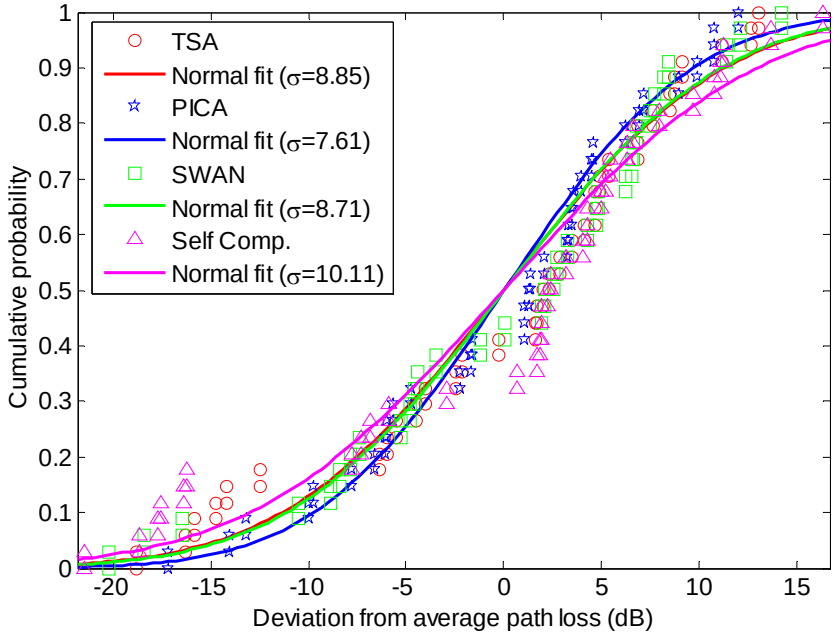

(b) Indoor

Fig. 5.27. Deviation of measurements from the average path loss fitted to a normal distribution for four different UWB antennas used; (a) Chamber and (b) Indoor.

Based on the results analysed in the previous sections, the UWB antenna specifications and design guidelines for body-centric wireless communications are provided. At the end of this chapter, a comparison between narrowband and UWB antenna parameters for body-centric wireless communications is summarised.

5.3 Ultra Wideband Antenna Specifications for Body-Centric Wireless Communications

- **Size and shape**: Due to the higher frequency band of operation, the size of UWB antennas is smaller compared with the narrowband antennas, which is one of the advantages of using UWB technology for BANs. The ultra wideband antenna for body-centric wireless communications needs to be compact, conformal to the body, unobtrusive, light-weight, low-cost and easily integrated with body worn-devices. The UWB antenna also needs to be low-power consumable in order to extend the battery life for body-worn devices and provide a green radio system. Since most of the UWB antennas show frequency shifting trends towards the left when placed on the body, very compact UWB antennas for on-body applications are possible but, careful consideration needs to be given to the antenna performance because, usually, smaller antennas show poorer performance.
- **Operating frequency**: The operating frequency of ultra wideband wearable antennas should be in the range of 3.1-10.6 GHz at -10 dB impedance. On the body, the lower frequency band at -10 dB impedance shifts to the left (by up to 2 GHz) with respect to the free space operation. On the body, for the UWB antenna case, the lower frequency shifting is not a major issue; the effect on impedance matching is more significant. On the body, though there is lower frequency shifting but still all the proposed UWB antennas work in the required frequency band except for some mismatch of antenna impedance within sub-bands. However, on the body, it is better to have the operating frequency of the UWB antenna as close possible as free space of operation. Multiple deep resonances over the UWB band are not good because they cause much distortion in the pulse shape. The frequency shifting may be controlled by the ground plane, antenna size and gap

between the antenna and the body. The separation distances to place the antenna from the body have the effects on the lower frequency shifting at -10 dB impedance as was noticed in the previous section. The distance to place the UWB antennas have higher effects on the lower frequency shifting for the smaller UWB antennas without ground plane while it has lower effects for the antenna with bigger in size. The lower frequency shifting of four UWB antennas (TSA, PICA, SWAN and Self complementary) for each separation distance between the antenna and the body was averaged. Table 5.11 shows the average lower frequency shifting and standard deviation of four ultra wide-band antennas for various separation distances. Placing the UWB antenna directly on the body, the average lower frequency shifting over different antennas is 1.2 GHz. It is noted that, the antenna-averaged lower frequency shifting reduces as the distance between the antenna and the body increases. The higher standard deviation is noticed when the antennas are very close to the body (direct on the body and 1 mm) which decreases as the distance between the antenna and the body increases. Results indicate that, for different antennas, the variation of lower frequency shifting is significant when the antenna placed at very close to the body (directly, 1mm) and insignificant at higher distance (16 mm).

Table 5.11. Average lower frequency shifting and standard deviation of four different UWB antennas for various distances from the body (the lower frequency shifting at -10 dB impedance for each distance was averaged over four UWB antennas).

Distance from the body	Mean (GHz)	Standard deviation (GHz)
Direct on the body	1.260	0.603
1 mm	0.780	0.646
4 mm	0.364	0.234
8 mm	0.238	0.245
16 mm	0.316	0.176

- **Impact of different locations of the body:** Follows the same trends as narrowband case. The lower frequency shifting at -10 dB impedance varies for different on-body locations by up to 0.916 GHz when placed directly on the body. Due to different on-body locations, the antenna lower frequency shifting variation is higher for the antenna without ground plane. The lower frequency shifting of four UWB antennas for each location on the body is averaged. Fig. 5.28 shows the average lower frequency shifting and standard

deviation of four UWB antennas for various on-body locations. On the body, the antenna-averaged frequency shifting is noticed to be higher when the antenna placed on the left waist, right thigh and right wrist. The variation of the standard deviation of four antennas for each location is very small.

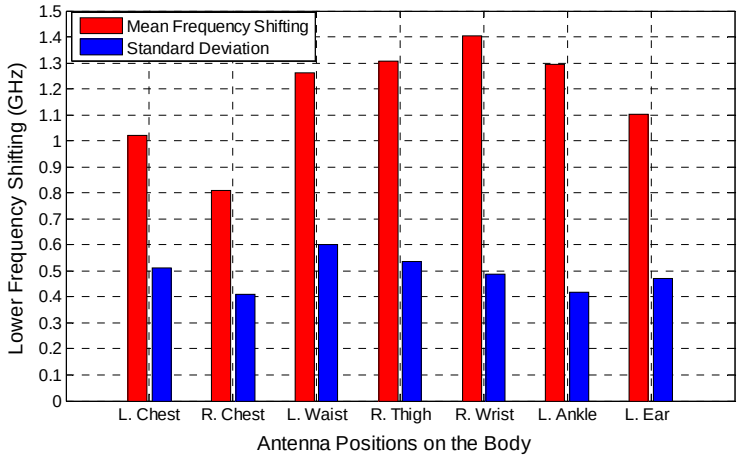

Fig. 5.28. Average lower frequency shifting and standard deviation of four UWB antennas for various locations on the body (the lower frequency shifting at -10 dB impedance for each on-body location was averaged over four UWB antennas).

- **Impedance:** The antenna input impedance should be 50 ohm. Antennas with very good impedance matching (return loss less than -10 dB across the whole band) are preferred and any strong resonance in the band is not good as far as pulse fidelity is concern. On the body, the antenna input impedance for all UWB antennas changes and, in some cases, the return losses reach as much as -5.5 to -6 dB within sub-bands. However, this may also be an acceptable level, because some of the mobile phone standards also work on the return loss at -6 dB. However, the antenna impedance can be improved by adding an extra matching network or possibly by placing full ground plane at the back of the UWB antenna.
- **Operational bandwidth**: The operational bandwidth of ultra wideband wearable antenna is required to be 3.1-10.6 GHz or 7.5 GHz at -10 dB impedance. According to the FCC first Report and Order, UWB systems are required to have a -10 dB impedance bandwidth of no less than 500 MHz, or UWB systems ought to have fractional bandwidth of at least 20%. On the body, the impedance bandwidth for all proposed UWB antennas

increases. Placing the UWB antennas on the body, the lower frequency band at -10 dB impedance shifts to the left with respect to free space, which ultimately increases the impedance bandwidth of the antenna. UWB antennas should have ultra wide impedance bandwidth with good impedance matching when placed on the body. UWB antenna requires the voltage standing wave ratio (VSWR) to be constant across the whole bandwidth of operation.

- **Radiation efficiency**: For UWB short-range indoor on-body communications, an efficient antenna is required. When the UWB antenna is on the body, the radiation efficiency decreases with respect to free space across the whole band for all antennas. The radiation efficiency reduction is higher at the lower frequency band than in the upper frequency band. The distance to place the antenna on the body has effects on the on-body radiation efficiency. In earlier section, it was reported that, on the body at 1 mm away, the wearable UWB antenna experiences up to 90.77 % reduction of radiation efficiency at 3 GHz and 59.7% at 9 GHz. As the distance between antenna and the body increases, the UWB antennas show better radiation efficiency. At 4 mm distance from the body, all UWB antennas used in this study, show acceptable levels of radiation efficiency. At this distance, on-body efficiency (averaged over frequency band of 3-10 GHz) for proposed UWB antennas is in the range of to 48.16 to 60.32%. However, placing the UWB antenna at 8 mm away from the body improves the radiation efficiency even more. The frequency averaged on-body radiation efficiency at 8 mm away from the body is in the range of 66.43 to 79.65%. Table 5.14 summarises the on-body performances of proposed four UWB antennas when placed at 8 mm away from the body. Smaller antenna shows poorer on-body radiation efficiency in compare to bigger antennas. There is not much difference of antenna radiation efficiency for the antennas with partial or without ground plane; the size is a more significant factor. The on-body radiation efficiency reduction may be improved for the UWB antenna with full ground plane, as found in narrowband case. The frequency-averaged (3-10 GHz) on-body radiation efficiency of four UWB antennas for each separation distance between the antenna and the body was averaged. Table 5.12 shows the frequency-averaged mean radiation efficiency and standard deviation of four UWB antennas for various separation distances. At 1 mm away from the body, the averaged on-body radiation efficiency of four UWB antennas is 30% while at 16 mm

away; it is found to be 85%. The lower standard deviation value is noticed when the antennas are very close to the body (1 mm) which increases as the distance between the antenna and the body increases. Results indicate that, for different UWB antennas, the variation of radiation efficiency is lower when the antenna placed at very close to the body (1 mm) and higher at higher distance (16 mm).

Table 5.12. Frequency-averaged mean radiation efficiency and standard deviation of four UWB antennas for various separation distances from the human body (the frequency-averaged efficiency was averaged over four UWB antennas).

Antenna	Mean (%)	Standard deviation (%)
Free space	99.12	0.7
1 mm	30.0	4.23
4 mm	55	5.42
8 mm	73.73	5.91
16 mm	84.90	6.80

- **Gain:** For UWB short-range on-body communications, antennas with good gain (gain with positive value) are suitable. On the body, the gain and radiation efficiency are frequency-dependent. When the UWB antenna is placed very close to the body (1 mm away), the gain reduces by up to 7.59 dB in the lower frequency band of 3 GHz, while increases up to 2.85 dB in the higher frequency band of 9 GHz. The antenna placement distance has the effect on the on-body gain for the UWB antennas. As discussed in previous, at 1 mm away from the body, the gain at 3 GHz for all antennas is negative, but, at 4 mm away from the body, the gain for all antennas is positive across the whole band; hence an acceptable level of gain is achieved and 4 mm gap is recommended to place the UWB antenna on the body. The on-body gain (averaged over the frequency of 3-10 GHz) at 4 mm from the body is in the range of 5.15 dBi to 7.09 dBi. However, placing the UWB antenna at 8 mm away from the body, results in an increase in the gain across the whole band, for all UWB antennas. The on-body gain for different UWB antennas at 8 mm from the body is in the range of 6.60 dBi to 8.04 dBi, as shown in Table 5.14. Furthermore, placing a full ground plane at the back of the UWB antenna is likely to improve the on-body gain across the whole band. It is important to know that, on the body, smaller UWB antennas provide lower gain in comparison with the antennas bigger in physical size. As mentioned earlier, antennas with higher gain on the XZ plane

(over the body surface) minimise the on-body link loss; therefore, antennas with higher gain in this plane are important. In this study, most of the proposed UWB antennas show very low gain on this plane. The gain on this plane (XZ) is antenna-dependent. The frequency-averaged (3-10 GHz) on-body peak gain of four UWB antennas for each separation distance between the antenna and the body was averaged. Table 5.13 shows the frequency-averaged mean peak gain and standard deviation of four UWB antennas for various separation distances. At 1 mm away from the body, the averaged on-body peak gain of four UWB antennas is 2.3 dBi while at 16 mm away, it is found to be 8 dBi. Results show that as the distance between the antenna and the body increases, the frequency-averaged gain of the UWB antenna increases. At lower distance, the standard deviation value is found to be higher which decreases as the distance between the antenna and the body increases. It is noted that, for the different UWB antennas, the variation of on-body gain is higher when the antenna placed at lower distance while the variation is lower when the antenna placed at higher distances.

Table 5.13. Frequency-averaged mean peak gain and standard deviation of four UWB antennas for various separation distances from the human body. (the frequency-averaged peak gain was averaged over the four antennas).

Antenna	Mean (dBi)	Standard deviation (dBi)
1 mm	2.32	1.36
4 mm	6.20	0.83
8 mm	7.36	0.67
16 mm	7.97	0.55

- **Radiation pattern**: As discussed in the narrowband case, antenna with quite omnidirectional radiation patterns over the body surface is required for power-efficient and reliable body-centric wireless communications. UWB antennas should have stable radiation patterns across the whole frequency band of operation. The UWB antennas used for this study are not quite omnidirectional over the body surface; however, antenna with omnidirectional radiation on the body surface may provide good on-body radio channel performances. On the body, the radiation pattern distorts for all studied UWB antennas; however, the distortion may be reduced for the antenna with full ground plane at the back as noticed for the narrowband case. The radiation pattern is dependent on the antenna type. For the UWB antennas, the on-body cross-polar radiation patterns show higher

performance compared to free space. In some cases, when the antenna is body worn, the cross-polar radiation patterns of the UWB antenna show the same performance as co-polar patterns or even higher.

- **Polarisation:** The UWB antenna polarisation should be normal to the body surface for minimised link loss in on-body communications. Dual-polarised UWB antennas will provide better on-body radio channel performance. For the UWB case, the antennas show good cross-polar radiation performance when placed on the body. Polarisation is dependent on the antenna type. The UWB antenna used in the thesis all linearly polarised.
- **Pulse fidelity**: Since the most appropriate setting for WBAN applications of the UWB antennas is side-by-side, the more omnidirectional the antenna radiation pattern over the body surface is, the better the pulse shape will be preserved. For indoor short-range UWB body-centric wireless communications, more than 70 % pulse fidelity is required. In this study, all UWB antennas show higher than 85 % pulse fidelity; hence, sufficient performance is obtained. Pulse fidelity is dependent on antenna radiation pattern and antenna size.
- **Ground plane:** For the UWB antennas examined in the previous section, it was shown that there was not much difference on the performance of the antenna without or partial ground plane; antenna size has more significant. However, UWB antennas with full ground planes may improve on-body performance as noticed in chapter four (narrowband antenna case). Furthermore, bigger ground planes may provide better results. The ground plane will be more useful for the narrowband case as compared to the UWB, due to frequency-dependent body effects.
- **Antenna placement distance from the body:** The on-body performance of the UWB antennas degrades when placed very close to the body, except for the gain in the higher frequency band. As it was found previously, that at 4 mm away from the body, all UWB antennas show acceptable level of on-body radiation efficiency and gain; therefore, the recommended minimum distance to place the UWB antenna on the body is 4 mm. The on-body performance of the UWB antennas, with partial ground plane or without ground plane is extremely dependent on the antenna placement distance from the body.
- **Frequency-dependent behaviour:** Due to wide-band characteristics, the on-body performance of the UWB antennas changes over the frequency band. Results in the

previous section shows that, at the lower frequency, the body has higher effects, as compared to the higher frequency. At the lower frequency, the signal penetrates the body tissue more, while at the higher frequency, it dissipates. The on-body gain, efficiency and radiation pattern are all frequency-dependent.

- **SAR:** Low SAR is required.

Table 5.14. Comparison of on-body performance of the proposed four ultra wideband antennas when placed at 8 mm away from the body (the gain and radiation efficiency were averaged over the frequency band of 3-10 GHz).

Performance parameters	TSA	PICA	SWAN	Self comp.
Frequency shift (GHz)	0.575	0.030	0.238	0.135
Radiation Efficiency (%)	71.62	79.65	77.22	66.43
Peak gain (dBi)	7.02	8.04	7.79	6.60
XZ plane gain (dBi)	-9.02	-6.78	-6.89	-7.00
YZ Plane gain (dBi)	7.00	6.58	7.10	5.41

The leading parameters that control the ultra wideband antenna performances when placed on the body are: the antenna type and size; antenna placement distance from the body; location of the body and the ground plane. A general summary of the effects of these parameters on the UWB antenna performance on the body is shown below in Table 5.15.

Table 5.15. General summary of the effects of leading parameters that control the UWB antenna performances when placed on the body.

Parameters	Frequency shifting	Radiation efficiency	Gain	Radiation pattern	Impedance matching	Pulse fidelity	Path loss
Without ground plane	Very sensitive. Significant lower frequency shifting at –10 dB impedance. More dependent on the locations of the body.	Very sensitive. Efficiency reduces significantly. Dependent on the gap between antenna and body. At 4mm reasonable efficiency across the whole band.	Very sensitive. Gain reduces significantly at lower band and increases at upper band. At 4 mm reasonable (positive) gain across the whole band.	Very sensitive. Distorts significantly. Independent of antenna placement distance.	Dependent. Impedance mismatch observed within band.	Will provide poor pulse shape due to distortion of radiation pattern.	--
Partial ground plane	Sensitive. Less frequency	Very sensitive. Efficiency	Very sensitive. Gain	Very sensitive. Distorts	Dependent. Impedance mismatch	Will provide poor pulse	Depends on antenna

	shifting at –10 dB impedance compared to antennas without ground plane. Less dependent on the locations of the body.	reduces significantly. Dependent on the gap between antenna and body. At 4mm, reasonable efficiency across the whole band.	reduces significantly at lower band and increases at upper band. At 4mm, reasonable (positive) gain across the whole band.	significantly. Independent of antenna placement distance.	observed within band.	shape due to distortion of radiation pattern.	radiation pattern and gain. Higher path loss.
Full ground plane (predicted, not investigated)	May be less sensitive. May see slight frequency shifting. The frequency shifting may be location independent.	May be less sensitive. Will reduce the efficiency reduction. May be less sensitive on the gap. May be reasonable efficiency for smaller gap.	May be less sensitive. May improve the gain across the whole frequency band of operations.	May be less sensitive. May be less distortion across the whole frequency band.	Impedance may be less mismatched.	Will provide better pulse shape since less distortion of radiation pattern.	May improve path loss but depends on the antenna radiation pattern and gain.
Antenna type	Less dependent on the antenna type.	Depends on the antenna type.	Depends on the antenna type.	Very much depends on the antenna type; also, the polarisation is dependent on antenna type.	Dependent on the antenna type	Dependent on antenna type and also on the radiation pattern.	Very much dependent
Antenna placement distance from the body	Sensitive extremely. Reduces as gap increases. Very sensitive for the antenna with partial and without ground plane.	Very sensitive. Depends significantly on the gap between the antenna and the body. Very sensitive for antenna with partial/no ground plane.	Very sensitive. Depends significantly on the gap between the antenna and the body. Very sensitive for antenna with partial/no ground plane.	Does not affect the antenna radiation pattern but affects the power/gain level. Full ground plane antennas minimise the antenna placement distance from the body.	Dependent on the gap between the antenna and the body.	--	--
Antenna size	Dependent on the antenna size. Less frequency shifting for bigger antennas. Independent	Dependent. Bigger antenna shows slightly higher on-body efficiency.	Dependent. Bigger antenna shows slightly higher on-body gain. Reduces less for bigger	Less dependent.	Less dependent.	Dependent. Smaller antenna shows less pulse fidelity. Also depends on the settings	--

	of body locations.		antenna.			of the antenna.	
Frequency dependent	--	Reduction of efficiency is frequency-dependent. At lower frequency, a higher reduction is observed.	Reduction of gain is frequency-dependent. At lower frequency, it reduces, but it increases at higher frequency.	Radiation pattern distortion is frequency-dependent. At higher frequency, slightly more distortion.	Not dependent	--	Dependent

Based on the specification, out of these four studied UWB antennas, the TSA and SWAN shaped antennas will be the suitable candidates for body-centric wireless communications. The PICA demonstrates good on-body performance but is probably too large for practical use. However, more suitable UWB antenna can be designed for future efficient and reliable body-centric wireless communications based on these specifications. The specifications provided here will be good guidelines for the system designer to design suitable UWB antenna for body area networks.

5.4 Narrowband vs. Ultra Wideband Antenna Parameters

A comparison between narrowband and UWB antenna parameters for body-centric wireless communications is summarised in Table 5.16.

Table 5.16. Comparison of narrowband and UWB antenna parameters for body-centric wireless communications.

No	Parameters	Narrowband	UWB
1	Size and shape	Due to lower frequency of operation, the antenna physical size is bigger compared to UWB. More space is needed on the printed circuit board (PCB) due to bigger size.	Higher frequency of operation; hence, the physical size of UWB wearable antenna can be more compact compared to narrowband antennas. For compact and light-weight UWB antenna will be cheaper and extended battery life. Due to being smaller in size, it is easy to integrate UWB antenna with the system and chip. Since, on the body, the lower frequency shifts to the left, the size of the UWB antenna can be very compact.
2	Operating frequency	The operating frequency is 2.45 GHz. For narrowband antennas, the operating frequency detuning is a very important	The operating frequency is higher and should be in the range of 3.1-10.6 GHz at -10 dB impedance. On the body, the lower frequency at

		issue and needs to be tuned on the body. On the body, if the operating frequency is not properly tuned, it may cause the loss of the communication link for very narrowband antennas.	-10 dB impedance shifts. The frequency shifting is less of an issue, because it increases antenna impedance bandwidth. Even on the body, the frequency shifts, the UWB antenna works in the required band.
3	Bandwidth	The narrowband antenna bandwidth needs to be 83.5 MHz at -10 dB impedance. Bandwidth is very narrow compared to UWB. Antenna bandwidth depends on the antenna types. On the body, the impedance bandwidth increases.	The bandwidth is very wide: 7.5 GHz at -10 dB impedance. On the body, the impedance bandwidth increases as well. All UWB antennas need to be made with the band of 7.5 GHz at -10 dB impedance.
4	Impedance	Should be 50 ohm. On the body, the narrowband antenna input impedance changes. The impedance mismatch is lower compared to UWB. On the body, the return loss remains less than -10 dB.	Should be 50 ohm as well. On the body, the antenna impedance changes. The impedance mismatch is higher. In some cases, the return loss reaches -5.5 dB. The return loss needs to be less than -10 dB across the whole band.
5	Radiation efficiency	On the body, radiation efficiency reduces and the reduction is higher compared to UWB. When the antenna is placed 8 mm away from the body acceptable radiation efficiency is obtained. At 8 mm away from the body the efficiency is in the range of (28 to 83 %).	On the body, the radiation efficiency reduces across the whole band. The reduction is lower than the narrowband antennas, due to frequency-dependent behaviour. When the antenna is placed 4 mm away from the body, acceptable radiation efficiency is obtained. At 8 mm away from the body, the efficiency is in the range of (66.43 79.65 %).
6	Gain	Positive gain required. On the body, gain reduces for antenna with partial ground plane and increases for with full plane. Gain reduction is higher. Lower gain on the body as compare to the UWB. When antenna placed at 8 mm away from the body acceptable gain is obtained. At 8 mm away from the body the gain is in the range of (1.34 to 6.75 dBi).	Positive gain required. Gain reduces at lower band increase at higher band when very close to the body. Gain reduction is lower. Higher gain on the body as compared to narrowband. When antenna placed at 4 mm away from the body acceptable gain is obtained. At 8 mm away from the body, the gain increases across the whole band. At 8 mm away from the body the gain is in the range of (6.60 to 8.04 dBi).
7	Polarisation	Normal to the body surface. Dual polarised better.	Normal to the body surface. Dual polarised is better.
8	Radiation Pattern	Omnidirectional over the body surface is required.	Omnidirectional over the body surface is required.
9	Antenna and body gap	The optimum distance to place the narrowband antenna is recommended to be 8 mm away from then body. Highly dependent on the gap.	The optimum distance to place the narrowband antenna is recommended to be 4 mm away from then body. Dependent on the gap but less as compare to narrowband.
10	Frequency dependent behaviour	Only one frequency band (2.45 GHz) of operation so the performance is concerned for one band.	Due to wide band (3.1-10.6 GHz) characteristics antenna performances change with frequency. At lower frequency band human body lossy tissue has higher effects on the antenna performances as compare to the higher.
11	Ground plane	Very effective and highly recommended.	Less effective as compare to narrowband due to less body effects at higher frequency, however, recommended.
12	Power consumption	Since bigger in size, high power consumable; hence, shorter battery life.	Since smaller in size, less power consumable hence longer battery life.
13	Transmit power (EIRP)	High as 36 dBm	Low as –41.25 dBm/MHz EIRP
14	Electromagnetic	Higher in compare to UWB	Extremely low; hence, green radio systems

	pollution		(heating of the surrounding body tissues and health concern).
15	User friendly	User friendly	More safer for user due to low transmitted power of -41 dBm and short nano pulses.
16	Sensitivity	Very sensitive to the human body. Power penetrates more on the human body at lower frequency band.	Less sensitive to the human body as compare to narrowband. Power dissipates at higher frequency bands.
17	Path Loss	The path loss at the reference distance is lower as compare to UWB. In the chamber for proposed antenna they are in the range of 23.1 to 43.7 dB while in the indoor they are in 25.2 to 45.1 dB.	The path loss at the reference distance is higher as compare to the narrowband. In the chamber they are in the range of 44.1 to 50 while in the indoor they are in 46.1to 51.3.
18	Path Loss exponent	The path loss exponent is higher for narrowband antennas. In the chamber the path loss exponents are in the range of 2.49-4.08 and while in indoor they are in the range of 2.29-3.65.	The path loss exponents are lower for UWB antennas. In the chamber the path loss exponents are in the range of 2.34-3.56 and while in indoor they are in the range of 2.01-2.91.
19	Robustness to multipath	Medium.	Highly robust in multipathing therefore path loss value is lower at the higher distance.
20	Data rate	Medium	High data rate due to wider bandwidth.
21	Location dependent performance	Yes. Frequency shifting and on-body bandwidth varies for different on-body locations.	Yes. Frequency shifting varies due to different on-body locations.

The UWB technology offers many advantages with respect to narrow band systems, such as:

- Compared to the narrowband case, the antenna placement distance from the human body is recommended to be less for the UWB. The UWB technology suffers less body effects on the antenna performance than narrowband systems.
- In the UWB systems, the transmission of short nanosecond pulses, rather than continuous waveforms, allows pulse generators, amplifiers and receivers to not work continuously, but to be turned on for only a few nanoseconds in each repetition period. In addition, UWB systems can transmit at a much faster data rate compared with narrow band systems due to their wide bandwidth. The combination of high data rate and intermittent signal reduces average power consumption, and hence UWB radio chips can have smaller and cheaper batteries.
- In the UWB systems, it is possible to transmit and receive pulses without generating a carrier. This makes possible to achieve smaller chip sizes which is a very important feature in the context of small and low-cost WBANs. Owing to being smaller in size, it is easy to integrate UWB antenna with the system and chip.

- UWB technology is safer for the user because of the very low peak power (-41 dBm). Besides, since in UWB systems short nano pulses are transmitted, the user is not continuously exposed to the radiation.
- A typical problem in wireless communication is the multipath. In a typical complex indoor environment, the presence of many scatterers produce reflected signals which can cause a destructive interference on the direct signal. In UWB, due to the short duration of pulses, it is easy to separate at the receiver the direct component from each single reflection, and hence is possible to achieve longer transmission range with the same power level. In this study, it is noted that the path loss exponents for on-body radio propagation are lower in the UWB systems as compared to narrowband.
- Combination of short duration pulses, low power requirements and random code spreading makes, the UWB robust to jamming as it is difficult to distinguish original signal from noise signal. Finally, UWB systems are more scalable and flexible.

- When the antennas are worn on the body, they show higher gain as compared to narrowband antennas. In the UWB case, when the antennas are placed on the body, the radiation efficiency reduction is lower than the narrowband antennas, due to frequency-dependent behaviour. When the UWB antennas are placed at 4 mm away from the body, an acceptable level of radiation efficiency and gain are noticed. On the other hand, in narrowband case, at 8 mm away from the body, the antennas show an acceptable level of gain and radiation efficiency.

- In the case of UWB, very compact antennas show good on-body performance, even if the antenna does not have a partial or full ground plane at the back. For narrowband antennas, the frequency detuning is a very important issue, but in the UWB case, the frequency shifting is less of an issue as compared to the narrowband systems.

In comparison to the narrowband, UWB has more advantages in terms of antenna parameters, on-body performances and overall; hence, UWB technology will be suitable for future efficient and reliable body-centric wireless communications.

5.5 Summary

The performance parameters in the presence of human body of four UWB antennas (namely, the TSA, PICA, SWAN Shaped and Self Complementary) were investigated and compared. Placing the UWB antenna on the body, the impedance changes; in some cases, the return loss reaches up to -5.5 to -6 dB. Results show that, on the body for all UWB antennas, the lower frequency band at -10 dB impedance shifts with respect to the free space by up to 2 GHz. The lower frequency shifting is more significant for the antenna smaller in size (TSA) and less for the antenna bigger in size (PICA). Results indicate that the partial ground plane helps to reduce the frequency shifting for the smaller antennas. Due to different locations of the body, the frequency shifting varies (up to 0.92 GHz) and the variation is significant for the antennas without a ground plane.

On the body, the radiation efficiency for all four UWB antennas reduces (maximum 90.77 %) with respect to free space across the whole UWB band; the efficiency reduction is higher at the lower frequency. When the UWB antenna is very close to the body, the gain reduces at the lower frequency band and increases at higher frequency band. However, at 8 mm away from the body, the gain increases across the whole UWB band, regardless of the antenna type. Results indicate that, at 4 mm away from the body, all UWB antennas show acceptable level of efficiency and gain; hence, the optimum distance to place the UWB antenna is recommended to be 4 mm. When the UWB antenna is body-worn, fewer effects are noticed on the antenna impedance but more significant effects are seen on the gain, efficiency and radiation pattern. On the body, the antenna performances (gain, efficiency, radiation pattern and pulse fidelity) are comparable for the PICA, SWAN and TSA, but a degradation in performance is noticed for the self complementary, compared to other three.

The four UWB antennas have also been used to characterise the on-body path loss; the PICA shows the highest path loss exponent. The path loss values for the TSA, SWAN and Self complementary antennas are very close. Although, the volume of the PICA is four times bigger than the other three antennas, it does not show much improvement in path loss. The TSA and SWAN shaped will be suitable candidates for BANs, due to their significant size reduction and overall good on-body performances. At the end, antenna specifications and design guidelines for UWB BCWCs are provided. Furthermore, a comparison between narrowband and UWB antenna parameters is provided. This study shows that, in comparison with narrowband, UWB shows some more advantages; therefore UWB technology is a suitable candidate for BCWCs.

References

[1] FCC First Report and Order, Revision of the Part 15 Commission's Rules Regarding Ultra-Wideband Transmission Systems, pp. 98–153, April 22, 2003.

[2] **P. S. Hall and Y. Hao,** *Antennas and Propagation for Body-Centric Wireless Communications*. Artech House, 2006.

[3] **J. Bernardhard, P. Nagel, J. Hupp, W. Strauss, and T. von der Grun**, "BAN – body area network for wearable computing," *9thWirelessWorld Research Forum Meeting, Zurich*, July 2003.

[4] **C. Kunze, U. Grossmann, W. Stork, and K. Muller-Glaser**, "Application of ubiquitous computing in personal health monitoring systems," *Biomedizinische Technik: 36th Annual meeting of the German Society for Biomedical Engineering*, pp. 360–362, 2002.

[5] **T.-G. Ma and C.-H. Tseng**, "An Ultra Wideband Coplanar Waveguide-fed Tapered Ring Slot Antenna," *IEEE Trans. Antenna Propag.*, vol. 54, no. 4, pp. 1105–1110, Apr. 2006.

[6] **J. Liang, L. Guo, C. C. Chiau, X. Chen, and C. G. Parini**, "Study of CPW-fed circular disc monopole antenna for ultra wideband application," *IEE Proc. Microw. Antennas Propag.*, vol. 152, no. 6, pp. 520–526, Nov. 2005.

[7] **H. G. Schantz and M. Barnes**, "The COTAB UWB magnetic slot antenna," in *Proc. IEEE AP-S Int. Symp.*, Boston, MA, Jul. 2001, vol. 4, pp. 104–107.

[8] **A. Rahman, A. Alomainy and Y. Hao**, "Compact Body-Worn Coplanar Waveguide Fed Antenna for UWB Body- Centric Wireless Communications,'' *Antennas and Prop., EuCAP* 2007. The Second European Conference on 11-16 Nov. 2007 Page(s):1 – 4.

[9] **A. Rahman and Y. Hao**, ''A Novel Tapered Slot CPW-fed Antenna for Ultra-Wideband Applications and Its On/Off Body Performance', *International Workshop on Antenna Technology, iWAT* 2007, 21–23 March, 2007, Cambridge, UK.

[10] A**. Alomainy, A. Sani, J. Santas, A. A Rahman, and Y. Hao**, "Transient Characteristics of Wearable Antennas and Radio Propagation Channels for Ultra Wideband Body-Centric Wireless Communications,'' *IEEE Transactions in Antenna and Propagation,* vol. 57, no.4, pp.875-884, April 2009.

[11] **S.Y. Suh, W. L. Stutz man, and W. A. Davis**, "A New Ultra Wideband Printed Monopole Antenna: The Planar Inverted Cone antenna (PICA)," *IEEE Transaction on Antennas and Propagation*, vol. 52, no. 5, pp. 1361–1364, May 2004.

[12] **A. Alomainy, Y. Hao, C. G. Parini, and P. S. Hall,** "Characterisation of Printed UWB Antenna for On-Body Communications,'' *IEEE Wideband and Multiband Antenna Arrays*, Birmingham, UK, Sep. 2005.

[13] **A. Alomainy, and Y. Hao**, "Radio Channel Models for UWB Body Centric Networks with Compact planar Antenna,'' in *Proc. IEEE APS Int Symp. Antennas Propag.,* Albuquerque, NM, Jul, 9-14, 2006, pp, 2173-2176.

[14] **S. Y, W. L. Stutz man, and W. A. Davis**, "A Novel CPW fed Disk Antenna,'' in *Proc. IEEE Antennas Propag. Soc. Symp.*, Jun. 2004, vol. 3, pp. 2919-2922.

[15] **Z. N. Chen, T. S. P. See, X. Qing**, ‘‘Small Printed Ultra Wideband Antenna with Reduced Ground Plane Effects,’’ *IEE Transactions on Antenna and Propagation*, vol, 55, no 2, Feb. 2007.

[16] **A. Sani, J. Santas, A. Alomainy, and Y. Hao**,‘‘ Time Domain Characterisation of Ultra Wideband Wearable Antennas and Radio Propagation for Body-Centric Wireless Networks in Health Care Applications,’’ *Proceeding of the 5th International Workshop on Wearable and Implantable Body Sensors Networks*, The Chinese University of Hong Kong, HKSAR, China, June. 1-3, 2008.

[17] **Q. H. Abbasi, A. Alomainy, Y. Hao**, ‘‘Recent Development of Ultra Wideband Body-Centric Wireless Communications,’’ *Proceeding of 2010 IEEE International Conference of Ultra-Wideband*, (ICUWB 2010).

[18] **L. Guo, S. Wang, X. Chen, and C. G. Parini**, ‘‘A Small Printed Quasi-Self-Complementary Antenna for Ultra Wideband Systems,’’ *IEEE Antennas and Wireless Propagation Letter*, vol. 8, 2009.

[19] ‘‘Calculation of the dielectric properties of body tissues,” *Institute for Applied Physics, Italian National Research council, URL:http:// niremf.ifac.cnr.it/tissprop/*.

[20] **C. Gabriel and S. Gabriel**, “Compilation of the dielectric properties of body tissues at RF andmicrowavefrequencies,”*URL:http://www.brooks.af.mil/AFRL/HED/hedr/reports/dielectric/Title/Title.html,1999.*

[21] **T. Yang, S.-Y. Suh, R. Nealy, W. Davis, and W. L. Stutzman**, “Compact antennas for UWB applications,” *2003 IEEE Ultra Wideband Systems and Technologies*, pp. 205–208, November 2003.

[22] **D. Lamensdorf and L. Susan,** “Baseband-pulse-antenna techniques,” *IEEE Antennas and Propagation Magazine*, vol. 36, no. 1, February 1994.

[23] **M. Klemm, I. Z. Kovacs, F. G. Pedersen, and G. Troster**, “Novel small-size directional antenna for UWB WBAN/WPAN applications,” *IEEE Transactions on Antennas and Propagation*, vol. 53, no. 12, pp. 3884–3896, 2005.

[24] **J. McLean, H. Foltz, and R. Sutton,** “Pattern descriptors for UWB antennas,” *IEEE transactions on antennas and propagation*, vol. 53, no. 1 Part 2, pp. 553–559, 2005.

[25] **T. Dissanayake and K. Esselle**, “Correlation-based pattern stability analysis and a figure of merit for UWB antennas,” *IEEE Transactions on Antennas and Propagation*, vol. 54, no. 11 Part 1, pp. 3184–3191, 2006.

[26] **Z. N. Chen,** “Novel bi-arm rolled monopole for UWB applications,” *IEEE Transactions on Antennas and Propagation*, vol. 53, no. 2, pp. 672–677, February 2005.

[27] **M. Kanda**, “A relatively short cylindrical broadband antenna with tapered resistive loading for picoseconds pulse measurements,” *IEEE Transactions on Antennas and Propagation*, vol. 26, no. 3, pp. 439–447, 1978.

[28] **T. Zasowski, F. Althaus, M. Stager, A. Wittneben, and G. Troster**, “UWB for non-invasive wireless body area networks: channel measurements and results,” *IEEE Conference on Ultra Wideband Systems and Technologies*, November 2003.

Chapter 6 Investigation of Subject-Specific Radio Propagation Channels for Body-Centric Wireless Communications

In body-centric wireless networks, various units/sensors are scattered on/around the human body to measure specified physiological data, as in patient monitoring for healthcare applications [1]. A body-worn base station will receive the medical data measured by the sensors located on/around the human body. Body-centric wireless networks have a range of applications, from monitoring of patients with chronic diseases and care for the elderly, to general well-being monitoring and performance evaluation in sports [2-6]. The human body is considered as an uninviting and even hostile environment for a wireless signal. The diffraction and scattering from body parts, in addition to the tissue losses, lead to a strong attenuation, distortion of the signal [1]. In order to design power-efficient on-body communication systems, accurate understanding the wave propagation, the radio channel characteristics and attenuation around the human body is extremely important. To ensure the efficient performance of WBANs, the propagation channels need to be modelled and characterised. In the past few years, researchers have been thoroughly investigating narrow band and ultra wideband on-body radio channels. In [7-12], on-body radio channel characterisation was presented at the unlicensed frequency band of 2.45 GHz. UWB on-body radio propagation channel characterisation for body-centric wireless networks have been presented extensively in the open literature [12-21]. In chapters four and five, the effects of various antenna types on the on-body radio propagation channels have been investigated. It was noted that for different types of antennas, the path loss for on-body radio channels varies greatly. However, the sizes and shapes of the human body will also affect the propagation path and cause large variations in path loss for on-body radio links, and hence lead to different system performances. Potential narrowband and ultra wide-band (UWB) body-centric wireless networks need to provide efficient and reliable communication channels. Critical issues remain with regard to the human body effect, shape and sizes of the body, indoor propagations and radio channel characterization, which all must be addressed before the concept can be deployed for commercial applications. In this chapter, subject-specific narrowband (2.45 GHz) and ultra wide-band (3-10.6 GHz) on-body radio propagation studies in Wireless Body Area Networks (WBANs) were

performed by characterising the path loss for eight different real human subjects (male) of different shapes and sizes**.** The body shapes of the test subjects used in this study are characterised as Endomorph (thin), Ectomorph (medium build), Mesomorph (fatty), short, average height, taller and so on. An experimental investigation was made in the indoor environment using a pair of Printed Monopoles (for the narrowband case) and a pair of Tapered Slot Antennas (for the UWB case). A frequency domain measurement set up was applied for both narrowband and UWB cases. The impact of different body shapes and sizes on the on-body radio communication channel was analysed at 2.45 GHz and 3-10 GHz. At the end of this chapter, a comparison between narrowband and ultra wide-band on-body radio propagation channel subject-specificity is also discussed.

6.1 Narrowband Subject-Specific On-Body Radio Propagation Channel Characterisation

A total of eight real male human subjects were considered in this study. The heights and weights of the test subjects are listed in Table 6.1, together with the chest and waist circumferences. Fig. 6.1 shows the photographs of the test subjects used in this experiment.

Measurement Settings

For the narrowband subject-specific on-body radio propagation channel study, a pair of Printed Monopole antennas (working at 2.45 GHz) was used (see Fig. 4.3). More details about the Printed Monopole antenna are provided in chapter 4. A HP8720ES vector network analyser (VNA) was used to measure the transmission response (S21) between two antennas of the same kind placed on the body. During the measurements, the transmitter antenna connecting with the cable was placed on the left waist, while the receiver antenna connecting with the cable was successively placed on 34 different locations on the front part of the standing human body; as shown in Fig. 4.21 (chapter 4). The test subjects were standing still during the measurements and, for each receiver location and measurement scenario, 10 sweeps were considered. The effects of the cable were calibrated out. The network analyser settings were the same as shown in the Table 4.10 (chapter 4). The measurement campaigns were performed in the Body-Centric Wireless Sensor Laboratory at Queen Mary, University of London (Fig. 4.22).

Table 6.1. The dimensions of eight real test subjects (male) used in this study.

Dimensions	**Male 1**	**Male 2**	**Male 3**	**Male 4**	**Male 5**	**Male 6**	**Male 7**	**Male 8**
Height (cm)	182	181	186	178	169	168	188	180
Weight (kg)	70	73	74	78	68	91	120	128
Chest Circumference (cm)	87	91	92	93	94	114	124	136
Waist Circumference (cm)	79	81	82	86	89	96	130	140

Male 1 Male 2 Male 3 Male 4 Male 5 Male 6

Male 7 Male 8

Fig. 6.1. The photographs of the eight test male subjects used for on-body radio propagation channel measurement (dimensions are shown in Table 6.1).

Narrowband On-Body Path Loss Characterisation

The path loss for the different receiver locations was calculated directly from the measurement data of S21 (10 sweeps) averaging at 2.45 GHz. In order to model the path loss as a linear function of the logarithmic distance, a least-square fit was performed on the measured path loss data for 34 different receiver locations, as shown in Fig. 6.2. Table 6.2 lists the value of path loss exponents, path loss at the reference distance d_0 (set to10 cm), obtained for the eight different test subjects. Due to the different body sizes, shapes and heights, the path loss exponent γ varies for the different human bodies. In this study for the narrowband case, a maximum variation in path loss exponent of 0.85 is noticed (Male 01 and Male 08). The results show that the path loss exponent generally increases with body size. It is noted that the path loss exponent is subject-specific.

In the case of subjects with the low value of body chest and waist circumferences, such as male 01, male 02 and male 03, the path loss exponent is lower and, with large values of chest and waist circumferences (male 06, male 07 and male 08), the path loss exponent is higher. In this case, for thinner subjects (male 01, male 02 and male 03), the propagation between the Tx and Rx is more line of sight (LOS) than the body with higher volume of the chest and waist circumference, resulting lower path loss exponents (γ=3.2, γ=3.25, γ=3.31 for male 01, male 02 and 03). For the subjects with a higher radius of curvature of the trunk, such as male 06, male 07 and male 08, the wave reaches the receiver through creeping wave propagation, which has higher signal attenuation, thus leading to a higher value of exponent (γ=3.71, γ=3.85, γ=4.05 for male 06, male 07 and 08). For the subject with higher volume of chest and waist circumferences, the communications for some of the receiver locations is heavily blocked by the different body parts, compared to the subject with lower value of chest and waist circumferences. In addition, the body tissues, reflection, diffraction and scattering from the body parts are also different for various subjects, which contribute to the variation of path loss. For the on-body radio channel, the propagation is mainly through creeping wave, free space and guided wave. Different shapes and sizes of the test subjects affect the propagation mode for on-body propagation links.

Fig. 6.3 shows the deviation of measurements from the average path loss fitted to a normal

distribution for the eight different test subjects for the narrowband case. Table 6.3 lists the values of standard deviation of the shadowing factor obtained for eight different test subjects. The standard deviation σ of the normal distribution was found to be higher for male 05 and male 08. Results indicate that the standard deviation value σ varies for different subjects.

Table 6.2. Narrowband on-body path loss parameters for the 8 different test subjects. The parameter γ is the path loss exponent, $PL_{dB}(d_0)$ is the path loss at the reference distance, and σ is the standard deviation of the normally distributed shadowing factor.

Path loss parameters	**Male 01**	**Male 02**	**Male 03**	**Male 04**	**Male 05**	**Male 06**	**Male 07**	**Male 08**
γ	3.20	3.25	3.31	3.39	3.48	3.71	3.85	4.05
$PL_{dB}(d_0)$ (dB)	41.0	40.8	40.7	43.8	42.0	42.8	44.2	41.7
σ (dB)	7.62	6.80	7.12	6.31	8.01	7.09	7.17	8.12

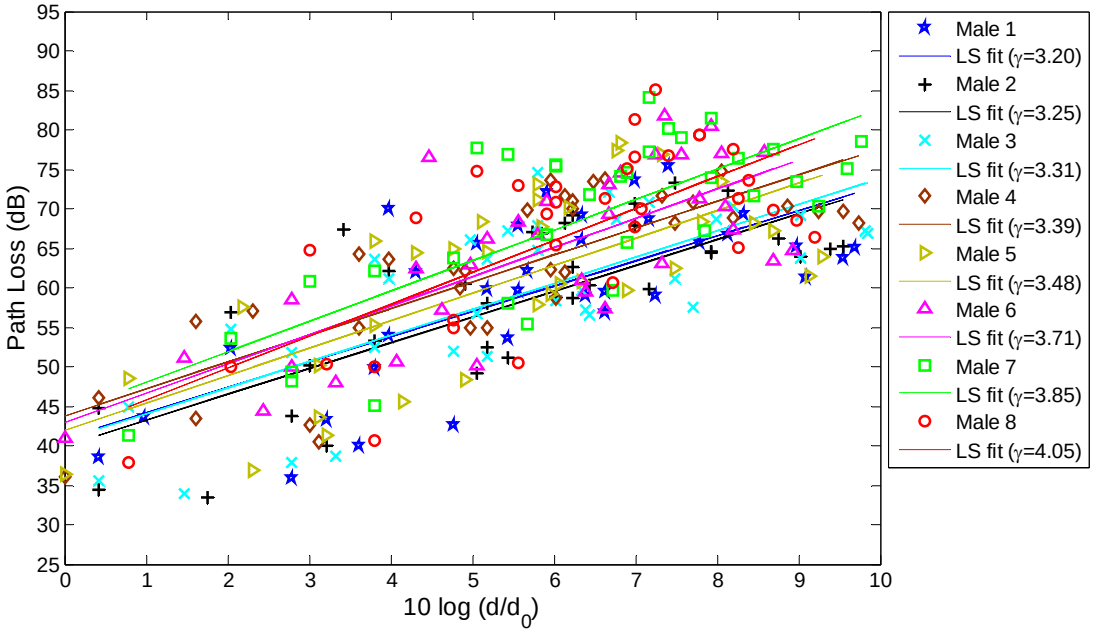

Fig. 6.2. Measured and modelled path loss for narrowband on-body channels versus logarithmic Tx-Rx separation distance of different human body (Male01-Male 08).

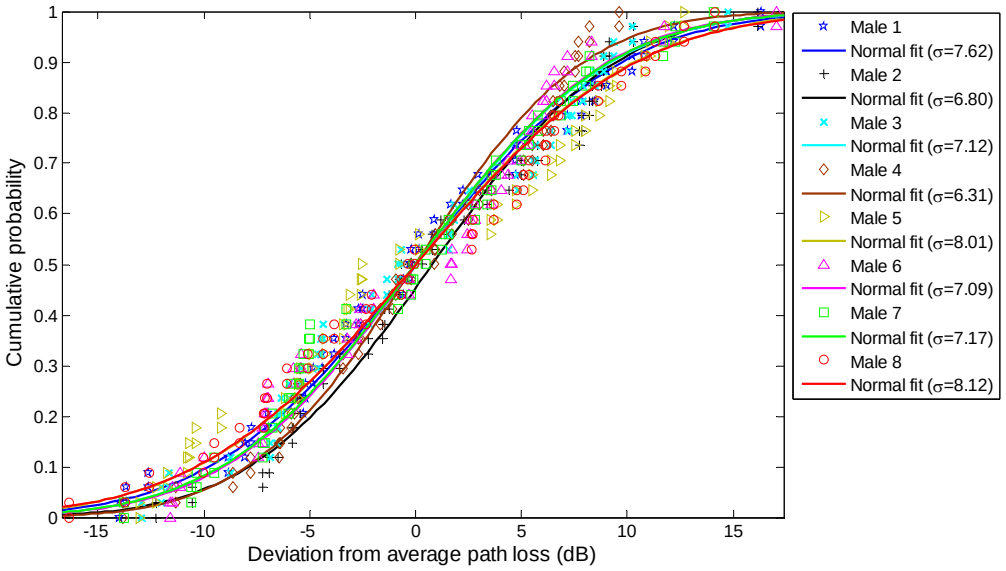

Fig. 6.3. Deviation of the measurements from the average path loss for different test subjects (Male01-Male 08) fitted to normal distribution at 2.45 GHz.

In order to compare the path loss for eight different human body types, eight different on-body channels (Fig. 6.4) have been chosen. Fig. 6.5 shows the variation in path loss for the eight different on-body links for the eight test subjects.

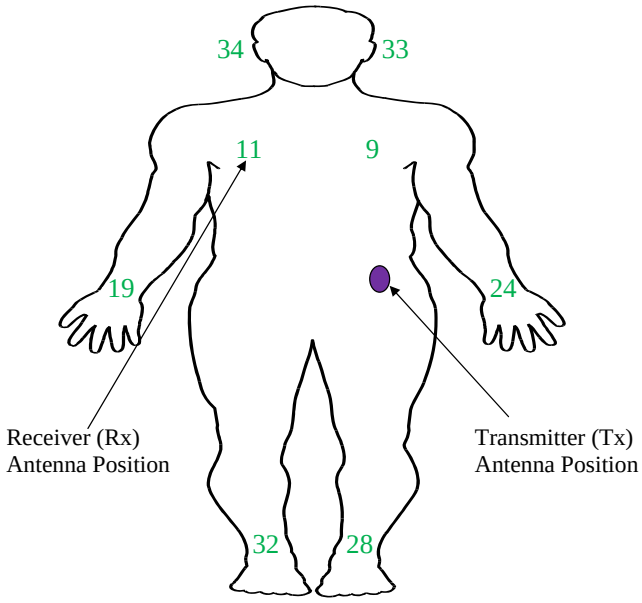

Fig. 6.4. Considered 8 different on-body links chosen for path loss comparison of different test subjects.

For the considered 8 different links, due to the different shapes and sizes of the human body, a maximum of 13.02 dB variation of path loss of an on-body channel was observed. It was noted for the transmitter to right wrist link (Rx 19) of male 01 and male 08, where the variation of path loss for this link of eight different subjects is mainly due to different trunk size of the different subjects. In the case of male 01, the trunk size is much smaller than the trunk of male 08, which creates less NLOS and less blocked communication, resulting in a lower path loss value for this link of the male 01. For the receivers on the wrists and on the ankles, the variation of path loss between the different subjects is found to be higher. The maximum variation of path loss of different subjects for left and right ankle links is 11.89 dB and 11.69 dB, respectively. For the ankle channels, the variation of path loss is due to different height and size of the legs of different subjects. The lowest path loss for both ankle links is noticed for the shorter subject with medium body size (male 05), whereas the highest is noticed for the taller subjects with a fatty body (male 07 and male 08). In the case of male 05, the legs are smaller than those of male 07 and male 08; hence, the communication distance in between Tx and Rx is less, leading to a lower path loss value of this channel for male 05.

For the receiver placed on the ear, it is possible to note that the path loss is higher for the taller subjects with a larger curvature radius at the trunk such as (male 07 and male 08) and lower for the thinner and shorter subjects with smaller curvature radius (male 05, male 01, male 02 and male 03). For the shorter subject with smaller value of curvature (male 05), the path loss for these left ear and right ear links is found to be a maximum 8.64 to 9.25 dB lower. In this study, for different subjects, the lowest path loss variation is noticed for the ear and chest links. Table 6.3 summarises the maximum path loss variation of each channel for different subjects.

Table 6.3. The maximum path loss variation of each link obtained among different test subjects (narrowband).

Channel	**Maximum path loss (dB) variation**
Left chest	7.52
Right chest	8.95
Left ear	9.25
Right ear	8.64
Left wrist	12.10
Right wrist	13.02
Left ankle	11.79
Right ankle	11.69

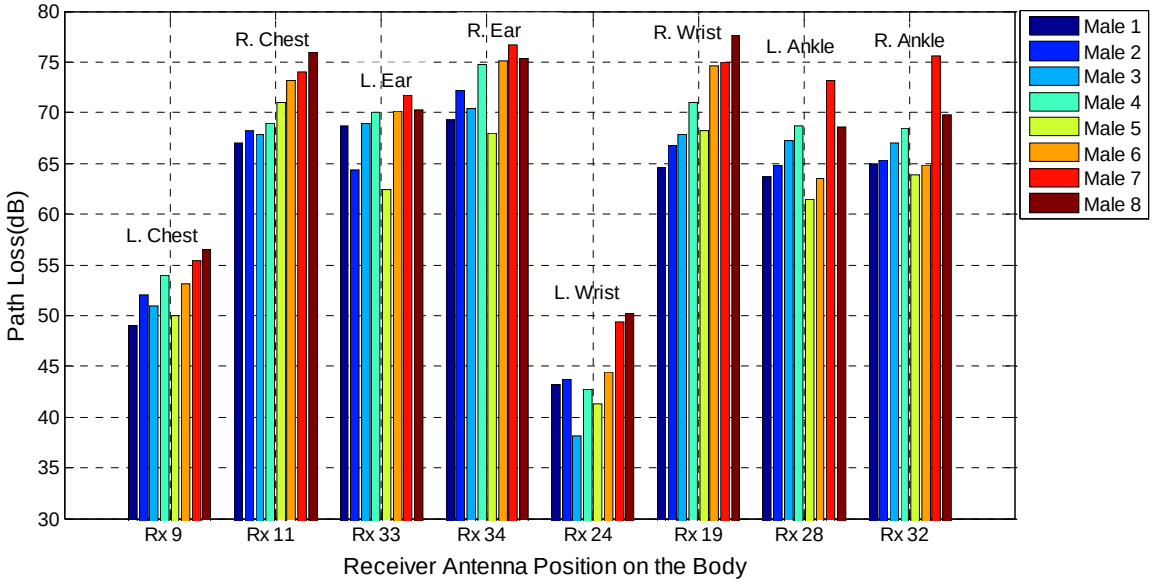

Fig. 6.5. Variation of path loss for 8 different narrowband on-body radio propagation channels of different human test subjects.

For the narrowband case, the lowest path loss is noticed for the left wrist and left chest links for all eight subjects. The path loss for each different location is averaged over the eight test subjects. The subject-averaged path loss values for the left chest, right chest, left ear, right ear, left wrist and right wrist, left ankle, right ankle are 52.64, 70.77, 68.32, 72.71, 44.14, 70.72, 66.41, 67.47 dB, respectively. Results show that, for the narrowband case, the subject-averaged highest path loss is noticed for the right ear, right wrist and right chest channels, while the lowest is at left wrist and left chest channels. The on-body channel path loss is also highly dependent on the antenna radiation pattern, as discussed in the previous chapter.

6.2 Ultra Wideband (UWB) Subject-Specific On-Body Radio Propagation Channel Characterisation

Similarly to the previous section, the subject-specificity of the ultra wide-band (UWB) on-body radio channel is investigated by considering the same eight real test subjects. For the ultra wide-

band subject-specific on-body radio propagation channel study, a pair of Tapered Slot antennas was used; see Fig. 5.1 in chapter 5. More details about the Tapered Slot Antenna (TSA) were provided in chapter 5. In order for a fair comparison to be made between narrowband and ultra wideband subject-specific on-body radio propagation channels, the printed monopole antenna was used for the narrowband case, while the tapered slot antenna was used for the UWB case. The printed monopole and the tapered slot antenna have the same radiation characteristics and both of them have partial ground plane at the back.

Measurement Settings

The UWB subject specific on-body radio channel measurements were also performed in the frequency domain, using a Vector Network Analyser (Hewlett Packard 8720ES-VNA) and two cables, connecting two stand-alone identical TSA antennas, to measure the transmission response (S21) in the frequency range of 3-10 GHz. The frequency range was set to 3-10 GHz, with 1601 points and with a sweep time of 800 ms. The network analyser settings were shown in the chapter 5 in Table 5.9. Like the narrowband study, 34 different receiver locations were considered. For this case, the transmitter and receiver antennas were placed exactly on the same locations as for the narrowband case; see Fig. 4.21 (chapter 4). During the measurements, the subject was standing still, and for each receiver location and measurement scenario, 10 sweeps were considered, as was performed for narrowband case. The UWB subject-specific on-body radio channel measurements were also performed in Body-Centric Wireless Sensor Lab, Queen Mary University of London (Fig. 4.22).

UWB On-Body Path Loss Characterisation

The path loss for each receiver location is directly calculated from the measurement, averaging over the frequency band of 3~10 GHz. A least-square fit method is applied on the measured path loss data for 34 different receiver locations to extract the path loss exponent for eight test subjects, as shown in Fig. 6.6. Table 6.4 lists the values of path loss exponent γ obtained for

different test subjects. It can be noted that the model path loss is affected by the body size. The conclusions are similar to the ones drawn in the previous section for a narrowband system. In particular, it is noted that subjects with a larger body size show higher values of path loss exponent. For the UWB case, the value of the path loss exponent γ ranges from 1.91 (Male 01) to 3.06 (Male 08). It can be noted that some subjects (such as male 06, male 07 and male 08) have a bigger curvature radius at the waist and chest, and hence they present a higher value of γ. For the UWB case, due to different body sizes, shapes and heights, a maximum variation in path loss exponent of 1.15 is noticed (Male 01 and Male 08). For this case, male 01 has the lowest chest and waist size circumferences compared with the male 08, resulting in the lowest path loss exponent.

Fig. 6.6 shows the deviation of measurements from the average path loss fitted to a normal distribution for the eight different test subjects for the UWB case. The values of the standard deviation σ of the shadowing factor obtained for eight different test subjects are listed in Table 6.4. As with the narrowband results, the standard deviation σ of the normal distribution was found to be higher for male 05 and male 08. Results indicate that the standard deviation value σ varies for different test subjects, as was found in the narrowband system.

Table 6.4. Ultra wide-band on-body path loss parameters for different test subjects. The parameter γ is the path loss exponent, $PL_{dB}(d_0)$ is the path loss at the reference distance, and σ is the standard deviation of the normally distributed shadowing factor.

Path loss parameters	**Male 01**	**Male 02**	**Male 03**	**Male 04**	**Male 05**	**Male 06**	**Male 07**	**Male 08**
γ	1.91	2.0	2.08	2.19	2.33	2.62	2.8	3.06
$PL_{dB}(d_0)$	51.2	51.6	50.4	51.8	50.7	50.5	49.0	48.7
σ	7.36	7.27	6.90	7.61	8.30	6.86	6.60	7.80

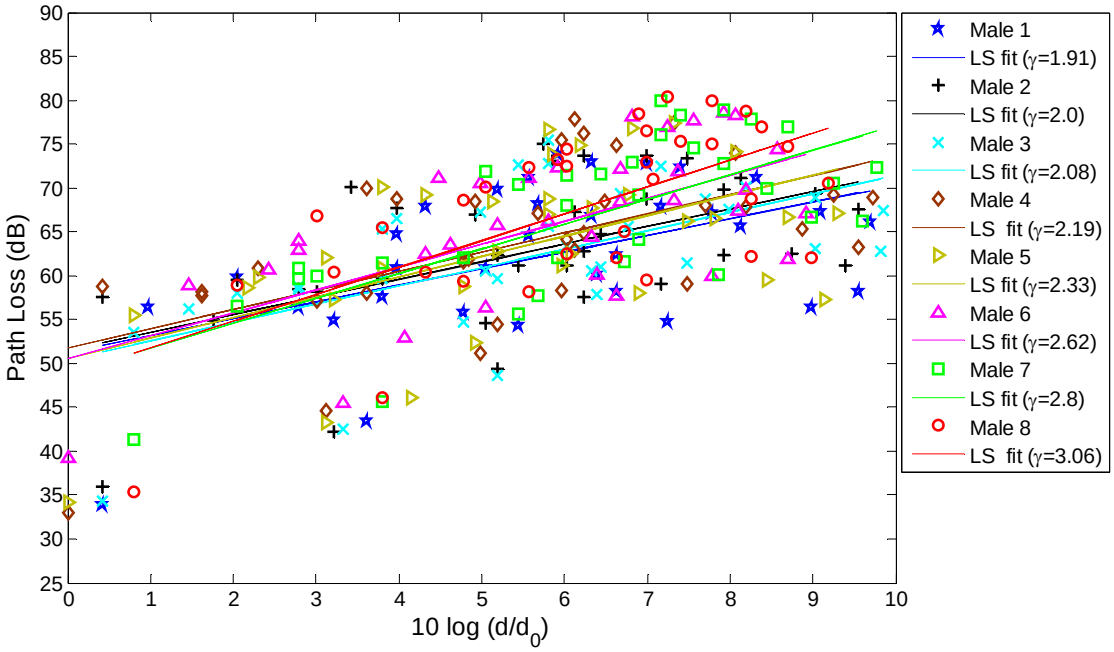

Fig. 6.6. Measured and modelled path loss for ultra wideband on-body channels versus logarithmic Tx-Rx separation distance of different human body (Male1-Male 8).

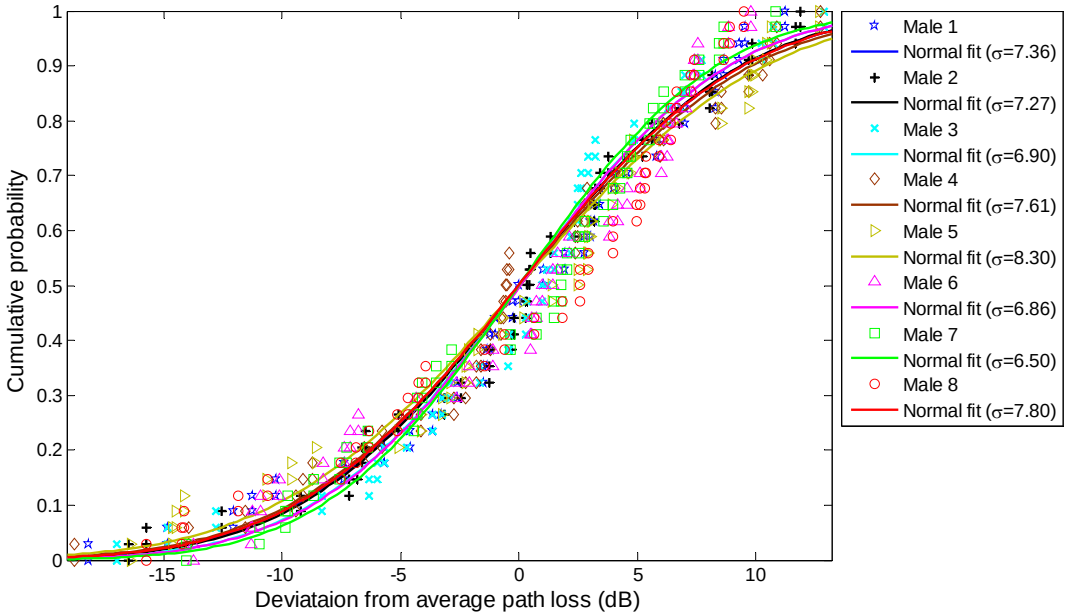

Fig. 6.7. Deviation of the measurements from the average path loss for different test subjects (Male 01 to Male 08) fitted to normal distribution at UWB.

Like the narrowband system, eight different on-body radio communication channels (as shown in Fig. 6.4) have been chosen for the UWB case, in order to compare the path loss for eight different human body types. Fig. 6.8 shows the variation in path loss for 8 different ultra wide-band on-body radio links of different human test subjects. Due to different shapes and sizes of the human body, the path loss varies for each different receiver location on the body. For the considered eight different radio links, a maximum of 14.21 dB variation in path loss of an ultra wide-band on-body radio channel was observed. It is noted for the transmitter to right wrist link (Rx 19) of male 01 and male 08. In this case, the same conclusion is drawn as in the previous section for a narrowband system. In particular, subjects with higher chest and waist circumferences (male 06, male 07, male 08) show higher path loss value for the wrist links, compared with the subjects with smaller chest and waist sizes (male 01, male 02, male 03). For different subjects, the higher path loss variation is noticed for the receivers on the wrists and on the ankles, while the lowest path loss variation is noticed for the ear and chest links. Table 6.5 summarises the maximum variation of path loss for different on-body channel of different subjects.

Table 6.5. The maximum path loss variation of each on-body radio link obtained among different subjects (UWB).

Channel	**Maximum path loss (dB) variation**
Left chest	8.8
Right chest	8.24
Left ear	9.4
Right ear	9.28
Left wrist	12.62
Right wrist	14.21
Left ankle	10.89
Right ankle	10.29

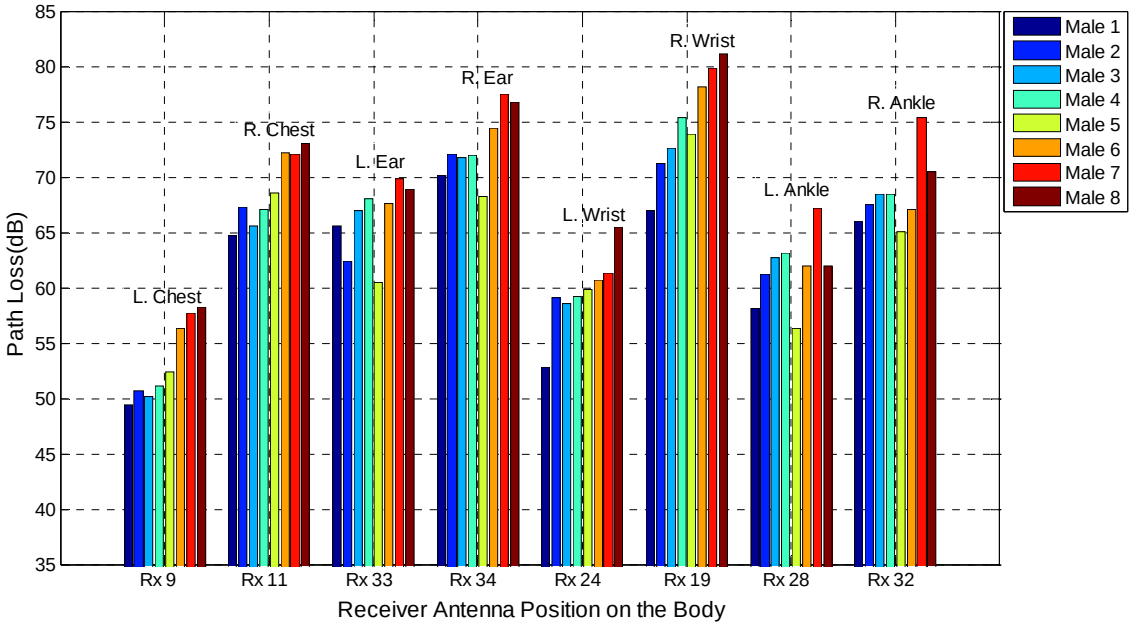

Fig. 6.8. Variation of path loss for 8 different UWB on-body radio propagation channels of different human body.

For the UWB system, the lowest path loss is noticed for the left wrist and left chest links for all eight subjects. The path loss for each different location is averaged over the eight test subjects. The averaged path loss for the left chest, right chest, left ear, right ear, left wrist and right wrist, left ankle, right ankle is 53.50, 68.80, 66.20, 72.84, 59.62, 74.87, 61.59, 68.55 dB, respectively. Results show that for UWB case, the subject-averaged highest path loss is noticed for the right wrist, right ear and right chest channels, while the lowest is at left chest and left wrist channels. For the UWB case, nearly the same trends are noticed as was noticed for the narrowband case.

6.3 Narrowband Vs Ultra Wideband Subject-Specific Radio Propagation Channels

Based on the studies in the previous two sections, a comparison between narrowband and ultra wide-band subject specific on-body channel characterisation is made here.

- For the narrowband case at 2.45 GHz, the path loss exponent is in the range of 3.20 to 4.05, while for the UWB (3-10 GHz) case, it is in the range of 1.91 to 3.06.
- It is noted that, for the narrowband on-body radio propagation case, due to the different sizes, shapes and heights of the test subjects, the path loss exponent value varies up to a maximum of 0.85. For the UWB case, for different subjects, the path loss exponent value varies up to maximum of 1.15. From this study, it is observed that, for different test subjects ultra wide-band system shows a higher variation of path loss exponent value (0.3). The variation of path loss exponent for different test subjects in the UWB case is not much compared with the narrowband system.
- For the considered 8 different on-body links in the narrowband case, for different test subjects, a maximum of 13.02 dB variation in path loss value of an on-body radio channel (right wrist) is noticed for the narrowband system, while for the UWB system, it is noticed to be 14.21 dB. For the UWB case nearly the same trends are noticed as was observed for the narrowband case.
- The values of path loss exponents γ are found to be higher for the narrowband case than the ones found for the UWB case. In the narrowband case, there is only one frequency band of operation (2.45 GHz) which has fewer effects (reflection, diffraction, scattering and so on) from the indoor environments and human body parts. On the other hand, in the UWB case, there are many frequency components (3-10 GHz) which have more effects from the indoor environments and the human body parts, results in lower path loss exponent as compared with the narrowband case. UWB technology is highly robust in multipathing; hence, path loss value is lower at the higher distance, resulting in lower path loss exponent.
- At the reference distance, the path loss is found to be higher for the UWB on-body radio channel (average 8 dB) compared with the narrowband system. At lower communication distances between Tx and Rx, the path loss for UWB on-body radio channels is found to be higher compared with the narrowband case (such as the left wrist and left chest links).

6.4 Summary

In this chapter, the subject-specificity of the narrowband (at 2.45 GHz) and ultra wide-band (3 GHz-10 GHz) on-body radio channels in Wireless Body Area Networks (WBANs) was investigated by considering eight real human test subjects of different shapes, heights and sizes. Experimental investigation was made in the indoor environment using a pair of Printed Monopole Antennas for the narrowband case, and a pair of Tapered Slot Antennas for UWB case. In both cases, a frequency domain measurement set up was applied. The impact of different body shape, height and size on the on-body radio communication channel path loss was investigated and analysed at 2.45 GHz and 3-10 GHz. It is noted that, for both narrowband and ultra wide-band on-body radio channel cases, the path loss exponent increases with the body size. In particular, the path loss exponent was found to be higher for subjects with bigger body size and larger radius of curvature at the chest and waist. Results demonstrated that both the narrowband and ultra wide-band on-body radio propagation channels are subject-specific.

A comparison between narrowband and UWB on-body radio propagation channel subject-specificity was summarised. Results demonstrated that, due to the different sizes, heights and shapes of the test subjects, the path loss exponent value varies up to maximum of 0.85 for the narrowband on-body case, whereas a maximum variation of path loss exponent value of 1.15 is noticed for the UWB case. Results show that the maximum path loss exponent variation for different test subjects in the UWB case is very close to the narrowband system. It is noted that, if the same antennas (same characteristics) are used for the narrowband and UWB systems, the on-body radio channels are subject-specific for both cases rather than the technology (UWB and narrowband). The path loss exponent is found to be higher for the narrowband on-body radio propagation case, compared with the UWB.

The effect of the human body shape and size variations on the 8 different on-body radio channels is studied where results demonstrated that, for certain on-body links (e.g. waist to right wrist) the changes in body shape can lead to a significant variation (up to 13.02 dB for narrowband and 14.21 dB for UWB case) in path loss. Results indicate that, for different subjects, the path loss varies maximum for the wrist and ankle channels and minimum for the ear and chest links in both cases. The UWB and narrowband systems show nearly the same trends of path loss for different on-body locations of different test subjects.

References

[1] **P. S Hall and Y. Hao**, Antennas and propagation for Body-Centric Wireless Communications. Artech House, 2006.

[2] **A. Fort, C. Desset, P. D. Doncker, and L.V. Biesen**, "Ultra wideband body area propagation: from statistics to implelmentation,'' *IEEE Transactions on Microwave Theory and Technique*, vol. 54, no. 4, pp. 1820 1826, June 2006.

[3] **S Drude**, "Requirements and application scenarios for body area networks,'' *Mobile and Wireless Commmunications Summit*, IST, Jul. 2007.

[4] **J. Bernardhard, P. Nagel, j. Hupp, W. Strauss, and T. Von Der Grun**, "BAN-body area network for wearable computing,'' The 9th *Wireless World Research Forum* Meeting, Zurich, July 2003.

[5] **E. Jovanov, A. O'D Raskovic, P. Cox, R. Adhami, and F. Andrasik**, " Stress monitoring using a distributed wireless intelligent sensor system,'' *IEEE Eng. Medicine Biology Mag*., Vol. 22, pp. 49-55, May 2003.

[6] **N. F Timmons and W. G. Scanlon,** "Analysis of the performance of IEEE 802.15.4 for medical sensor body area networking,'' 1st annual *IEEE Communications Conference Sensor and Ad Hoc Communications and Networks* (SECON), pp, 16-24, Oct. 4-7, 2004. (2002).

[7] **A. Alomainy, Y. Hao, A. Owadally, C. G. Parini, Y. Nechayev, C. C. Constantinou, and P. S. Hall**, "Statistical analysis and performance evaluation for on-body radio propagation with microstrip patch antenna,'' *IEEE Transactions on Antennas and Propagation,* Vol, 55, No, 1 January 2007.

[8] **Y. Nechayev, P. Hall, C.C. Constantinou, Y. Hao, A. Owadally and C. G. Parini**, "Path loss measurements of on-body propagation channels,'' in Proc. 2004 *International Symposium on Antennas an Propagation*, Sendai, Japan, pp. 745-748, Aug. 2004.

[9] **P. S. Hall, Y. Nechayev, Y. Hao, A. Alomainy, M. R. Kamaruddin, C. C. Constantinou, R. Dubrovka and C. G. Parini**, "Radio characterisation and antennas for on-body communications,'' In Proc. *Loughborough Antennas and Propagation Conference*, Loughborough, UK, pp. 330-333, Apr. 2005. "PDCA12-70 data sheet,'' Opto Speed SA, Mezzovico, Switzerland.

[10] **Y. Hao, A. Alomainy, P. S. Hall, Y. I. Nechayev, C. G. Parini, and C. C. Constantinou**, "Antennas and propagation for body-centric wireless communications,'' *IEEE/ACES International Conference on Wireless Communications and Applied Computational Electromagnetics*, Honolulu, Hawaii, USA, 3-7 April 2005.

[11] **A. Alomainy, Y. Hao, A. Owadally, C. G. Parini, Y. I. Nechayev, C. C. Constantinou, and P. S. Hall**, "Antennas and propagation for body-centric wireless communications,'' *IEEE/ACES International Conference on Wireless Communications and Applied Computational Electromagnetics*, Honolulu, Hawaii, USA, 3-7 April 2005.

[12] **Z. Hu, Y. Nechayev, P. S Hall, C. Constantinou, and Y. Hao**, "Measurements and statistical analysis of on-body channel fading at 2.45 GHz, *IEEE antennas and Wireless Propag. Lett.* vol. 6, pp. 612-615, 2007.

[13] **A. A. Alomainy, Y. Hao, C. G. Parini, and P. S. Hall**, "Comparison between two different antennas for UWB on body propagation measurements,'' *IEEE Antennas and Wireless Propagation Letter.* 2005, 4, (1), pp. 31-34.

[14] **A. Sani and Y. Hao**, "Modeling of Path Loss for Ultrawide Band Body Centric Wireless Communications,'' Electromagnetics in advance applications, 2009. ICEAA'09, *International Conference on* 14-18 sept.,2009 pages(s):998-1001.

[15] **A. Fort, C. Desset, J. Ryckaert, P. D. Donker, L. V. Biesen , and P. Wambackq**, "Characterization of Ultra wideband body area propagation channel,'' *International Conference on Ultra- Wideband*, September 2005.

[16] **Q, Wang, J. Wang**, "Performances of On-Body Chest-to-Waist UWB Communication Link,'' *IEEE microwave and wireless components letters*, vol. 19, no. 2, Feb.2009.

[17] **T. Zasowski, F. Althaus, M. Stager, A, Wittneben, and G. Troster**, "UWB for non-invasive wireless body area networks: channel measurements and results,'' *IEEE Conference on Ultra Wideband Systems and Technologies*, November 2003.

[18] **A. Alomainy, Y. Hao, X. Hu, C. G. Parini, and P.S Hall**, "UWB on-body radio propagation and system modeling for wireless body-centric networks,'' *IEE proceedings communications*-Special Issue on Ultra Wideband Systems, technologies and Applications, vol. 153, no.1, pp 107-114, Feb. 2006.

[19] **Q. H. Abbasi, A. Sani, A. Alomainy and Y. Hao**, "Radio Channel characterization and system-Level Modeling for Multiband OFDM Ultra Wideband Body-Centric wireless networks,'' accepted in special issue of *IEEE Transactions on Microwave Theory and Techniques.*

[20] **A. Sani, G. Palikaras, A. Alomainy and Y. Hao**, "Time Domain UWB Radio Channel Characterisation for Body-Centric Wireless Communications in Indoor Environment,'' *Wideband and Ultrawide-band Systems and Technologies: Evaluating current Research Development, 2008 IET Seminar*.

[21] **A. Sani, A. Alomainy, and Y. Hao**, "Effect of the Indoor Environment on the UWB On-Body Radio Propagation Channel,'' *Antennas and Propagation, 2009. EuCAP 2009. 3rd European Conference on,* 23-27 March 2009 Page(s):455 – 458.

[22] **A. Alomainy, Y. Hao and D. M Davenport**, "Parametric Study of Wearable Antennas Varying Distances from the Body and Different On-Body Positions,'' *Antennas and Propagation for Body-Centric Wireless Communications, 2007 IET Seminar on* 24-24 April 2007 Page(s):84 – 89.

[23] **A. Rahman, A. Alomainy and Y. Hao**, "Compact Body-Worn Coplanar Waveguide Fed Antenna for UWB Body- Centric Wireless Communications,'' *Antennas and Prop., EuCAP* 2007. The Second European Conference on 11-16 Nov. 2007 Page(s):1–4.

[24] **A. Rahman and Y. Hao**, ''A Novel Tapered Slot CPW-fed Antenna for Ultra-Wideband Applications and Its On/Off Body Performance', *International Workshop on Antenna Technology, iWAT* 2007, 21–23 March, 2007, Cambridge, UK.

[25] A**. Alomainy, A. Sani, J. Santas, A. A Rahman, and Y. Hao**, "Transient Characteristics of Wearable Antennas and Radio Propagation Channels for Ultra Wideband Body-Centric Wireless Communications,'' *IEEE Transactions in Antenna and Propagation,* vol. 57, no.4, pp.875-884, April 2009.

Chapter 7 Conclusions and Future Work

7.1 Summary

Recently, there have been many efforts made to design the wearable antennas and to investigate the on-body radio propagation channels. In the presented work, a parametric study was performed in order to study the human body effects on the performance parameters of five different narrowband antennas at 2.45 GHz. According to the study, when narrowband antennas are placed on the body, they suffer huge effects on the performances from the human body, especially the antennas with partial ground planes. The dependency of the wearable antenna parameters on the distance between the antenna and the body and also on-body position to which the antennas were attached were demonstrated through numerical simulation and experimental analysis. The study illustrated the benefit of applying the full ground plane in minimising the influence of lossy human tissues on antenna performance parameters. For wearable antennas, a full ground plane will be suitable in order to minimise the influence of lossy human tissues on the antenna performance, therefore it is recommended. However, if we don't want the full ground plane, the narrowband antennas need to be placed at least 8 mm away from the body, but the frequency needs to be tuned properly. For wearable narrowband antennas, the frequency detuning is very important issue and antenna with very narrow bandwidth is not suitable for on-body applications unless the frequency is tuned properly. The performance parameters of the patch and wire monopole are much less sensitive to the human body tissues. As compared to the patch, the wire monopole has the advantage of on-body performance. Experimental investigations were carried out to study the effects of various antenna types on the on-body radio propagation channels, where Wire Monopole is found to be the most power-efficient for on-body communications. However, due to its shape, the wire monopole antenna will be not suitable for on-body applications.

A novel dual-band and diverse radiation pattern antenna is proposed for reliable and power-efficient on-body and off-body communications intended to be applied in various applications in healthcare and sport monitoring. The DBDM antenna is conformal and, it shows excellent on-body performance at both frequency bands. The DBDM offers advantage of performances at 2.45 GHz compared to the other narrowband antennas used and this antenna (DBDM) is suitable

candidate for future BCWCs in order to establish power efficient co-operative on-body and off-body communications. Statistical analysis was also provided to evaluate the on-body performances of different narrowband antennas. Based on the results analysed for six antennas, the narrowband (2.45 GHz) antenna specifications and guidelines for body-centric wireless communications are provided. The DBDM antenna meets the specifications and guidelines.

Over the past few years, the attention towards the UWB technology for wearable applications has experienced considerable growth. In this work, the performance parameters at 3-10 GHz of four different UWB antennas in the presence of a human body were investigated and compared. The performance of the UWB antennas were investigated by placing the antenna at various distances away from the body, where results show that, having no ground plane or a partial ground plane has limited effect on the on-body performance parameters, but the antenna size seems to be more significant. However, it is possible that having a full ground plane on the back of the antenna may improve the on-body performance for the UWB antenna. For UWB system, the optimum distance to place the antenna from the body is recommended to be 4 mm. The frequency shifting of the UWB antennas was studied placing them at different locations on the body, where results indicate that the frequency shifting is very much dependent on the on-body location for the antennas without ground plane.

Results and analysis show that the on-body performance of the TSA, PICA and SWAN are not much different, while degradation of the performance is noticed for the self complementary antenna as compared to the other three. The four UWB antennas were used for on-body radio channel path loss characterisation where PICA shows the highest path loss exponent. Even though, the volume of the PICA is four times bigger than the other three antennas, it doesn't show much improvement in path loss. Thus although, the size of the TSA and SWAN antenna are nearly four times smaller than the PICA, the on-body performances (in terms of efficiency, gain, and radiation patterns) are not much different. Based on overall on-body performances, and due to their significant size reduction, the TSA and SWAN will be ideal candidates for BANs.

Based on the result analysed in chapter five, the UWB antenna specifications and guidelines for BCWCs are provided. A comparison of UWB and narrowband antenna parameters was provided, where UWB shows more advantages; hence, UWB technology will be the suitable candidate for BCWCs. The results in chapters 4 and 5, together with the analysis and antenna specifications, will be suitable guidelines and understanding for the system designers to design

the best narrowband and UWB antennas for future reliable and efficient body-centric wireless communications.

Finally, the subject-specificity of the on-body radio channel at 2.45 GHz and 3-10 GHz was experimentally investigated in an indoor environment by considering eight real human test subjects of different shapes, heights and sizes, and it was concluded that the physical parameters, such as the height of the subject, size and the curvature radius at the trunk, affect the path loss in on-body radio channels for both UWB and narrowband cases. The subject-specificity of the on-body radio channels was compared between narrowband and UWB systems, where results show that the on-body radio channels are subject-specific for both cases rather than the technology (UWB and narrowband), if the same antennas (same characteristics i.e., radiation and structure) are used. In this study, the values of path loss exponents γ are found to be higher for the narrowband case than the ones found for the UWB system.

7.2 Key Contributions

The major contributions of this thesis are:

- Characterisation of narrowband antennas at 2.45 GHz for on-body applications in body-centric wireless communications. This work involves investigating and comparing the performance parameters of five different body-worn antennas in the presence of the human body. A parametric study was performed to investigate the human body effects on the performance parameters of different body-worn antenna types to identify the best body-worn antenna for narrowband system to be applied in Body Area Networks. The study was performed by a combination of simulation and experimental investigation. A novel dual-band and dual-mode antenna for power-efficient and reliable body-centric wireless communications (on-body and off-body) was designed. On-body and free space performances are investigated in simulation and experimentally. The proposed DBDM antenna is found to be the suitable candidate for future body-centric wireless communications in order to establish power-efficient and reliable cooperative on-body and off-body communications.
- Characterisation of UWB antennas at 3-10.6 GHz for on-body applications in body area networks. Like narrowband, the on-body performances of four different UWB antennas

are investigated and compared in close proximity to the human body. A parametric study was performed to investigate the human body effects on the performance parameters of different body-worn antenna types to identify the best body-worn antenna for UWB system to be applied in Body Area Networks.

- Provide the narrowband and ultra wideband antenna specifications and guidelines for body-centric wireless communications. These works involve providing narrowband and ultra wideband body-worn antenna specifications and guidelines for system designers to select and design the best body-worn wearable antenna for future efficient and reliable narrowband and UWB body-centric wireless communications. Statistical analyses were performed in order to evaluate the on-body parameters for different narrowband and UWB body-worn antennas. It also involves a comparison between narrowband and UWB antenna parameters.
- The narrowband and UWB on-body radio propagation channels were experimentally investigated for 8 different body shapes, sizes and heights. The investigation was conducted by considering 8 human subjects and the results demonstrated that different body sizes, shapes and heights can lead to variations in path loss, and hence, to different system performance. The subject specificity of the on-body radio propagation channels was compared between narrowband and UWB system, where results show that the on-body radio channels are subject specific in both cases rather than the technology, if same antennas are used.

7.3 Future Work

Based on the conclusions drawn and the limitations of the work presented, the following research aspects and issues would provide potential and natural progression to the accomplished works in this thesis:

Wearable Antennas for Body-Centric Wireless Communications

- The size of the proposed dual-band and dual-mode antenna can be reduced further. In addition, the DBDM antenna can be tuned to operate three or more bands.

- The operating frequency of both resonating elements in the DBDM antenna can be tuned to operate at 2.45 GHz with different radiation modes (Omnidirectional radiation pattern over the body surface and directive radiation towards off-body direction) for power-efficient and reliable on-body and off-body communications. This antenna can be used to characterise body-to- body communication channels.

- Design a compact UWB antenna with full ground plane at the back which has omnidirectional radiation pattern characteristics over the body surface for future efficient and reliable body-centric wireless communications. Investigation of the performances of this antenna in close proximity to the human body. Finally, application of the antenna to on-body radio channel characterisation.

- Design a compact narrowband antenna at 2.45 GHz which does not experience any frequency detuning when placed on the body. The antenna can be designed with frequency tuning technique, or new material needs to be applied on the antenna structure to overcome frequency detuning.

- Design best body-worn narrowband and UWB antennas for future efficient and reliable body-centric wireless communications based on the specification provided in this thesis.

- Investigation of on-body performance of the narrowband and UWB antennas for different human test subjects. In this study, the on-body performance (in terms of frequency detuning, bandwidth, gain, radiation pattern and so on) of the narrowband and UWB antennas can be tested for various subjects with different shapes, sizes and heights.

- Design UWB and narrowband antennas placed on the human body (digital phantom/three layer human body model).

Radio Channel Characterisation for Body-Centric Wireless Communications

- Experimental investigation of subject-specific off-body radio channels characterisation for both ultra wideband and narrowband cases. This work also involves more thorough analysis of on-body and off-body radio channel characterisation and comparison.

- Characterisation of UWB body-to-body radio channels needs to be investigated. The body-to-body communication link can offer wireless communications between individuals with a seamless exchange of information. For example, patients could exchange vital information with their doctors, such as transmitting their medical history files to the doctor's personal base station, or may be soldiers exchanging information with the base station.

- UWB (3.1-10.6 GHz) off-body radio channel measurements should be made using omnidirectional, directional and high gain UWB antennas, in order to study the effects of the antenna as a part of the radio channels. This includes the design of directional and array antennas, to be applied to off-body communications in body-centric wireless communications.

- Study of smart antenna techniques to overcome fading of off-body radio channels in indoor body-centric wireless communications. Due to blocked communications by the human body, the off-body radio channel experiences huge fading of the transmitted signal. In order to overcome this fading, smart antenna techniques will be helpful.

- Radio propagation channel characterisation in sport applications, including a thorough analysis, must be performed. The DBDM antenna can be used in this study.

Millimetre-Wave for Body-Centric Wireless Communications

- Millimetre-wave frequencies are appealing for short-range, high-rate communications, with the advantage of a significant size reduction of the wearable device. Therefore, the on-body radio channel at 60 GHz and beyond needs to be investigated.

- Design of optimised wearable antennas for millimetre-wave applications. Design a millimetre-wave antenna which has omnidirectional radiation characteristics over the body surface.

- Characterisation of millimetre-wave antennas for body-centric wireless communications.

- Millimetre-wave antenna specifications for body-centric wireless communications. This work can also be compared with the narrowband and ultrawide band antenna specifications for cross-referencing.
- Investigation of subject-specific on-body radio channel at mm-wave frequencies.

Appendix A

Fabricated Narrowband and UWB Antennas

A.1 Fabricated Narrowband Antennas

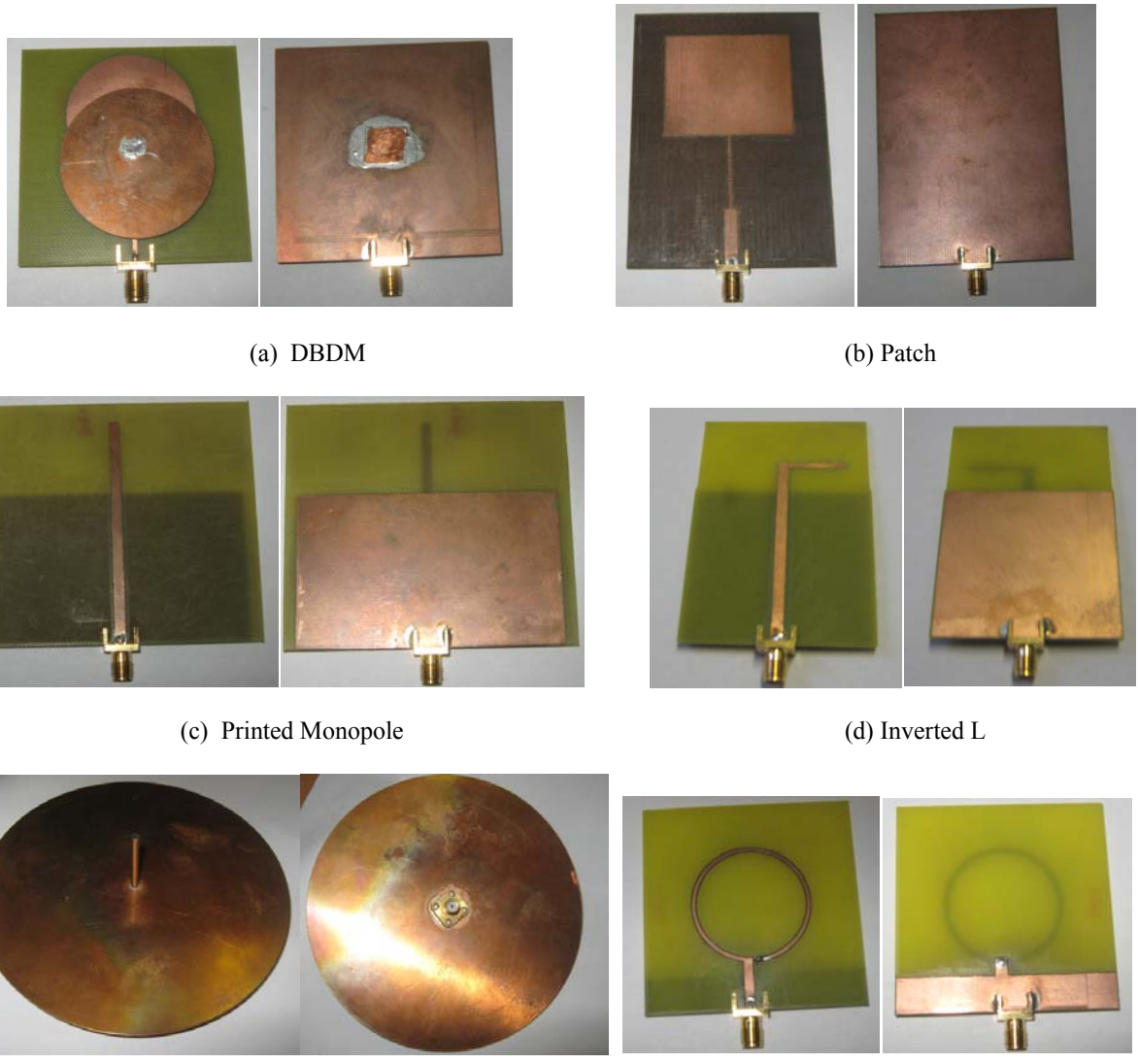

(a) DBDM (b) Patch

(c) Printed Monopole (d) Inverted L

(e) Wire Monopole (f) Loop

Fig. A 1. Narrowband fabricated antenna showing front and back side, respectively.

A.2 Fabricated UWB Antennas

(a) TSA

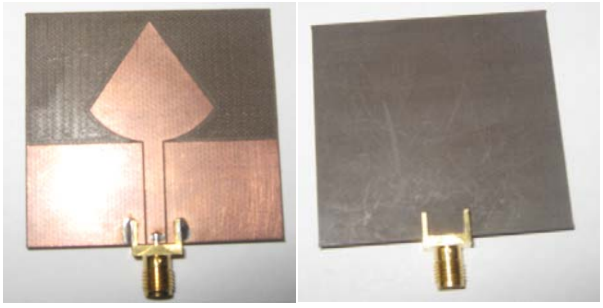

(b) PICA

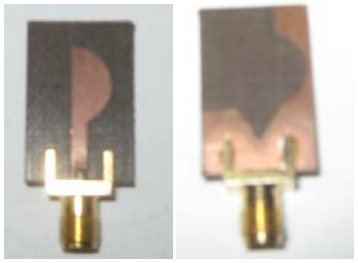

(c) Self Complementary

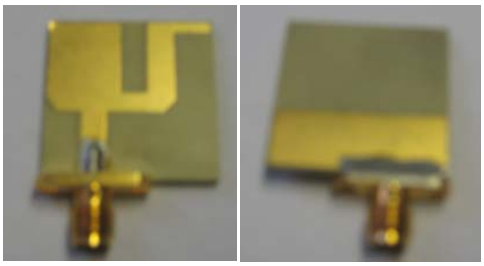

(d) SWAN Shaped

Fig. A 2. UWB fabricated antenna showing front and back side, respectively.

Appendix B

On-Body Measurements

Fig. B 1. HP8720ES Vector Network Analyser used for on-body measurement.

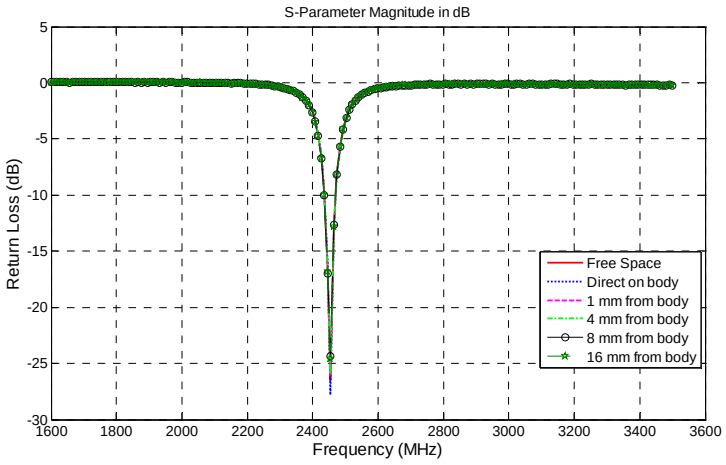

(a) Patch

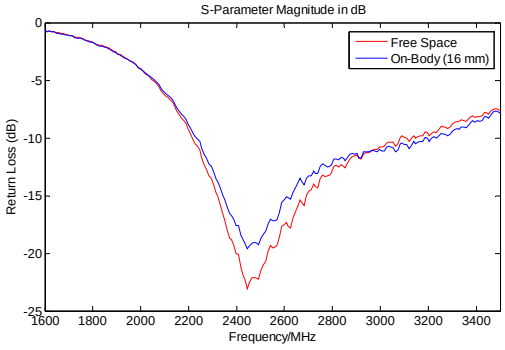

(b) Wire Monopole

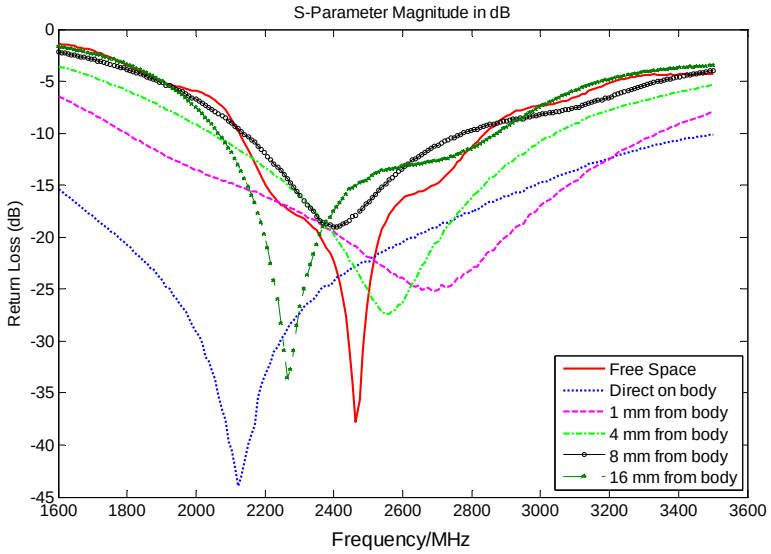

(c) Printed Monopole

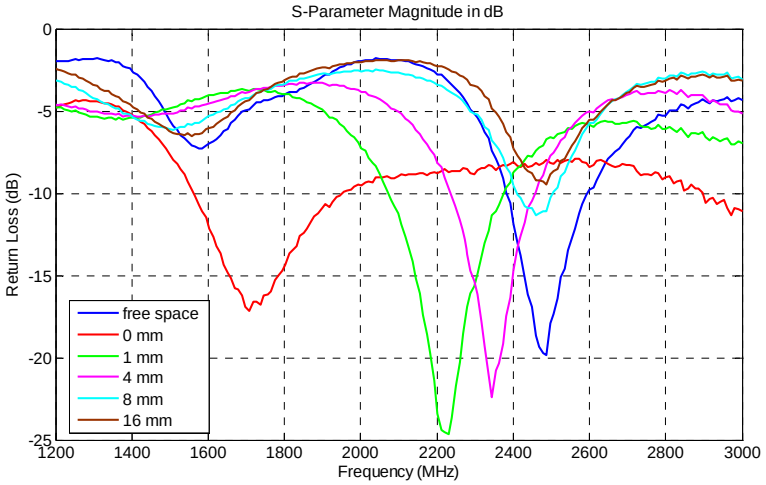

(d) Printed Circular Loop

Fig. B 2. Measured on-body S11 of narrowband antennas when placed at different distances away from the body.